CUMBERLAND SOUND AND KINGS BAY PRE-TRIDENT AND BASIC TRIDENT CHANNEL HYDRODYNAMIC AND SEDIMENT TRANSPORT HYBRID MODELING

VOLUME I

MAIN TEXT AND APPENDIXES A, C, AND D

by

Mitchell A. Granat, Nobie J. Brogdon

Hydraulics Laboratory

DEPARTMENT OF THE ARMY
Waterways Experiment Station, Corps of Engineers
3909 Halls Ferry Road, Vicksburg, Mississippi 39180-6199

AD-A231 434

December 1990

Final Report

Approved For Public Release; Distribution Unlimited

91 1 29 087

BLOCK 8a. NAME OF FUNDING/SPONSORING ORGANIZATION and
BLOCK 8c. ADDRESS (Continued).

Officer in Charge of Construction
TRIDENT
DEPARTMENT OF THE NAVY
Naval Facilities Engineering Command
St. Marys, GA 31558-0768

and

Naval Submarine Base
Kings Bay, GA 31547

19. ABSTRACT (Continued).

elevations in both the physical and numerical models. Variations were close to, but greater than, model detection limits. Low-water elevations between the models were inconsistent. Based on more recent field data, it was concluded that tide range will probably not change as a result of Trident channel improvements, and mean water level in Cumberland Sound may increase a small amount, less than the normal annual variation in mean sea level.

The subtle base-to-plan hydrodynamic differences and the increased plan channel area resulted in dramatic sedimentation responses. The numerical model predictions indicated a 150 percent increase in required annual plan channel maintenance dredging. Based on previous shoaling history and this study's findings, the typical annual plan channel maintenance dredging requirement is predicted to vary from a low of about 0.9 million cubic yards per year to a high of about 4.9 million cubic yards per year. The long-term average submarine channel maintenance is predicted to increase from approximately 1.0 million cubic yards per year for pre-Trident channel conditions to approximately 2.5 million cubic yards per year for the Trident channel condition.

Accession For		
NTIS GRA&I	☒	
DTIC TAB	☐	
Unannounced	☐	
Justification		
By		
Distribution/		
Availability Codes		
Dist	Avail and/or Special	
A-1		

REPORT DOCUMENTATION PAGE		Form Approved OMB No. 0704-0188

1a. REPORT SECURITY CLASSIFICATION Unclassified	1b. RESTRICTIVE MARKINGS

2a. SECURITY CLASSIFICATION AUTHORITY	3. DISTRIBUTION/AVAILABILITY OF REPORT Approved for public release; distribution unlimited.
2b. DECLASSIFICATION/DOWNGRADING SCHEDULE	

4. PERFORMING ORGANIZATION REPORT NUMBER(S) Technical Report HL-90-21	5. MONITORING ORGANIZATION REPORT NUMBER(S)

6a. NAME OF PERFORMING ORGANIZATION USAEWES Hydraulics Laboratory	6b. OFFICE SYMBOL (If applicable) CEWES-HE-E	7a. NAME OF MONITORING ORGANIZATION

6c. ADDRESS (City, State, and ZIP Code) 3909 Halls Ferry Road Vicksburg, MS 39180-6199	7b. ADDRESS (City, State, and ZIP Code)

8a. NAME OF FUNDING/SPONSORING ORGANIZATION See reverse.	8b. OFFICE SYMBOL (If applicable)	9. PROCUREMENT INSTRUMENT IDENTIFICATION NUMBER

8c. ADDRESS (City, State, and ZIP Code) See reverse.	10. SOURCE OF FUNDING NUMBERS			
	PROGRAM ELEMENT NO.	PROJECT NO.	TASK NO.	WORK UNIT ACCESSION NO.

11. TITLE (Include Security Classification)
Cumberland Sound and Kings Bay Pre-Trident and Basic Trident Channel Hydrodynamic and Sediment Transport Hybrid Modeling; Volume I: Main Text and Appendixes A, C, and D

12. PERSONAL AUTHOR(S)
Granat, Mitchell A.; Brogdon, Noble J.

13a. TYPE OF REPORT Final report in 2 vols.	13b. TIME COVERED FROM _____ TO _____	14. DATE OF REPORT (Year, Month, Day) December 1990	15. PAGE COUNT Vol I, 190

16. SUPPLEMENTARY NOTATION A limited number of copies of Appendix B were published under separate cover. Copies of this report and Appendix B are available from National Technical Information Service, 5285 Port Royal Road, Springfield, VA 22161.

17.	COSATI CODES		18. SUBJECT TERMS (Continue on reverse if necessary and identify by block number)
FIELD	GROUP	SUB-GROUP	Channel deepening Kings Bay (Georgia)
			Cumberland Sound Sediment modeling
			Hydrodynamic modeling Trident channel

19. ABSTRACT (Continue on reverse if necessary and identify by block number)

A previously verified hybrid modeling system (coupled physical and numerical models) of the Kings Bay/Cumberland Sound estuarine system was used to investigate hydrodynamic and sedimentation variations associated with Trident channel expansion. The models generally demonstrated small velocity differences between the pre-Trident base channel condition and the enlarged Trident channel condition tested. Reduced velocity magnitudes in the deepened upper Kings Bay turning basin demonstrated the largest base-to-plan velocity differences.

Subtle circulation differences were identified. The deepened and widened Trident plan channel increased flood and ebb volume transport efficiency of the submarine channel through St. Marys Inlet into Cumberland Sound and Kings Bay. Increased discharge through and past Kings Bay changed the phasing relationships north of Kings Bay.

Although not an explicit objective of the modeling efforts, tidal effects were examined. The tested plan condition resulted in higher high-water and midtide level

(Continued)

20. DISTRIBUTION/AVAILABILITY OF ABSTRACT ☒ UNCLASSIFIED/UNLIMITED ☐ SAME AS RPT. ☐ DTIC USERS	21. ABSTRACT SECURITY CLASSIFICATION Unclassified
22a. NAME OF RESPONSIBLE INDIVIDUAL	22b. TELEPHONE (Include Area Code)	22c. OFFICE SYMBOL

DD Form 1473, JUN 86   Previous editions are obsolete.   SECURITY CLASSIFICATION OF THIS PAGE

EXECUTIVE SUMMARY

A hybrid modeling system (coupled physical and numerical models) was used to investigate the hydrodynamic and sedimentation processes of the interior submarine channel through Cumberland Sound into Kings Bay. The components of the hybrid modeling system, the modeling procedures, and their verifications are presented in detail in Technical Report HL-89-14.

Briefly, the Kings Bay physical model was a distorted-scale, fixed-bed, concrete model built to length scales of 1:100 vertical and 1:1,000 horizontal. The model was approximately 126 ft long and 108 ft wide and accurately reproduced the three-dimensional tide, velocity, and salinity characteristics of the Cumberland Sound estuarine system including Kings Bay.

The other component of the hybrid modeling system was the US Army Corps of Engineers Generalized Computer Program System: Open-Channel Flow and Sedimentation, TABS-2 (Instruction Report HL-85-1). TABS-2 is a collection of two-dimensional, depth-averaged, finite element computational programs and utility codes. The numerical hydrodynamic code RMA-2V uses physical-model-derived boundary forcing conditions to solve the depth-integrated equations of conservation of mass and momentum. Water-surface elevation and velocity results were used by the numerical sediment transport code STUDH to solve the depth-integrated convection-diffusion equation and model the interaction of the flow (transport) and cohesive (clay and silt) and noncohesive (sand and silt) sedimentation (erosion and deposition).

The hybrid modeling system was used to assess hydrodynamic and sedimentation variations between the pre-Trident 1982 base channel condition and the Trident channel condition planned in 1985. The physical model base data collected in 1983 were used for comparison to the basic plan data collected in 1985. These data sets provided the hydrodynamic boundary forcing conditions for the numerical modeling portion of the investigation. Both models included the most up-to-date information available at the time of testing. Ideally, a new pre-Trident base channel physical model test should have been conducted during the 1985 testing period. The need for expedited testing of the revised basic plan channel did not permit the schedule to be adjusted for that purpose. The lower Kings Bay turning basin and the St. Marys Inlet turning and sediment basins, designed subsequent to model testing, were not included in the modeling study.

1

The modeling work did not include as an explicit objective prediction of tidal elevation effects; however, they were measured. Physical model and numerical model results indicated a slight trend of increased water levels within Kings Bay and Cumberland Sound for the plan channel condition. These variations were close to, but greater than, model detection limits. Appendix B provides a more detailed analysis of potential water level changes using available modeling results and recent field data. Based on the more recent field data, it was concluded that tide range will probably not change as a result of the Trident channel improvements and that mean water level in Cumberland Sound may increase a small amount, less than the normal variation in mean sea level. As such, any changes will be extremely difficult to detect until several years of data are available.

The hybrid modeling system generally predicted small velocity differences between the pre-Trident base channel and the Trident plan condition. Reduced velocity magnitudes in the deepened upper Kings Bay turning basin demonstrated the largest base-to-plan velocity differences. A low-velocity recirculation eddy in the upper turning basin, downstream from the Trident dry dock, was enhanced during the plan condition ebb cycle.

Subtle circulation changes were predicted comparing the base and plan channel conditions. The deepened and widened Trident plan channel increased flood and ebb volume transport efficiency of the submarine channel through St. Marys Inlet into Cumberland Sound and Kings Bay. Flood and ebb tidal cycle discharge within each tributary, at the numerical model boundary locations, was reduced for the plan channel condition relative to the base channel condition. The northern Cumberland Sound boundary was the only boundary to demonstrate a discharge dominance change; net flow changed from slightly flood dominated for the base condition to slightly ebb dominated for the plan condition. Increased discharge through Kings Bay changed the tidal phasing relationships (earlier times of arrival) north of Kings Bay.

The plan channel condition increased the maintained interior channel area by about 70 percent. Approximately 43 percent of the increased channel area was within the high shoaling zones of Kings Bay. The subtle circulation changes predicted by the physical and numerical models plus the much larger maintained channel areas resulted in dramatic changes in the sedimentation responses. The numerical model results indicated a potential 150 percent increase in plan channel shoaling. The long-term average submarine channel

2

maintenance dredging requirement was predicted to increase from about 1.0 million cubic yards per year for the pre-Trident channel condition to approximately 2.5 million cubic yards per year for the Trident channel condition tested.

The numerical sedimentation model was verified to reproduce observed prototype average channel sedimentation rates for the period July 1979 to August 1982. Thus the base-to-plan sedimentation absolute results should reflect the changes that would occur on average over a comparable period with similar sediment supply. Individual years may experience sedimentation rates appreciably lower or higher than those predicted by the model. The long-term average change in sedimentation rate may be quantitatively different from the predicted rates, but should be qualitatively similar.

Based on previous shoaling history and this study's findings, typical annual plan channel maintenance dredging requirements are predicted to vary from a low of about 0.9 million cubic yards per year to a high of about 4.9 million cubic yards per year. Over 90 percent (2.3 million cubic yards) of the total plan channel shoaling is predicted to be located within Kings Bay. Cohesive material (clay and silt) is predicted to account for over 80 percent (2.0 million cubic yards) of the total plan channel shoaling volume.

The pre-Trident Kings Bay was an efficient sediment trap. The increased discharge through Cumberland Sound and Kings Bay and the reduced current velocities associated with the plan channel modifications are predicted to make Kings Bay an even more efficient sediment trap.

PREFACE

The modeling study reported herein was requested by the Department of
the Navy, Officer in Charge of Construction (OICC), Trident, Kings Bay, in a
letter to the US Army Engineer Waterways Experiment Station (WES) dated
16 September 1982. The modeling portion of the study was conducted during the
period October 1982 through September 1986. WES was requested to undertake a
modeling study to examine the hydrodynamic and sedimentation processes of the
Kings Bay Submarine Base harbor facilities and channels, to predict long-term
average maintenance dredging requirements for planned channel enlargements,
and to evaluate possible remedial measures. A two-part model study was devel-
oped. Part one, referred to as Model A, was a hybrid model (coupled physical
and numerical models) designed to address the interior portion of the system--
inland of the throat of St. Marys Inlet. The second part, Model B (Technical
Report CERC-88-3), developed at the Coastal Engineering Research Center, WES,
addressed the outer portion--seaward from the inlet throat. This report
describes the Model A hybrid model findings for the pre- and post-Trident
channel conditions. An earlier report (Technical Report HL-89-14) described
the hybrid modeling system in detail and addressed the physical and the numer-
ical model verifications. Subsequent reports address physical model and
numerical model evaluations of some potential remedial measures.

This study was conducted in the Hydraulics Laboratory of WES under the
general supervision of Messrs. H. B. Simmons and F. A. Herrmann. Jr., former
and present Chiefs of the Hydraulics Laboratory, respectively; R. A. Sager,
Assistant Chief of the Hydraulics Laboratory; W. H. McAnally, Chief of the
Estuaries Division, Hydraulics Laboratory; W. D. Martin, Chief of the
Estuarine Engineering Branch, Estuaries Division; R. A. Boland and J. V.
Letter, former Chiefs of the Estuarine Simulation Branch, Estuaries Division;
and M. A. Granat, Estuarine Engineering Branch, Project Manager. Mr. N. J.
Brogdon, Jr., Estuarine Simulation Branch, was Project Engineer for the physi-
cal model and Mr. Granat was Project Engineer for both numerical models.
Ms. C. Coleman, Estuarine Processes Branch, Estuaries Division, and Mr. D.
Stewart, Estuarine Engineering Branch, assisted as numerical model technicians
during several stages of this investigation. Physical model technicians who
assisted throughout the investigation included Messrs. J. Ashley,
J. Cartwright, D. M. White, C. Holmes, and J. Cessna, Jr., all of the

4

CONTENTS

---

* A limited number of copies of Appendix B were published under separate
  cover. Copies are available from National Technical Information Service,
  5285 Port Royal Road, Springfield, VA 22161.

CONVERSION FACTORS, NON-SI TO SI (METRIC)
UNITS OF MEASUREMENT

Non-SI units of measurement used in this report can be converted to SI (metric) units as follows:

Multiply	By	To Obtain
acres	4,046.873	square metres
cubic feet	0.02831685	cubic metres
cubic yards	0.7645549	cubic metres
feet	0.3048	metres
miles (US nautical)	1.852	kilometres
miles (US statute)	1.609347	kilometres
pounds (force)-second per square foot	47.88026	pascals-second
square feet	0.09290304	square metres
square miles	2.589988	square kilometres

CUMBERLAND SOUND AND KINGS BAY PRE-TRIDENT AND BASIC TRIDENT CHANNEL
HYDRODYNAMIC AND SEDIMENT TRANSPORT HYBRID MODELING

PART I: INTRODUCTION

Background

1. The Naval Submarine Base, Kings Bay, is located in southeast
Georgia, about 9.6 nautical miles* north of the St. Marys Inlet entrance
jetties at the Atlantic Ocean. Figure 1 shows the general Cumberland Sound
and Kings Bay study area. The base is within the Cumberland Sound estuarine
system, which includes extensive salt marshes and sand flats (stippled areas
on Figure 1) typical of the Sea Island system of southeast Georgia. The mean
tidal range at the ocean entrance between Amelia Island, in the State of
Florida, and Cumberland Island, in the State of Georgia, is 5.8 ft. Maximum
spring tide ranges can exceed 8.0 ft in the interior portions of the estuary.

2. The primary source of fresh water for the Cumberland Sound estuarine
system is the St. Marys River. The river originates in the Okefenokee Swamp,
approximately 140 statute miles upstream from Cumberland Sound, and enters the
Sound about 5.5 nautical miles south of the Kings Bay entrance. The St. Marys
drainage basin includes about 1,500 square miles of swampland and coastal
plain. The long-term average freshwater discharge at the mouth of the river
is about 1,500 cfs. Freshet discharges as high as 18,000 cfs have been
reported. Suspended sediment loads within the St. Marys River are generally
low.

3. The Crooked River, located approximately 2 nautical miles north of
Kings Bay, is the second largest contributor of fresh water into the Cumber-
land Sound system. This river is much smaller than the St. Marys and consists
of a drainage basin of about 90 square miles with an average freshwater dis-
charge of about 100 cfs. The total fresh water entering Cumberland Sound from
the remaining drainage basins is estimated to be less than the Crooked River
flow.

4. The relatively low average total freshwater discharge into

---

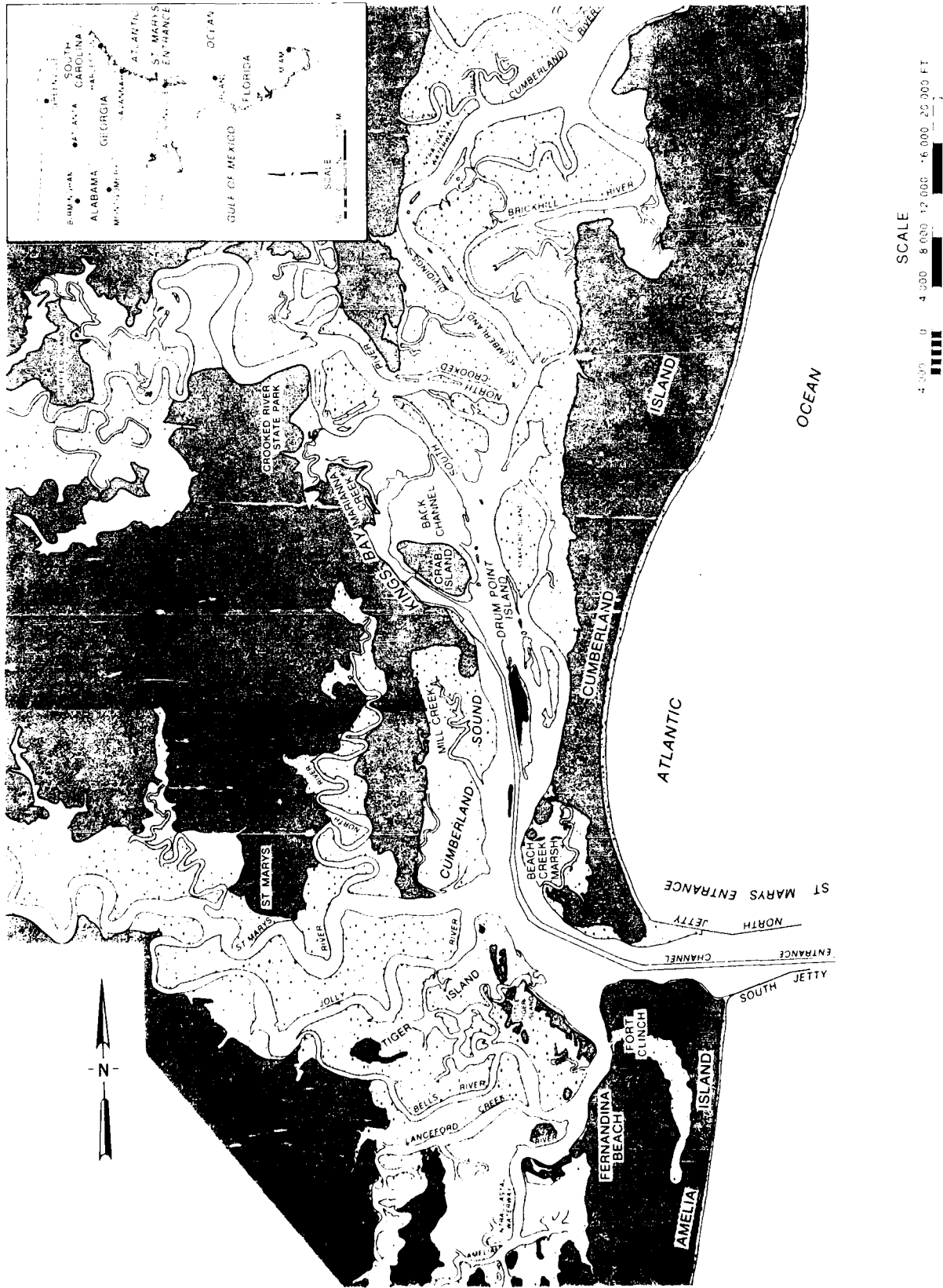* A table of factors for converting non-SI to SI (metric) units is presented
on page 8.

Figure 1. General study area location map

Cumberland Sound and the relatively high tidal range and associated strong current velocities generally maintain the sound as a well-mixed estuarine system. Salinity within the sound and Kings Bay is generally vertically and laterally homogeneous. Longitudinally, salinity within the sound is only slightly reduced from the ocean entrance conditions. Salinity in Kings Bay typically varies from about 26 to 32 ppt during the year.

5. The original Kings Bay facility was designed and developed as an emergency Army Munitions Operation Transportation facility in the late 1950's. Initial channel depths were authorized at 32 ft mean low water (mlw).* The facility was in a standby mobilization status with channel depths of about 32 ft maintained on an "as time and money permitted" basis.

6. In July 1978, ownership of the Kings Bay facility was transferred to the Department of the Navy for use as a Naval submarine base for Poseidon class submarines. Between July 1978 and July 1979 approximately 8.6 million cubic yards of material were removed for Poseidon facility expansion. Major channel realignment, widening, and deepening were performed. The lower entrance channels had project depths of 38 to 40 ft and a width of 400 ft. The remaining interior approach channel had a project depth of 34 ft and a width of 300 ft. Kings Bay had a project depth of 37 ft.

7. The total length of the interior Poseidon (pre-Trident) channel, from the throat of St. Marys entrance adjacent to Fort Clinch to the end of the main docking facility, was about 7 nautical miles. The narrowest point between land masses within Kings Bay was about 1,000 ft and occurred at the entrance to the submarine base. The channel width widened from about 650 ft at the entrance to about 1,200 ft at the downstream end of the main docking facility. At this location, a 643-ft-long Poseidon submarine support tender was usually anchored perpendicular to the channel. A floating dry dock was located parallel to the channel about 0.5 nautical mile downstream from the Kings Bay entrance.

8. Limited pre-Trident channel sedimentation history indicated an average channel shoaling rate of about 1.2 million cubic yards per year; seasonal extreme values varied from 0.4 million cubic yards per year to 2.6 million cubic yards per year. Most of the required maintenance dredging was

---

* All depths and elevations (el) described in this report are in feet referred to local mean low water, which is 2.75 ft below National Geodetic Vertical Datum (NGVD).

concentrated within the Kings Bay area of the channel. Relatively low shoaling rates, less than 1.0 ft per year, were indicated for the navigation channel in Cumberland Sound. High shoaling rates, greater than 3.0 ft per year, were indicated for the channel areas within Kings Bay. Long-term hydrodynamic processes, including ebb and flood circulation cells and reduced current velocities within Kings Bay, are primarily responsible for transporting already flocculated clay sediments and causing the high shoaling rates at Kings Bay. Sedimentation is not the result of localized flocculation (geochemistry associated with a freshwater-saltwater interface).

Objectives

9. A hybrid modeling study (coupled physical and numerical models) to investigate hydrodynamic and sedimentation processes of the Cumberland Sound and Kings Bay estuarine system was undertaken by the US Army Engineer Waterways Experiment Station (WES). The primary objectives of the modeling study were to (a) predict average currents, (b) predict long-term average maintenance dredging requirements for enlarged channel and port facilities for the submarine base, and (c) develop and evaluate remedial measures that might reduce sedimentation without adversely affecting ship handling and enhance base operational readiness. Another primary goal of the entire study effort was to maintain a fast-track pace to provide the Navy with results on priority tasks while maintaining the required flexibility to adapt to project design changes. Results were provided to the Navy in memorandum format as they became available.

Scope

10. The complete modeling study included many different tasks and subtasks. Some of the final design plans for channel expansion evolved during the 7 years of construction and during model testing. The models were updated in a timely fashion as additional information was provided. This report describes the hybrid modeling hydrodynamic and sedimentation results for the pre-Trident and basic Trident channel conditions planned through August 1985. The hybrid modeling procedures developed and their verification are described

in detail in an earlier report * The main purpose of this report is to
address variations between pre-Trident and basic Trident channel hydrodynamic
and sediment model predictions. Subsequent reports address model evaluations
of potential remedial measures.

11. The most recent basic Trident plan channel conditions addressed in
this report included all revisions requested by the Officer in Charge of Con-
struction (OICC) through January 1985 for the physical model and August 1985
for the numerical model. Details of the base and plan submarine channel will
be discussed in paragraph 62. The modeling efforts did not include the lower
Kings Bay turning basin or the St. Marys Inlet turning and sediment basins,
which were designed subsequent to model testing. The incorporated revisions
included all channels widened to a minimum 500-ft width; an ocean entrance
channel widened 100 ft to the north and deepened to 49 ft; an interior
approach channel widened 200 ft to the west and deepened to 46 ft; some addi-
tional channel widening to the east at the entrance bend into Cumberland
Sound; the relocated 46-ft-deep magnetic silencing facility adjacent to the
main channel across from Drum Point Island; development of a 41-ft-deep
Poseidon waterfront docking area adjacent to and west of the floating dry
dock; relocation of the Poseidon tender from perpendicular to the channel at
Kings Bay to parallel to the channel above the floating dry dock; and a Tri-
dent Kings Bay operational area that was widened, deepened to 48 ft, and
lengthened 1 nautical mile to the northwest, to include an upper turning
basin, a Trident dry dock, and other support facilities including a 23-ft-deep
small boat facility. Approximately 25.5 million cubic yards of material were
removed to accomplish this planned interior channel expansion. The requested
plan testing condition also included the anticipated relocation of the
Atlantic Intracoastal Waterway (AIWW) to an alignment east of Drum Point
Island. Paragraphs 31 and 61, respectively, describe the physical and numeri-
cal model schematizations of the relocated waterway.

---

* Mitchell A. Granat, Noble J. Brogdon, John T. Cartwright, and William H.
   McAnally, Jr. 1989 (Jul). "Verification of the Hydrodynamic and Sediment
   Transport Hybrid Modeling System for Cumberland Sound and Kings Bay Naviga-
   tion Channel, Georgia," Technical Report HL-89-14, US Army Engineer Water-
   ways Experiment Station, Vicksburg, MS.

PART II: THE HYBRID MODELING SYSTEM

12.   The hybrid modeling system (coupled physical and numerical models)
was developed to investigate the hydrodynamic and sedimentation processes of
the interior submarine navigation channel through Cumberland Sound into Kings
Bay.   This hybrid system used the advantages of each modeling approach (physi-
cal and numerical) while reducing or avoiding associated model limitations.

The Physical Model

13.   The Kings Bay physical model was a distorted-length-scale, fixed-
bed, concrete model that reproduced approximately 206 square miles of
southeast Georgia and northeast Florida, and about 220 square miles of the
adjacent Atlantic Ocean.   The model was constructed to linear scale ratios,
model-to-prototype, of 1:100 vertical and 1:1,000 horizontal; the vertical
scale in the physical model was stretched 10 times relative to the horizontal
scale.   The model was approximately 126 ft long and 108 ft wide and covered an
area of about 12,600 sq ft.   The vertical and horizontal scales dictated the
other scaling factors (time, velocity, discharge) based on Froudian relation-
ships.   Time, for example, was compressed in the physical model so that one
complete ebb and flood semidiurnal tidal cycle (12.42 hr) occurred in
7.452 min on the model.

14.   The physical model was an accurate scaled reproduction of the
Cumberland Sound/Kings Bay estuarine system.   Figure 2 illustrates the physi-
cal model limits.   Salinity in the model was reproduced at a 1:1 ratio.   The
physical model was verified* to reproduce observed tide, velocity, and salin-
ity field measurements to ensure the reliability of model results.   Two dis-
tinct verifications were demonstrated.   Stainless steel artificial roughness
or resistance strips projecting from the molded concrete bed of the model
served as the primary means of adjusting the physical model to reproduce
November 1982 pre-Trident channel hydrodynamic field conditions for Kings Bay
and the areas to the south.   Additional roughness strip and geometry adjust-
ments were performed in the physical model areas north of Kings Bay prior to
final verification to the January 1985 transitional channel field conditions

---

* Granat et al., op. cit.
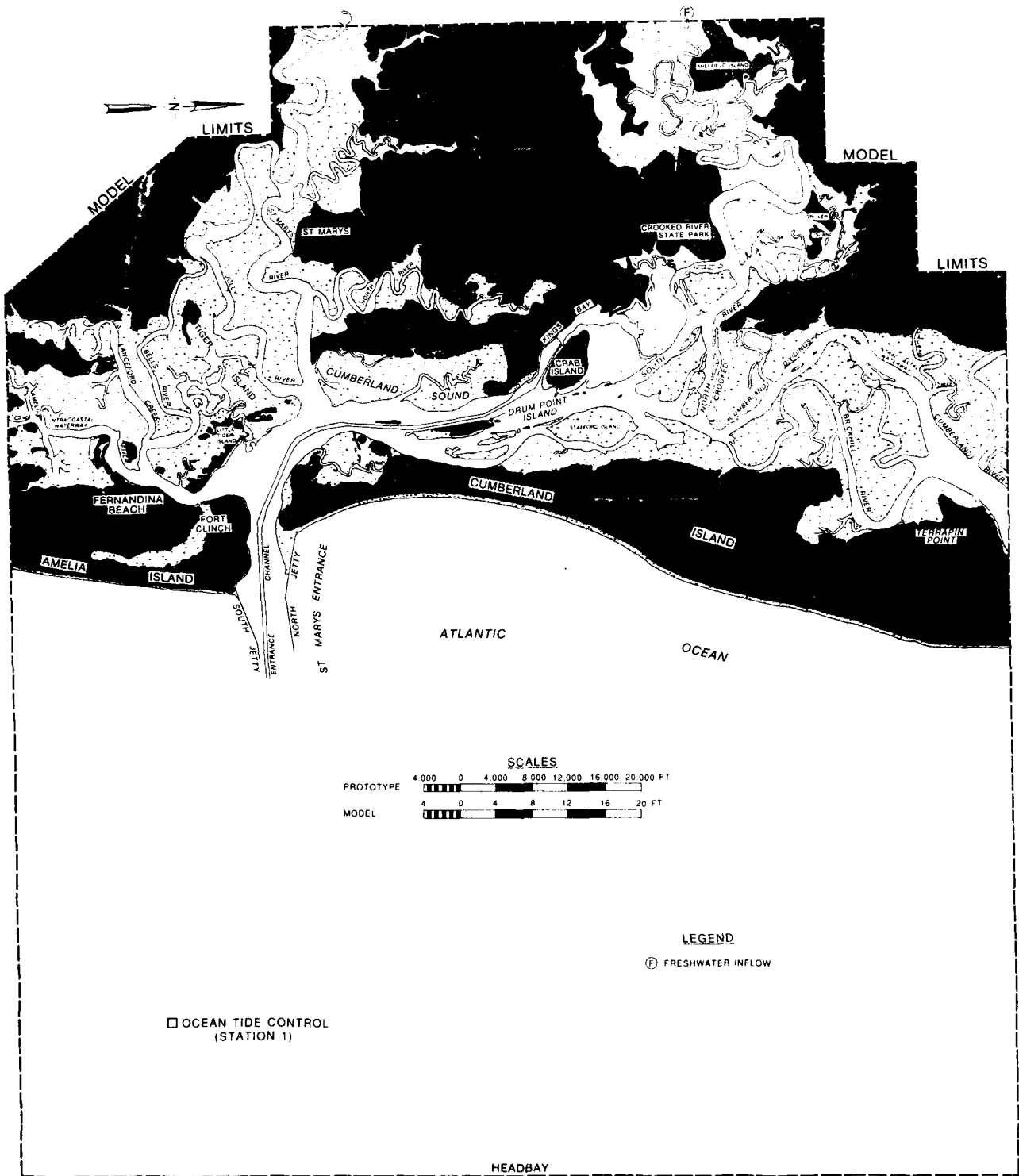
Figure 2. Physical model limits

15

for the areas north of and including Kings Bay.

15. As verified, the physical model can be used to investigate the three-dimensional flow characteristics of the Cumberland Sound/Kings Bay estuarine system associated with the long-term average freshwater discharge and average tidal conditions. Geometry in the model can be modified physically to examine any desired alternative plan condition. Comparison of results between two model runs with identical conditions except for the plan modification provides a means of assessing potential hydrodynamic impacts associated with the plan modification.

16. A limitation of the physical model involves quantitative sedimentation predictions, especially when cohesive sediment is the primary sediment constituent, as is the case for Kings Bay; numerical models are superior sedimentation predictor tools. The physical model provided the hydrodynamic boundary forcing conditions for the numerical model. Physical model tidal cycle water levels collected at the St. Marys Inlet entrance were used as the numerical model ocean boundary forcing condition. Depth-averaged physical model tidal cycle velocity observations collected at each of the tributary boundary locations of the numerical model were used as numerical model upstream boundary forcing conditions. Physical model tide and velocity measurements at selected interior model locations throughout the modeled area of interest were used for numerical model verification purposes.

The TABS-2 Numerical Models

17. The numerical modeling system used was the US Army Corps of Engineers Generalized Computer Program System: Open Channel Flow and Sedimentation, TABS-2.* TABS-2 is a collection of preprocessor and postprocessor utility codes and three main finite element, two-dimensional, depth-averaged computational programs. The finite element method provides a means of obtaining an approximate solution to a system of governing equations (i.e., equations of motion and conservation) by dividing the area of interest into

---

* William A. Thomas and William H. McAnally, Jr. 1985 (Jul). "User's Manual for the Generalized Computer Program System: Open-Channel Flow and Sedimentation, TABS-2," Instruction Report HL-85-1, US Army Engineer Waterways Experiment Station, Vicksburg, MS.

smaller subareas called elements; time-varying partial differential equations are transformed into finite element form and then solved in a global matrix system for the modeled area of interest. The solution is smooth across each element and continuous over the computational area. Figure 3 illustrates the basic Kings Bay numerical model mesh. An elemental wetting and drying algorithm was used in modeling the extensive marsh and intertidal areas of the estuarine system. These areas are shaded in Figure 3. Appendix A provides a concise summary of the TABS-2 modeling system.

Numerical hydrodynamic model RMA-2V

18. The numerical model code RMA-2V used the boundary forcing conditions derived from the physical model to solve the depth-integrated equations of conservation of mass and momentum in two horizontal directions and provided hydrodynamic solutions for water-surface elevations and horizontal velocity components over the entire modeled area. Verification of RMA-2V was accomplished through comparisons of water-surface elevation and velocity with corresponding physical model data. Numerical model bottom roughness (Manning's n) and eddy viscosity coefficients based on physical characteristics and marsh elevation schematization provided the necessary means for verifying the numerical model.

19. Marsh-estuarine circulation interaction was found to be important in achieving proper reproduction of Cumberland Sound and Kings Bay hydrodynamic characteristics. A compromise between tidal reproduction and velocity reproduction was made in achieving the desired agreement between the numerical model and the physical model measurements. A nominal marsh elevation of +4.0 was selected in schematizing the numerical model marsh areas that flooded and dried during the tidal cycle. Higher numerical model marsh elevations improved tidal reproduction (higher high-water and lower low-water elevations) but resulted in overall reduced current velocities. Precise field marsh elevations were not known. The +4.0 elevation was felt to be a valid average marsh elevation approximation for modeling purposes.

20. The developed numerical modeling procedures and coefficients demonstrated excellent main channel ebb and flood velocity phase and magnitude agreement with the physical model measurements. Tributary and secondary channels adjacent to marsh areas demonstrated excellent velocity phase agreement and a slightly reduced numerical model ebb and flood velocity magnitude relative to the physical model measurements. Excellent tidal phase and midtide

17

LEGEND

FLOODING AND DRYING AREAS

PROPOSED RELOCATED AIWW
ALTERNATE ROUTE C

CRAB ISLAND

KINGS BAY
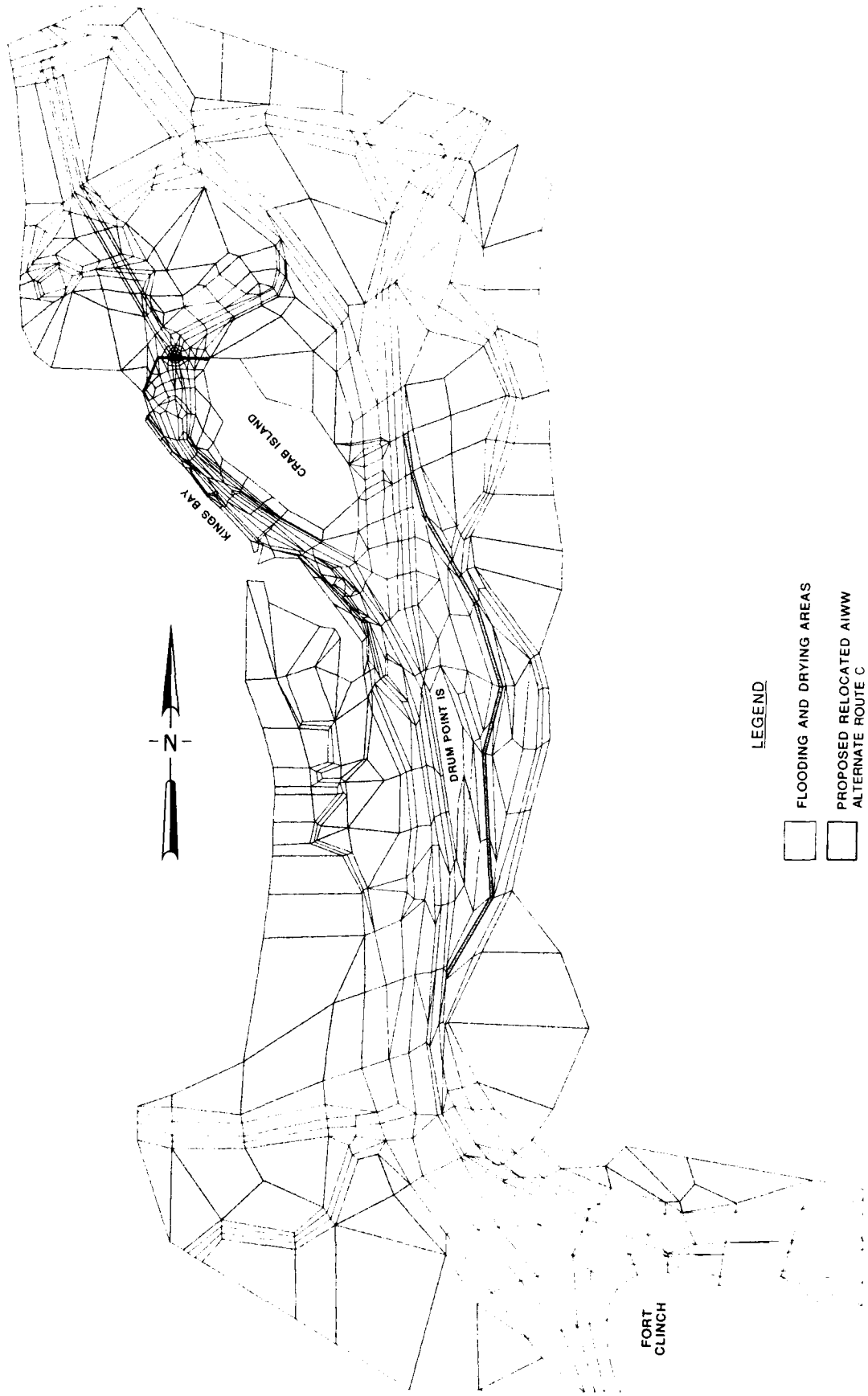
DRUM POINT IS

FORT
CLINCH

-N-

Figure 3. Numerical model Mesh 4

level agreement was also demonstrated. Numerical model high- and low-water elevations were generally within 0.1 to 0.3 ft of the physical model measurements (i.e., numerical model tidal range was reduced relative to the physical model). This agreement (and compromise discussed in the preceding paragraph) was considered acceptable since tidal predictions were not an explicit objective of the modeling effort. An improved numerical model to physical model agreement in tide and velocity characteristics was generally achieved during the transitional channel (1985) verification. The greatest improvements were in the areas north of Kings Bay, the areas in which additional physical model geometry and roughness adjustments were performed. A finer resolution of the marsh areas and of the wetting and drying process would improve the local comparisons; however, additional modifications were not attempted due to the excellent agreement of the main channel velocity characteristics, the uncertainties of precise marsh elevations and their history, and the primary goals of the modeling effort (i.e., channel velocity and sedimentation predictions).

21. Based upon the physical characteristics of each element, the same Manning's n and eddy viscosity coefficients and marsh elevations determined during the verification process were used during the various channel conditions examined. For comparison in this report, the same basic mesh (Mesh 4) with the required depth adjustments was used for pre-Trident and Trident channel conditions to eliminate the possibility of mesh resolution refinement as a possible cause for anomalous variations in the model predictions. Physical-model-derived base and plan channel boundary forcing conditions were used for the base and plan numerical model runs, respectively.

Numerical sediment model, STUDH

22. The hydrodynamic results from RMA-2V were used in the numerical sediment transport code STUDH as input information to solve the depth-integrated convection-diffusion equation for a single sediment constituent. The interaction of the flow (transport) and the bed (sedimentation) was treated in routines that computed source/sink (erosion/deposition) terms over the entire modeled area. Cohesive (clay and silt) and noncohesive (sand and silt) sedimentation and transport were handled separately. Sediment modeling results provided an average sedimentation (erosion or deposition) approximation across each computational element.

23. The RMA-2V hydrodynamic data sets were considered to be approximations of the long-term average hydrodynamic conditions associated with the

19

long-term sedimentation processes affecting the navigation channel through Cumberland Sound and Kings Bay. Several cohesive and noncohesive sediment model runs were performed separately to initialize model sediment concentrations and bed conditions. Results for each sediment type were then extrapolated to provide model predictions for a complete year of sedimentation. Results for each sediment type were arithmetically combined to produce a yearly sedimentation rate for comparison and planning.

24. STUDH was verified through comparison of model predictions with actual field shoaling rates for pre-Trident channel conditions. Model testing coefficients were based upon the latest field data, laboratory testing analyses, and previous modeling experience, as available. Sediment grain size distribution was the primary adjustment means for noncohesive sedimentation, and bed density was the primary adjustment means for cohesive sedimentation. Results presented in this report reflect the most up-to-date grain size distribution and bed density characteristics (i.e., a medium-grain-sized sand north of Kings Bay and a cohesive bed density of 300 kg/cu m). These sediment coefficients were the same for the base and plan conditions.

25. Excellent numerical model and field pre-Trident channel sedimentation agreement was demonstrated during the model verification. The same modeling procedures and model coefficients were used to examine shoaling rates associated with the January 1985 transitional channel geometry conditions. Field shoaling rates were determined for the recently dredged upper Trident turning basin for the January 1985-January 1986 period. This area had no previous survey information for determining a shoaling history. Model predictions for the upper turning basin area indicated higher shoaling rates than the limited field data. Several possible explanations for this difference included low field sediment loads associated with the prolonged east coast drought conditions at that time, the ongoing dredging operations and the transitional nature of the channel, and the possible need for further model adjustments. The sediment model was developed and verified for long-term average conditions, and additional model adjustments could not be justified based on the limited data available for this area. Additional time and monitoring are required before any other model adjustments can be made with confidence.

Modeling Limitations

26. Any solution method or model is an approximation of the prototype.

Each has its own set of limitations, simplifications, and underlying assumptions. Results obtained from any technique must always be considered as approximate solutions to the given set of conditions. A verification process is required to demonstrate the degree of reasonableness for all predictions. The degree of sophistication of the technique and the resulting verification are offset by time and cost constraints.

27. Many approximations, simplifications, and assumptions have been made in the present hybrid approach, and only part of them are explicitly stated in this report. Each approximation, simplification, and assumption can be arguably justified as necessary or desirable, but the net result must be considered only an approximation to a very complex system and its processes. The developed hybrid method was the most advanced modeling method available to assess potential changes in submarine channel velocity and sedimentation characteristics. In comparison to the complex interaction of processes within Cumberland Sound and Kings Bay, the modeling approach was greatly simplified.

28. After completion of the base test and before the plan testing reported here, portions of northern Cumberland Sound were revised in the physical model and reverified.* Examination of model results showed that the changes were small enough to proceed with testing for the stated objectives; however, tidal elevation comparisons between base and this plan should be made with extreme caution. (See Appendix B for further discussion.)

---

* Granat et al., op. cit.

PART III: PHYSICAL MODEL HYDRODYNAMIC RESULTS AND ANALYSIS

Testing Conditions

29. The same physical model ocean boundary conditions were maintained between the pre-Trident channel base condition and the basic Trident channel plan condition requested in January 1985. The ocean tide control (station 1, Figure 4), located in the modeled offshore Atlantic Ocean, was established as the tide control station to avoid potential geometry-induced hydrodynamic variations associated with the plan channel modifications. A long-term average +6.2-ft high-water to +0.5-ft low-water repetitive ocean tide was generated at the control station for the base and plan tests. C ean salinity was maintained at 32.5 ppt throughout each test. A constant long-term freshwater discharge was also maintained during each test. The freshwater inflow at the St. Marys River boundary was maintained at 1,000 cfs and the inflow at the Crooked River boundary was maintained at 100 cfs.

30. Pre-Trident channel conditions obtained during the July 1982 examination survey conducted by the US Army Engineer District, Savannah, were molded into the model for the base testing condition. As described in paragraphs 6 and 7, this channel condition consisted of a 400-ft-wide lower entrance channel with depths maintained between 38 and 40 ft, a 300-ft-wide interior approach channel maintained at a depth no shallower than 34 ft (generally between 36 and 39 ft), and the Poseidon Kings Bay operational area maintained at a depth between 37 and 41 ft.

31. The basic Trident plan channel condition addressed in this report included all OICC-requested revisions through January 1985, as described in detail in paragraph 11. At the time the physical model basic plan (P4-1) was tested, the AIWW relocated to alternate Route C (Figure 3) was requested to be modeled at a depth of 16 ft. Subsequent to this test, the testing depth was revised to 12 ft. Subtle localized differences were indicated by comparing results from the P4-1 condition to the revised 12-ft-deep AIWW basic plan test (P4-Z) that was conducted during the upper basin remedial measures testing program. No AIWW-related impacts were identified at any of the stations to be used for deriving the numerical model boundary forcing conditions.

32. The major differences in pre-Trident base and Trident Plan P4-1 conditions were the navigation channel changes. However, during the 1985
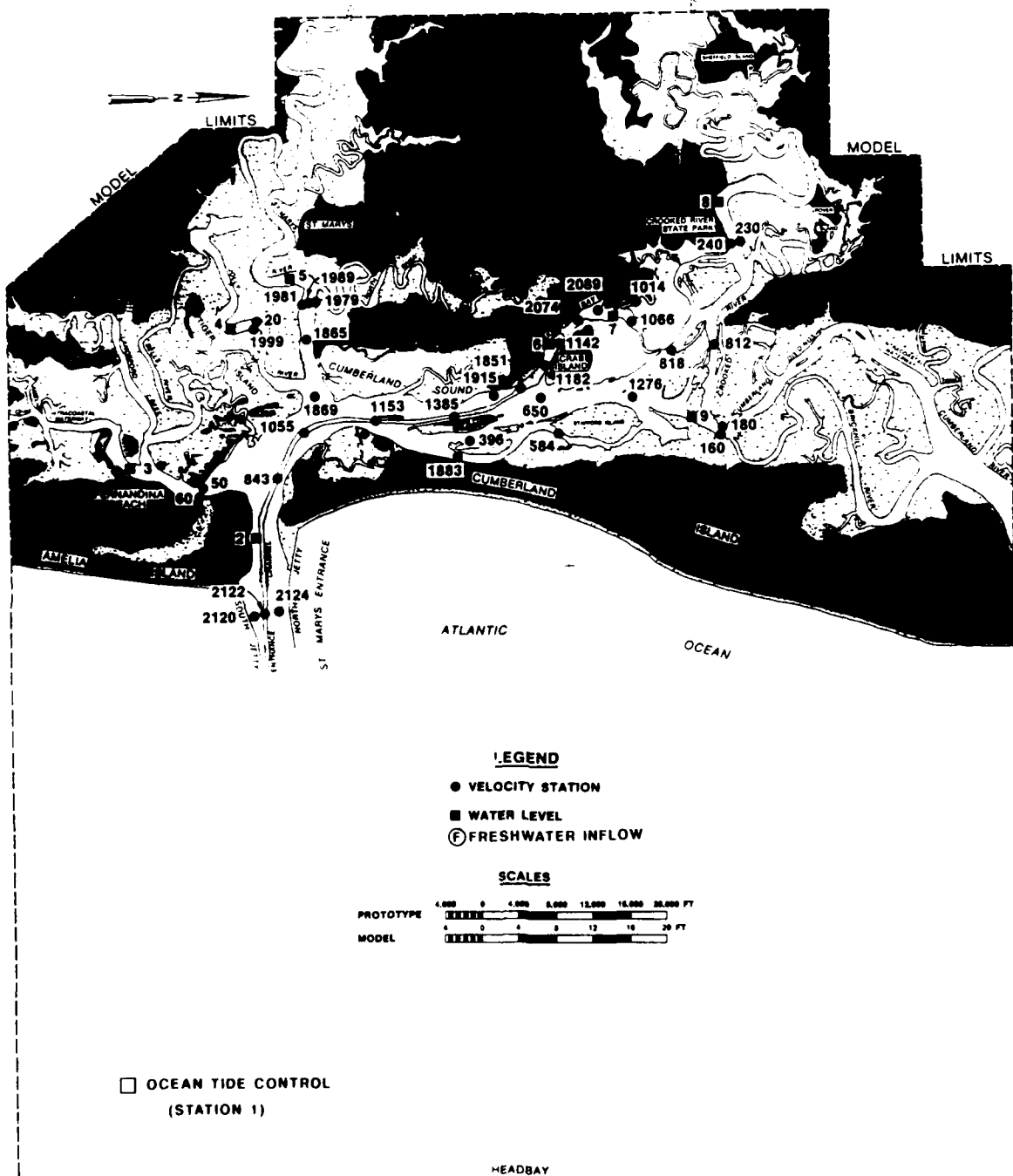
22

Figure 4. Physical model base and plan testing station location map

23

transitional channel verification effort (verification of the areas west and north of Drum Point Island), roughness and bathymetric changes were made in the areas north of Kings Bay. Roughness adjustments were performed in northern Cumberland Sound, Cumberland Dividings, and Cumberland and Crooked Rivers, in addition to bathymetric changes in the channels north of the upper turning basin and in the south and north forks of the Crooked River. Care was taken to leave intact existing roughness within and south of Kings Bay, the area previously verified to the November 1982 pre-Trident channel prototype data.

33. St. Andrew Sound Inlet, located about 17 nautical miles north of the St. Marys Inlet, was about 3 nautical miles beyond the northern limit of the physical model. In the interior, the Cumberland Sound and St. Andrew Sound estuarine systems are connected by a system of small rivers, sloughs, and marsh areas. Propagation of tidal flows through St. Andrew Sound Inlet was reproduced at the northern limit of the model by an artificial labyrinth system opening to the model ocean. During the 1982 pre-Trident channel verification, the labyrinth system was adjusted so that hydrodynamic conditions in the study area were reproduced to an acceptable degree. During the 1985 transitional channel verification, it was necessary to readjust the labyrinth configuration in the artificial opening to maintain acceptable hydrodynamic conditions with the revised geometry and roughness conditions.

34. Funding and time constraints prevented rerunning the pre-Trident channel base condition with these changes incorporated into the model. Therefore, the differences between Trident channel Plan P4-1 results and pre-Trident base conditions presented herein are a combination of channel and Kings Bay improvements along with the effects of these model changes north of Kings Bay (roughness, bathymetry, and labyrinth configuration). The degree of impact of these model modifications compared to impact of Plan P4-1 channel improvements cannot be precisely defined. As described in Appendix B, results from the preliminary plan channel condition tested in 1983, immediately after the pre-Trident base condition and prior to the model adjustments north of Kings Bay, indicated trends of change similar to those of the P4-1 condition although the magnitude was slightly reduced. The preliminary plan channel design tested included less extensive interior channel expansion than the P4-1 condition. The specific channel configuration is described in the

verification report* and the preliminary plan channel results are documented by Brogdon.**

Tidal Elevation Comparisons

35. Water-surface elevations were obtained in the model with point gages and automatic water level detectors. Point gage water level observations were taken every 18 sec on the model (prototype half hourly) for three complete tidal cycle observations at each of the interior tide stations (Figure 4). These data were read to the nearest 0.0005 ft on the model (0.05 ft prototype), averaged, and then rounded to the nearest 0.10 ft (prototype). Plates C1-C3 present hourly time-history water-surface elevations at each station. Figure 5 summarizes high-water, midtide level (average elevation between high and low water), and low-water elevations.

36. Tide height comparisons at stations 1-3 are shown in Plate C1. Station 1, located in the model ocean area, was the tide control, and every effort was made to reproduce water levels at this location as closely as possible for the base and plan conditions. A comparison of the base and plan conditions shows very little elevation difference at the tide control station. At St. Marys Inlet (station 2), Trident Plan P4-1 high water was about 0.3 ft higher than the pre-Trident base condition. The low-water elevation did not change between the base and plan conditions. The plan condition midtide level was elevated about 0.15 ft. Tidal phase with the plan was slightly later (15-30 min) than with the base condition. Data from tide station 3, located in the Amelia River, showed that Plan P4-1 resulted in a slightly higher high water (0.2 ft) and a slightly higher low water (0.1 ft). Very little difference was observed in tidal phase at this station. The plan condition midtide level was about 0.15 ft higher than the base condition at station 3.

37. Tide height comparisons at stations 4-6 are shown in Plate C2. Tide station 4 data, from the Jolly River, showed that Plan P4-1 resulted in an increased high-water level of about 0.3 ft ⌐' an increased low-water level

---

* Granat et al., op. cit.
** N. J. Brogdon. 1989 (21 Feb). "Kings Bay Physical Model Tests of Preliminary Facility Plan," Memorandum for Record, US Army Engineer Waterways Experiment Station, Vicksburg, MS.
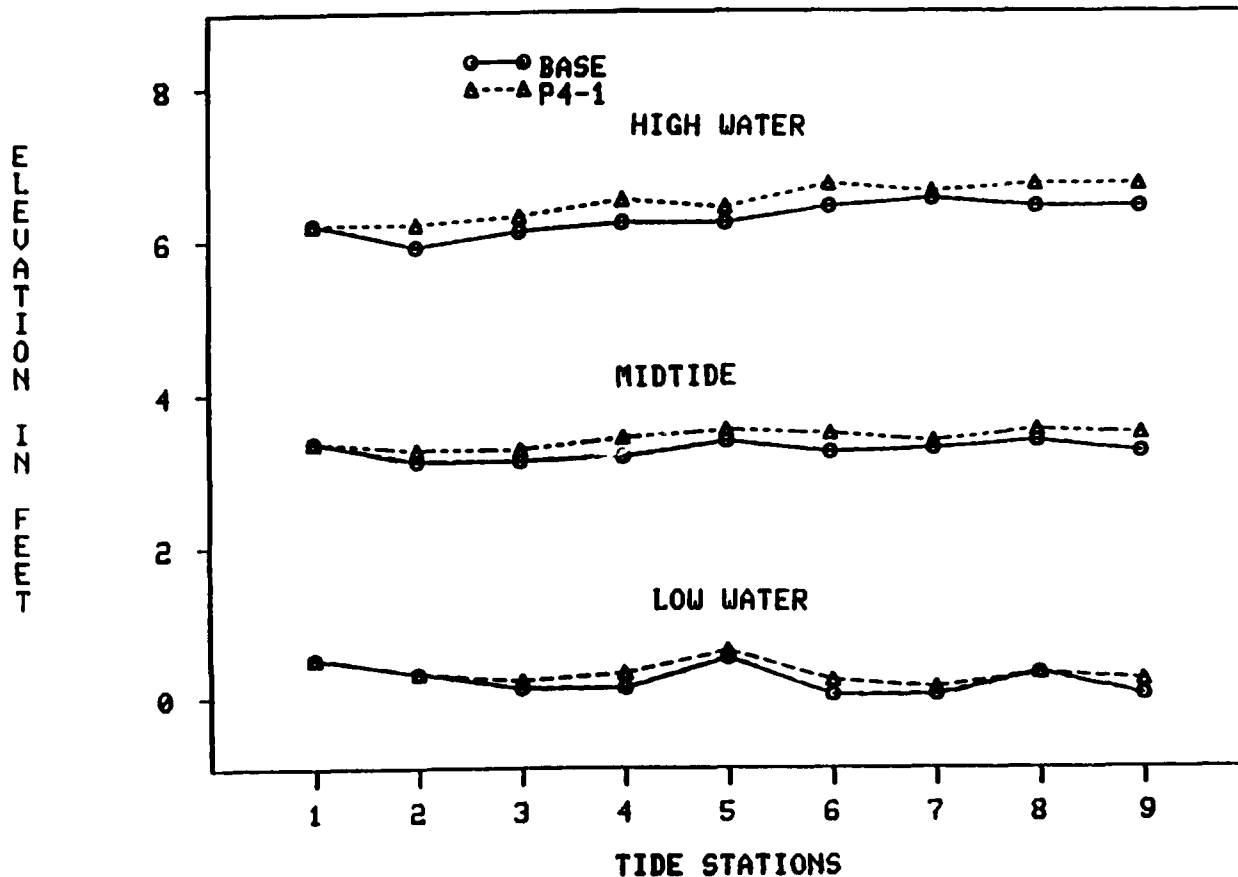
Figure 5. Physical model base and plan water level summary

of about 0.20 ft. Midtide level was increased by about 0.25 ft. The plan had very little effect on water level phase during the flood portion of the tidal cycle; however, plan condition water level phase during the ebb portion of the tidal cycle was about 15-30 min later than the base condition. The St. Marys River tide data (station 5) indicated that plan condition high- and low-water elevations were increased 0.20 ft and 0.10 ft, respectively. Midtide level was increased about 0.15 ft for the plan condition. Very little water level phase difference was observed during the flooding portion of the tidal cycle, but plan condition phase was between 15 and 30 min later during the ebb portion of the tidal cycle. Tide station 6 data collected in lower Kings Bay indicated that high- and low-water elevations during the plan condition were increased about 0.30 ft and 0.20 ft, respectively. Midtide level was increased about 0.25 ft for the plan condition. Base and plan tidal phase relationships in lower Kings Bay (station 6) were similar to those at stations 4 and 5; i.e., plan condition water level phase during the ebb portion of the

26

tidal cycle was about 15-30 min later than in the base condition.

38. Tidal height comparisons at stations 7-9, located north of Kings Bay, are shown in Plate C3. It should be noted that geometry and roughness distributions in this general area were modified (during the transitional channel verification) between the base and plan testing conditions and may be responsible for the reduced differences between the two conditions. Tide station 7, located north of the Trident upper turning basin, demonstrated that plan condition high- and low-water elevations were about 0.10 ft higher than those observed during the base condition. Midtide level was increased about 0.10 ft. Tidal phase at this station with Plan P4-1 installed was slightly later (15 min) than base. Tide station 8, located in Crooked River upstream from Crooked River State Park, demonstrated that plan condition high-water elevation was increased 0.30 ft while low-water elevation was unchanged. Midtide level was increased about 0.15 ft. Little change was observed in water level phase during the flood portion of the tidal cycle, but plan condition phase during the ebb portion of the tidal cycle was delayed by about 30 min. Tide station 9, located in the northern Cumberland Sound, demonstrated that plan condition high- and low-water elevations were 0.30 ft and 0.20 ft higher than the base condition, respectively. Midtide level was increased by about 0.25 ft for the plan condition. Tidal phase during the flooding portion of the tidal cycle was unchanged, but plan condition phase during the ebb portion of the tidal cycle was delayed by about 30 min.

39. Following completion of the model study and the analyses described in paragraphs 35-38, concerns expressed by persons interested in the submarine base and Cumberland Sound led to a thorough reevaluation of the test results and an analysis of recent prototype data. The results of those analyses are provided in Appendix B. It was concluded that Plan P4-1 tide results must be used with greater than usual caution, that tide range probably will not change appreciably, and that mean tide level may increase by a small amount as a result of the Trident project.

Current Velocity Comparisons

40. Current velocity data for base and plan tests were analyzed to determine flow predominance. This analysis approach reduces magnitude, direction, and duration of the currents to a single number that defines the

predominant direction and percentage of total flow at any given point.

41. To obtain flow predominance values, the areas subtended by both ebb and flood portions of the velocity versus time curve were integrated. The area subtended by the flood portion of the curve was then divided by the sum of flood and ebb areas to determine the fraction of the total in the flood direction. The fraction was converted to a percentage and 50 percent was subtracted to obtain the flow predominance value. A predominance of zero indicates that flows in the ebb and flood direction are balanced; the ebb area and flood area of the curve are equal. A value of +50 indicates that flow at that point is in the flood direction at all times during a tidal cycle, while a -50 percent value indicates flow in the ebb direction throughout a tidal cycle. Flow predominance calculations at locations where current velocities are less than 0.5 fps should be used with caution. Measurements of this low magnitude are close to the limits of the current meter and model repeatability; therefore, lack of accuracy may contaminate the integration. Flow predominance values provide an assessment of flow dominance at each depth for the specific condition tested. Comparisons of flow predominance values between two different conditions, especially at stations with depth modifications, do not provide a means of assessing discharge differences.

42. Stations 2120, 2122, and 2124 were located in the St. Marys Inlet. Hourly current velocity data are shown in Plates C4-C6, respectively. Flow predominance values are presented in Table 1. Maximum plan ebb current changes at station 2120, south of the navigation channel, varied from an increase of 0.3 fps at the surface to a decrease of 0.7 fps at the bottom. Maximum flood current velocities were increased slightly, 0.2, 0.2, and 0.6 fps at the surface, middepth, and bottom, respectively. Station 2122, located within the navigation channel, demonstrated the greatest effects of the plan channel deepening. Middepth maximum ebb current was increased 2.3 fps. Maximum ebb currents at the surface and bottom at station 2122 were increased by 1.7 fps and 2.0 fps, respectively. Maximum flood velocities at station 2122 observed during the plan test varied from an increase of 0.1 fps at the surface to a decrease of 0.4 fps at middepth. The greatest impact of the plan at station 2124, located north of the navigation channel, was observed at the surface where the maximum ebb current velocity was increased 1.6 fps. Maximum ebb currents at middepth and bottom were increased 0.2 fps and 0.4 fps, respectively. Maximum flood current velocities at station 2124

were generally 0.6 fps to 0.9 fps lower than base with the plan installed.

43. Stations 50 and 60 were located in Amelia River. Hourly current velocity data are shown in Plates C7 and C8, respectively. The greatest changes occurred at station 50 at surface and middepth. Maximum flood current velocities at these depths were reduced by the plan by 1.2 fps at surface and 0.3 fps at middepth. Maximum ebb current velocities were increased by 1.1 fps and 0.5 fps at surface and middepth, respectively. Changes at other depths at these two stations were generally less than 0.25 to 0.50 fps. There was very little difference between base and plan maximum currents at station 60.

44. Stations 20 and 1999 were located in the Jolly River. Current velocity data at these two stations are shown in Plates C9 and C10, respectively. The greatest change was at station 20 for the surface ebb flow, where the maximum current velocity was increased 0.8 fps. Maximum flood velocity was decreased slightly, less than 0.5 fps. The greatest effect at station 1999 occurred during flood flow, where maximum currents at the surface and middepth were increased 1.1 fps and 1.0 fps, respectively. There was very little change to the maximum ebb currents.

45. Hourly current velocity data at stations 1981, 1989, and 1979 are shown in Plates C11-C13, respectively. These stations are located in the St. Marys River. The surface maximum ebb currents at station 1979 were increased 0.4 fps by the plan. There were no changes to maximum flood currents. Maximum flood currents at station 1981 were increased slightly (less than 0.5 fps), while maximum ebb currents were decreased by 1.2 fps and 1.0 fps at middepth and bottom, respectively. The maximum ebb current velocity at the surface was increased by 0.3 fps. Maximum flood velocity at station 1989 changed very little, but changes to maximum ebb currents with Plan P4-1 installed were variable. Maximum ebb currents at the surface and middepth at station 1989 were decreased 0.9 fps and 0.5 fps, respectively, by the plan, while maximum ebb currents at the bottom were increased 0.7 fps.

46. Stations 1865 and 1869 are located in lower St. Marys River. Hourly current velocity observations at these stations are shown in Plates C14 and C15, respectively. Both maximum ebb and flood current velocities at each station were generally decreased from 0.1 fps to 1.0 fps by the plan. The exception was observed at the surface at station 1869, where the maximum flood current velocity was increased 0.2 fps.

47. Stations 843, 1055, and 1153 were located along the navigation

29

channel in lower Cumberland Sound. Hourly current velocity observations at these three stations are shown in Plates C16-C18, respectively. Both maximum ebb and flood current velocities at these stations were decreased slightly with the plan installed, generally less than 1.0 fps. Exceptions were noted at the bottom at station 1055 and at the surface at station 1153, where the maximum current velocities, both ebb and flood, were increased by the plan on the order of 0.2 to 0.9 fps.

48. Stations 1883 and 396 were located east of Drum Point Island, and station 1385 was located in the navigation channel west of Drum Point Island. Hourly current velocity observations at these stations are shown in Plates C19-C21. Maximum flood currents at station 1883 were decreased 0.50 fps and 0.8 fps, surface and bottom, respectively, with Plan P4-1 installed. Maximum ebb currents were likewise decreased 1.0 fps and 0.7 fps at the surface and bottom, respectively. Maximum flood current velocities at station 396 were influenced very little by the plan, less than 0.2 fps. Maximum ebb current velocities at station 396 were decreased 0.5 fps and 0.1 fps at the surface and bottom, respectively. Maximum flood currents at station 1385 were increased about 0.3 fps and 0.1 fps at the surface and middepth, respectively, while the maximum current velocity at the bottom depth was decreased 0.1 fps. Maximum ebb current velocities at station 1385 were decreased between 0.1 to 0.7 fps.

49. Hourly current observations for stations 650 and 584 are shown in Plates C22 and C23, respectively. These stations were located east of Kings Bay. Maximum ebb and flood current velocities were influenced very little by the plan. Changes were generally less than 0.5 fps.

50. Stations 1915 and 1851 are located immediately downstream of the Kings Bay entrance. Station 1915 is located in the magnetic silencing facility area west of the main navigation channel, and station 1851 is located in the navigation channel east of the Poseidon floating dry dock. Hourly current velocity observations are shown in Plates C24 and C25, respectively. The plan resulted in small changes in both maximum ebb and flood velocities, generally less than 0.6 fps. At station 1915, the maximum bottom ebb current velocity was reduced about 1.2 fps.

51. Hourly current velocity observations at stations 1182, 1142, 2074, and 2089, located within Kings Bay, are shown in Plates C26-C29, respectively. Maximum flood currents at station 1182 were increased slightly by the plan.

30

The changes varied from 0.0 fps to a maximum change of 0.4 fps at middepth. Maximum ebb currents were reduced at middepth and bottom by 0.7 fps and 0.8 fps, respectively, and increased by 0.3 fps at the surface. The greatest impact on maximum current velocities by the plan in the Kings Bay area was observed at stations 1142 and 2074. The plan effected a reduction in both maximum ebb and flood currents at these two locations. The reductions ranged from a minimum of 0.3 fps at station 1142 (middepth and bottom) to a maximum of 1.6 fps at station 2074 (bottom). Reductions in maximum current velocities at station 1142 averaged about 0.5 fps for flood currents and about 0.9 fps for ebb currents. Reductions in maximum current velocities at station 2074 averaged about 1.0 fps for flood velocities and about 1.5 fps for ebb velocities. Changes to maximum current velocities at station 2089 varied from no change to an increase of 0.6 fps at the surface depth.

52. The location of station 2089 had an influence on the changes observed at this station. Station 2089 was located in 26 ft of water for the base test, but when the plan was installed, the water depth was increased to 48 ft. This station was also located very near the upstream limits of the upper turning basin and Trident dry dock and was in an eddy zone of slow and erratic currents. Its location was not in the primary path of currents moving through Kings Bay. The reported data are correct and reflect the eddy circulation adjacent to the Trident dry dock.

53. Stations 1014 and 1066 are located in small channels north of Kings Bay feeding into Crooked River. Hourly current observations for these stations are shown in Plates C30 and C31, respectively. Both maximum ebb and flood current velocities were increased by the plan at station 1014 (Marianna Creek) by 0.4 fps and 0.1 fps, respectively. Both maximum ebb and flood current velocities were decreased at station 1066 (Back Creek adjacent to Crab Island) by 1.2 fps and 0.6 fps, respectively. Bathymetric conditions (widening and deepening) in each of these small channels were changed during the 1985 transitional channel verification process. The total changes observed at these two locations reflect both bathymetric and plan effects.

54. Stations 230 and 240 were located in the Crooked River in the vicinity of Crooked River State Park. Hourly current velocity observations are presented in Plates C32 and C33, respectively. Both maximum ebb and flood current velocities were decreased slightly at each station with the plan installed, with the exception at station 240, where an increase in the maximum

31

bottom ebb current velocity of 0.1 fps was observed. The decreases were generally less than 0.5 fps, with the greatest decrease of 0.9 fps being observed at the surface at station 230 during ebb flow.

55. Stations 818 and 812 are located in the south and north branches of the Crooked River, respectively. Hourly current observations are shown in Plates C34 and C35, respectively. Bathymetric conditions in these channels (widening and deepening) were altered during the course of the transitional channel verification; therefore, the total effects at these stations reflect both plan effects and bathymetric change effects. Decreases in both maximum ebb and flood currents at station 818 were observed with the plan installed. The changes ranged from 0.1 fps at the bottom during flood flow to 0.8 fps at middepth during flood flow. Maximum ebb currents at each depth were decreased 0.7 fps. Maximum flood current velocity at station 812 was decreased 1.8 fps, and the maximum ebb current velocity was increased 0.2 fps.

56. Station 1276 was located immediately northwest of Stafford Island in relatively shallow water. This was the region of the nodal point between the Cumberland Sound and St. Andrew Sound circulation systems. Hourly current velocity data for this station are shown in Plate C36. These data show that Plan P4-1 resulted in increasing both maximum ebb and flood currents. The greatest increase (about 1.1 fps) occurred during the ebb portion of the tidal cycle at the surface. The smallest change (0.2 fps) occurred at the surface during flood conditions.

57. Stations 160 and 180 are located at the confluence of Cumberland Sound and Crooked, Cumberland, and Brickhill Rivers (Cumberland Dividings). Hourly current velocity observations are shown in Plates C37 and C38, respectively. These data show that Plan P4-1 resulted in reducing both the maximum ebb and flood current velocities. A reduction in maximum ebb current velocity of 1.6 fps was observed at the surface depth at station 160. Other reductions at station 160 were about 0.8 fps. Maximum flood and ebb current velocities at station 180 were reduced 1.2 fps and 0.4 fps, respectively.

Navigation Channel Center-Line Flow Predominance

58. From the data shown in Table 1, flow predominance profiles were constructed for the surface, middepth, and bottom at stations located along the center line of the navigation channel. These profiles are presented in

F'gures 6-8. Data shown in Figure 6 (surface) show that Plan P4-1 resulted in a slight shift toward stronger ebb flow. This change became more pronounced when approaching Kings Bay. Data shown in Figures 7 and 8 (middepth and bottom, respectively) reflect generally the opposite effect of that observed at the surface, as the majority of change was toward stronger flood predominance. Station 2122, located in the estuary entrance, showed a consistent change toward stronger ebb predominance at all depths. In general, data at the other stations indicated that the overall effect of Plan P4-1 was toward stronger flood predominance.
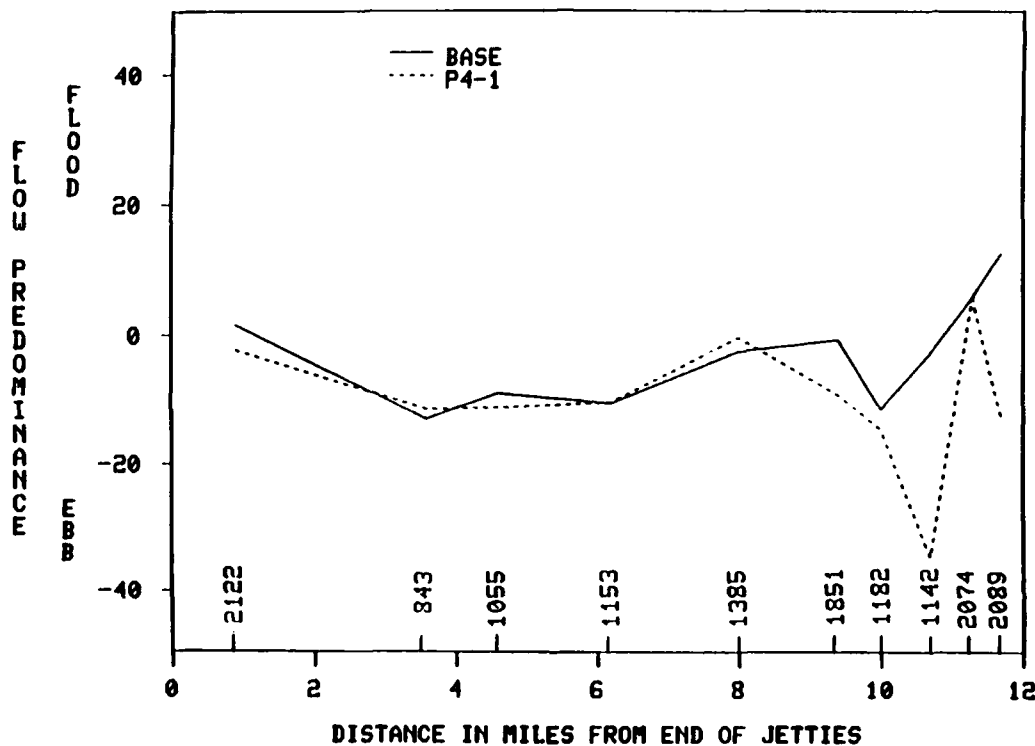
Figure 6. Physical model base and plan navigation channel surface flow predominance

Summary

Tidal elevations

59. Plan P4-1 resulted in an average increase of tide range in the estuary of about 0.15 ft. Midtide levels were raised on the average about 0.20 ft throughout the estuary. Both high- and low-water elevations were generally raised as a result of the plan; however, effects on high-water
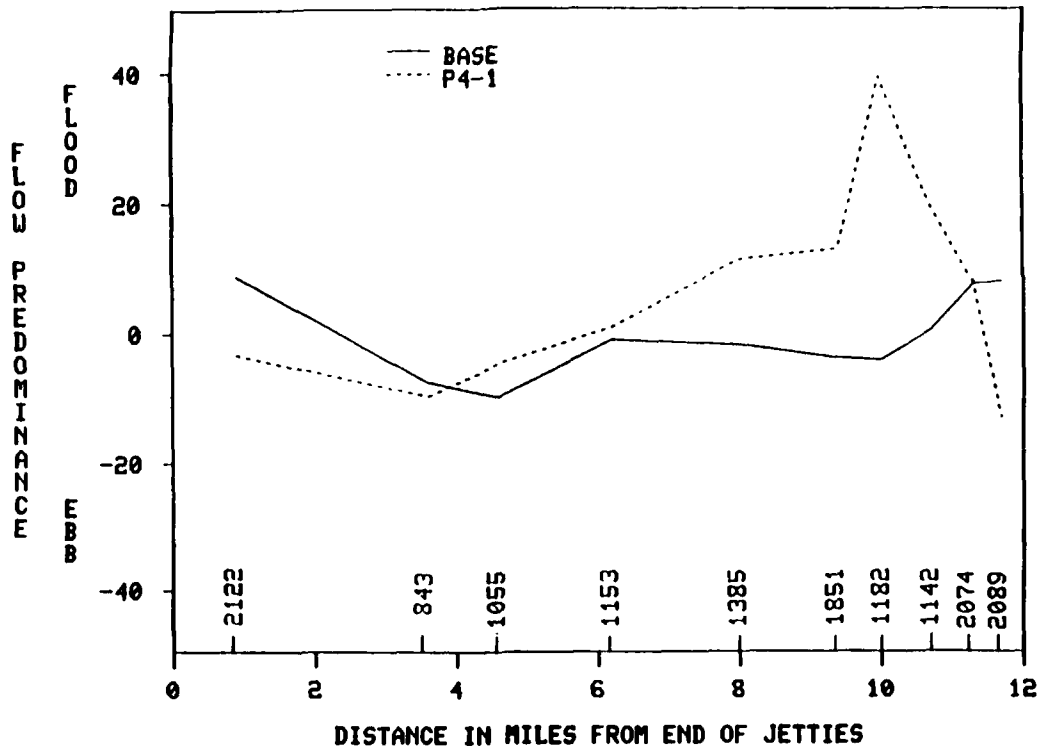
Figure 7. Physical model base and plan navigation channel
middepth flow predominance
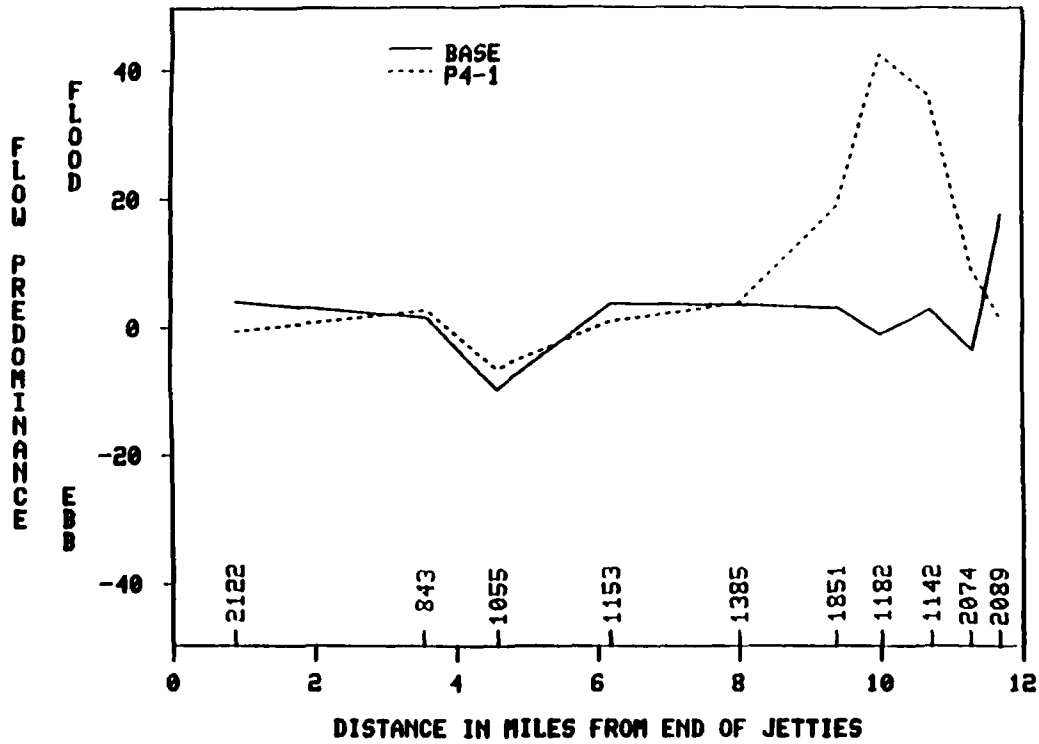
Figure 8. Physical model base and plan navigation channel
bottom flow predominance

elevations were about twice that observed for low-water elevations.

Current velocities

60.   The flow predominance data at stations in the immediate Kings Bay area show that Plan P4-1 resulted in changing an existing weak ebb-dominated condition to a flood dominated condition.   Flow predominance at several stations located in lower Crooked River and Cumberland Dividings showed a slight increase in the ebb direction.   Although maximum current velocities through Kings Bay and in the Crooked River (north and south branches) were reduced, the plan resulted in routing more flood flow through Kings Bay.

PART IV: NUMERICAL MODEL MESH 4 HYDRODYNAMIC RESULTS AND ANALYSES

Testing Conditions

61. The OICC-requested pre-Trident submarine base channel conditions
are described in paragraphs 6 and 7. Channel geometry conditions obtained
from the Savannah District November 1982 examination survey were used in sche-
matizing the pre-Trident base channel. Geometry conditions from the August
1985 examination survey for the areas east of and including Drum Point Island
were used in the schematization of this area for the base condition. The
numerical model basic Trident pla ι channel condition tested and discussed in
this report included the channel revisions requested by OICC through August
1985, as described in paragraph 11. At the time of the numerical model test-
ing, relocation of the AIWW to the east side of Drum Point was anticipated.
WES was requested to conduct the numerical model plan tests with the AIWW
relocated to the preferred alternate Route C at a depth of 12 ft. Plans for a
lower Kings Bay turning basin and St. Marys Inlet entrance channel turning and
sediment basins had not been finalized and were not included in the plan
modeling efforts.

62. Figure 9 illustrates the basic numerical model Mesh 4 base (pre-
Trident) and plan (Trident) channel schematizations tested. This mesh was
developed for the upper basin remedial measures testing program, which was
conducted following the transitional channel verification. The mesh included
resolution for examining a tide gate barrier above the planned upper turning
basin, a sediment trap below the tide gate area but above the turning basin,
and additional channelization from the upper end of Kings Bay into the south
fork of the Crooked River through either Marianna Creek or the back channel
around Big Crab Island.

63. A small mesh revision was required between the base and plan chan-
nel schematization for the Poseidon waterfront docking area to allow proper
reproduction of the wetting and drying process. This revision, illustrated in
the insets of Figure 9a, increased the number of nodes and elements by one for
the base condition (i.e., from 1,117 elements and 3,223 nodes for the plan
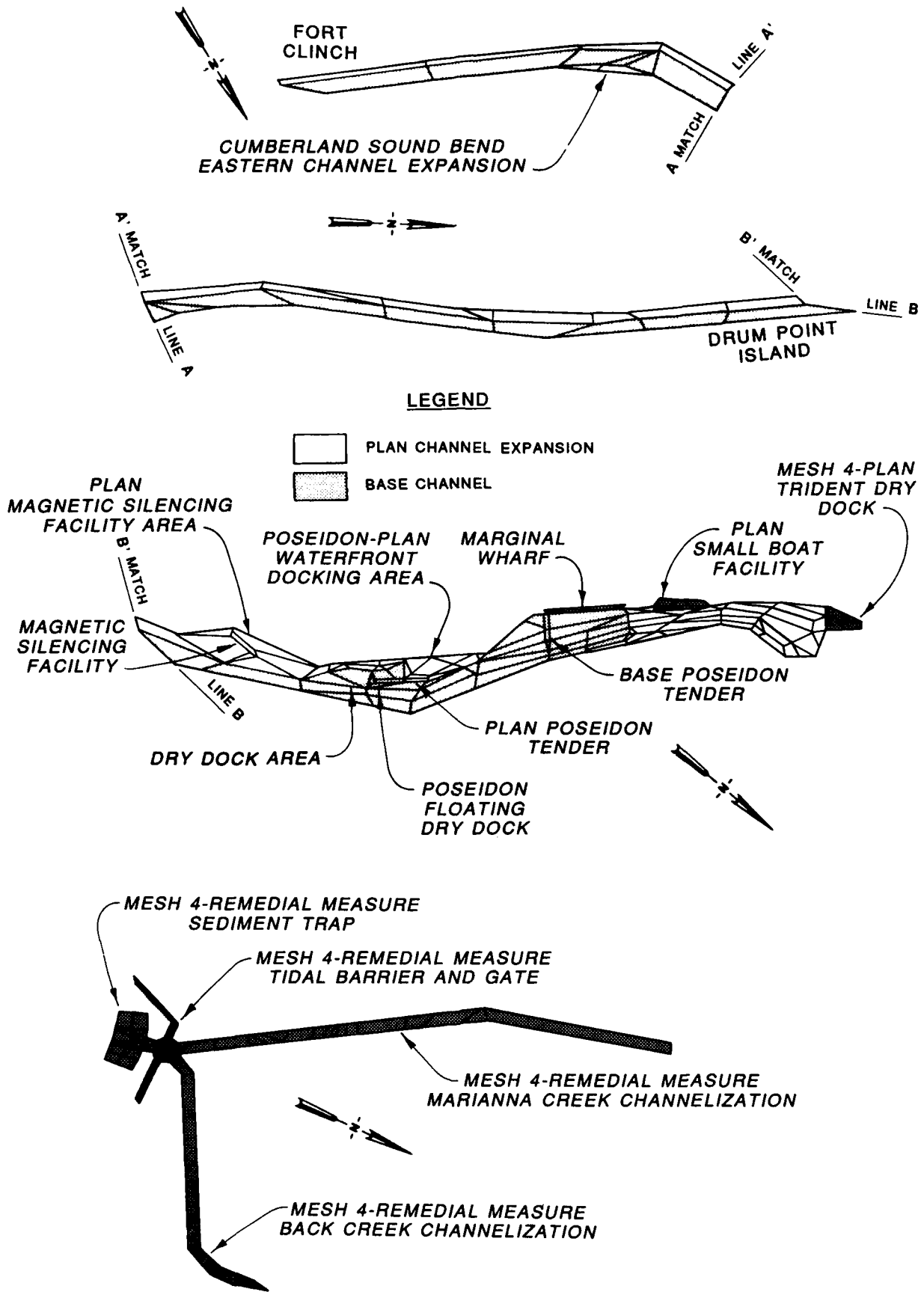condition to 1,118 elements and 3,224 nodes for the base)

64. For base and plan testing purposes, the numerical hydrodynamic
model RMA-2V was run from hour 5.0 to hour 22.0; hours 9.5 to 22.0 were used

LEGEND

☐ FLOODING AND DRYING AREAS

■ PROPOSED RELOCATED AIWW ALTERNATE ROUTE C

▨ PRE-TRIDENT CHANNEL

▨ TRIDENT EXPANSION
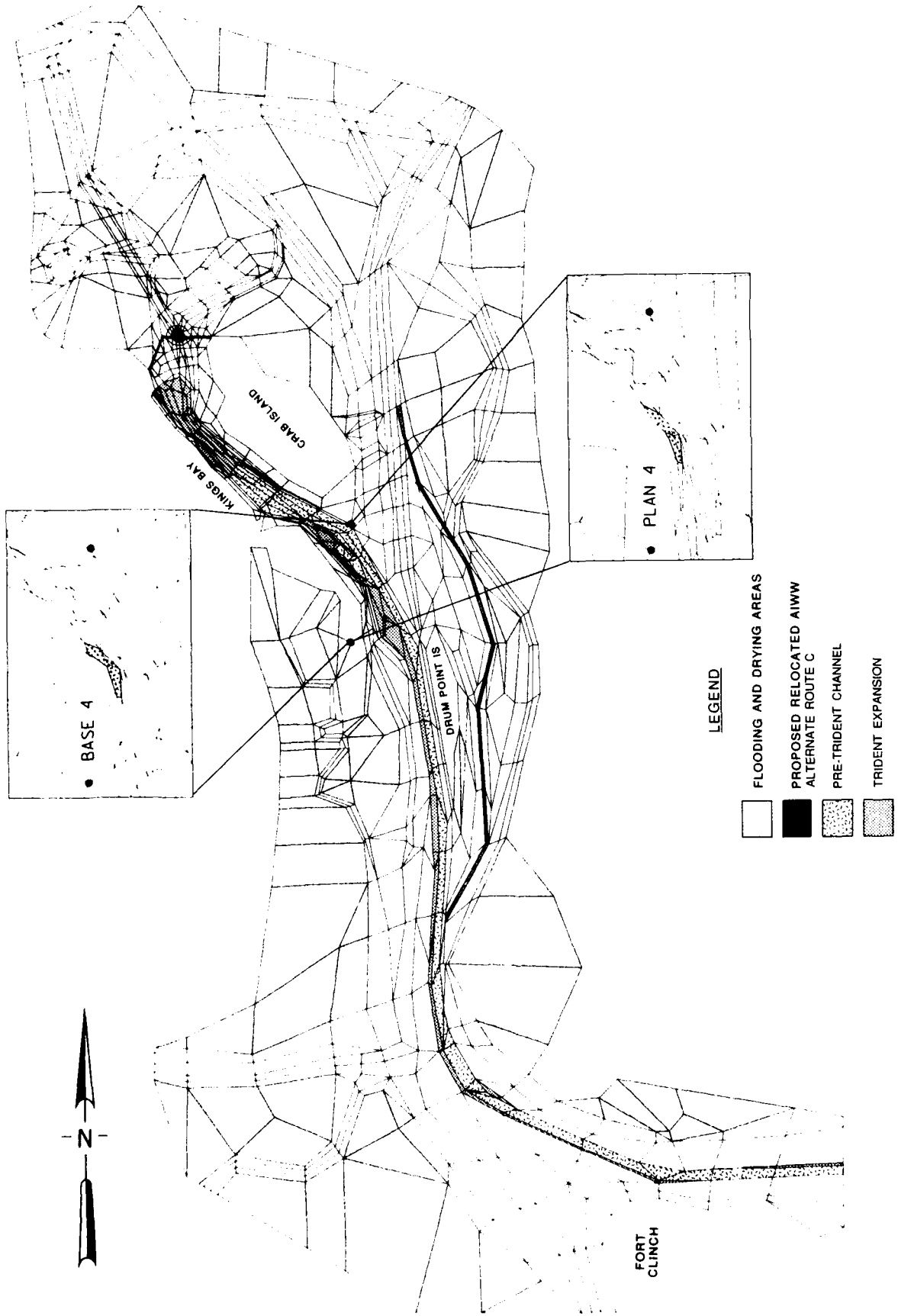
a.   Computational mesh with insets of base and plan differences

Figure 9.   Numerical model Mesh 4 (Continued)

FORT
CLINCH

LINE A'

A MATCH

CUMBERLAND SOUND BEND
EASTERN CHANNEL EXPANSION

A' MATCH

B' MATCH

LINE A

LINE B

DRUM POINT
ISLAND

LEGEND

PLAN CHANNEL EXPANSION

BASE CHANNEL

PLAN
MAGNETIC SILENCING
FACILITY AREA

POSEIDON-PLAN
WATERFRONT
DOCKING AREA

MARGINAL
WHARF

MESH 4-PLAN
TRIDENT DRY
DOCK

PLAN
SMALL BOAT
FACILITY

B' MATCH

MAGNETIC
SILENCING
FACILITY

LINE B

BASE POSEIDON
TENDER

DRY DOCK AREA

PLAN POSEIDON
TENDER

POSEIDON
FLOATING
DRY DOCK

MESH 4-REMEDIAL MEASURE
SEDIMENT TRAP

MESH 4-REMEDIAL MEASURE
TIDAL BARRIER AND GATE

MESH 4-REMEDIAL MEASURE
MARIANNA CREEK CHANNELIZATION

MESH 4-REMEDIAL MEASURE
BACK CREEK CHANNELIZATION

b. Detail of Mesh 4, base and plan navigation channel and
potential remedial measures

Figure 9. (Concluded)

for analysis and comparison. Physical-model-derived boundary forcing conditions (water levels for the ocean and velocities for the tributary boundaries) from the pre-Trident condition were used for the numerical model base boundary forcing conditions. The numerical model pre-Trident Mesh 4 base data set was used for comparison to the plan channel data set. Plan boundary forcing conditions were derived from the physical model upper basin remedial measures basic plan testing condition (P4-1). The same basic physical and numerical modeling procedures and conditions developed during the numerical model verification were used for the base and plan tests. Table 2 summarizes the roughness and turbulent exchange coefficients assigned to each element type. These coefficients were assigned to each element based upon the physical characteristic each element was representing in each condition. Depth, roughness, and turbulent exchange coefficients were accordingly adjusted between the base and plan condition (i.e., some base marsh/channel transition areas were changed to smooth channel areas for the plan condition). Figure 10 illustrates the base and plan test sampling locations.

Tidal Elevation Comparisons

65. Plate D1 presents the time-history water-surface elevations generated at the physical model ocean tide control (station 1, Figure 4) during the base and plan physical model data collection efforts. Small variations, within the 0.1-ft accuracy of the physical model data, included a slightly reduced plan elevation at hours 17.0 and 17.5 and a slightly increased (less than 0.1 ft) high-water elevation (hour 20.0) during the plan. Data from station 2 in the physical model were the ocean boundary forcing conditions used in the numerical model base and plan tests. The conditions at node 2170 (Figure 10) in the numerical model were derived from these data. Plate D2 shows the numerical model base and plan water-surface elevations generated at node 2170. A base-to-plan phase shift with a time of arrival approximately 20 min later for the plan condition was indicated for the boundary forcing condition. Base and plan channel low-water elevations were in close agreement at node 2170. The plan condition high-water elevation was about 0.3 ft greater than the base condition. It is stressed that these data were derived directly from physical model base and plan channel tests and the half-hour values represented the average of three replicate tidal cycle observations.

39
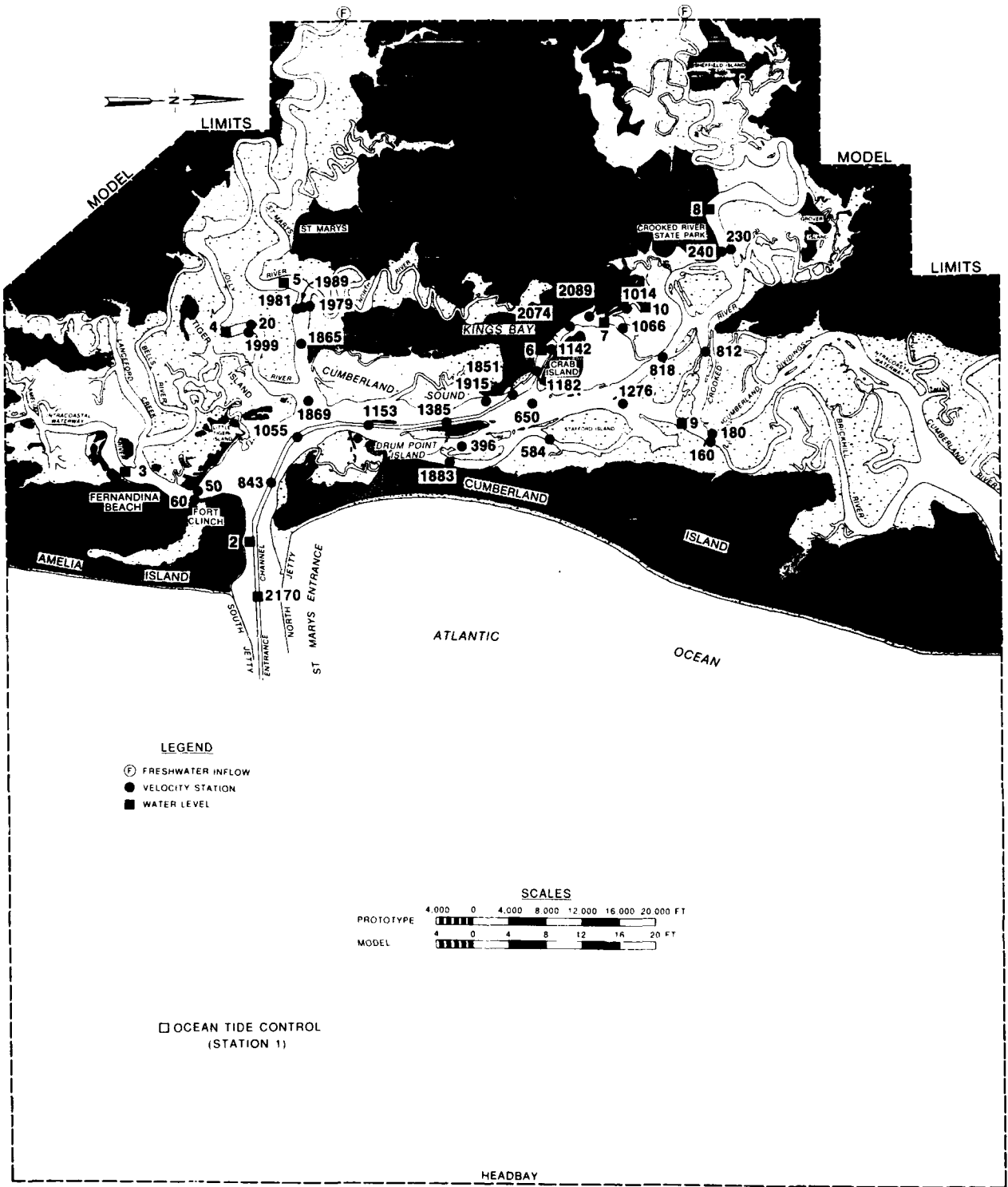
Figure 10. Numerical model verification, base, and plan testing
station location map

66. Plates D3-D10 illustrate the base and plan time-history water-surface elevations for the numerical model interior stations examined. A phase shift, similar to the boundary forcing condition, with a time of arrival approximately 20 min later for the plan condition was indicated at the tide stations south of Kings Bay (Plates D3-D6). This phase shift was reduced at station 1150 in Kings Bay (Plate D7). The phase shift was reduced more at stations 2227 and 240 north of Kings Bay (Plates D8 and D9).

67. Tidal elevation differences between base and plan conditions were generally increased at the interior stations relative to the boundary forcing condition (node 2170). Plan condition high-water elevations were about 0.4 ft greater than base condition elevations. Base and plan low-water elevations south of Kings Bay were generally unchanged. Plan condition low-water elevations within and north of Kings Bay were about 0.1 ft lower than those of the base condition. The plan condition midtide levels (mean elevation between high and low water) were elevated about 0.2 ft at the stations south of Kings Bay and were elevated about 0.15 ft at and north of Kings Bay. Figure 11 summarizes the high, low, and midtide elevations for the numerical model base and plan conditions for all stations.

68. Comparison of numerical model base and plan elevations (Figure 11) with physical model base and plan elevations (Figure 5) reveals some interesting trends. As summarized in paragraph 19 and explained in detail in the verification report,* numerical model marsh elevation schematization was found to be a sensitive parameter in establishing the desired hydrodynamic reproduction. A compromise between tidal agreement and velocity agreement was made in achieving the desired reproduction (verification) between the numerical model and the physical model measurements. This type of compromise is common physical and numerical modeling practice. As described in paragraph 19, for the verification condition (the base test), agreement of numerical model and physical model tides was sacrificed somewhat to improve velocity reproduction. A consistent marsh elevation of +4.0 was selected as the nominal elevation for the base and plan testing conditions so a similar trend of numerical model and physical model tidal reproduction was expected for the plan condition.

69. The most consistent tidal observations between the numerical and

---

* Granat et al., op. cit.
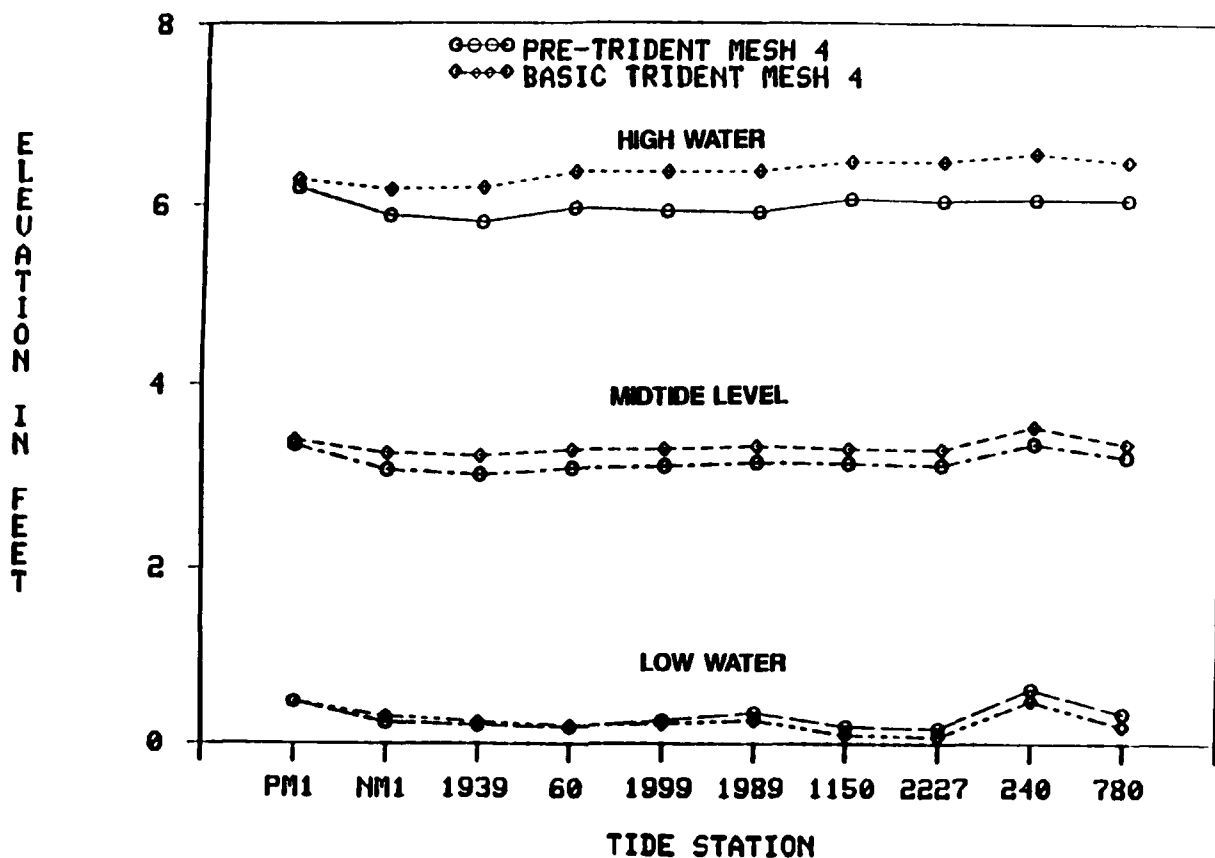
PHYSICAL AND NUMERICAL MODEL TIDE STATIONS

Physical Model	Location	Numerical Model Node
1	Physical model ocean tide control/ numerical model ocean boundary	2170
2	St. Marys Inlet	1939
3	Amelia River	60
4	Jolly River	1999
5	St. Marys City Dock	1989
6	Lower Kings Bay	1150
7	Marianna Creek	2227
8	Crooked River State Park	240
9	Northern Cumberland Sound	780

Figure 11. Numerical model base and plan water level summary

physical models were for the midtide levels. Both models indicated about a 0.15- to 0.2-ft increase in the plan condition midtide levels (Figures 5 and 11). Numerical model and physical model midtide levels generally agreed within 0.1 ft. The St. Marys River was an exception with the physical model midtide level elevated about 0.2 ft above the numerical model midtide level. This difference is attributed to the three-dimensional density (salinity) characteristics of the physical model.

70. The plan condition consistently resulted in higher high-water elevations in both models (Figures 5 and 11). Numerical model base-to-plan high-water elevation differences were generally 0.1 to 0.2 ft greater than physical model base-to-plan differences (i.e., physical model plan condition high-water elevations were generally 0.2 to 0.3 ft higher than base conditions while numerical model plan condition high-water elevations were generally about 0.4 ft greater than base conditions).

71. Low-water elevation differences did not demonstrate a consistent trend between the two models. Physical model plan condition low-water elevations generally demonstrated a 0.1- to 0.2-ft increase in elevation compared to the base condition (Figure 5). Numerical model low-water elevations south of Kings Bay (Figure 11) generally demonstrated a closer base and plan agreement than did the physical model. In contrast to the physical model, the low-water elevations in the numerical model plan condition at and north of Kings Bay were generally 0.1 to 0.15 ft lower than those of the base condition.

72. As mentioned in paragraph 20 and explained in more detail in the verification report,* the physical model geometry adjustments made prior to the 1985 transitional channel verification generally resulted in improved physical and numerical model tide agreements. Figures 12a and b illustrate the numerical model and physical model water level summary comparisons for the original Mesh 1 pre-Trident channel and transitional channel verifications. The transitional channel verification was conducted with a slightly elevated boundary forcing condition, so results between the pre-Trident and transitional channel conditions cannot be directly compared. As illustrated, the greatest improvements were in the areas north of Kings Bay, and were associated with improved low-water elevation agreement.

73. Figures 13a and 13b illustrate physical model to numerical model

---

* Granat et al., op. cit.
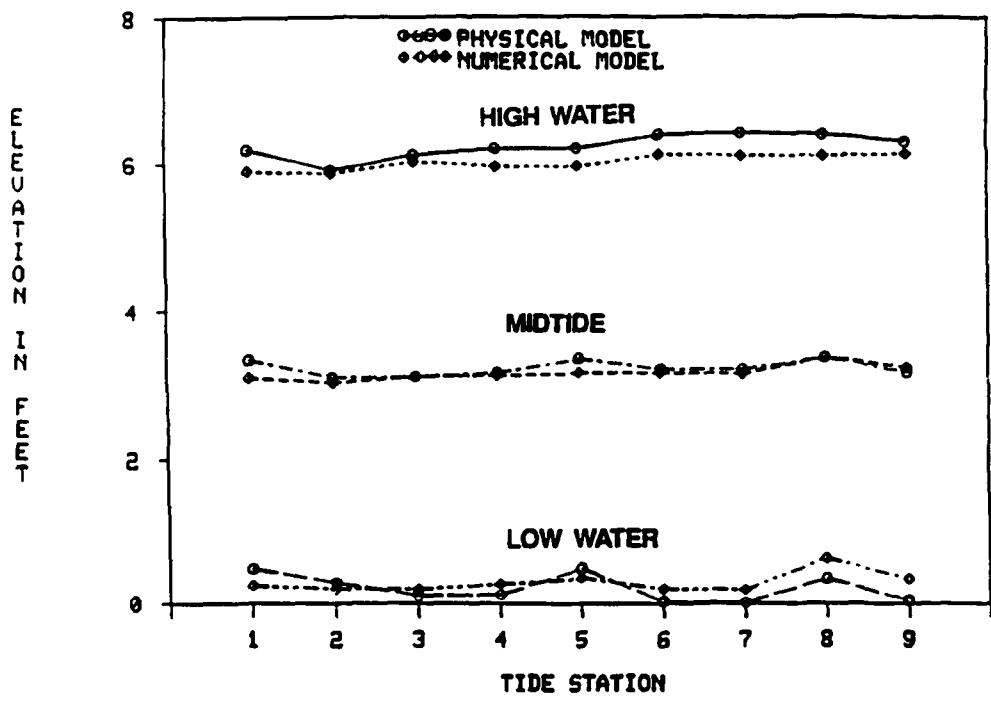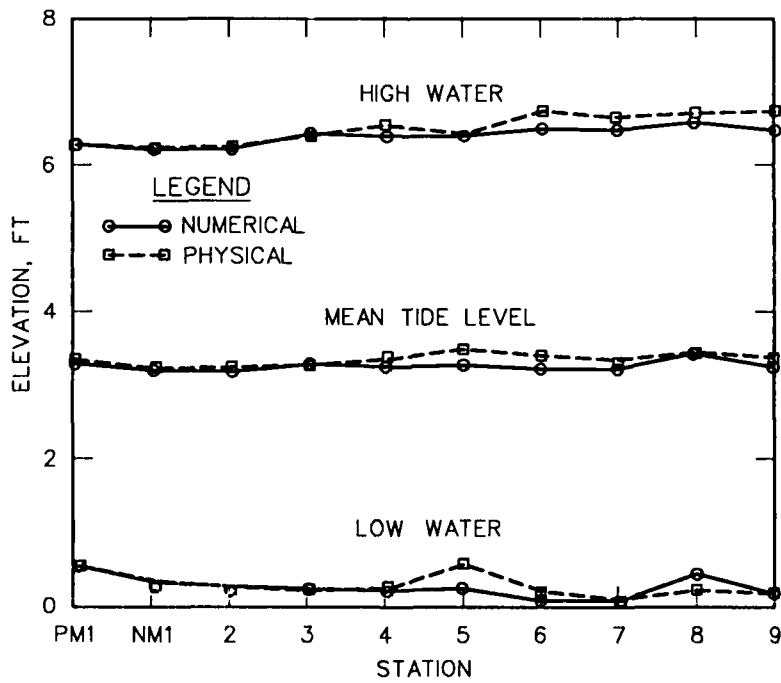
a. Pre-Trident Mesh 1
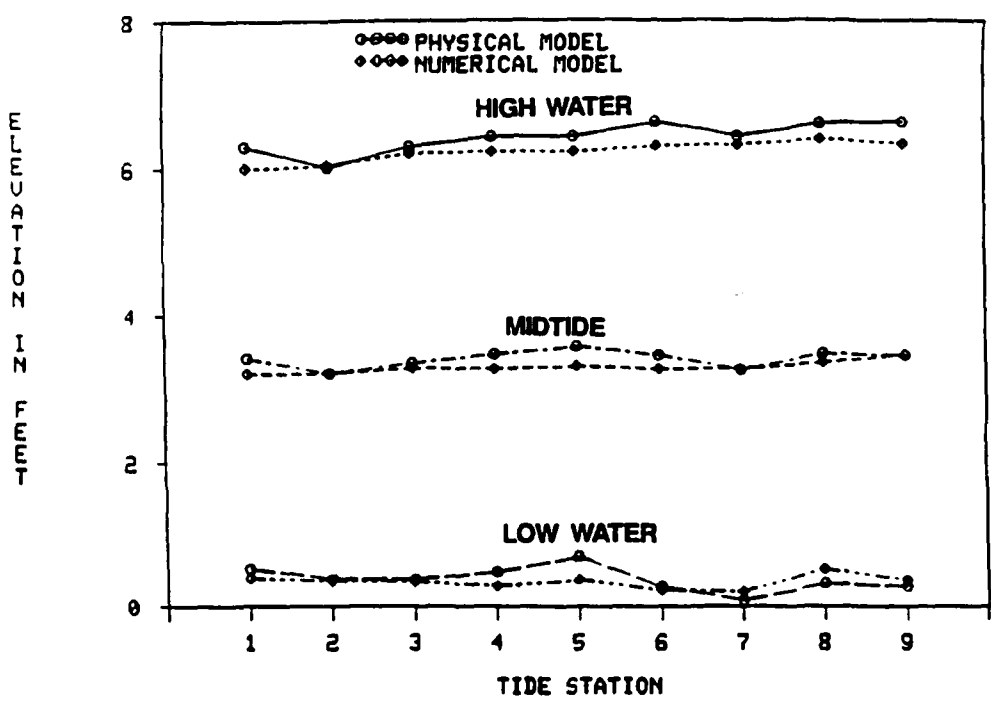
b. Transitional channel

Figure 12. Water level summaries for Mesh 1
pre-Trident and transitional channel
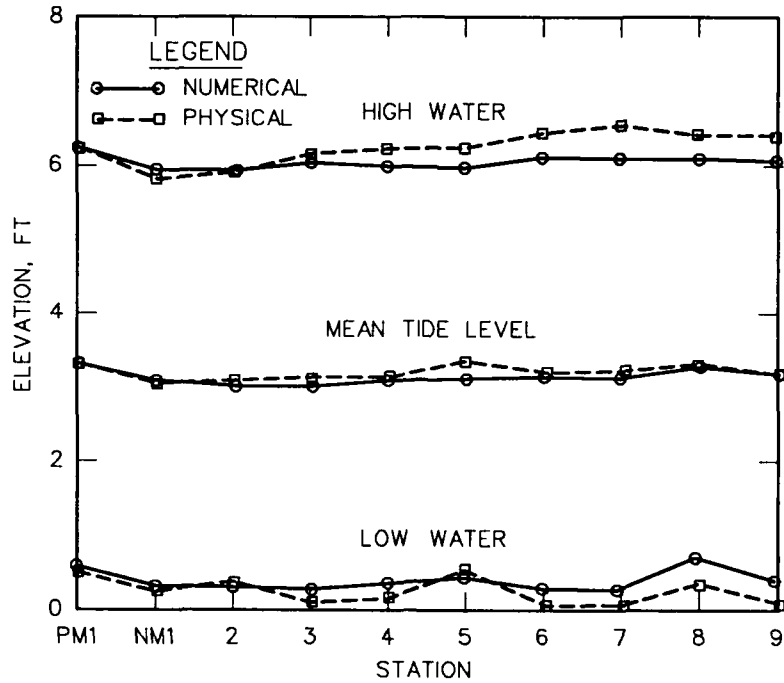
a. Pre-Trident Mesh 4 base

b. Trident plan channel

Figure 13. Water level summaries for Mesh 4
base and plan channels

water level summary comparisons for Mesh 4 base and plan channel conditions, respectively. In general, closer numerical model to physical model tidal agreement was illustrated for the plan condition compared to the base condition. This finding suggested a possible modeling perturbation not directly related to base and plan channel geometry differences (i.e., the deepened and widened channel).

Tidal Sensitivity Findings

74. Two numerical model sensitivity tests were examined in an attempt to investigate potential boundary forcing condition impacts. The first test, PGBF (plan channel geometry and base channel boundary forcing conditions), used the numerical model Trident plan channel geometry conditions and the physical-model-derived pre-Trident channel base boundary forcing conditions. The second test, BGPF (base channel geometry and plan channel forcing conditions), used the numerical model pre-Trident base geometry conditions and the physical-model-derived Trident plan channel boundary forcing conditions. These two sensitivity tests may be used to examine potential hydrodynamic impacts associated solely with geometry differences (i.e., comparing PGBF with the actual base test, BSE4, demonstrates the plan geometry impact) while permitting no channel deepening impact on the boundary conditions. In a physical sense, the sensitivity test results (the crossed geometry and boundary conditions) are nonrepresentative since separating the geometry from its impact on the boundary conditions is not truly possible in the present application (i.e., the boundaries are impacted by the channel expansion). They do, however, offer a qualitative check on the physical model tide results.

75. Figure 14 summarizes the tidal elevation sensitivity findings. High-water, low-water, and midtide elevations for these tests are illustrated along with the actual base and plan modeling results. Data from the sensitivity tests appear to group with the associated boundary condition rather than with the associated geometry condition (i.e., the base test data, BGBF, and the PGBF data group together and the BGPF data are closely associated with the plan test data, PGPF). These findings indicate that the boundary forcing conditions had a much larger influence on the resulting numerical model water level elevations than did the geometry condition by itself. It is also interesting to note that the sensitivity results (the crossed boundary and geometry
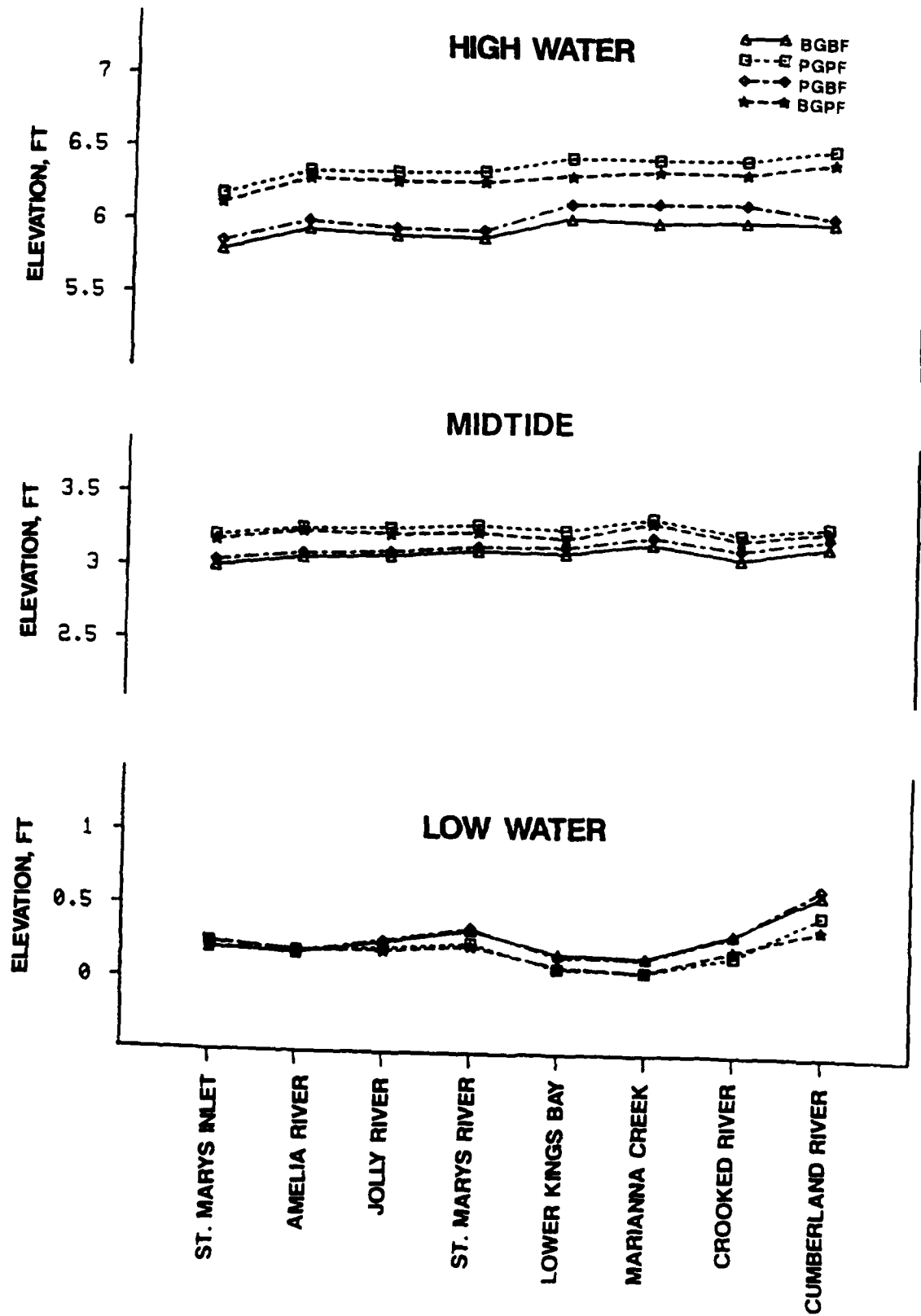
Figure 14. Numerical model water level sensitivity summary

47

conditions) produced intermediate elevations relative to the actual base and plan condition tests.

76. Comparing results from the PGBF test with the actual base testing condition demonstrated that if the base boundary conditions were maintained (i.e., no geometry-induced effects at the boundaries) during the plan condition, the Trident channel expansion would result in an increased high-water elevation of about 0.05 ft at the tide stations south of Drum Point and about a 0.10-ft increase at the stations north of Drum Point Island. Low-water elevations would basically be unaffected. Increases in the midtide levels for the PGBF condition, relative to the base condition, would generally be less than 0.1 ft. Comparing results from the BGPF condition with results from the actual base testing condition indicated a 0.3- to 0.4-ft increase in high-water elevation and about a 0.1-ft decrease in low-water elevation. The midtide levels for the BGPF condition increased between 0.1 and 0.2 ft relative to the actual base condition.

77. Results obtained comparing the BGPF with the actual plan channel condition demonstrated elevations close to but slightly smaller than the actual plan results. The BGPF base geometry sensitivity condition resulted in slightly reduced elevations relative to the actual plan condition. These variations were of a similar magnitude but in the opposite direction of the PGBF to actual base condition variations. Compared to the actual plan condition, the PGBF sensitivity test resulted in reduced high-water elevations between 0.3 to 0.4 ft and increased low-water elevations by about 0.1 ft. Midtide elevations for the PGBF test were between 0.1 and 0.2 ft lower than the actual plan condition.

78. Results from the sensitivity tests with the crossed geometry and boundary forcing conditions demonstrated geometry-related water level variations in the same direction as the actual base and plan variations but at a reduced magnitude. The tidal differences predicted by the actual base and plan numerical model channel tests were greater than the findings of the sensitivity tests and of the physical model comparisons. Based on these results, the actual tidal differences predicted by the numerical model base and plan tests may be somewhat overestimated. This magnitude difference may be explained by the physical and numerical model differences predicted during the base channel condition. A further discussion of these water level differences is warranted.

Water Level Variations

79. The hybrid modeling approach allowed the geographic extent of the numerical model to be reduced. As demonstrated by the sensitivity studies, the closeness of the numerical model boundaries, however, caused the numerical water level solution to be very sensitive to and dependent on the boundary forcing conditions derived from the physical model. The differences in water level elevation between the base and plan tests in the physical model St. Marys Inlet were close to, but greater than, the model detection limits. The raw physical model data (triplicate base and plan observations) and the reduced data were reviewed and found to be correct. The datum agreement between the ocean tide control and the St. Marys Inlet tide station was verified during a February 1989 physical model survey. These analyses provided additional support that the observed physical model differences were real and that the findings were accurately reported.

80. As described in paragraphs 19, 20, and 68, the results from the numerical model were also found to be sensitive to the marsh schematization and the associated wetting and drying process as affected by the prescribed marsh elevations. As indicated by comparisons of the base and plan numerical model elevations, the reported marsh-estuarine circulation interaction appeared to be modified by the plan channel expansion; i.e., preliminary marsh elevation sensitivity studies indicated that increased marsh elevations (reduced depth of water over the marsh) resulted in increased tidal range. However, the demonstrated base and plan differences indicated that the predicted increased water levels associated with the plan condition (increased depth of water over the marsh) resulted in increased numerical model plan tidal range compared to the base condition. This same type response was indicated in the physical model comparisons.

81. Results from the tidal sensitivity studies, for example, the PGBF numerical model tidal sensitivity test compared to the actual base test, support the trend of increased water levels associated with the plan channel modifications. As will be addressed in the velocity section, velocity boundary sensitivity studies suggested that some change to the boundaries would be expected as a result of the channel expansion.

82. Information from the transitional channel verification tests and the preliminary plan channel condition tests were reviewed in an attempt to

49

further document water level impacts associated with channel expansion. Results from these analyses indicated consistent trends of increasing water level as channel expansion evolved. Appendix B and the verification report* provide the details of these analyses. Appendix B also describes some other channel expansion model studies where water level impacts were documented and reviews available National Ocean Survey (NOS) field information from Fernandina Beach, FL; Mayport, FL; Savannah, GA; Charleston, SC; Wilmington, NC; and Hampton Roads, VA.

Summary of Water Level Findings

83. The modeled Trident plan channel condition demonstrated a 0.15- to 0.20-ft increase in midtide levels relative to the pre-Trident base channel condition in both the numerical and physical models. As explained in paragraph 68, during the numerical model verification process, agreement of base condition high- and low-water tides between numerical and physical models was sacrificed somewhat for improved velocity agreement. The same modeling procedures and coefficients were used for the base and plan conditions; however, agreement between numerical and physical model high- and low-water elevations was generally improved for the plan condition. Numerical model high-water elevations generally demonstrated an addiitonal 0.1- to 0.2-ft increase over the physical model in plan-to-base differences; i.e., the physical model indicated a 0.2- to 0.3-ft increase in plan condition high-water elevations while the numerical model indicated a 0.4-ft increase in plan condition high-water levels. Low-water elevations for the physical model plan condition were generally elevated 0.1 to 0.2 ft over those of the base condition. Numerical model low-water elevations south of Kings Bay did not vary between the plan and base condition. Low-water elevations at and north of Kings Bay were generally reduced 0.10 to 0.15 ft for the numerical model plan condition. The numerical model marsh schematization and the associated wetting and drying process may be responsible for the apparent differences from the physical model findings. Both models predicted a 0.15- to 0.20-ft increase in midtide level and a possible small increase in tide range for the Trident channel condition tested relative to the pre-Trident channel condition.

---

* Granat et al., op. cit.

84. As discussed in paragraph 39, a thorough reevaluation of all model testing results and analysis of recent prototype data led to the conclusion that the numerical model tide results are less useful than physical model results and physical model results indicated a consistent trend of increasing water level as channel expansion evolved. Based on analyses of recent field data, it was concluded that tide range will probably not change as a result of the Trident channel improvements and that mean water level in Cumberland Sound may increase a small amount, less than the normal annual variation in mean sea level. As such, any changes will be extremely difficult to detect until several years of data are available.

Velocity Comparisons

85. Numerical model base and plan velocity time-history boundary forcing conditions derived from the physical model tributary data sets are illustrated in Plates D11-D21. The data are presented in clockwise order from Amelia River, in the south, to Cumberland Dividings in the north. Plates D22-D31 illustrate the resulting base and plan velocity time-history comparisons for the main submarine channel stations progressing from lower Cumberland Sound to the upper Trident turning basin. Plates D32-D42 illustrate resulting velocity time-history comparisons for the tributary and secondary channel stations, from south to north. Plan condition velocities demonstrated subtle phase shifts, generally with times of arrival slightly later than the base condition. Figure 15 summarizes the base and plan maximum ebb and flood velocity magnitudes at each of the interior stations examined. In general, only subtle base-to-plan velocity variations were indicated. The largest ebb and flood velocity magnitude differences were found at the two upper Trident operational area stations 2074 and 2089 (Plates D30 and D31, respectively). The largest base-to-plan depth changes existed at these two stations (from about 26 ft for the base condition to 48 ft for the plan condition). As indicated at these two stations, the increased plan channel depths within the upper turning basin resulted in reduced plan channel velocities.

Discharge Comparisons

86. The time-history plots illustrate the depth-integrated velocity

51
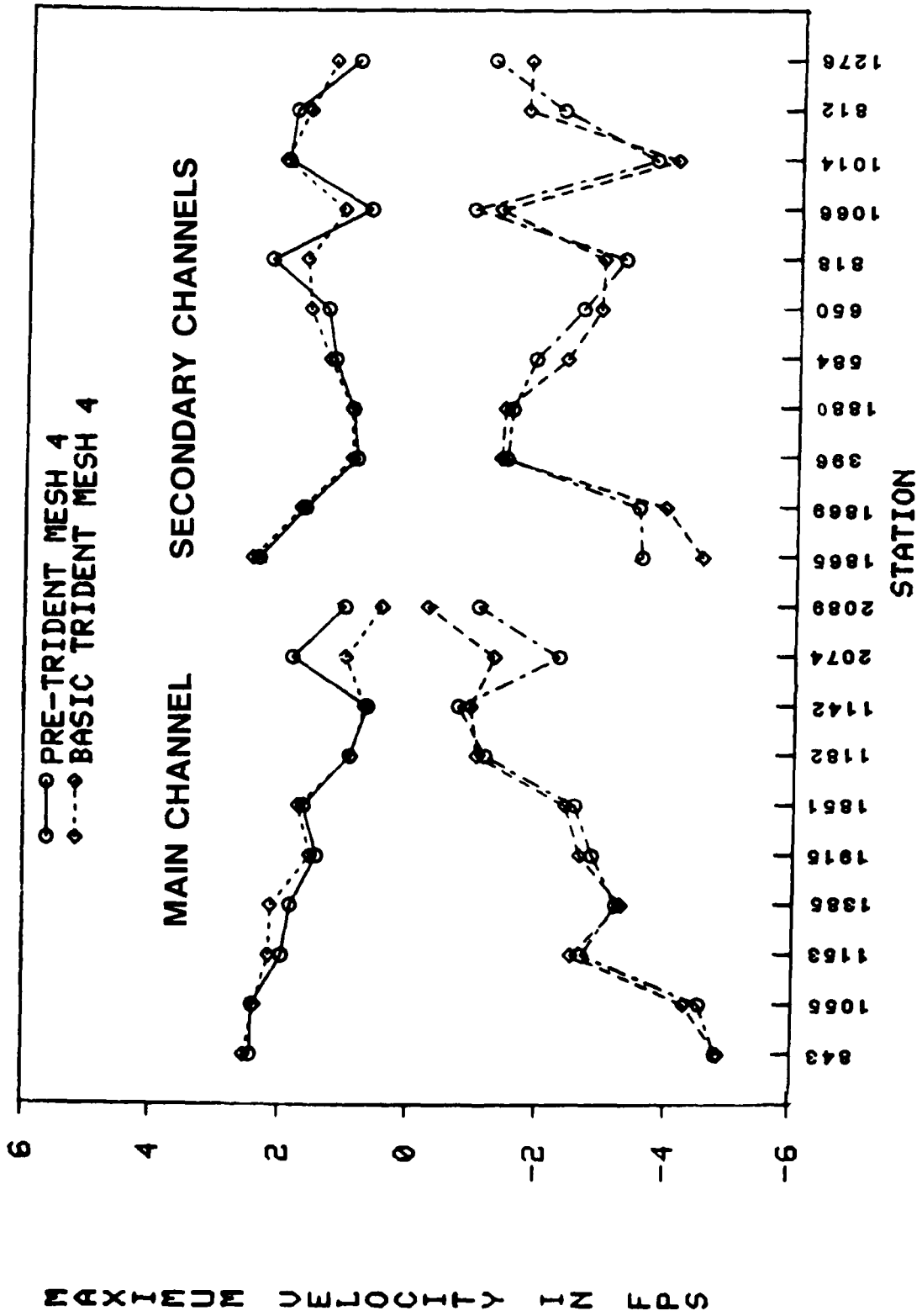
Figure 15. Base and plan velocity comparison summary

condition predicted by the numerical model and the changes between base and plan values at the specific locations. As such, they do not provide a direct indication of volume transport (discharge) or the variation in transport for stations or conditions at different depths. Discharge computations at each numerical model tributary boundary and at other specified cross sections were performed to examine general circulation changes between the base and plan conditions. This approach used the continuity check routine from RMA-2V and provided values in terms of discharge (velocity times depth times width). The total ebb discharge and flood discharge over the tidal cycle was calculated for each of the specified cross sections for the base and the plan condition.

87. Numerical model discharge dominance, calculated as the ebb discharge divided by the sum of the absolute value of ebb and flood discharge, was used to summarize base and plan variations at the numerical model boundaries. These boundary forcing conditions were derived directly from the physical model base and plan velocity observations (Plates C7-C13, C32, C33, C37, and C38). Replicate half-hourly velocity measurements were collected over three tidal cycles, averaged for each depth, and then depth-averaged (Plates D11-D21) and distributed across the tributary boundary. The St. Marys Inlet boundary, as expected, was found to be slightly ebb-dominated for both the base and plan condition. Although the inlet ebb and flood tidal cycle discharge was increased slightly for the plan condition (a 2 to 3 percent increase over base conditions), the same degree of ebb discharge dominance was indicated for the base and plan condition.

88. The Amelia River was found to be flood dominated for the base and plan conditions (see paragraph 89). The ebb and flood discharge for the Amelia River was decreased slightly for the plan condition. The largest decrease was for the flood period, resulting in a slightly reduced plan flood dominance. The Jolly River was similarly found to be flood dominated for the base and plan conditions, also with a slightly reduced ebb and flood discharge. The largest decrease in discharge was for the ebb cycle, resulting in a slightly increased flood dominance for the plan condition. The St. Marys River was found to be ebb dominated for the base and plan conditions, as would be expected because of freshwater inflow. As with the Jolly and Amelia Rivers, the ebb and flood tidal cycle discharge was decreased slightly for the plan condition. The degree of plan ebb dominance was not changed from that of the base condition.

53

89. All three southern tributary systems (Amelia, Jolly, and St. Marys) are interconnected by marsh and secondary channel systems in the prototype and in the physical model. This fact greatly complicates the resulting circulation processes. Briefly, the physical model data indicated that the plan condition resulted in reduced ebb and flood tidal cycle discharge through these tributary systems. Approximately 45 percent of the total ocean ebb and flood discharge was associated with the southern tributaries during the base condition; this value was reduced to about 40 percent during the plan condition. This reduction can be attributed to the improved plan channel hydraulic efficiency in Cumberland Sound.

90. The Crooked River and Black Point Creek boundaries were found to be ebb dominated for the base and plan conditions. As with the lower tributaries, ebb and flood discharge for the plan condition was reduced. Flood discharge was reduced more than the ebb discharge, resulting in a slightly increased ebb dominance for the plan condition at the Crooked River boundary. The reduced velocities at this boundary may be associated with the earlier plan condition tidal phase (time of arrival) described in paragraph 66, resulting in a reduced water level gradient up the Crooked River.

91. The plan ebb and flood discharge at the Cumberland Dividings boundary was also found to be slightly reduced. This boundary was the only boundary to demonstrate a dominance change between the two conditions. Flood discharge during the base condition was slightly greater than ebb discharge, resulting in a slightly flood-dominated boundary (a dominance value of 0.46; more water flowed into the Cumberland Sound system on the flood cycle than was transported out through the boundary on the ebb cycle). Ebb discharge for the plan channel condition at the Cumberland Dividings was slightly greater (it was reduced by a smaller amount) than flood discharge, resulting in a slightly ebb-dominated boundary (a dominance value of 0.54). More flow was transported out through this boundary on the ebb cycle than was transported into the system on the flood cycle. The velocity and discharge variations illustrated at this boundary may again be associated with subtle variations in phase relationships and/or physical model modifications undertaken during the transitional channel verification (paragraphs 14 and 33).

92. In summary, the plan condition discharge values south of Kings Bay indicated a small increase in ebb and flood flow efficiency at the ocean entrance, a reduced ebb and flood tidal cycle discharge at the southern

54

tributary boundaries, and an associated increase in discharge along Cumberland Sound. The corresponding reduced plan discharges at the northern tributary boundaries were associated with phase relationships and increased plan condition interior water levels, a fact substantiated by the time-history water-surface elevations (Plates D3-D10). The northern Cumberland Sound (Cumberland Dividings) boundary was the only boundary to illustrate a change in net tidal cycle flow direction, a change from slight flood dominance during the base condition to slight ebb dominance during the plan condition.

93. Figure 16 illustrates a schematic of the interior continuity lines examined in detail for the base and plan conditions. The obtained transport values have inherent limitations associated with the finite element approach and the wetting and drying procedure (i.e., finite element models conserve mass on a global basis and may demonstrate localized perturbations from cross section to cross section, whereas most finite difference models compensate for flow continuity errors by local adjustments to the water level). Comparisons between base and plan values provide a means of identifying potential circulation variations between the two conditions. An attempt was made to reduce some of the underlying uncertainty associated with localized continuity calculations. For comparison and illustration, base and plan flood and ebb values at each line were normalized by dividing each value by the respective ocean values. The length of each vector in Figure 16 represents the percentage of ocean flood and ebb discharge across each line. As illustrated, small base-to-plan variations generally resulted.

94. Lines 1 and 2, west of Drum Point Island, indicated that the ebb and flood discharges for the plan channel condition were increased. The plan condition flood discharge increased more than the ebb discharge. Flood discharge at line 3, east of Drum Point Island, did not demonstrate a base-to-plan variation, while the ebb discharge was reduced for the plan condition. Lines 4-8 and 10, associated with Kings Bay and Cumberland Sound, demonstrated increased ebb and flood discharge for the plan condition. Lines 9, 11, and 12, associated with the south and north forks of the Crooked River, demonstrated reduced plan channel ebb and flood discharge.

95. In summary, although subtle discharge variations were indicated, a consistent trend was demonstrated. The plan condition generally resulted in increased ebb and flood discharge along Cumberland Sound and through Kings

BASE AND PLAN FLOW TRANSPORT
PERCENT OF OCEAN FLOW

BIG CRAB ISLAND

DRUM POINT ISLAND

10 PERCENT

BASE

PLAN

-N-

EBB   FLOOD
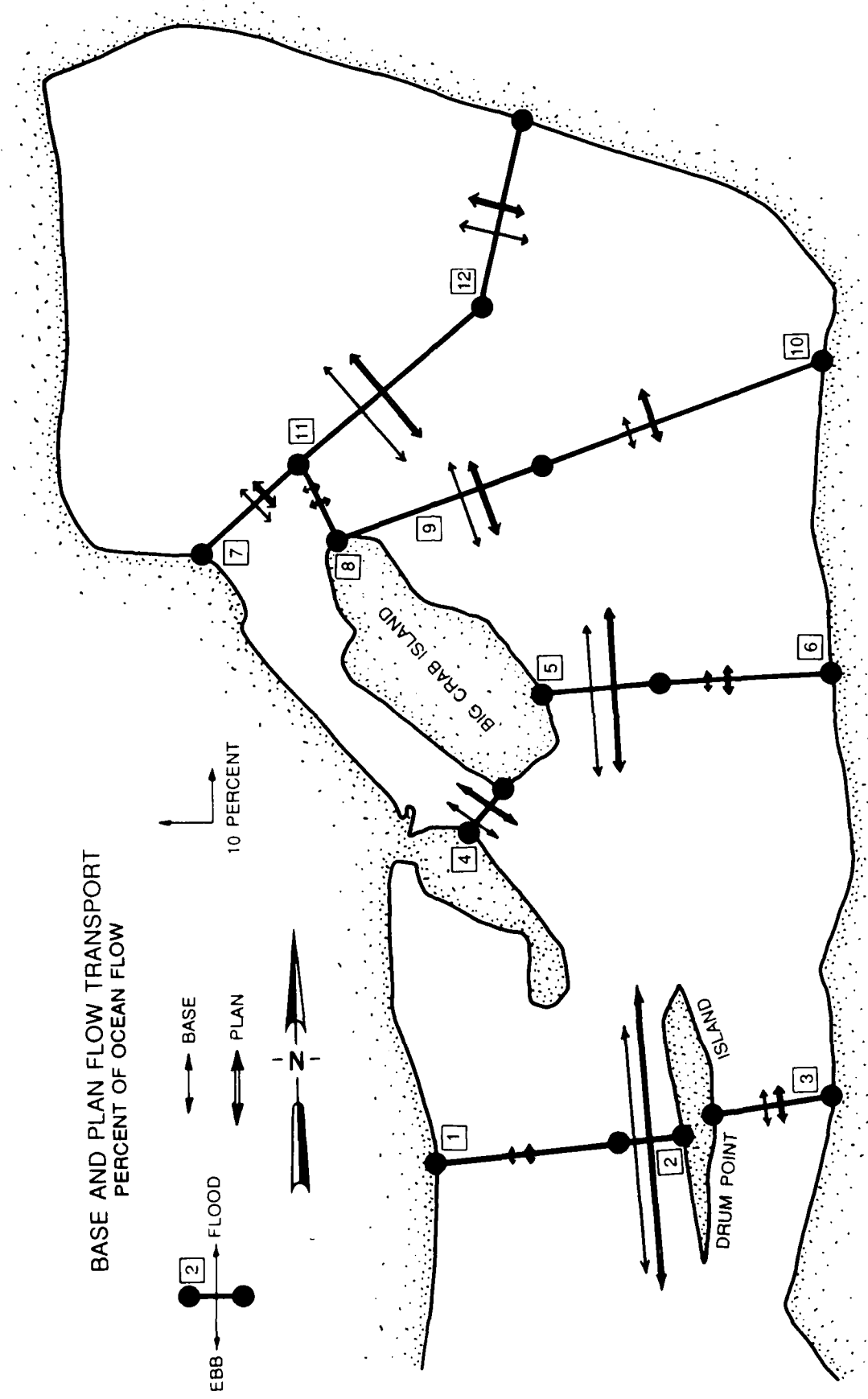
Figure 16. Base and plan flow discharge comparison

56

Bay. The ebb and flood discharges along the lower south and north forks of the Crooked River were reduced for the plan condition.

Flow Distribution Comparisons

96. Flow distribution and base-to-plan distribution changes along five specific cross sections were an additional means of examining circulation changes associated with the plan channel condition. Figure 17 illustrates the selected cross sections and provides a pictorial summary. The percentage of total ocean ebb and flood discharge for each cross section was determined, and then the distribution of this flow across each line segment of the cross section was calculated. This procedure provided a normalized flow distribution for each cross section. As expected, subtle base-to-plan variations were generally indicated.

97. Cross-section 1, across Cumberland Sound and Drum Point Island, south of Kings Bay, consisted of continuity lines 1-3. As indicated, most of the ebb and flood cross-section flow (76-81 percent) was concentrated along line 2, between Drum Point Island and the eastern side of Mill Creek Marsh (line 1 is associated with Mill Creek and Mill Creek Marsh). The deepened plan channel resulted in increasing the relative volume of flow along Cumberland Sound across line 2, while reducing the relative volume along line 3, east of Drum Point Island (a 3 to 4 percent change).

98. Cross-section 2 included line 4 across the entrance to Kings Bay, line 5 across Cumberland Sound between Crab Island and the western shore of Stafford Island Marsh, and line 6 across Stafford Island to the western shore of Cumberland Island. The pre-Trident condition flow through Kings Bay (line 4) accounted for 31 percent of the cross-section flood flow and 20 percent of the cross-section ebb flow. Although the total flood and ebb Trident channel discharge was increased from the base condition, the cross-section percentage of Trident condition flood flow was reduced slightly to 30 percent while the ebb flow distribution was increased to 25 percent. A majority of the base and plan flow (60 to 68 percent) was across line 5, along Cumberland Sound.

99. Cross-section 3 examined the flow distribution north of upper Kings Bay. It included line 7, from the mainland above the Trident dry dock area across Marianna Creek to the adjacent marsh, and line 8, from this marsh

CROSS-SECTION FLOW DISTRIBUTION

PERCENT OF CROSS-SECTION FLOW

VALUES (BASE/PLAN) ARE ON THE SIDE
OF LINE TO WHICH FLOW OCCURS
(i.e. FLOOD FLOW IS UP ESTUARY)

- N -
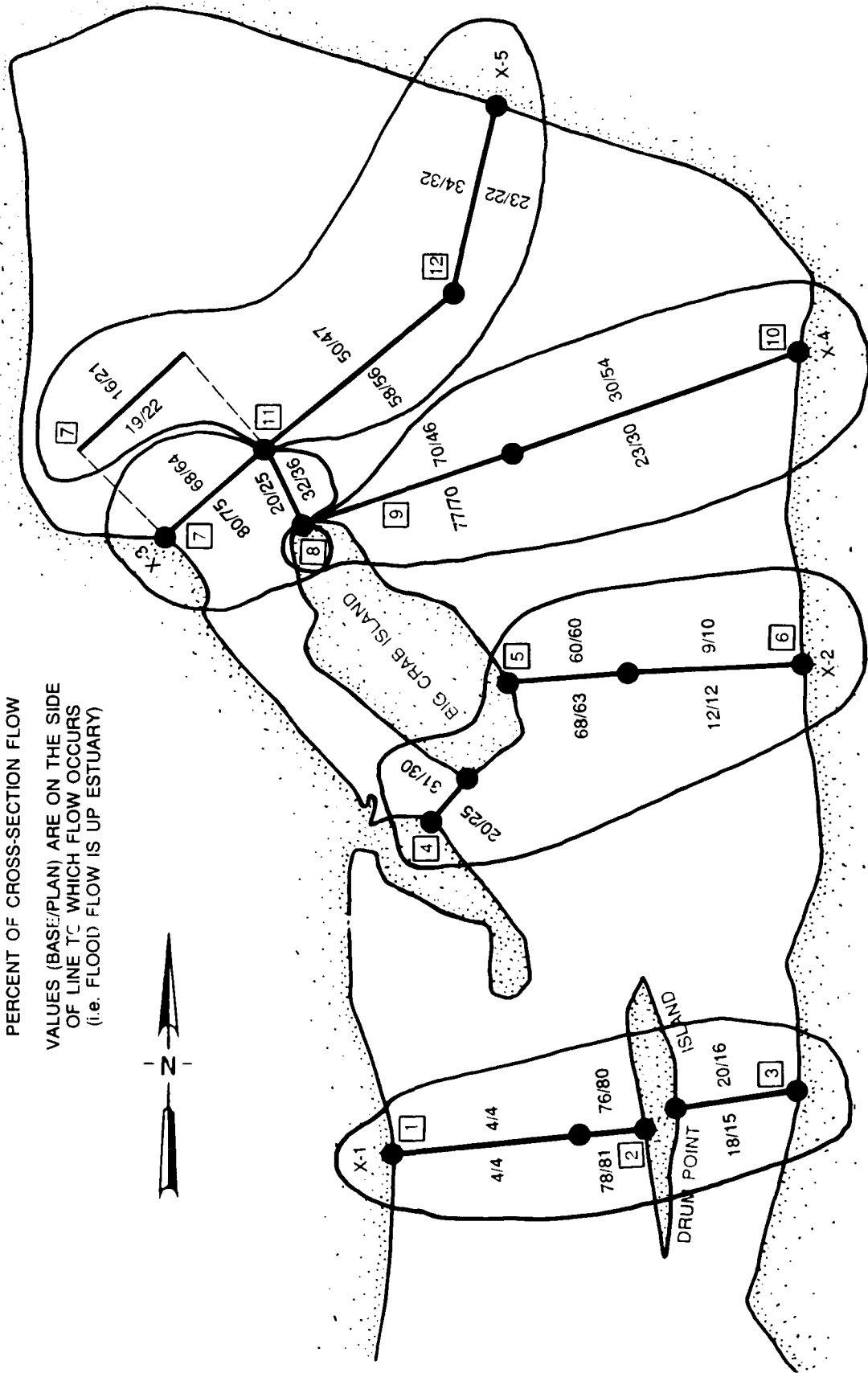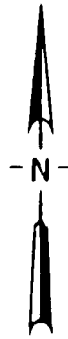
Figure 17. Cross-section flow distribution

58

location to the upper end of Crab Island. For the pre-Trident condition, 68 percent of the flood flow and 80 percent of the ebb flow was across line 7 through Marianna Creek. The total ebb and flood discharge through the upper end of Kings Bay was increased for the Trident plan channel condition; however, the percentage of plan flood and ebb flow across line 7 was reduced relative to line 8. The flow across line 8 through the back channel around Crab Island was increased about 5 percent for the Trident plan channel condition.

100. Cross-section 4 examined the flow distribution between lines 9 and 10. Line 9 extended from the upper end of Crab Island across the lower south fork of the Crooked River to the edge of the adjacent marsh. Line 10 extended from the edge of this marsh across Cumberland Sound, above Stafford Island, to Cumberland Island. As will be illustrated in the next section, some of the flow passing line 10 flowed to the west across the marsh and into the Crooked River region. For the pre-Trident condition, most of the flow at this cross section was associated with the lower south fork of the Crooked River; approximately 70 percent of the flood flow and 77 percent of the ebb flow was across line 9. The plan condition flood and ebb discharge at line 9 was reduced while the discharge at line 10 was increased. The percentage of the cross-section flood flow across line 10 was increased from 30 to 54 percent for the plan condition; the ebb flow was increased from 23 to 30 percent.

101. The final cross-section examined in detail included lines 7, 11, and 12. As previously addressed, flood and ebb discharge at lines 11 and 12 (Crooked River south and north forks, respectively) were reduced and discharge at line 7 (Marianna Creek) was increased for the plan condition. The flow distribution followed a similar pattern. Marianna Creek (line 7) accounted for about 16 and 19 percent of the normalized pre-Trident cross-section flood and ebb flow, respectively. Trident plan condition flood and ebb values for Marianna Creek were increased to 21 and 22 percent, respectively. Pre-Trident flood and ebb values for the south fork Crooked River (line 11) were reduced from 50 and 58 percent, respectively, to 47 and 56 percent for the Trident condition. Pre-Trident values for line 12 (north fork Crooked River) were slightly reduced from 34 percent for the flood and 23 percent for the ebb to Trident plan values of 32 percent for the flood and 22 percent for the ebb.

Circulation Summary

102. In general, subtle hydrodynamic variations were indicated between the pre-Trident base condition and the Trident plan channel condition. RMA-2V-derived vector plots for times around maximum flood (hour 22.0) and maximum ebb (hour 11.5) for the area adjacent to and north of Drum Point Island help in summarizing the circulation variations between the base and plan conditions. The illustrated vector plots (Figures 18-21) are based on a regularized grid pattern, i.e., the finite element solution has been interpolated to a uniform spacing throughout the computational mesh. As described in paragraphs 65 and 66, a slight phase shift existed between the base and plan conditions. The marsh wetting and drying process was affected by this phase shift and accounts for the variation in the dried portion of the mesh, comparing base (Figure 20) and plan (Figure 21) conditions.

103. The deepened Trident plan channel improved the hydrodynamic efficiency of the channel resulting in increased discharge of ebb and flood flows through St. Marys Inlet and Cumberland Sound. Ebb and flood discharge through the lower tributary systems (Amelia, Jolly, and St. Marys Rivers) was reduced during the plan condition. Plan condition ebb and flood discharge west of Drum Point Island was increased. Plan ebb discharge east of Drum Point Island was reduced. Less than 20 percent of the ebb and flood flow along Cumberland Sound was between Drum Point Island and Cumberland Island for the base and plan conditions. The plan condition resulted in increasing the relative flow distribution to the west of Drum Point Island.

104. Ebb and flood discharge was also increased through lower Kings Bay for the deepened Trident channel condition. Approximately 30 percent of the base and plan Cumberland Sound flood flow was transported through Kings Bay. The relative percentage of Cumberland Sound ebb flow through Kings Bay was increased from about 20 percent for the base condition to about 25 percent for the plan condition. As discussed in paragraph 85, the reduced velocity in upper Kings Bay associated with the deepened Trident channel is clearly illustrated in Plates D30 and D31 and Figures 15 and 18-21. Although the velocity magnitude was reduced for the plan condition, the total ebb and flood discharge through upper Kings Bay was increased (Figure 16). As indicated by a comparison of the base condition (Figure 20) with the plan condition (Figure 21), a low-velocity eddy circulation cell downstream of the Trident dry

60

PRE-TRIDENT BASE4

MAXIMUM FLOOD VELOCITY

VELOCITY VECTOR

SCALE

(FPS)

0.0

4.0

↑ N
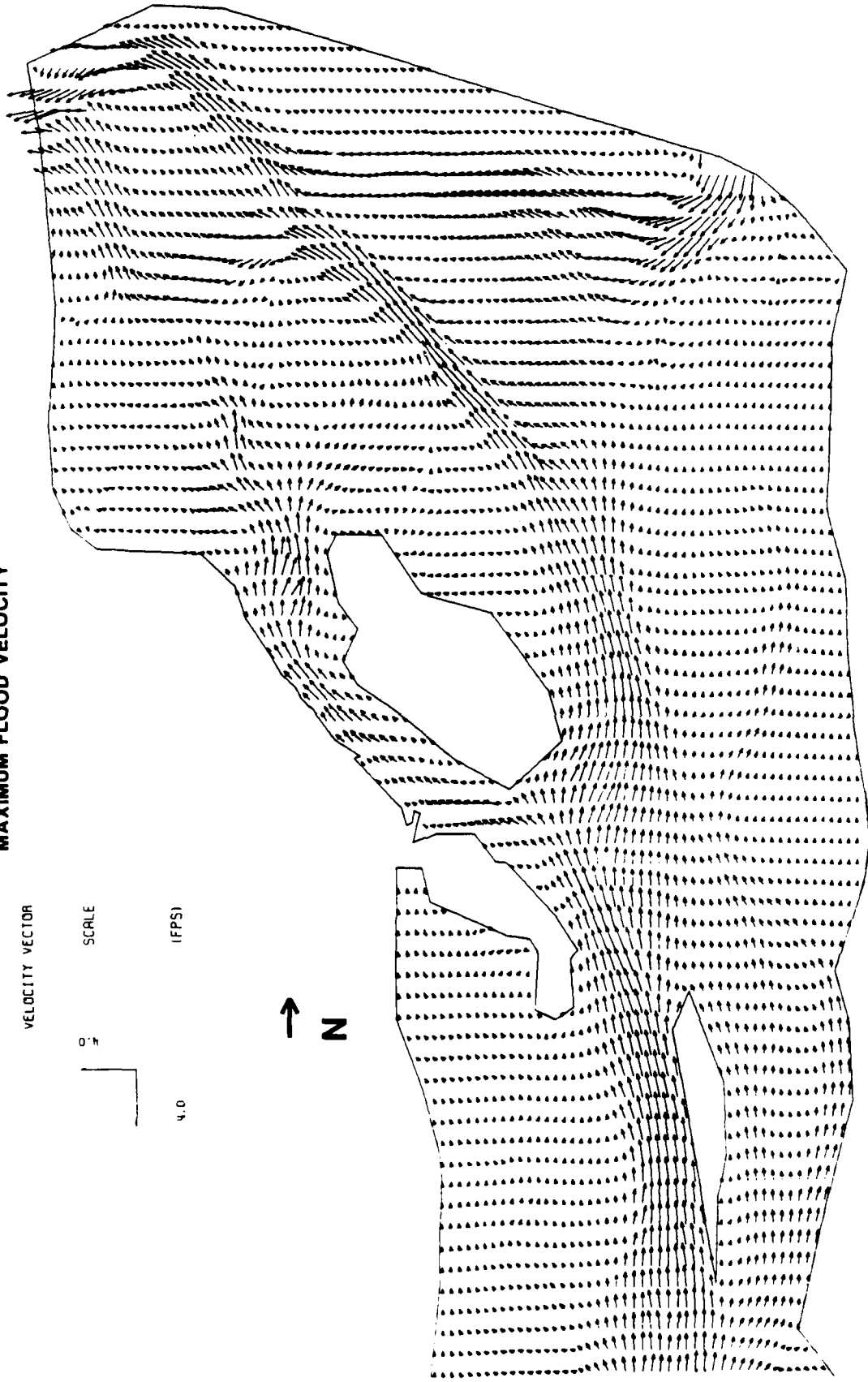
Figure 18. Pre-Trident channel maximum flood velocity vectors

61

TRIDENT PLAN4

MAXIMUM FLOOD VELOCITY

VELOCITY VECTOR

SCALE

(FPS)

4.0

4.0

N
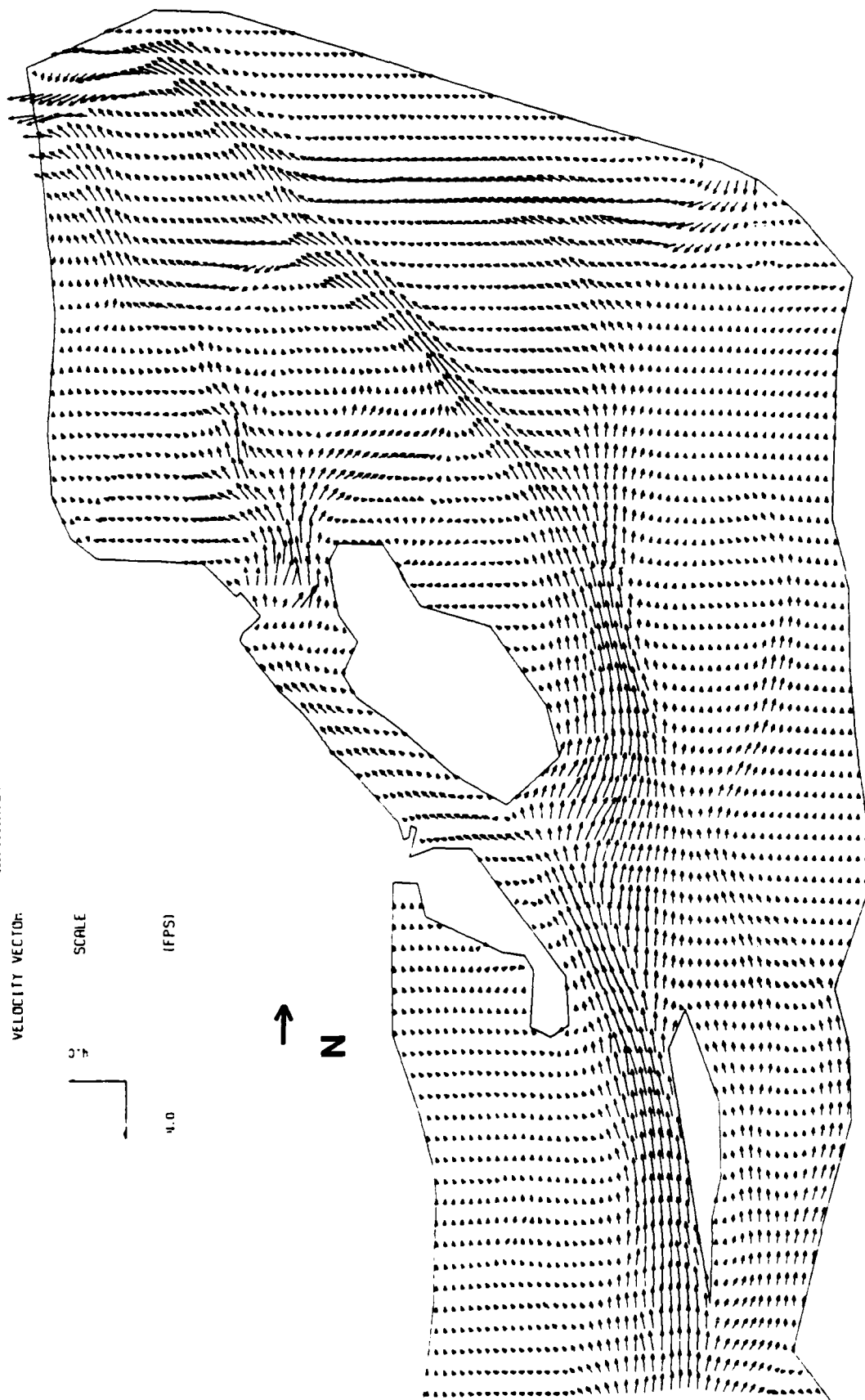
Figure 19. Trident channel maximum flood velocity vectors

62

PRE-TRIDENT BASE4

MAXIMUM EBB VELOCITY

VELOCITY VECTOR

SCALE

(FPS)

4.0

4.0

↑N
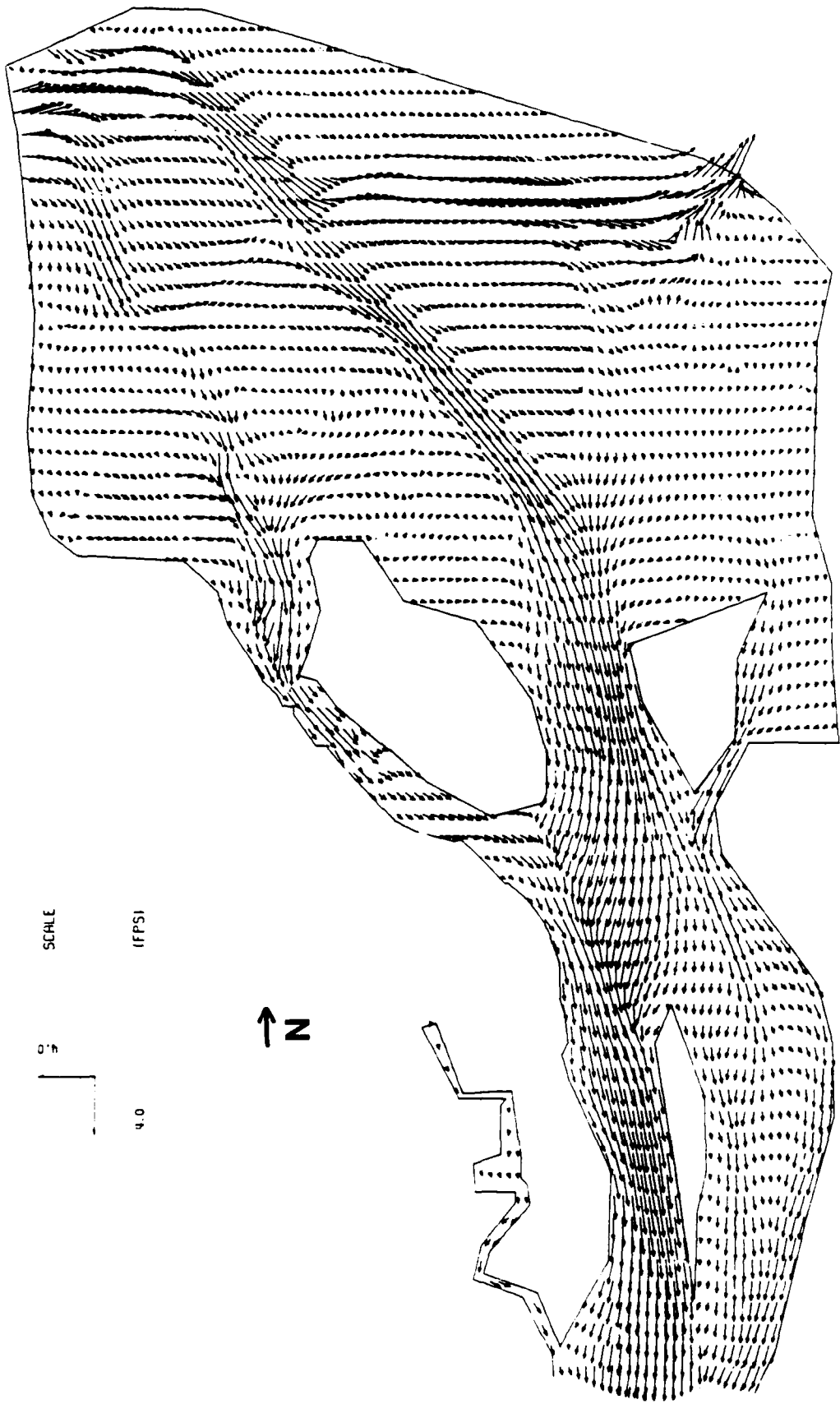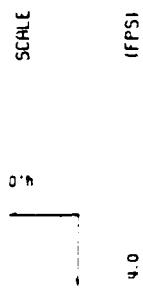
Figure 20. Pre-Trident channel maximum ebb velocity vectors

63

TRIDENT PLAN4

MAXIMUM EBB VELOCITY

VELOCITY VECTOR

SCALE

(FPS)

0.0   4.0
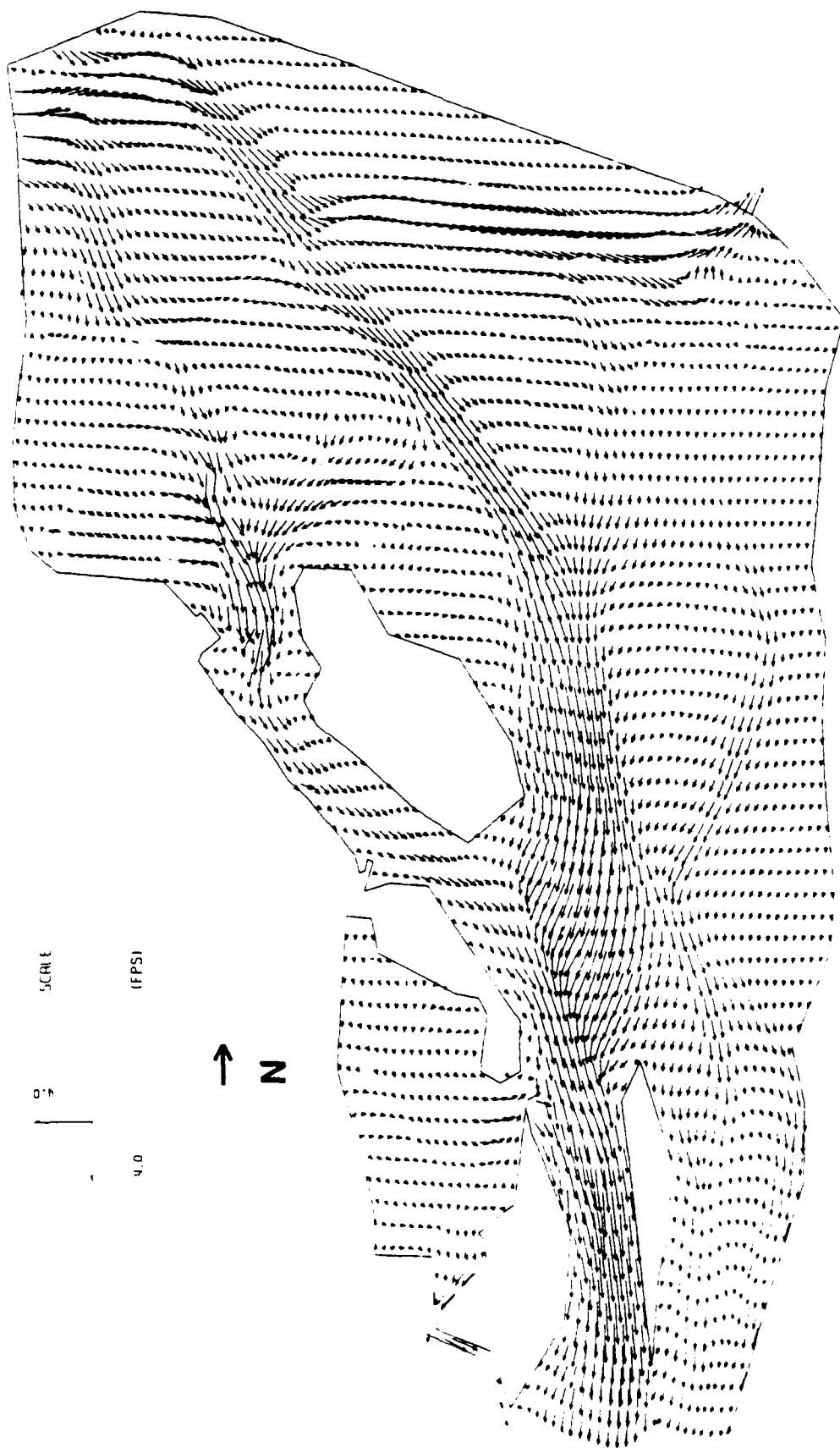
Figure 21. Trident channel maximum ebb velocity vectors

dock was also enhanced during the ebb cycle for the plan condition. This plan condition recirculation in the upper Trident turning basin also developed in the physical model.

105. Most of the base and plan flow through upper Kings Bay was transported through Marianna Creek; however, the percentage of flow through the back channel around the upper end of Crab Island was increased somewhat during the plan condition. Under the plan condition, an increased percentage of the flow associated with the marsh areas north of Kings Bay and the upper Crooked River was transported through Kings Bay rather than by the lower south and north forks of the Crooked River, as was the case during the base condition (Figure 16).

106. The increased efficiency of the plan Kings Bay channel did not accommodate the entire increased flood transport of lower Cumberland Sound. Flood transport east of Crab Island was also increased for the plan condition. As a result of the increased plan flow through Kings Bay, transport associated with the lower south fork of the Crooked River (line 9) was reduced. In a relative sense, the increased Cumberland Sound plan flood flow passing Crab Island was directed northward (i.e., across line 10), past the south fork of the Crooked River. As explained in paragraph 100 and illustrated in Figure 19, some of this flow was transported northwestward across the marsh adjacent to and north of the south fork of the Crooked River.

107. Station 1276 (Figure 10), north of line 10 in northern Cumberland Sound, was located close to the nodal point between the Cumberland Sound/St. Marys system to the south and the Cumberland Dividings/St. Andrew system to the north. The general location of this nodal point in the numerical model was consistent with the physical model and aerial reconnaissance observations made in April 1983. Plate D42 and Figures 16-21 illustrate increased plan condition ebb and flood velocity and transport across this region. This increased plan condition discharge changed the phase and circulation relationship between the Cumberland Sound/St. Marys system and the Cumberland Dividings/St. Andrew system. As indicated in paragraphs 91 and 92, the total ebb and flood discharge through the Cumberland Dividings boundary was reduced for the plan condition. Flow dominance at the Cumberland Dividings boundary varied from a slightly flood-dominated condition during the base to an ebb-dominated condition during the plan.

Velocity Sensitivity Findings

108. Velocity results from the sensitivity tests provide additional insight to boundary forcing condition impacts. As discussed in paragraph 74, these sensitivity tests provide nonrepresentative results due to the unmatched (crossed) geometry and boundary forcing conditions. For example, the previously described circulation variations at the lower tributary boundaries and the increased submarine channel discharge along Cumberland Sound and Kings Bay associated with the actual plan condition will not have the increased cross-sectional area available for transport in the BGPF sensitivity test. As another example, the tidal phase and discharge variations north of Kings Bay and at the upper tributary boundaries associated with the deepened submarine channel will be suppressed during the PGBF sensitivity test. Results from the sensitivity tests do, however, provide additional understanding of the complex hydrodynamic characteristics of the Cumberland Sound system.

109. Figure 22 illustrates the maximum ebb and flood velocity magnitudes for the interior stations for the two sensitivity tests and the actual base and plan conditions. Velocity magnitudes at each of the main channel stations demonstrated larger variations than at the secondary stations, indicating that velocity impacts are more directly focused along the main submarine channel. The sensitivity tests resulted in extreme velocities relative to the actual base and plan conditions. The BGPF sensitivity test resulted in the highest flood and ebb velocities. The PGBF test resulted in minimum velocities. These results are as expected considering discharge, cross-sectional area, the mixed conditions, and continuity (i.e., $Q = VA$; if cross-sectional area A is reduced, to maintain the same discharge Q , velocity V must increase).

110. Sensitivity test velocity magnitudes at stations 2074 and 2089 in the upper Kings Bay Trident area were the only two stations to demonstrate a distinct association with the same geometry condition (i.e., the two base geometry conditions demonstrated increased velocity relative to the two plan conditions). The two lower Kings Bay stations, 1182 and especially 1142, demonstrated the closest main channel velocity agreement among the four testing conditions. These findings indicate that circulation within Kings Bay is more sensitive to the geometry changes than to the boundary forcing conditions.
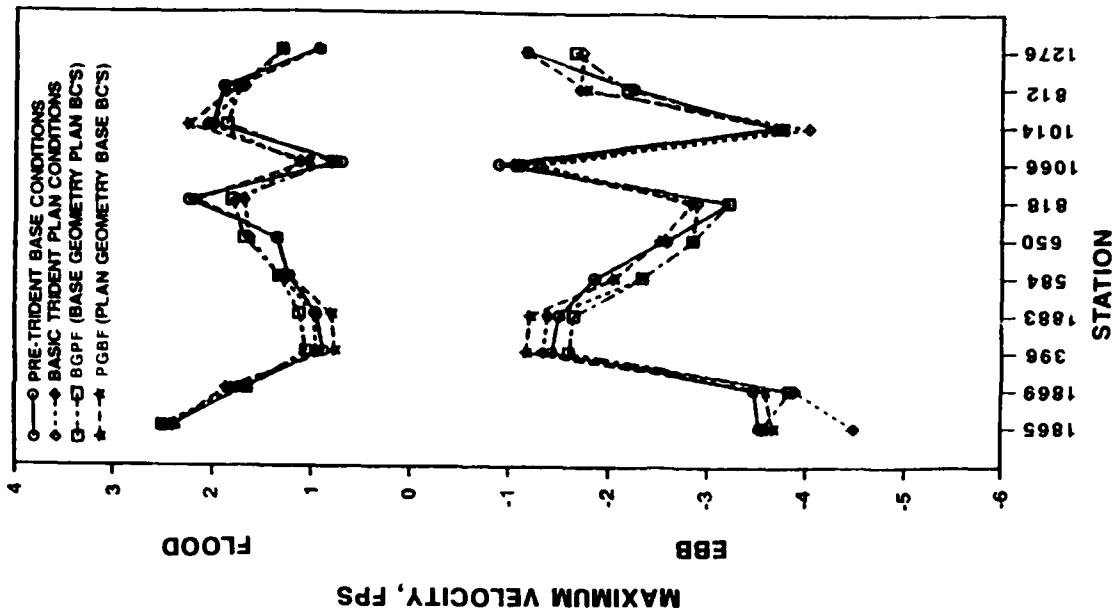
a. Main channel

b. Secondary channels and tributaries
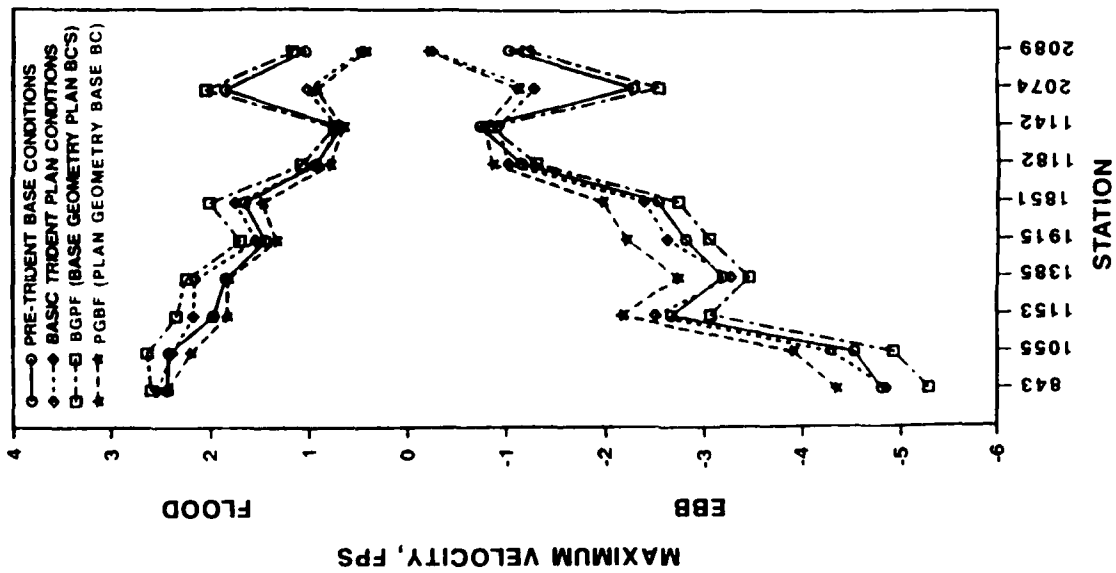
Figure 22. Velocity sensitivity summary

111. As with the base and plan tests, a closer look at sensitivity test discharge values provide a better indication of circulation variations. The sensitivity results confirmed the general findings of the base and plan comparisons with regard to increased submarine channel discharge associated with the deepened plan channel.

112. Comparing PGBF with the actual base condition indicated increased flood and ebb discharge across lines 2, 4, 7, and 8. These lines are all associated with the main submarine channel. This increased submarine channel discharge resulted without changes to the boundary forcing conditions; i.e., the channel geometry was the only condition to change. The additional main channel discharge associated with the deeper channel geometry generally resulted in reduced flood and ebb discharge across the other lines. Lines 1 and 10 were the only two exceptions. Line 10 indicated increased flood discharge and line 1 indicated increased ebb discharge for the PGBF condition relative to the actual base condition. Both of these increases were greatly reduced compared to the increases associated with the actual plan condition.

113. Compared to the actual plan condition, results from PGBF indicated reduced ebb and flood discharge at all lines except lines 9, 11, and 12 in the south and north forks of the Crooked River. Since channel deepening usually does not result in reducing the transport efficiency of a channel, this contrary indication of reduced channel discharge for the sensitivity test indicates that some modification to the boundary conditions would appear likely as a result of the Trident channel expansion. The fact that lines 9, 11, and 12 demonstrated increased discharge during this sensitivity test relative to the actual plan test tends to indicate that the boundary forcing conditions have a more direct influence on the discharge in these areas than does the submarine channel geometry. The boundary forcing conditions were the only changes between these two tests.

114. The discharge values across lines 2, 4, 7, and 8 (lines directly associated with the submarine channel) were reduced for the BGPF sensitivity test compared to the actual plan condition test. The channel geometry was the only condition that changed between these two tests. Discharge at all other lines was increased during the sensitivity test relative to the actual plan condition. These results are as expected based upon the geometry conditions; i.e., relative to the plan condition, the reduced channel depths and associated increased frictional resistance of the BGPF condition reduced the

channel discharge and resulted in redistributing some of the flow to areas adjacent to the main channel.

115. Comparison of discharge values between the BGPF sensitivity test and the actual base condition test provides an assessment of the boundary condition impacts on the pre-Trident channel geometry condition. Discharge at all lines except lines 9, 11, and 12 was increased for the BGPF sensitivity test relative to the actual base condition test. In fact, during the BGPF test, ebb and flood discharge at lines 1, 3, 5, 6, and 10 (lines not associated with the submarine channel) resulted in the largest discharge values of the four conditions examined. These findings, associated with boundary forcing condition differences, can be explained by basic continuity, as described in paragraph 109. The increased discharge through St. Marys Inlet and the reduced discharge through the lower tributaries prescribed by the plan boundary forcing conditions resulted in increased transport through the lower cross sections. The reduced BGPF discharge at lines 9, 11, and 12 is associated with the reduced discharge through the Crooked River and Cumberland Dividings boundaries.

116. As explained in this section, the velocity sensitivity test findings provide additional understanding of the complex hydrodynamic characteristics of the Cumberland Sound system. The velocity impacts were more directly focused along the main submarine channel. Circulation within Kings Bay was shown to be more sensitive to the channel geometry than to boundary condition differences. These tests confirmed the increased submarine channel discharge associated with the deepened and widened plan channel. They also indicated that some modification to the numerical boundary conditions are likely as a result of channel expansion.

PART V: NUMERICAL MODEL MESH 4 SEDIMENTATION RESULTS AND ANALYSIS

Sedimentation Comparisons

117. Subtle hydrodynamic changes in a complex estuarine circulation system such as Cumberland Sound and Kings Bay can result in dramatic changes in the resulting sedimentation responses. Sedimentation predictions presented in this section were derived from the Mesh 4 pre-Trident base and basic Trident plan channel modeling runs. The same modeling procedures, coefficients, and analysis routines developed during the Mesh 4 verification process were used in determining base and plan model sedimentation predictions. A complete description of the STUDH model and its application as used in this study is provided in the verification report.*

118. In brief, the base and plan RMA-2V data sets were considered to be approximations of the hydrodynamic conditions associated with the long-term sedimentation processes. RMA-2V results from hours 9.5 to 22.0 were used as the hydrodynamic forcing conditions for each of the base and plan sediment runs. The interaction of the flow (transport) and the bed (sedimentation) was treated in routines that computed source/sink (erosion/deposition) terms over the entire modeled area. Several cohesive and noncohesive sediment model tidal cycle runs were performed separately taking advantage of hot-start capabilities (using output data from previous runs as initial conditions in following runs) to initialize model sediment concentrations and bed conditions. In this manner, the sediment model was brought into a dynamic equilibrium with the prescribed hydrodynamic conditions.

119. Tables 3 and 4 summarize the coefficients used during the cohesive and noncohesive modeling runs, respectively, for the base and plan conditions. Figure 23 illustrates the noncohesive sediment grain size distribution used for the base and plan modeling runs. During the verification process, this distribution and the indicated cohesive and noncohesive coefficients were found to result in an excellent reproduction of pre-Trident channel field shoaling rates.

120. Figure 24 illustrates the base and plan channel shoaling zone locations used for the reported sedimentation computations. Numeric zones

---

* Granat et al., op. cit.
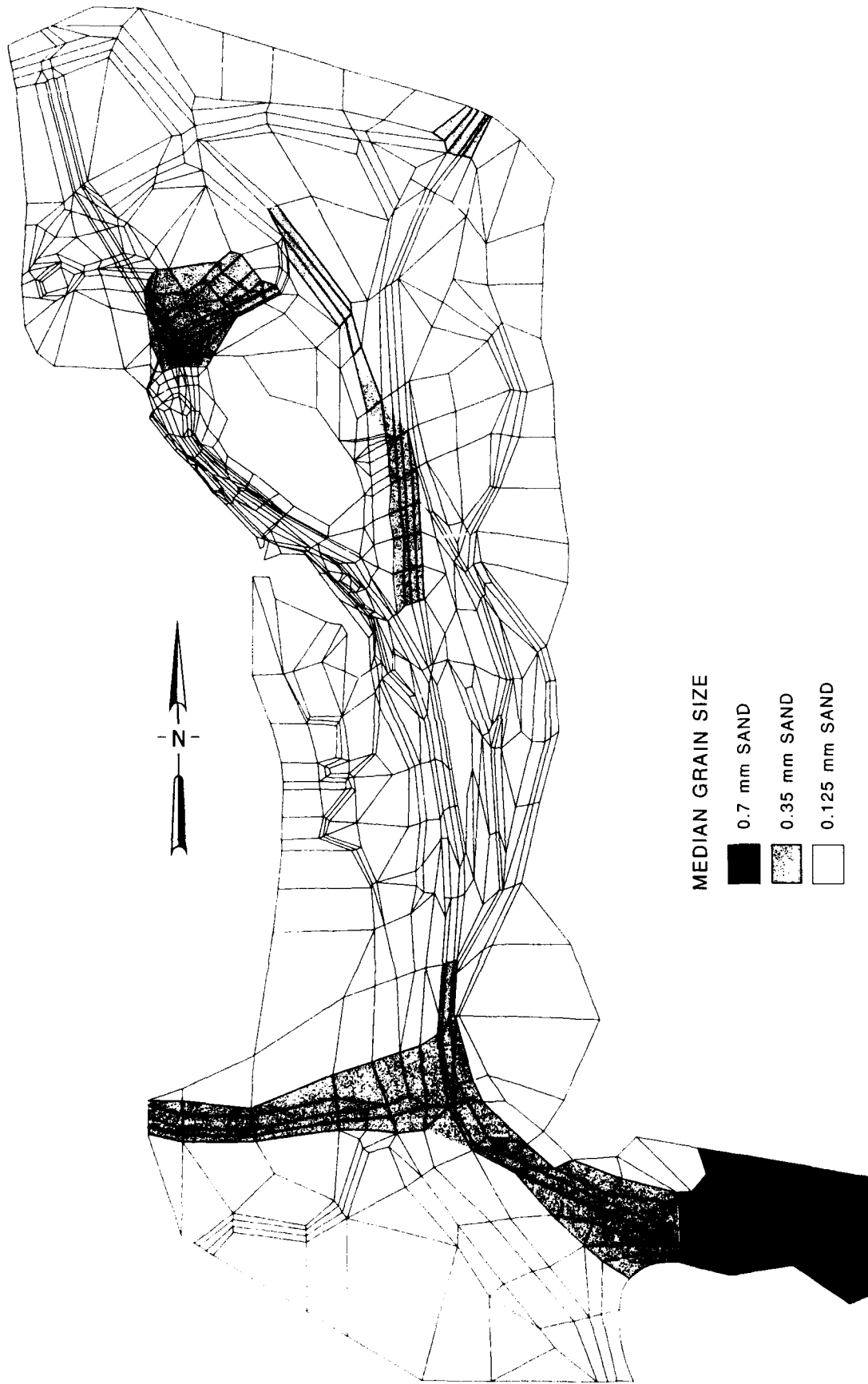
MEDIAN GRAIN SIZE

0.7 mm SAND

0.35 mm SAND

0.125 mm SAND

Figure 23. Noncohesive sediment grain size distribution
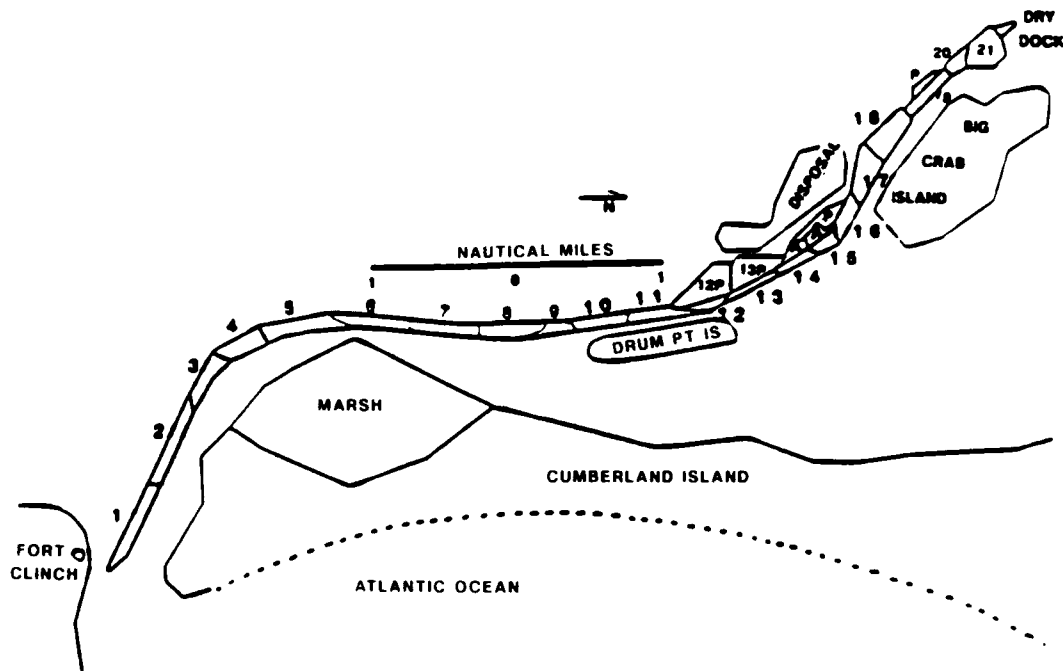
Figure 24. Shoaling zones

correspond to main channel locations while alphanumeric zones correspond to facility areas adjacent to the main channel. Table 5 summarizes the results, by zone, in terms of shoaling volumes in cubic yards per year and shoaling rates in feet per year for cohesive sediments, noncohesive sediments, and total sedimentation (cohesive plus noncohesive). Figure 25 summarizes the predicted total base and plan submarine channel shoaling rates by zone. The predicted shoaling volumes and depths presented in Table 5 and Figures 25 and 26 represent an estimate of long-term average annual shoaling that would occur if the channels were fully maintained at design dimensions. Thus, the predicted quantities do not necessarily represent what will occur in any particular year. A predicted range of sedimentation rates is described in paragraph 126.

121. Low shoaling rates, less than 1.0 ft per year, were predicted for base and plan channel conditions in zones 1 to 13, from the St. Marys/ Cumberland Sound entrance area to the areas south of Kings Bay and the Poseidon docking area. As indicated in Table 5, no appreciable cohesive deposition was predicted for zones 1 to 13; current velocities in these zones were sufficiently high to limit cohesive sediment deposition. High shoaling rates, basically cohesive deposition greater than 3.0 ft per year, were
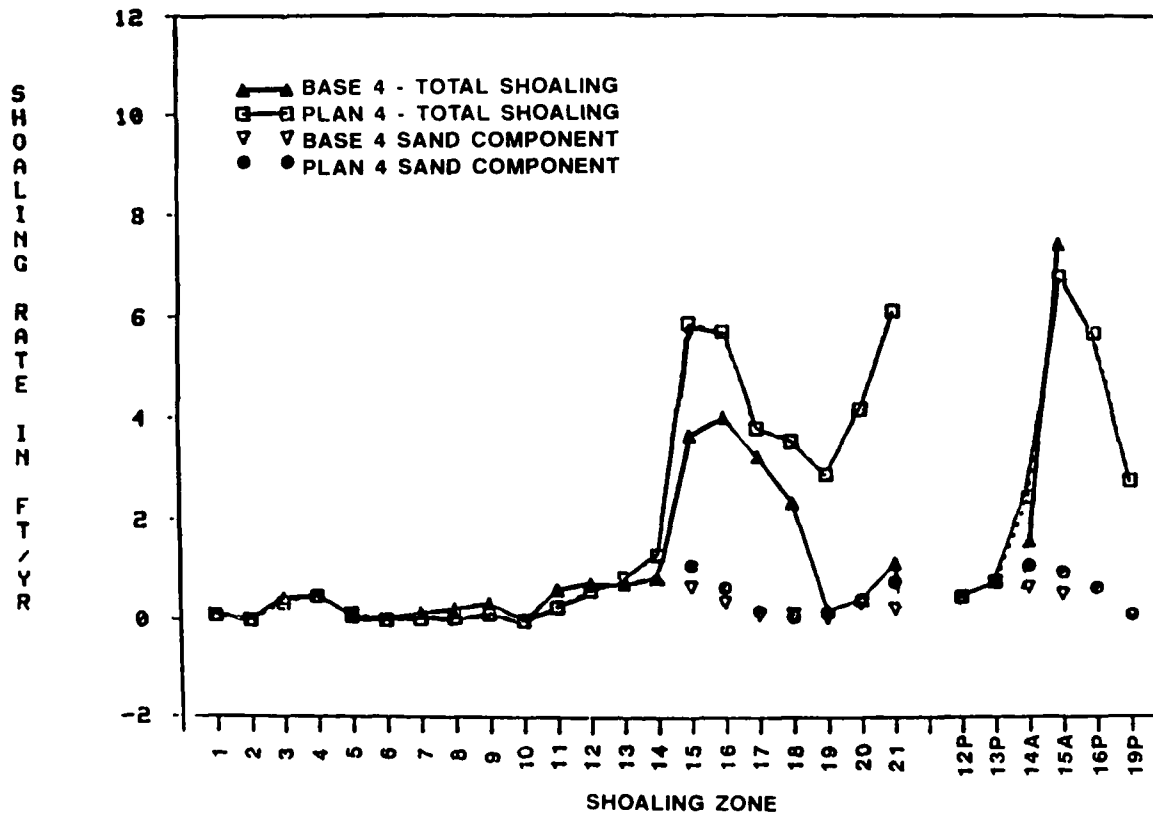
Figure 25.   Base and plan channel predicted shoaling rates

indicated for the interior Kings Bay and facility areas (zones 15 to 21).

122.   The plan channel condition tested did not include the lower Kings
Bay turning basin or the St. Marys Inlet turning and sediment basins that were
constructed after model testing was completed.   The conditions tested in-
creased the maintained interior channel areas by about 70 percent, from
475 acres for the pre-Trident channel geometry condition to 811 acres for the
plan channel geometry condition.   Approximately 43 percent of the increased
channel area was located within the high shoaling zones of Kings Bay.   For the
plan condition, model predictions indicated a 150 percent increase in required
annual channel maintenance dredging, from approximately 1.0 million cubic
yards per year for the pre-Trident channel condition to approximately 2.5 mil-
lion cubic yards per year for the Trident channel condition tested.   Approxi-
mately 92 percent of the total plan channel shoaling (i.e., 2.3 million cubic
yards) was located within Kings Bay.   About 48 percent of the total (i.e.,
1.2 million cubic yards) was associated with the new Trident channel areas.
As indicated in Table 5, cohesive deposition accounted for 80 percent of the
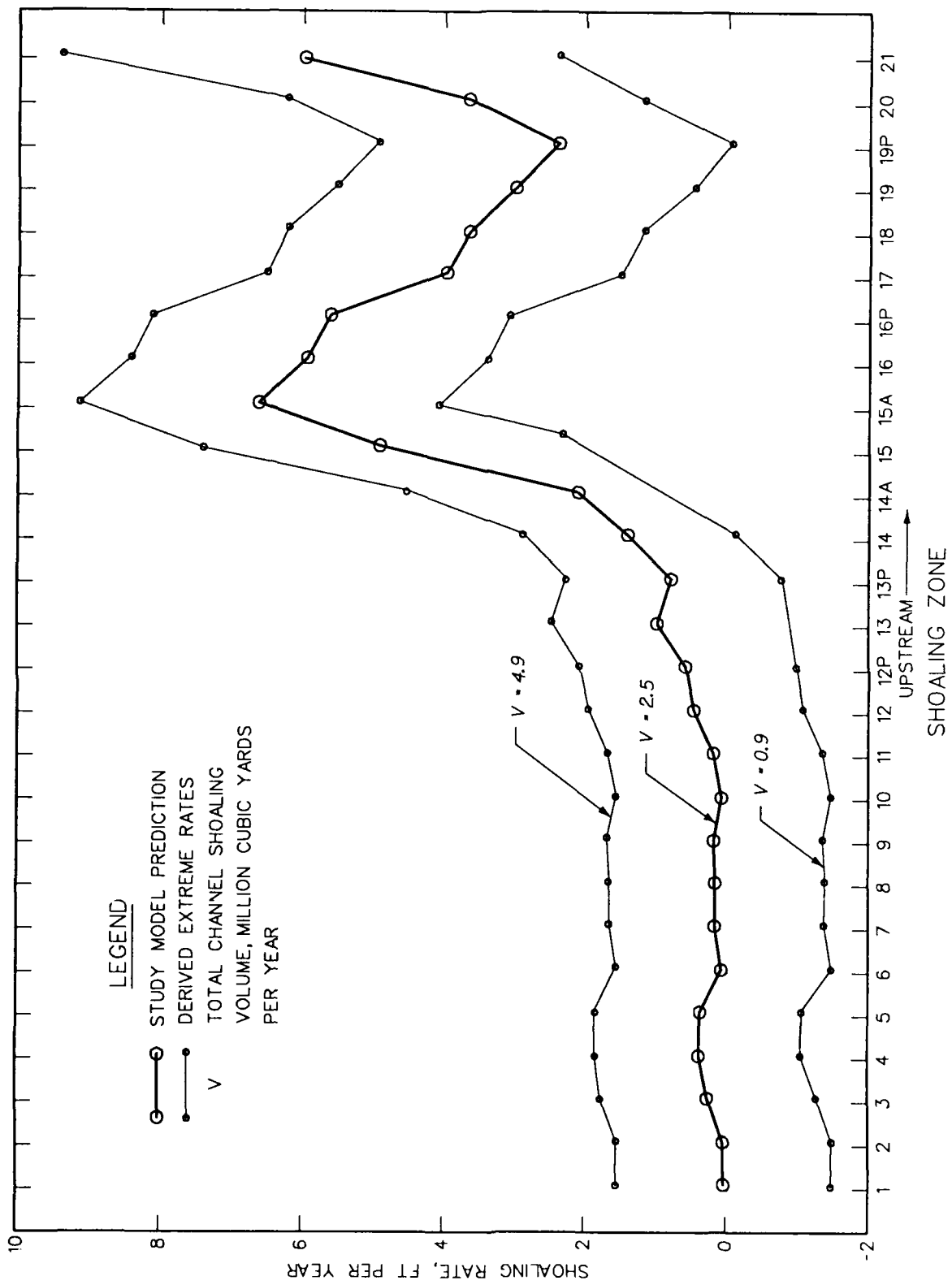
Figure 26. Trident plan channel predicted long-term average and extreme shoaling rates

total base and plan channel shoaling volume (i.e., 0.8 million cubic yards for the pre-Trident channel and 2.0 million cubic yards for the tested plan channel).

123. A closer analysis of Table 5 values provides additional insight to the plan channel sedimentation impacts. The widened and deepened plan channel areas adjacent to and south of Drum Point Island (zones 12 and below) demonstrated the same or, more usually, reduced shoaling rates relative to the pre-Trident condition. In some cases, shoaling volumes may have increased, but this increase was caused by the increased plan channel surface area. The increased channel area and increased discharge of the plan channel, as described in Part IV, generally resulted in reduced noncohesive sediment transport and deposition and increased cohesive sediment transport in this portion of the Kings Bay approach channel.

124. Cohesive and noncohesive deposition in the channel areas above Drum Point Island (zones 13 to 21) generally demonstrated increased shoaling rates and volumes for the plan channel. The area associated with the Poseidon floating dry dock (zone 15A) was the only area that demonstrated a reduced plan channel total (cohesive plus noncohesive) shoaling rate. Cohesive deposition in this area was reduced from about 7 ft per year for the base condition to about 6 ft per year for the plan condition. Noncohesive deposition for the plan condition was increased a lesser amount in this zone relative to the base condition. This zone demonstrated the largest base and plan shoaling rates for the entire Kings Bay channel. The reduced plan channel total shoaling rate in this area (zone 15A) was the result of the increased channel area associated with the development of the adjacent Poseidon waterfront docking area (zone 16P), which was also predicted to be a high shoaling area (i.e., available shoaling material was distributed across a much larger area).

125. The increased plan channel shoaling rates in Kings Bay were the result of the increased discharge through Kings Bay and reduced current velocities associated with increased plan channel cross-sectional area (depth and width). The upper Kings Bay turning basin (zone 21) demonstrated the second highest plan channel shoaling rate, approximately 6 ft per year. The enhanced plan channel eddy circulation described in Part IV also influenced the high shoaling rate of this zone.

126. As summarized in paragraph 8 and described in detail in the

verification report,* available pre-Trident channel field shoaling rates indicated a wide range of natural variability in channel sedimentation rates. The average pre-Trident channel shoaling rate was about 1.2 million cubic yards per year with extreme values ranging from 0.4 million cubic yards per year to 2.6 million cubic yards per year. This magnitude of variability is common in natural estuarine systems such as Cumberland Sound and Kings Bay. Figure 26 illustrates the average yearly Trident channel shoaling rates predicted by STUDH and associated extreme high and low shoaling rates derived using the pre-Trident channel shoaling rate history as a guide. The predicted long-term average Trident channel shoaling rate is approximately 2.5 million cubic yards per year; however, based on pre-Trident channel shoaling history, the range of yearly channel sedimentation may be as low as 0.9 million cubic yards per year or as high as 4.9 million cubic yards per year. It must be stressed that this does not include catastrophic phenomena such as potentially higher shoaling rates associated with hurricane island breaching.

127. Also, as described in paragraphs 8, 24, and 25 and developed in more detail in the verification report,* the model adjustments and predictions are based upon only a few years of field data collected following pre-Trident channel deepening. The extensive channel expansion undertaken for development of the Trident submarine channel and facilities may have exceeded the model's ability to reproduce the system's sedimentation response to these modifications. The possibility of the need for further model adjustments, i.e., potential sediment armoring reducing the availability of source material, should not be ruled out. However, additional time and field monitoring are required before any other model adjustments can be made with confidence.

Boundary Condition Sensitivity Findings

128. Results from the two RMA-2V sensitivity runs (PGBF and BGPF) were used to investigate sensitivity of STUDH sedimentation to the hydrodynamic boundary forcing conditions. Although the resulting shoaling distributions (location and type) varied between the actual base and plan conditions and these sensitivity runs, the total shoaling volumes for each geometry condition were in agreement (rounded to the newest 100,000 cubic yards). Figure 27

---

* Granat et al., op. cit.
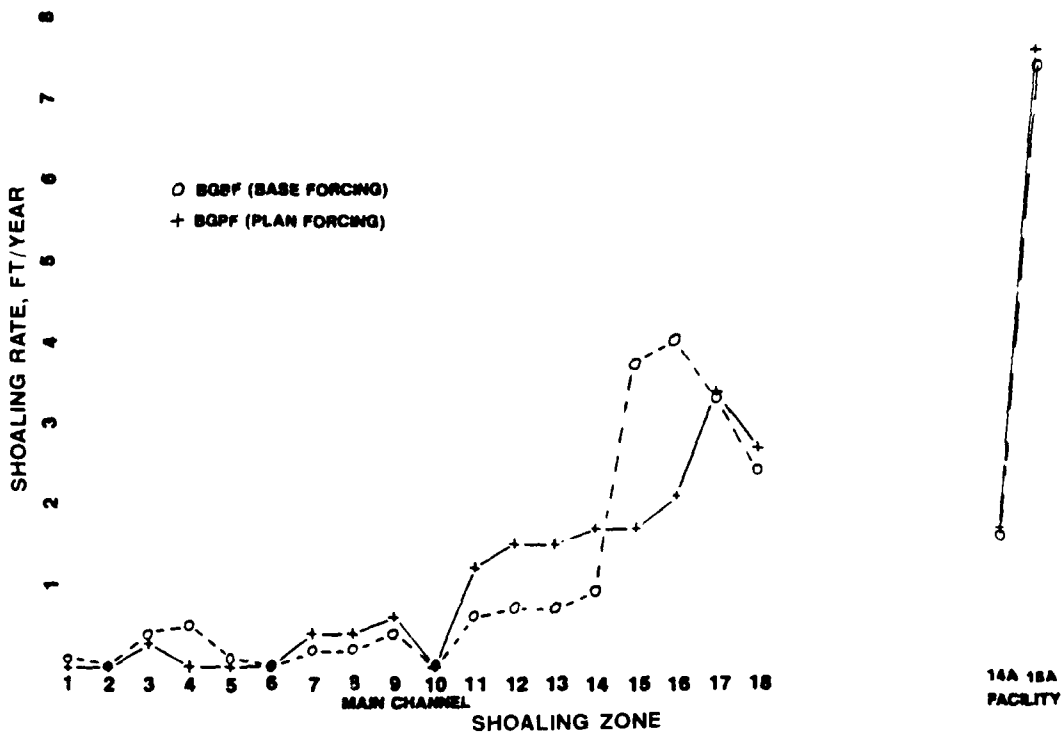
a. Base geometry
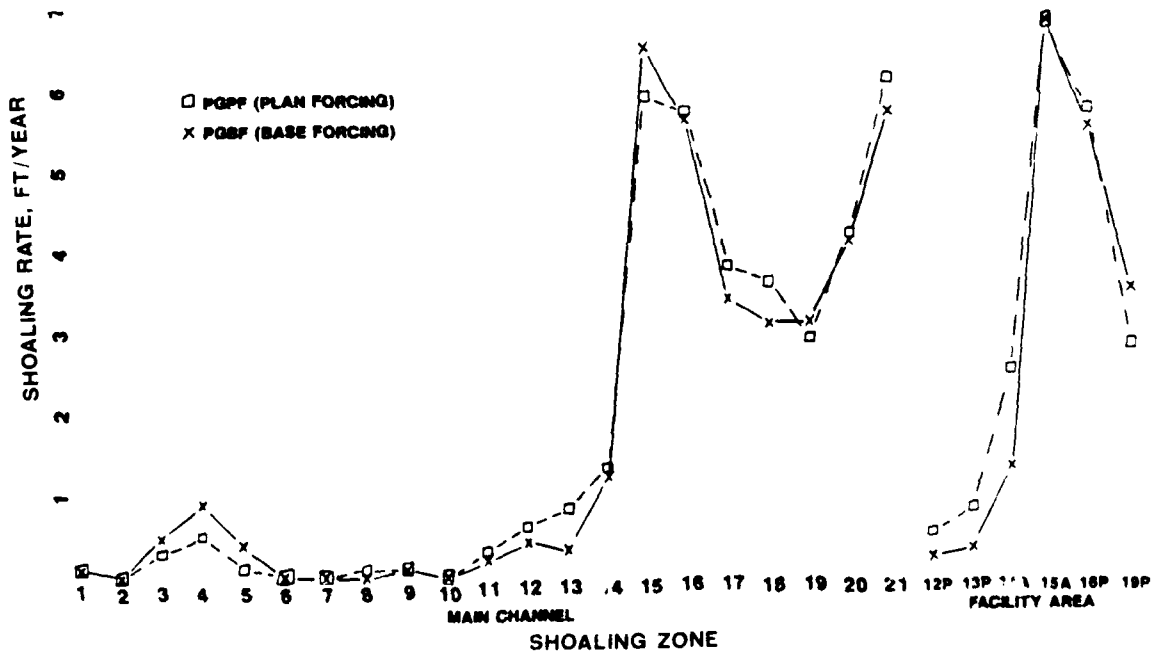
b. Plan geometry

Figure 27. Sensitivity of base and plan channel shoaling rates to hydrodynamic boundary forcing conditions

compares the sensitivity of shoaling rates for the actual base and plan channel geometry conditions to base and plan hydrodynamic boundary forcing conditions.

129. The two plan conditions (plan geometry with plan boundary forcing conditions and plan geometry with base boundary forcing conditions) demonstrated closer shoaling distribution agreement than did the two base geometry conditions. A 5 percent increase in cohesive deposition (from 2.0 million cubic yards per year for the actual plan condition to 2.1 million cubic yards per year for the plan geometry and base boundary condition) was indicated for the sensitivity condition and a 25 percent reduction in noncohesive deposition (from 0.4 million cubic yards per year for the actual plan test to 0.3 million cubic yards per year for the sensitivity condition) were indicated.

130. Although the channel total shoaling volume for each of the two base channel runs were in agreement, the predicted base geometry shoaling distributions demonstrated greater variations than the two plan geometry model runs. Cohesive shoaling was reduced from about 0.8 million cubic yards per year for the actual base condition to about 0.7 million cubic yards per year for the base geometry and plan boundary forcing condition run (i.e., the sensitivity testing condition demonstrated a 12 percent reduction in cohesive deposition). The sensitivity testing condition resulted in a 50 percent increase in noncohesive deposition over that of the actual base condition (from 0.2 million cubic yards per year for the actual base test to 0.3 million cubic yards for the mixed base geometry-plan forcing test). The indicated variations can be logically explained by the mixed boundary and geometry condition. The increased Cumberland Sound channel velocities associated with the crossed condition (BGPF, Figure 22) resulted in an almost twofold increase in noncohesive transport and deposition above zone 6 in Cumberland Sound and into Kings Bay. The increased Cumberland Sound velocities reduced cohesive deposition in the submarine channel south of Kings Bay (below zone 17) and resulted in a slight increase in cohesive deposition in Kings Bay (zones 17 and 18).

131. The findings of these sensitivity runs indicated that the predicted shoaling rates were sensitive to the geometry conditions and the resulting interior hydrodynamic variations and not very sensitive to the hydrodynamic boundary forcing conditions.

132. Boundary condition suspended sediment concentration was another

type of sensitivity analysis examined. The findings of this analysis indicated a nonlinear response trend between submarine channel shoaling rate and boundary condition cohesive suspended sediment concentration. A 30 percent reduction in suspended sediment boundary concentration (from 100 to 70 mg/ℓ) resulted in a 6 percent reduction in total submarine channel cohesive deposition. A 50 percent boundary concentration reduction (to 50 mg/ℓ) resulted in about a 20 percent reduction in total submarine channel cohesive deposition. Little shoaling rate variation (a 3 percent reduction) resulted when the boundary concentration was further reduced from 50 to 25 mg/ℓ. These findings indicate that in the modeling procedure developed for the Kings Bay study, the submarine channel shoaling rates are sensitive to boundary condition suspended sediment concentrations between 50 and 70 mg/ℓ. Concentration variations between 70 to 100 mg/ℓ or 25 to 50 mg/ℓ had a small relative impact on model-predicted submarine channel shoaling rates.

Summary

133. The plan channel condition tested increased the maintained interior channel areas by about 70 percent. Approximately 43 percent of the increased channel area was located within the high shoaling zones of Kings Bay. For the plan condition, model predictions indicated a 150 percent increase in required annual channel maintenance dredging. The long-term average submarine channel maintenance dredging requirement was predicted to increase from approximately 1.0 million cubic yards per year for pre-Trident channel conditions to approximately 2.5 million cubic yards per year for the Trident channel condition tested. Approximately 92 percent (2.3 million cubic yards) of the total plan channel shoaling was located within Kings Bay. Cohesive material (clay and silt) accounted for approximately 80 percent (2.0 million cubic yards) of the total shoaling volume.

134. The hybrid sedimentation model was verified to reproduce observed prototype average channel sedimentation rates for the period July 1979 to August 1982. Thus the base-to-plan sedimentation absolute results should reflect the changes that would occur on average over a comparable period with similar sediment supply. Individual years may experience sedimentation rates appreciably lower or higher than those predicted by the model. The long-term average change in sedimentation rate may be quantitatively different than the

predicted rates, but should be qualitatively similar. Based on previous shoaling history and this study's findings, typical annual plan channel maintenance dredging requirements may vary from a low of about 0.9 million cubic yards per year to a high of about 4.9 million cubic yards per year.

135. In summary, the pre-Trident Kings Bay was an efficient sediment trap. The reduced current velocities and increased discharge through Kings Bay associated with the plan channel modifications are predicted to result in an even more efficient sediment trap. The sedimentation processes of Cumberland Sound and Kings Bay model were found to be sensitive to the channel geometry changes and the resulting interior hydrodynamic changes and were not very sensitive to the hydrodynamic boundary forcing conditions.

PART VI: SUMMARY AND CONCLUSIONS

136. The Kings Bay hybrid modeling system (coupled physical and numeri-
cal models) was used to investigate hydrodynamic and sedimentation variations
between the pre-Trident 1982 base channel condition and the Trident channel
condition planned in 1985. The plan channel condition tested increased the
maintained interior channel area by about 70 percent, from 475 acres for pre-
Trident conditions to 811 acres for Trident channel condition. The lower
Kings Bay turning basin and the St. Marys Inlet turning and sediment basins
designed subsequent to model testing were not included in the modeling study.

137. The Kings Bay hybrid modeling system demonstrated small velocity
differences between the pre-Trident base channel and Trident plan channel con-
ditions. These differences were rather subtle and the results generally pro-
vided trends that could be explained by realistic hydrodynamic variations
associated with the Trident channel expansion.

138. The numerical model information, by the nature of the finite ele-
ment approach, allowed a more detailed but depth-averaged view over the
modeled area of interest compared to the three-dimensional station-specific
information provided by the physical model. The general well-mixed conditions
of the Cumberland Sound/Kings Bay system (vertical and lateral) greatly en-
hanced the reliability of the depth-averaged approach used by the numerical
model. Another advantage of the numerical model data is the repeatable nature
of the solution to the governing equations and the ability of the model to
perform boundary condition sensitivity analyses. In the present application,
however, physical model tide and salinity results are considered superior to
numerical model results since the physical model is fully three-dimensional
(including the extensive marsh areas), and its boundaries are further from the
problem area.

139. Based on the model findings, small base-to-plan hydrodynamic dif-
ferences were identified. The deepened and widened Trident plan channel in-
creased flood and ebb volume transport efficiency of the submarine channel
through St. Marys Inlet into Cumberland Sound and Kings Bay. Flood and ebb
discharge within each tributary at the numerical model boundaries was reduced
for the plan channel condition relative to the base condition. The northern
Cumberland Sound boundary was the only boundary to demonstrate a discharge
dominance change; flow changed from slightly flood-dominated for the base

condition to slightly ebb dominated for the plan condition. Increased dis-
charge through Kings Bay changed the phasing relationships (earlier times of
arrival) north of Kings Bay. Reduced velocity magnitudes in the deepened
upper Kings Bay turning basin demonstrated the largest base-to-plan velocity
differences. A low-velocity recirculation eddy in the upper turning basin,
downstream from the Trident dry dock, was enhanced during the plan condition
ebb cycle.

140. Although tidal effects were not an explicit objective of the
modeling efforts, they were examined. The tested plan condition resulted in
higher high-water and midtide level elevations in the physical and numerical
models. These variations were close to, but still greater than, model detec-
tion limits. Numerical model sensitivity tests demonstrated that numerical
model tidal predictions were more sensitive to boundary conditions than to
geometry variations and therefore were less useful than physical model re-
sults. The sensitivity results did confirm the physical model results of
increased plan channel high-water and midtide level elevations. Concerns ex-
pressed by persons interested in Kings Bay and Cumberland Sound led to a
thorough reevaluation of all model testing results and analysis of recent pro-
totype data. The physical model results were found to indicate a consistent
trend of increasing water level as channel expansion evolved. Based on the
more recent field data, tide range will probably not change as a result of the
Trident channel improvements and mean water level in Cumberland Sound may
increase a small amount, less than the normal annual variation in mean sea
level.

141. The subtle base-to-plan hydrodynamic velocity changes indicated by
the physical and numerical models and the increased plan channel surface area
resulted in dramatic changes in the sedimentation response. The numerical
model predictions indicated a 150 percent increase in required annual plan
channel maintenance dredging. Based on previous shoaling history and this
study's findings, typical annual plan channel maintenace dredging requirements
may vary from a low of about 0.9 million cubic yards per year to a high of
about 4.9 million cubic yards per year. The long-term average maintenance
dredging requirement for the submarine channel was predicted to increase from
approximately 1.0 million cubic yards per year for pre-Trident channel condi-
tions to approximately 2.5 million cubic yards per year for the Trident chan-
nel condition tested. Approximately 92 percent (2.3 million cubic yards) of

the total plan channel shoaling was located within Kings Bay. Cohesive material (clay and silt) accounted for approximately 80 percent (2.0 million cubic yards) of the total shoaling volume.

142. The pre-Trident Kings Bay was an efficient sediment trap. The increased discharge and reduced current velocities associated with the plan channel modifications are predicted to make Kings Bay an even more efficient sediment trap.

143. The numerical model investigations indicated that the sedimentation processes of Cumberland Sound and Kings Bay were sensitive to the channel geometry changes and the resulting interior hydrodynamic changes and were not sensitive to the physical model-derived hydrodynamic boundary forcing conditions.

Table 1

Kings Bay Physical Model Flow Predominance Values

Station Number	Depth	Base Pre-Trident	Plan P4-1
20	Surface	27.0	9.7
	Middepth	26.7	18.7
50	Surface	18.5	-12.3
	Middepth	21.9	7.8
	Bottom	23.6	23.2
60	Surface	-4.5	-5.3
	Middepth	-6.7	-1.1
	Bottom	3.4	6.0
160	Surface	-8.2	-20.9
	Middepth	-5.5	-9.4
180	Middepth	23.9	15.8
230	Surface	-11.7	-5.7
	Bottom	-2.5	-6.4
240	Surface	-14.9	-19.0
	Bottom	-8.9	-18.1
396	Surface	-4.5	-9.7
	Bottom	-4.7	-6.1
584	Surface	18.7	12.5
	Bottom	17.5	11.9
650	Surface	-14.0	-11.8
	Middepth	-9.8	-10.4
	Bottom	-6.2	-3.9
812	Middepth	-2.0	-10.4
818	Surface	-2.4	-0.9
	Middepth	-3.0	-1.5
	Bottom	-3.5	0.1
843	Surface	-13.0	-11.5
	Middepth	-7.5	-9.7
	Bottom	1.5	2.7
1014	Middepth	-6.8	-9.3

(Continued)

Note: Negative values indicate ebb dominance.

Table 1 (Continued)

Station Number	Depth	Base Pre-Trident	Plan P4-1
1055	Surface	-9.1	-11.3
	Middepth	-9.9	-4.7
	Bottom	-9.9	-6.6
1066	Middepth	ND	33.5
1142	Surface	-2.8	-34.6
	Middepth	0.3	19.7
	Bottom	2.7	36.0
1153	Surface	-10.7	-10.5
	Middepth	-1.1	0.8
	Bottom	3.6	0.9
1182	Surface	-11.6	-14.6
	Middepth	-4.2	39.3
	Bottom	-1.2	42.5
1276	Surface	8.4	-19.1
	Bottom	-0.7	-8.4
1385	Surface	-2.6	-0.4
	Midepth	-1.9	11.0
	Bottom	3.4	3.6
1851	Surface	-0.8	-9.3
	Middepth	-3.9	12.8
	Bottom	3.0	18.7
1865	Surface	-2.8	-8.9
	Middepth	-1.8	-8.8
	Bottom	-0.7	-7.3
1869	Surface	-7.5	-8.0
	Middepth	0.0	-7.6
	Bottom	-0.7	-5.3
1883	Surface	-6.6	-8.7
	Bottom	-6.1	-11.7
1915	Surface	-10.7	-13.3
	Middepth	-11.5	3.5
	Bottom	-16.0	7.2
1979	Surface	-13.0	-17.7
	Bottom	-14.0	-16.0

(Continued)

Table 1 (Concluded)

Station Number	Depth	Base Pre-Trident	Plan P4-1
1981	Surface	6.9	11.5
	Middepth	−2.6	7.3
	Bottom	−4.4	1.2
1989	Surface	−20.4	−13.8
	Middepth	−17.7	−17.8
	Bottom	−14.2	−18.2
1999	Surface	−25.0	−12.7
	Middepth	−23.8	−9.4
	Bottom	−17.6	−11.1
2074	Surface	5.7	5.6
	Middepth	7.4	7.8
	Bottom	−3.7	8.9
2089	Surface	12.5	−12.7
	Middepth	7.8	−13.2
	Bottom	17.5	1.2
2120	Surface	−16.2	−17.5
	Middepth	−11.8	−5.4
	Bottom	−7.8	−3.6
2122	Surface	1.5	−2.3
	Middepth	8.7	−3.2
	Bottom	4.0	−0.6
2124	Surface	12.8	0.5
	Middepth	6.2	1.1
	Bottom	3.7	−0.3

Table 2

RMA-2V Hydrodynamic Coefficients

Type	Description	Turbulent Exchange lb-sec/sq ft	Manning's n
1	Small channel	100	0.025
2	Normal channel	100	0.020
3	Smooth channel	100	0.015
4	Main marsh	200	0.050
5	Secondary marsh	170	0.040
6	Marsh/channel transition	150	0.030
7	Ocean	500	0.020
8	Dock facility	300	0.030
9	Dry dock/tender	70	0.030

Table 3

Cohesive Sedimentation Coefficients

Coefficient	Cycle 1	Cycle 2	Cycle 3
Crank-Nicholson THETA	0.66	0.66	0.66
Critical shear stress deposition, N/sq m	0.05	0.05	0.05
Dry weight density of freshly deposited layer, kg/cu m	300	300	300
Particle specific gravity	2.65	2.65	2.65
Erosion rate constant, kg/sq m/sec	0.002	0.002	0.002
Effective diffusion, sq m/sec	50	50	50
Boundary inflow sediment concentration, kg/cu m	0.10	0.10	0.10
Exterior boundary particle settling velocity, m/sec	0.0	0.0	0.0
Interior boundary particle settling velocity, m/sec	0.0006	0.0003	0.0003
Critical shear stress particle erosion, N/sq m	0.15	0.12	0.12
Sediment bed initialization	Non-eroding	Hot start cycle 1	Hot start cycle 2
Initialization of suspended sediment concentration	0.10	0.10	Hot start cycle 2

Table 4

Noncohesive Sedimentation Coefficients

Crank–Nicholson THETA	0.66
Particle specific gravity	2.65
Particle shape factor	0.70
Length factor for deposition (times depth)	0.50
Length factor for erosion (times depth)	10.0
Effective diffusion, sq m/sec	250
Boundary inflow sediment concentration, kg/cu m	0.01
Median sediment grain size D_{50}, mm	
Coarse sand	0.70
Medium sand	0.35
Fine sand	0.125
Particle settling velocity, m/sec	
Coarse sand	0.090
Medium sand	0.045
Fine sand	0.0105
Manning's n value	
Ocean	0.025
Channel bend at Lower Cumberland Sound	0.015
Channel bend at Kings Bay entrance	0.010
All other areas	0.020

Table 5

Numerical Model Shoaling Predictions

Zone	Area 1,000 sq ft		Cohesive Shoaling				Noncohesive Shoaling				Total Shoaling*			
			Volume 1,000 cu yd/year		Rate ft/year		Volume 1,000 cu yd/year		Rate ft/year		Volume 1,000 cu yd/year		Rate ft/year	
	Base	Plan	Base	Plan	Base	Plan	Base	Plan	Base	Plan	Base	Plan	Base	Plan
1	1,338	1,688	NA	NA	NA	NA	5	6	0.1	0.1	5	6	0.1	0.1
2	1,485	1,839	NA	NA	NA	NA	NA	NA	NA	NA	NA	NA	NA	NA
3	1,077	1,641	NA	NA	NA	NA	18	21	0.4	0.3	18	21	0.4	0.3
4	1,304	1,722	NA	NA	NA	NA	24	31	0.5	0.5	24	31	0.5	0.5
5	1,511	1,997	NA	NA	NA	NA	5	11	0.1	0.1	5	11	0.1	0.1
6	965	2,264	NA	NA	NA	NA	NA	NA	NA	NA	NA	NA	NA	NA
7	892	1,489	NA	NA	NA	NA	5	2	0.2	NA	5	2	0.2	NA
8	796	1,580	NA	NA	NA	NA	7	3	0.2	0.1	7	3	0.2	0.1
9	594	848	NA	NA	NA	NA	8	4	0.4	0.1	8	4	0.4	0.1
10	661	1,147	NA	NA	NA	NA	NA	NA	NA	NA	NA	NA	NA	NA
11	834	1,221	NA	NA	NA	NA	19	12	0.6	0.3	19	12	0.6	0.3
12	710	710	NA	NA	NA	NA	20	16	0.7	0.6	20	16	0.7	0.6
13	718	718	NA	NA	NA	NA	19	22	0.7	0.8	19	22	0.7	0.8
14	666	666	NA	NA	NA	NA	21	32	0.9	1.3	21	32	0.9	1.3
15	661	661	73	117	3.0	4.8	16	27	0.7	1.1	90	144	3.7	5.9
16	1,109	1,109	151	207	3.7	5.1	15	27	0.4	0.7	156	235	4.0	5.7
17	1,966	1,966	229	264	3.1	3.6	9	14	0.1	0.2	238	278	3.3	3.8
18	2,305	2,305	177	297	2.2	3.5	11	7	0.1	0.1	188	304	2.4	3.6
19	NI	1,646	(9)	167	0.2	2.8	(NA)	10	(0.1)	0.2	(10)	177	(0.2)	2.9
20	NI	709	(2)	99	0.1	3.8	(9)	11	(0.4)	0.4	(11)	110	(0.4)	4.2
21	NI	2,137	(73)	423	0.9	5.3	(18)	62	(0.2)	0.8	(92)	484	(1.2)	6.1

(Continued)

Note: Values were rounded to significant figures after all computations were completed. NI or ( ) indicates zone not part of channel condition. NA indicates no appreciable shoaling.

* Summation of cohesive and noncohesive deposition.

Table 5 (Concluded)

Zone	Area 1,000 sq ft		Cohesive Shoaling Volume 1,000 cu yd/year		Cohesive Shoaling Rate ft/year		Noncohesive Shoaling Volume 1,000 cu yd/year		Noncohesive Shoaling Rate ft/year		Total Shoaling* Volume 1,000 cu yd/year		Total Shoaling* Rate ft/year	
	Base	Plan	Base	Plan	Base	Plan	Base	Plan	Base	Plan	Base	Plan	Base	Plan
12P	NI	1,803	NI	NA	NI	NA	NI	32	NI	0.5	NI	32	NI	0.5
13P	NI	515	NI	NA	NI	NA	NI	15	NI	0.8	NI	15	NI	0.8
14A	529	529	18	27	0.9	1.4	13	21	0.7	1.1	31	48	1.6	2.5
15A	588	588	151	127	6.9	5.8	11	21	0.7	1.1	162	148	7.4	6.8
16P	NI	1,426	NI	266	NI	5.0	NI	34	NI	0.7	NI	300	NI	5.7
19P	NI	418	NI	41	NI	2.7	NI	2	NI	0.1	NI	43	NI	2.8
Total	20,708	35,340	799	2,035			225	443			1,023	2,478		

APPENDIX A: THE TABS-2 SYSTEM

1. TABS-2 is a collection of generalized computer programs and utility
codes integrated into a numerical modeling system for studying two-dimensional
hydrodynamics, sedimentation, and transport problems in rivers, reservoirs,
bays, and estuaries. A schematic representation of the system is shown in
Figure A1. It can be used either as a stand-alone solution technique or as a
step in the hybrid modeling approach. The basic concept is to calculate
water-surface elevations, current patterns, sediment erosion, transport and
deposition, the resulting bed surface elevations, and the feedback to hydrau-
lics. Existing and proposed geometry can be analyzed to determine the impact
on sedimentation of project designs and to determine the impact of project
designs on salinity and on the stream system. The system is described in de-
tail by Thomas and McAnally (1985).

2. The three basic components of the system are as follows:

<u>a</u>. "A Two-Dimensional Model for Free Surface Flows," RMA-2V.

<u>b</u>. "Sediment Transport in Unsteady 2-Dimensional Flows, Horizontal
Plane," STUDH.

<u>c</u>. "Two-Dimensional Finite Element Program for Water Quality,"
RMA-4.

3. RMA-2V is a finite element solution of the Reynolds form of the
Navier-Stokes equations for turbulent flows. Friction is calculated with
Manning's equation and eddy viscosity coefficients are used to define the
turbulent losses. A velocity form of the basic equation is used with side
boundaries treated as either slip or static. The model automatically recog-
nizes dry elements and corrects the mesh accordingly. Boundary conditions may
be water-surface elevations, velocities, or discharges and may occur inside
the mesh as well as along the edges.

4. The sedimentation model, STUDH, solves the convection-diffusion
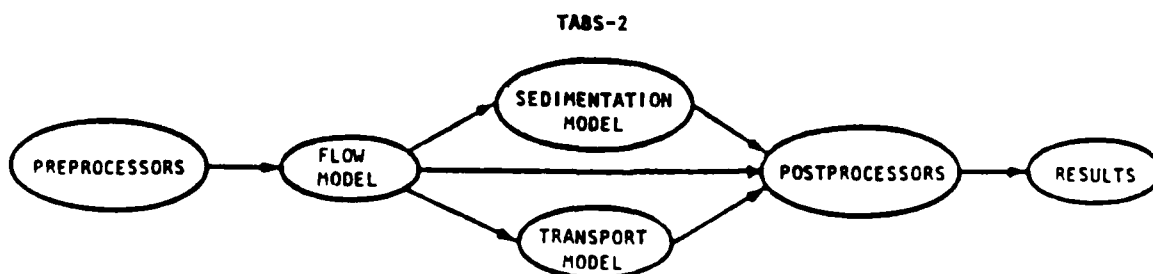
Figure A1. TABS-2 schematic

A3

equation with bed source terms. These terms are structured for either sand or cohesive sediments. The Ackers-White (1973) procedure is used to calculate a sediment transport potential for the sands from which the actual transport is calculated based on availability. Clay erosion is based on work by Partheniades (1962) and Ariathurai and the deposition of clay utilizes Krone's equations (Ariathurai, MacArthur, and Krone 1977). Deposited material forms layers, as shown in Figure A2, and bookkeeping allows up to 10 layers at each node for maintaining separate material types, deposit thickness, and age. The code uses the same mesh as RMA-2V.

5. Salinity calculations, RMA-4, are made with a form of the convective-diffusion equation which has general source-sink terms. Up to seven conservative substances or substances requiring a decay term can be routed. The code uses the same mesh as RMA-2V.

6. Each of these generalized computer codes can be used as a stand-alone program, but to facilitate the preparation of input data and to aid in analyzing results, a family of utility programs was developed for the following purposes:

      <u>a</u>. Digitizing

      <u>b</u>. Mesh generation

      <u>c</u>. Spatial data management

      <u>d</u>. Graphical output

      <u>e</u>. Output analysis

      <u>f</u>. File management

      <u>g</u>. Interfaces

      <u>h</u>. Job control language

Finite Element Modeling

7. The TABS-2 numerical models used in this effort employ the finite element method to solve the governing equations. To help those who are unfamiliar with the method to better understand this report, a brief description of the method is given here.

8. The finite element method approximates a solution to equations by dividing the area of interest into smaller subareas, which are called elements. The dependent variables (e.g., water-surface elevations and sediment concentrations) are approximated over each element by continuous functions

A4
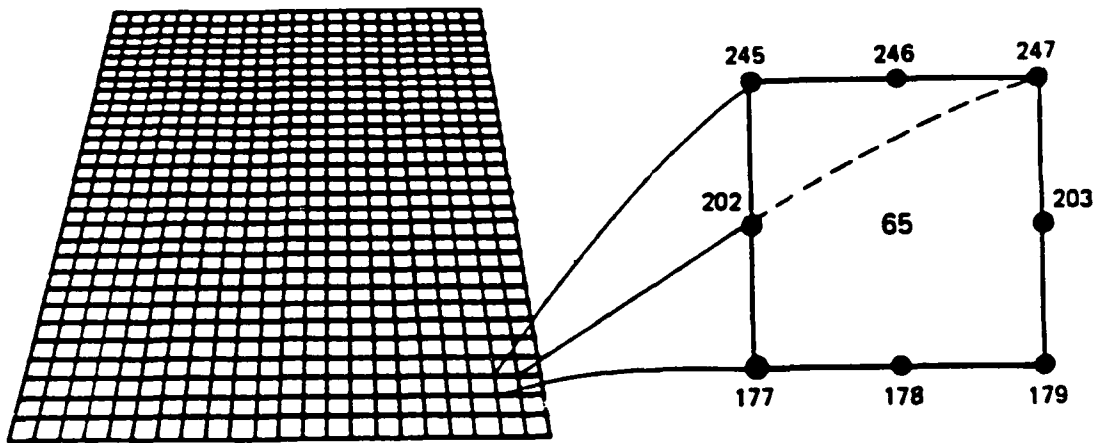
a. Eight nodes define each element
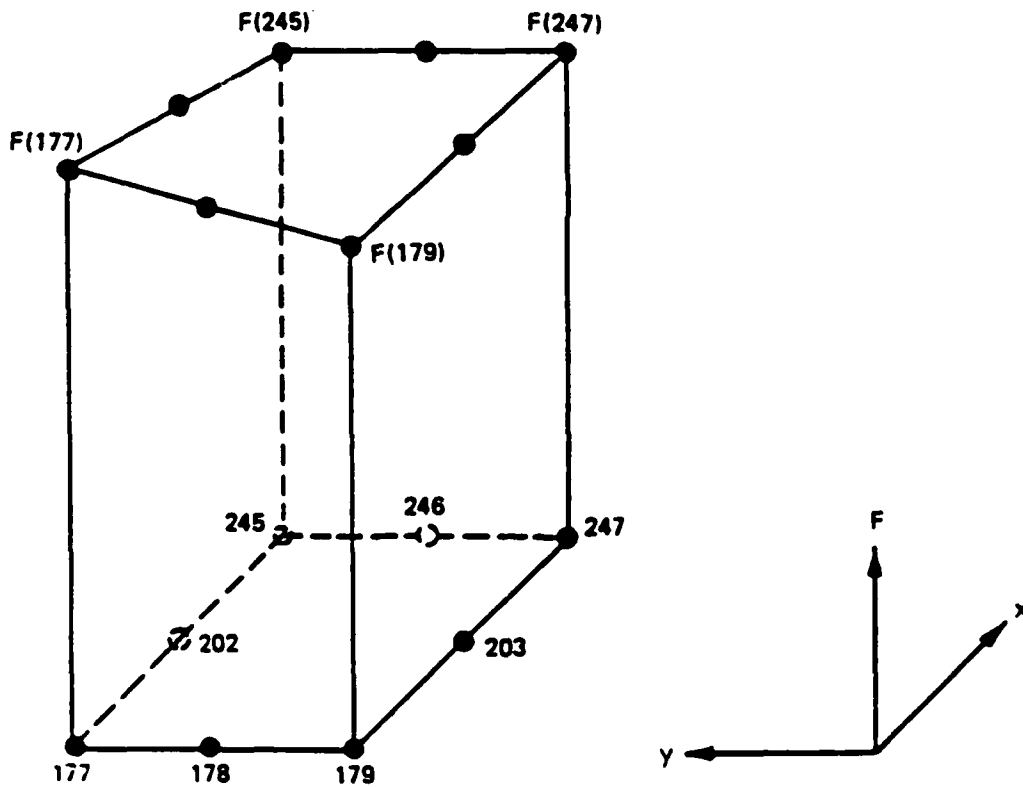
b. Linear interpolation function

Figure A2. Two-dimensional finite element mesh

A5

which interpolate in terms of unknown point (node) values of the variables. An error, defined as the deviation of the approximation solution from the correct solution, is minimized. Then, when boundary conditions are imposed, a set of solvable simultaneous equations is created. The solution is continuous over the area of interest.

9. In one-dimensional problems, elements are line segments. In two-dimensional problems, the elements are polygons, usually either triangles or quadrilaterals. Nodes are located on the edges of elements and occasionally inside the elements. The interpolating functions may be linear or higher order polynomials. Figure A2 illustrates a quadrilateral element with eight nodes and a linear solution surface where F is the interpolating function.

10. Most water resource applications of the finite element method use the Galerkin method of weighted residuals to minimize error. In this method the residual, the total error between the approximate and correct solutions, is weighted by a function that is identical with the interpolating function and then minimized. Minimization results in a set of simultaneous equations in terms of nodal values of the dependent variable (e.g. water-surface elevations or sediment concentration). The time portion of time-dependent problems can be solved by the finite element method, but it is generally more efficient to express derivatives with respect to time in finite difference form.

The Hydrodynamic Model, RMA-2V

Applications

11. This program is designed for far-field problems in which vertical accelerations are negligible and the velocity vectors at a node generally point in the same directions over the entire depth of the water column at any instant of time. It expects a homogeneous fluid with a free surface. Both steady and unsteady state problems can be analyzed. A surface wind stress can be imposed.

12. The program has been applied to calculate flow distribution around islands; flow at bridges having one or more relief openings, in contracting and expanding reaches, into and out of off-channel hydropower plants, at river junctions, and into and out of pumping plant channels; and general flow patterns in rivers, reservoirs, and estuaries.

Limitations

13. This program is not designed for near-field problems where flow-structure interactions (such as vortices, vibrations, or vertical accelerations) are of interest. Areas of vertically stratified flow are beyond this program's capability unless it is used in a hybrid modeling approach. It is two-dimensional in the horizontal plane, and zones where the bottom current is in a different direction from the surface current must be analyzed with considerable subjective judgment regarding long-term energy considerations. It is a free-surface calculation for subcritical flow problems.

Governing equations

14. The generalized computer program RMA-2V solves the depth-integrated equations of fluid mass and momentum conservation in two horizontal directions. The form of the solved equations is

$$h \frac{\partial u}{\partial t} + hu \frac{\partial u}{\partial x} + hv \frac{\partial u}{\partial y} - \frac{h}{\rho} \left[\epsilon_{xx} \frac{\partial^2 u}{\partial x^2} + \epsilon_{xy} \frac{\partial^2 u}{\partial y^2} \right] + gh \left[\frac{\partial a}{\partial x} + \frac{\partial h}{\partial x} \right]$$

$$+ \frac{gun^2}{\left[1.486 h^{1/6} \right]^2} \left[u^2 + v^2 \right]^{1/2} - \varsigma V_a^2 \cos \psi - 2h\omega v \sin \phi = 0 \qquad (A1)$$

$$h \frac{\partial v}{\partial t} + hu \frac{\partial v}{\partial x} + hv \frac{\partial v}{\partial y} - \frac{h}{\rho} \left[\epsilon_{yx} \frac{\partial^2 v}{\partial x^2} + \epsilon_{yy} \frac{\partial^2 v}{\partial y^2} \right] + gh \left[\frac{\partial a}{\partial y} + \frac{\partial h}{\partial y} \right]$$

$$+ \frac{gvn^2}{\left[1.486 h^{1/6} \right]^2} \left[u^2 + v^2 \right]^{1/2} - \varsigma V_a^2 \sin \psi + 2\omega hu \sin \phi = 0 \qquad (A2)$$

$$\frac{\partial h}{\partial t} + h \left[\frac{\partial u}{\partial x} + \frac{\partial v}{\partial y} \right] + u \frac{\partial h}{\partial x} + v \frac{\partial h}{\partial y} = 0 \qquad (A3)$$

where

h = depth

u, v = velocities in the Cartesian directions

x, y, t = Cartesian coordinates and time

ρ = density

A7

ϵ = eddy viscosity coefficient, for xx = normal direction on x-axis surface; yy = normal direction on y-axis surface; xy and yx = shear direction on each surface

g = acceleration due to gravity

a = elevation of bottom

n = Manning's n value

1.486 = conversion from SI (metric) to non-SI units

ζ = empirical wind shear coefficient

V_a = wind speed

ψ = wind direction

ω = rate of earth's angular rotation

ϕ = local latitude

15.   Equations A1, A2, and A3 are solved by the finite element method using Galerkin weighted residuals. The elements may be either quadrilaterals or triangles and may have curved (parabolic) sides. The shape functions are quadratic for flow and linear for depth. Integration in space is performed by Gaussian integration. Derivatives in time are replaced by a nonlinear finite difference approximation. Variables are assumed to vary over each tim_ interval in the form

$$f(t) = f(0) + at + bt^c \qquad t_0 \leq t < t \qquad (A4)$$

which is differentiated with respect to time, and cast in finite difference form. Letters a , b , and c are constants. It has been found by experiment that the best value for c is 1.5 (Norton and King 1977).

16.   The solution is fully implicit and the set of simultaneous equations is solved by Newton-Raphson iteration. The computer code executes the solution by means of a front-type solver that assembles a portion of the matrix and solves it before assembling the next portion of the matrix. The front solver's efficiency is largely independent of bandwidth and thus does not require as much care in formation of the computational mesh as do traditional solvers.

17.   The code RMA-2V is based on the earlier version RMA-2 (Norton and King 1977) but differs from it in several ways. It is formulated in terms of velocity (v) instead of unit discharge (vh), which improves some aspects of the code's behavior; it permits drying and wetting of areas within the grid;

and it permits specification of turbulent exchange coefficients in directions other than along the x- and z-axes. For a more complete description, see Appendix F of Thomas and McAnally (1985).

The Sediment Transport Model, STUDH

Applications

18. STUDH can be applied to clay and/or sand bed sediments where flow velocities can be considered two-dimensional (i.e., the speed and direction can be satisfactorily represented as a depth-averaged velocity). It is useful for both deposition and erosion studies and, to a limited extent, for stream width studies. The program treats two categories of sediment: noncohesive, which is referred to as sand here, and cohesive, which is referred to as clay.

Limitations

19. Both clay and sand may be analyzed, but the model considers a single, effective grain size for each and treats each separately. Fall velocity must be prescribed along with the water-surface elevations, x-velocity, y-velocity, diffusion coefficients, bed density, critical shear stresses for erosion, erosion rate constants, and critical shear stress for deposition.

20. Many applications cannot use long simulation periods because of their computation cost. Study areas should be made as small as possible to avoid an excessive number of elements when dynamic runs are contemplated yet must be large enough to permit proper posing of boundary conditions. The same computation time interval must be satisfactory for both the transverse and longitudinal flow directions.

21. The program does not compute water-surface elevations or velocities; therefore these data must be provided. For complicated geometries, the numerical model for hydrodynamic computations, RMA-2V, is used.

Governing equations

22. The generalized computer program STUDH solves the depth-integrated convection-dispersion equation in two horizontal dimensions for a single sediment constituent. For a more complete description, see Appendix G of Thomas and McAnally (1985). The form of the solved equation is

$$\frac{\partial C}{\partial t} + u\frac{\partial C}{\partial x} + v\frac{\partial C}{\partial y} - \frac{\partial}{\partial x}\left(D_x\frac{\partial C}{\partial x}\right) + \frac{\partial}{\partial y}\left(D_y\frac{\partial C}{\partial y}\right) + \alpha_1 C + \alpha_2 = 0 \qquad (A5)$$

where

C = concentration of sediment

u = depth-integrated velocity in x-direction

v = depth-integrated velocity in y-direction

D_x = dispersion coefficient in x-direction

D_y = dispersion coefficient in y-direction

α_1 = coefficient of concentration-dependent source/sink term

α_2 = coefficient of source/sink term

23. The source/sink terms in Equation B5 are computed in routines that treat the interaction of the flow and the bed. Separate sections of the code handle computations for clay bed and sand bed problems.

Sand transport

24. The source/sink terms are evaluated by first computing a potential sand transport capacity for the specified flow conditions, comparing that capacity with the amount of sand actually being transported, and then eroding from or depositing to the bed at a rate that would approach the equilibrium value after sufficient elapsed time.

25. The potential sand transport capacity in the model is computed by the method of Ackers and White (1973), which uses a transport power (work rate) approach. It has been shown to provide superior results for transport under steady-flow conditions (White, Milli, and Crabbe 1975) and for combined waves and currents (Swart 1976). Flume tests at the US Army Engineer Waterways Experiment Station have shown that the concept is valid for transport by estuarine currents.

26. The total load transport function of Ackers and White is based upon a dimensionless grain size

$$D_{gr} = D \left[\frac{g(s - 1)}{\nu^2} \right]^{1/3} \tag{A6}$$

where

D = sediment particle diameter

s = specific gravity of the sediment

ν = kinematic viscosity of the fluid

and a sediment mobility parameter

A10

$$F_{gr} = \left[\frac{\tau^{n'} \tau'^{(1-n')}}{\rho g D (s - 1)} \right]^{1/2}$$

(A7)

where

  τ = total boundary shear stress

  n' = a coefficient expressing the relative importance of bed-load and suspended-load transport, given in Equation A9

  τ' = boundary surface shear stress

The surface shear stress is that part of the total shear stress which is due to the rough surface of the bed only, i.e., not including that part due to bed forms and geometry. It therefore corresponds to that shear stress that the flow would exert on a plane bed.

27. The total sediment transport is expressed as an effective concentration

$$G_p = C \left[\frac{F_{gr}}{A} - 1 \right]^m \frac{sD}{h} \left[\frac{\rho}{\tau} U \right]^{n'}$$

(A8)

where U is the average flow speed, and for $1 < D_{gr} \leq 60$

$$n' = 1.00 - 0.56 \log D_{gr}$$

(A9)

$$A = \frac{0.23}{\sqrt{D_{gr}}} + 0.14$$

(A10)

$$\log C = 2.86 \log D_{gr} - (\log D_{gr})^2 - 3.53$$

(A11)

$$m = \frac{9.66}{D_{gr}} + 1.34$$

(A12)

For $D_{gr} < 60$

$$n' = 0.00$$

(A13)

A11

$$A = 0.17 \tag{A14}$$

$$C = 0.025 \tag{A15}$$

$$m = 1.5 \tag{A16}$$

28. Equations A6-A16 result in a potential sediment concentration G_p This value is the depth-averaged concentration of sediment that will occur if an equilibrium transport rate is reached with a nonlimited supply of sediment. The rate of sediment deposition (or erosion) is then computed as

$$R = \frac{G_p - C}{t_c} \tag{A17}$$

where

   C = present sediment concentration

   t_c = time constant

For deposition, the time constant is

$$t_c = \text{larger of} \begin{cases} \Delta t \\ \text{or} \\ \dfrac{C_d h}{V_s} \end{cases} \tag{A18}$$

and for erosion it is

$$t_c = \text{larger of} \begin{cases} \Delta t \\ \text{or} \\ \dfrac{C_e h}{U} \end{cases} \tag{A19}$$

where

   Δt = computational time-step

   C_d = response time coefficient for deposition

   V_s = sediment settling velocity

   C_e = response time coefficient for erosion

A12

The sand bed has a specified initial thickness which limits the amount of ero-
sion to that thickness.

Cohesive sediments transport

29. Cohesive sediments (usually clays and some silts) are considered to
be depositional if the bed shear stress exerted by the flow is less than a
critical value τ_d . When that value occurs, the deposition rate is given by
Krone's (1962) equation

$$S = \begin{cases} -\dfrac{2V_s}{h} C \left(1 - \dfrac{\tau}{\tau_d}\right) & \text{for} \quad C < C_c \qquad\qquad (A20) \\[3em] -\dfrac{2V_s}{hC_c^{4/3}} C^{5/3}\left(1 - \dfrac{\tau}{\tau_d}\right) & \text{for} \quad C > C_c \qquad\qquad (A21) \end{cases}$$

where

  S = source term

  V_s = fall velocity of a sediment particle

  h = flow depth

  C = sediment concentration in water column

  τ = bed shear stress

  τ_d = critical shear stress for deposition

  C_c = critical concentration = 300 mg/ℓ

30. If the bed shear stress is greater than the critical value for par-
ticle erosion τ_e , material is removed from the bed. The source term is then
computed by Ariathurai's (Ariathurai, MacArthur, and Krone 1977) adaptation of
Partheniades' (1962) findings:

$$S = \frac{P}{h}\left[\frac{\tau}{\tau_e} - 1\right] \quad \text{for } \tau > \tau_e \qquad\qquad (A22)$$

where P is the erosion rate constant, unless the shear stress is also
greater than the critical value for mass erosion. When this value is
exceeded, mass failure of a sediment layer occurs and

$$S = \frac{T_L P_L}{h \Delta t} \quad \text{for } \tau > \tau_s \tag{A23}$$

where

T_L = thickness of the failed layer

P_L = density of the failed layer

Δt = time interval over which failure occurs

τ_s = bulk shear strength of the layer

31. The cohesive sediment bed consists of 1 to 10 layers, each with a distinct density and erosion resistance. The layers consolidate with overburden and time.

Bed shear stress

32. Bed shear stresses are calculated from the flow speed according to one of four optional equations: the smooth-wall log velocity profile or Manning equation for flows alone; and a smooth bed or rippled bed equation for combined currents and wind waves. Shear stresses are calculated using the shear velocity concept where

$$\tau_b = \rho u_*^2 \tag{A24}$$

where

τ_b = bed shear stress

u_* = shear velocity

and the shear velocity is calculated by one of four methods:

    <u>a</u>. Smooth-wall log velocity profiles

$$\frac{\bar{u}}{u_*} = 5.75 \ \log \left(3.32 \ \frac{u_* h}{\nu} \right) \tag{A25}$$

which is applicable to the lower 15 percent of the boundary layer when

$$\frac{u_* h}{\nu} > 30$$

where u is the mean flow velocity (resultant of u and v components)

b. The Manning shear stress equation

$$u_* = \frac{\left(\overline{un}\right)\sqrt{g}}{CME\ (h)^{1/6}} \qquad (A26)$$

where CME is a coefficient of 1 for SI (metric) units and 1.486 for non-SI units of measurement.

c. A Jonsson-type equation for surface shear stress (plane beds) caused by waves and currents

$$u_* = \sqrt{\frac{1}{2}\left(\frac{f_w u_{om} + f_c \bar{u}}{u_{om} + \bar{u}}\right)\left(\bar{u} + u_{om}\right)^2} \qquad (A27)$$

where

f_w = shear stress coefficient for waves

u_{om} = maximum orbital velocity of waves

f_c = shear stress coefficient for currents

d. A Bijker-type equation for total shear stress caused by waves and current

$$u_* = \sqrt{\frac{1}{2}f_c \bar{u}^2 + \frac{1}{4}f_w u_{om}^2} \qquad (A28)$$

Solution method

33. Equation A5 is solved by the finite element method using Galerkin weighted residuals. Like RMA-2V, which uses the same general solution technique, elements are quadrilateral and may have parabolic sides. Shape functions are quadratic. Integration in space is Gaussian. Time-stepping is performed by a Crank-Nicholson approach with a weighting factor (θ) of 0.66. A front-type solver similar to that in RMA-2V is used to solve the simultaneous equations.

A15

References

Ackers, P., and White, W. R. 1973. (Nov). "Sediment Transport: New Approach and Analysis," Journal, Hydraulics Division, American Society of Civil Engineers, Vol 99, No. HY-11, pp 2041-2060.

Ariathurai, R., MacArthur, R. D., and Krone, R. C. 1977 (Oct). "Mathematical Model of Estuarial Sediment Transport," Technical Report D-77-12, US Army Engineer Waterways Experiment Station, Vicksburg, MS.

Krone, R. B. 1962. "Flume Studies of Transport of Sediment in Estuarial Shoaling Processes," Final Report, Hydraulics Engineering Research Laboratory, University of California, Berkeley, CA.

Norton, W. R., and King, I. P. 1977 (Feb). "Operating Instructions for the Computer Program RMA-2V," Resource Management Associates, Lafayette, CA.

Partheniades, E. 1962. "A Study of Erosion and Deposition of Cohesive Soils in Salt Water," Ph.D. Dissertation, University of California, Berkeley, CA.

Swart, D. H. 1976 (Sep). "Coastal Sediment Transport, Computation of Longshore Transport," R968, Part 1, Delft Hydraulics Laboratory, The Netherlands.

Thomas, W. A., and McAnally, W. H., Jr. 1985 (Aug). "User's Manual for the Generalized Computer Program System; Open-Channel Flow and Sedimentation, TABS-2, Main Text and Appendices A through O," Instruction Report HL-85-1, US Army Engineer Waterways Experiment Station, Vicksburg, MS.

White, W. R., Milli, H., and Crabbe, A. D. 1975. "Sediment Transport Theories: An Appraisal of Available Methods," Report Int 119, Vols 1 and 2, Hydraulics Research Station, Wallingford, England.

APPENDIX B: TIDES IN CUMBERLAND SOUND, GEORGIA, BEFORE AND AFTER
ENLARGEMENT OF THE KINGS BAY NAVAL BASE CHANNELS

This appendix is bound separately in Volume II.

APPENDIX C: PHYSICAL MODEL PRE-TRIDENT BASE
AND TRIDENT PLAN 4 COMPARISONS
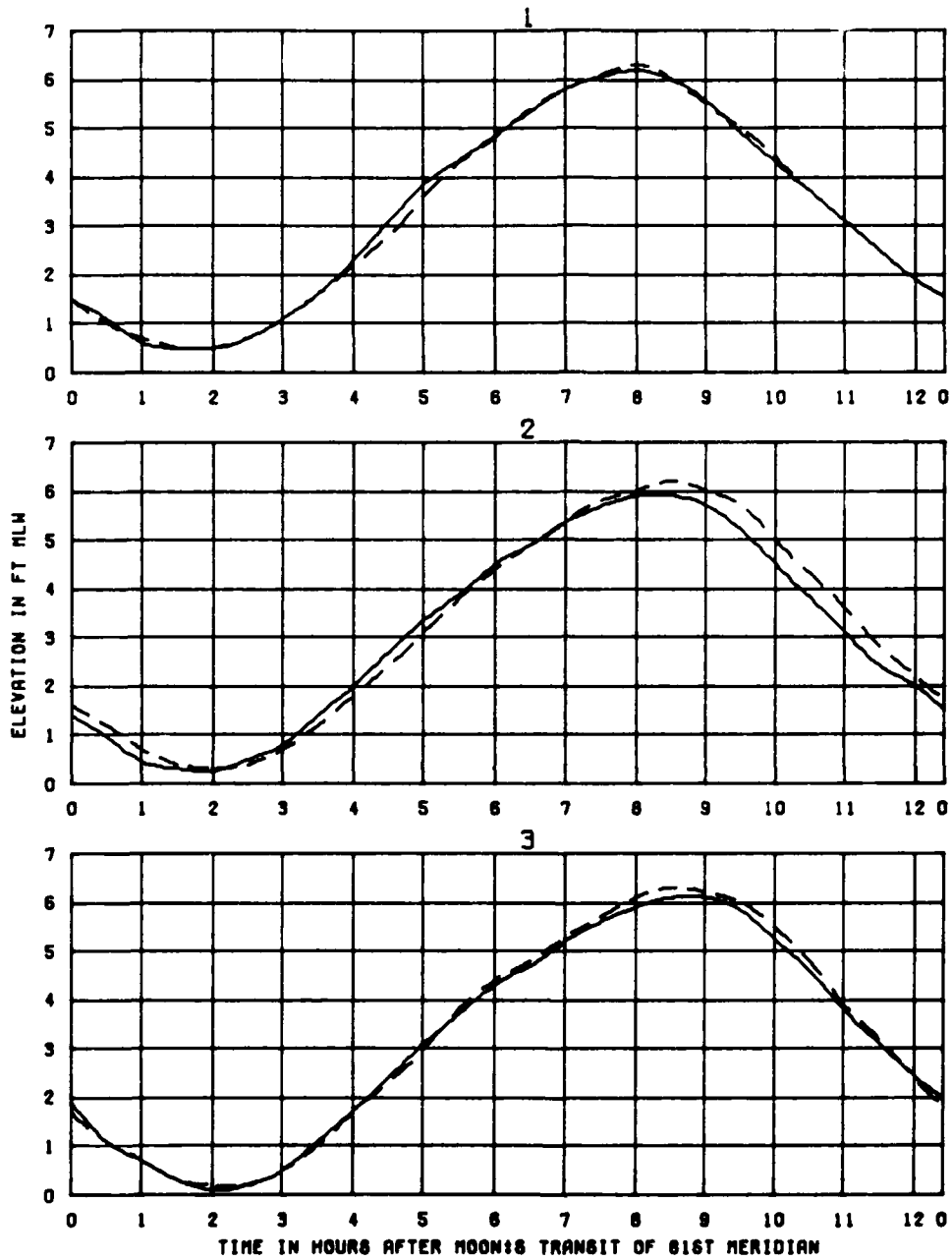
Graph 1 (top): Elevation in ft MLW vs Time in hours. Y-axis 0-7, X-axis 0-12 0.

Graph 2 (middle): ELEVATION IN FT MLW vs Time. Y-axis 0-7, X-axis 0-12 0.

Graph 3 (bottom): Elevation vs TIME IN HOURS AFTER MOON'S TRANSIT OF 81ST MERIDIAN. Y-axis 0-7, X-axis 0-12 0.

TEST CONDITIONS

TIDE RANGE AT GAGE 1	5.8 FT
OCEAN SALINITY(TOTAL SALT)	32.5 PPT
FRESHWATER INFLOW	1100 CFS

KINGS BAY MODEL

**EFFECTS OF
PLAN P4-1
ON TIDAL HEIGHTS**
STATIONS

1,   2, AND   3

LEGEND
BASE ———————
PLAN 1 — — —
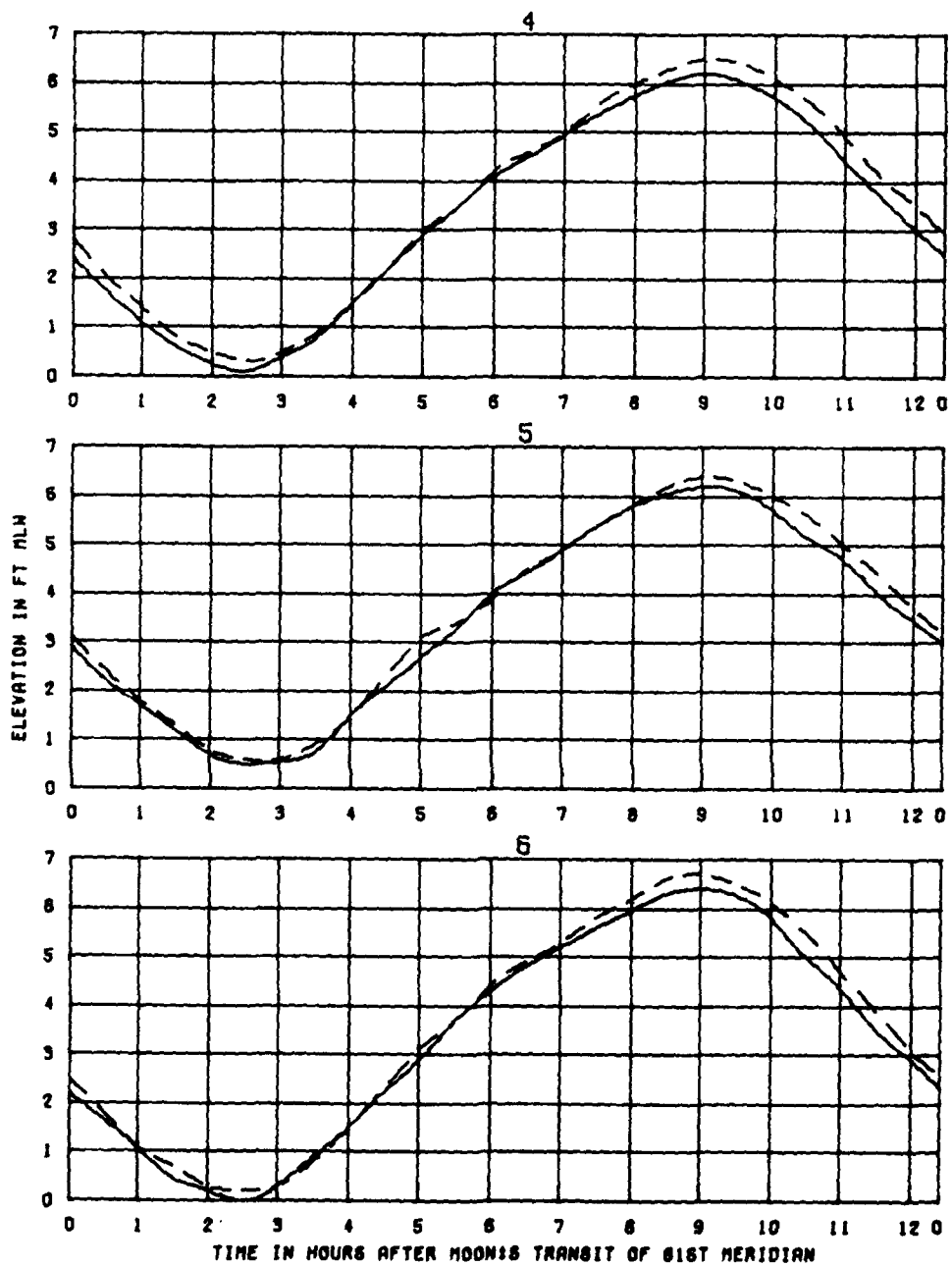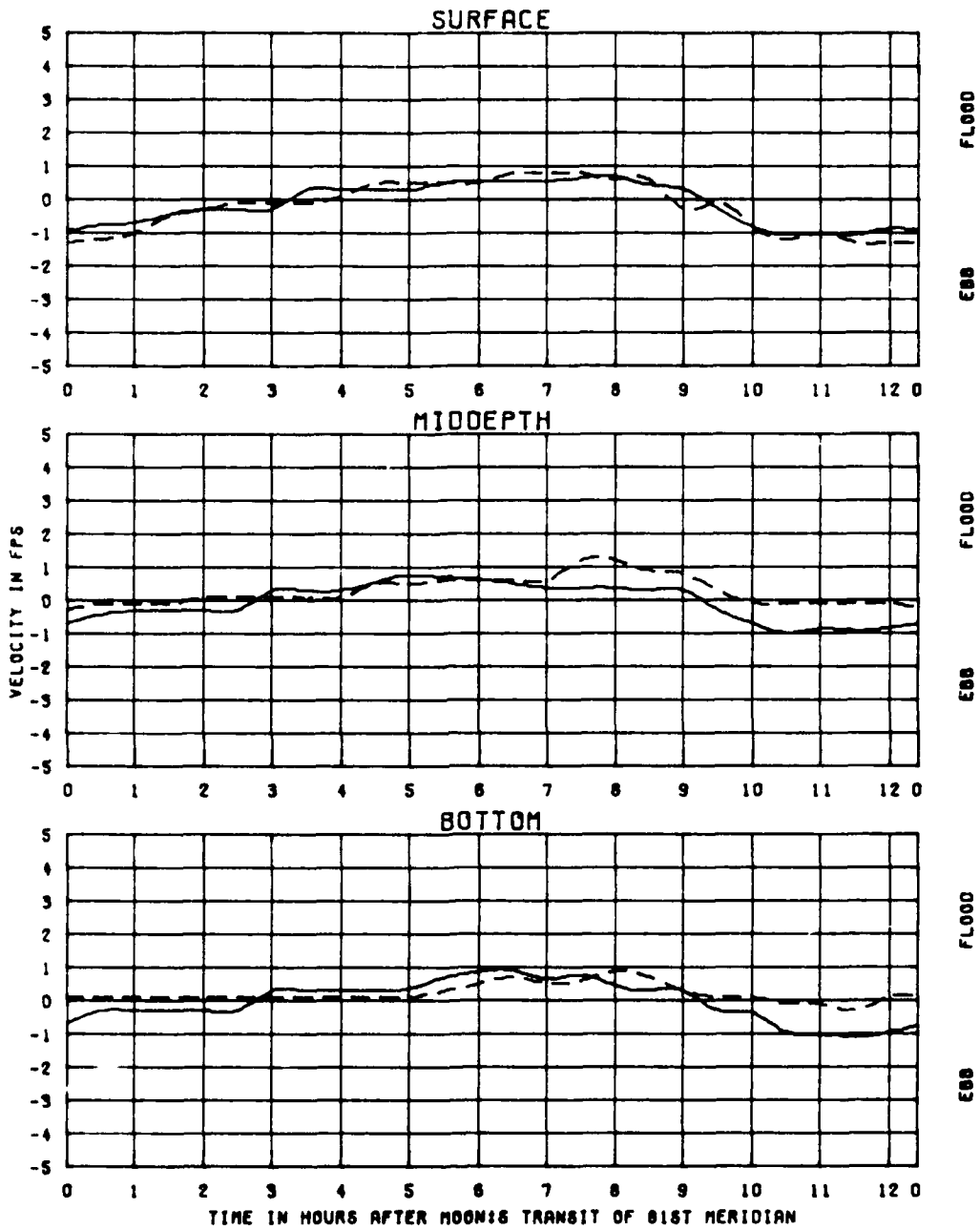
TEST CONDITIONS
TIDE RANGE AT GAGE 1   5.8 FT
OCEAN SALINITY(TOTAL SALT)   32.5 PPT
FRESHWATER INFLOW   1100 CFS

KINGS BAY MODEL

EFFECTS OF
PLAN P4-1
ON TIDAL HEIGHTS
STATIONS
4,   5, AND   6

LEGEND
BASE ————
PLAN 1 — — —
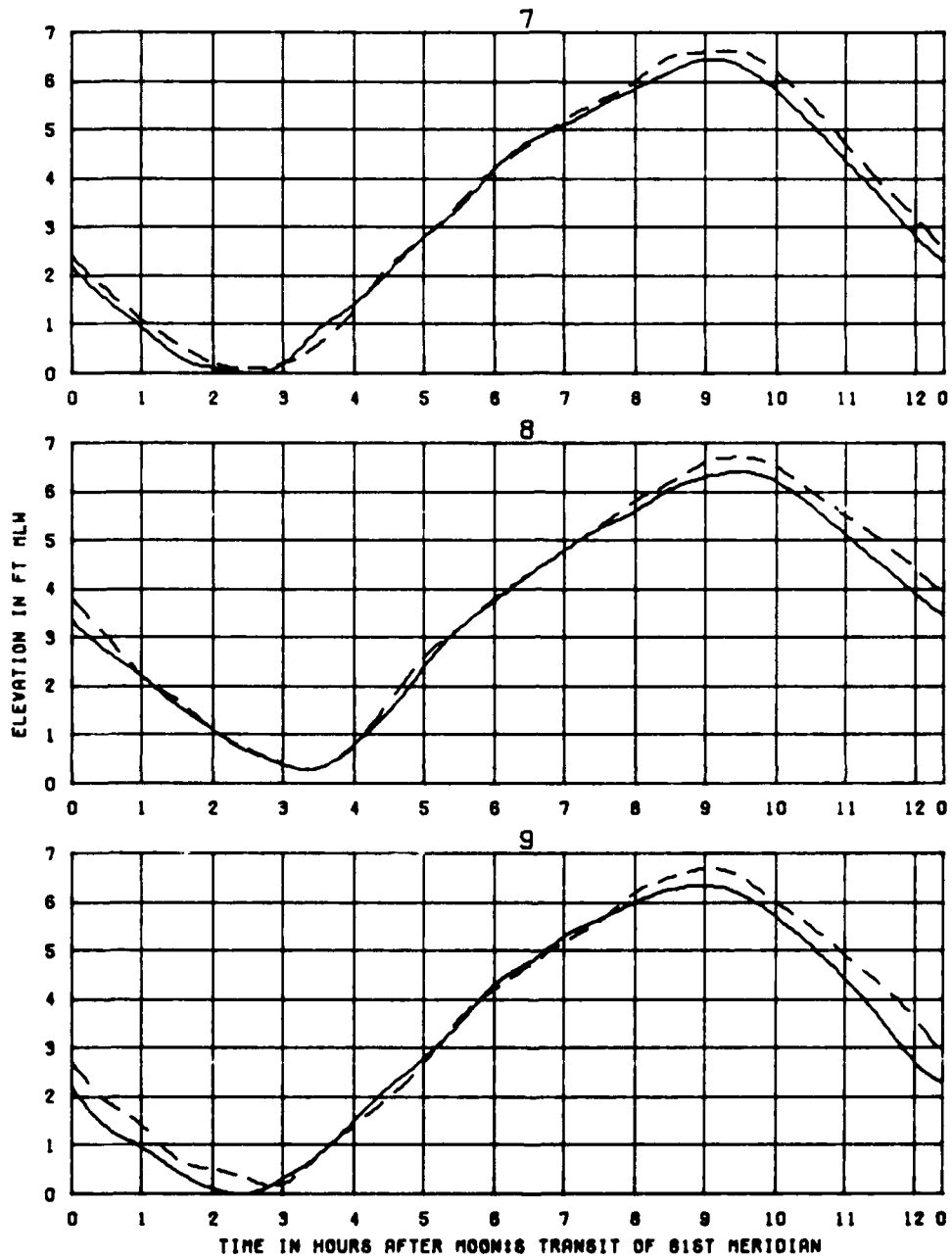
PLATE C2

TEST CONDITIONS
TIDE RANGE AT GAGE 1   5.8 FT
OCEAN SALINITY(TOTAL SALT)   32.5 PPT
FRESHWATER INFLOW   1100 CFS

KINGS BAY MODEL

EFFECTS OF
PLAN P4-1
ON TIDAL HEIGHTS
STATIONS
7,   8, AND   9

LEGEND
BASE   ———————
PLAN 1   — — — —
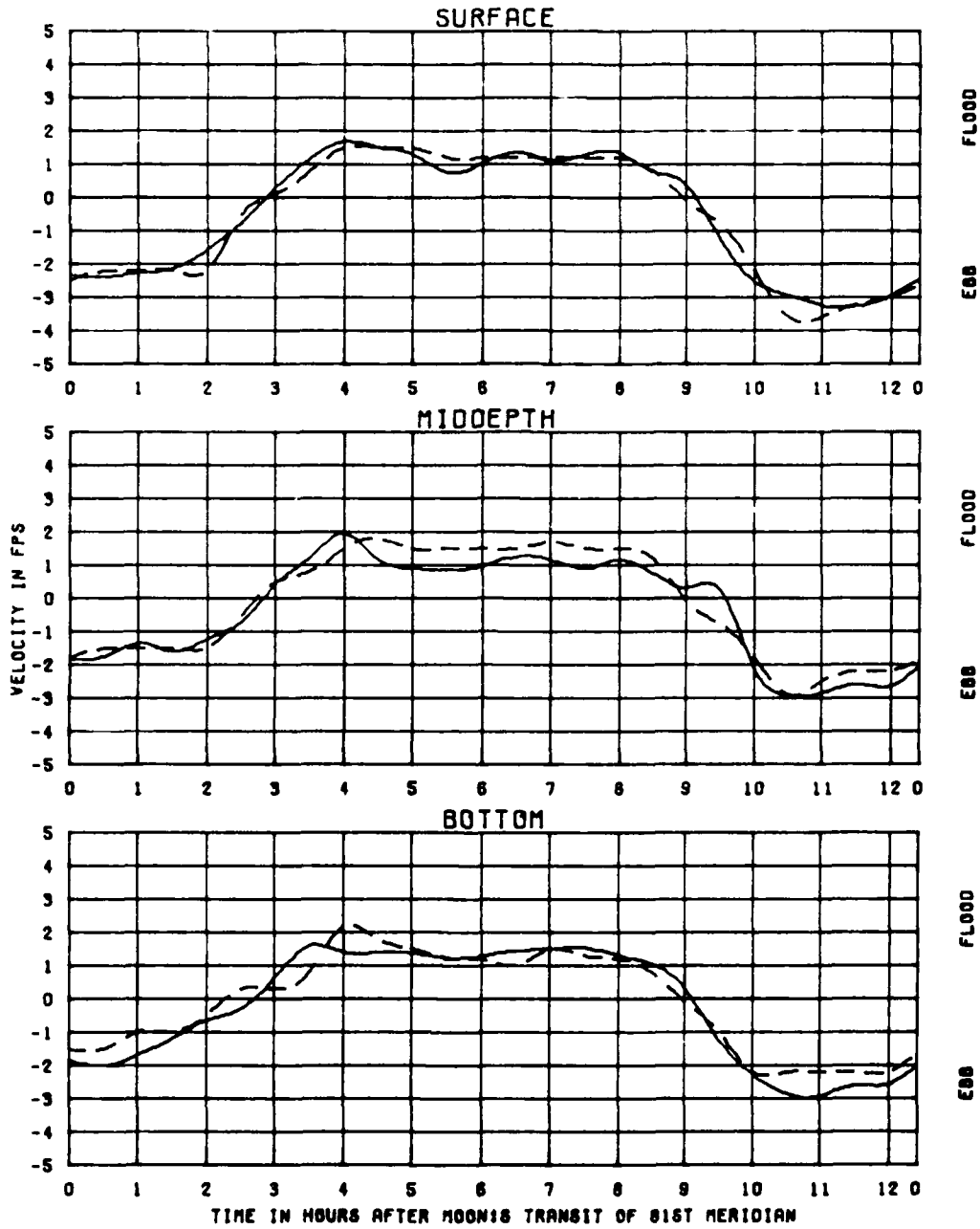
PLATE C3

SURFACE

MIDDEPTH

BOTTOM

VELOCITY IN FPS

TIME IN HOURS AFTER MOON'S TRANSIT OF 81ST MERIDIAN

FLOOD

EBB

TEST CONDITIONS
TIDE RANGE AT GAGE 1   5.8 FT
OCEAN SALINITY(TOTAL SALT) 32.5 PPT
FRESHWATER INFLOW   1100 CFS

KINGS BAY MODEL

EFFECTS OF
PLAN P4-1
ON VELOCITIES
STATION
2120

LEGEND
BASE   ————
PLAN 1 — — —
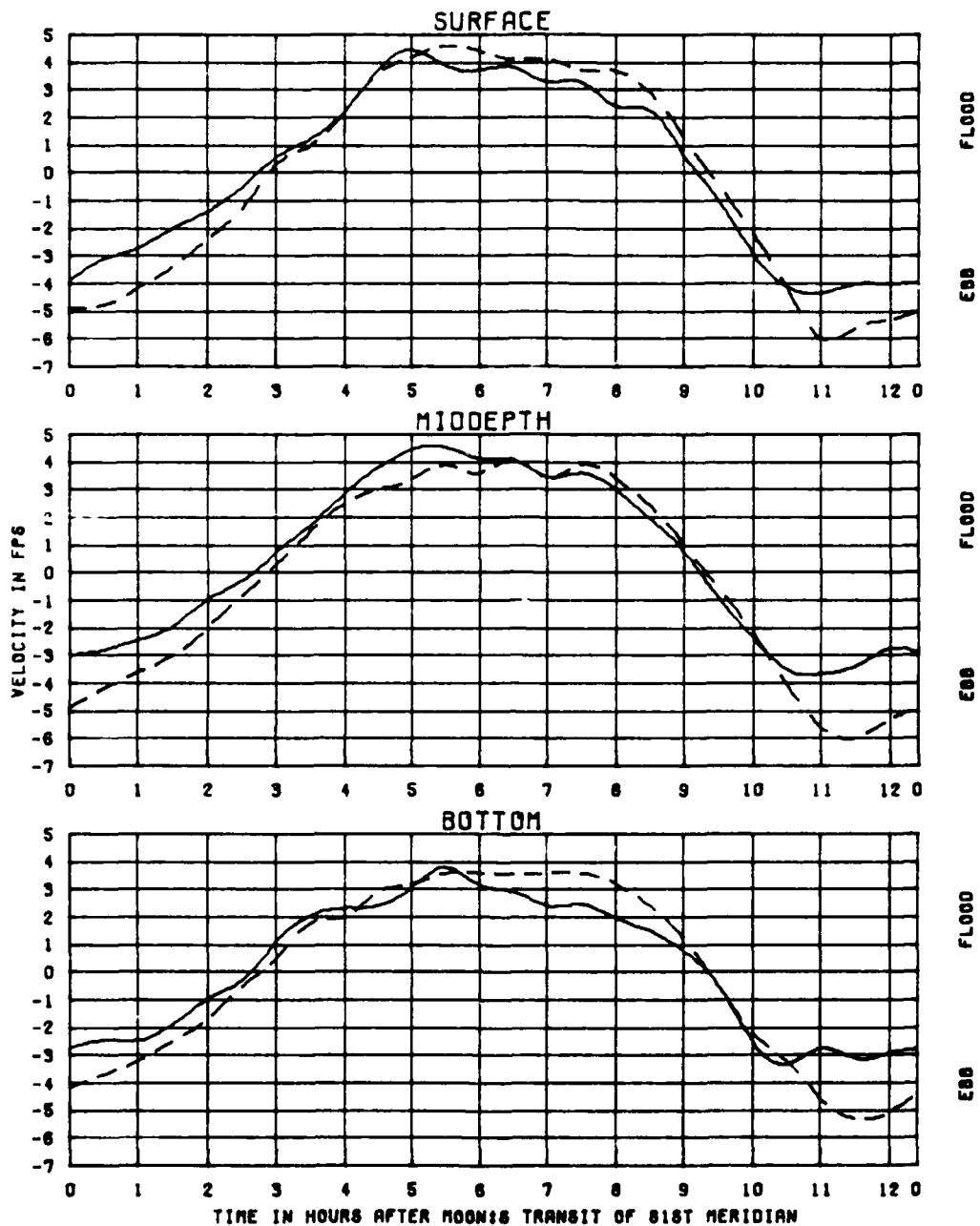
PLATE C4

SURFACE

MIDDEPTH

BOTTOM

VELOCITY IN FPS

TIME IN HOURS AFTER MOON'S TRANSIT OF 81ST MERIDIAN

FLOOD

EBB

TEST CONDITIONS
TIDE RANGE AT GAGE 1   5.8 FT
OCEAN SALINITY(TOTAL SALT)   32.5 PPT
FRESHWATER INFLOW   1100 CFS

KINGS BAY MODEL

EFFECTS OF
PLAN P4-1
ON VELOCITIES
STATION
2122

LEGEND
BASE   _____
PLAN 1   _ _ _ _
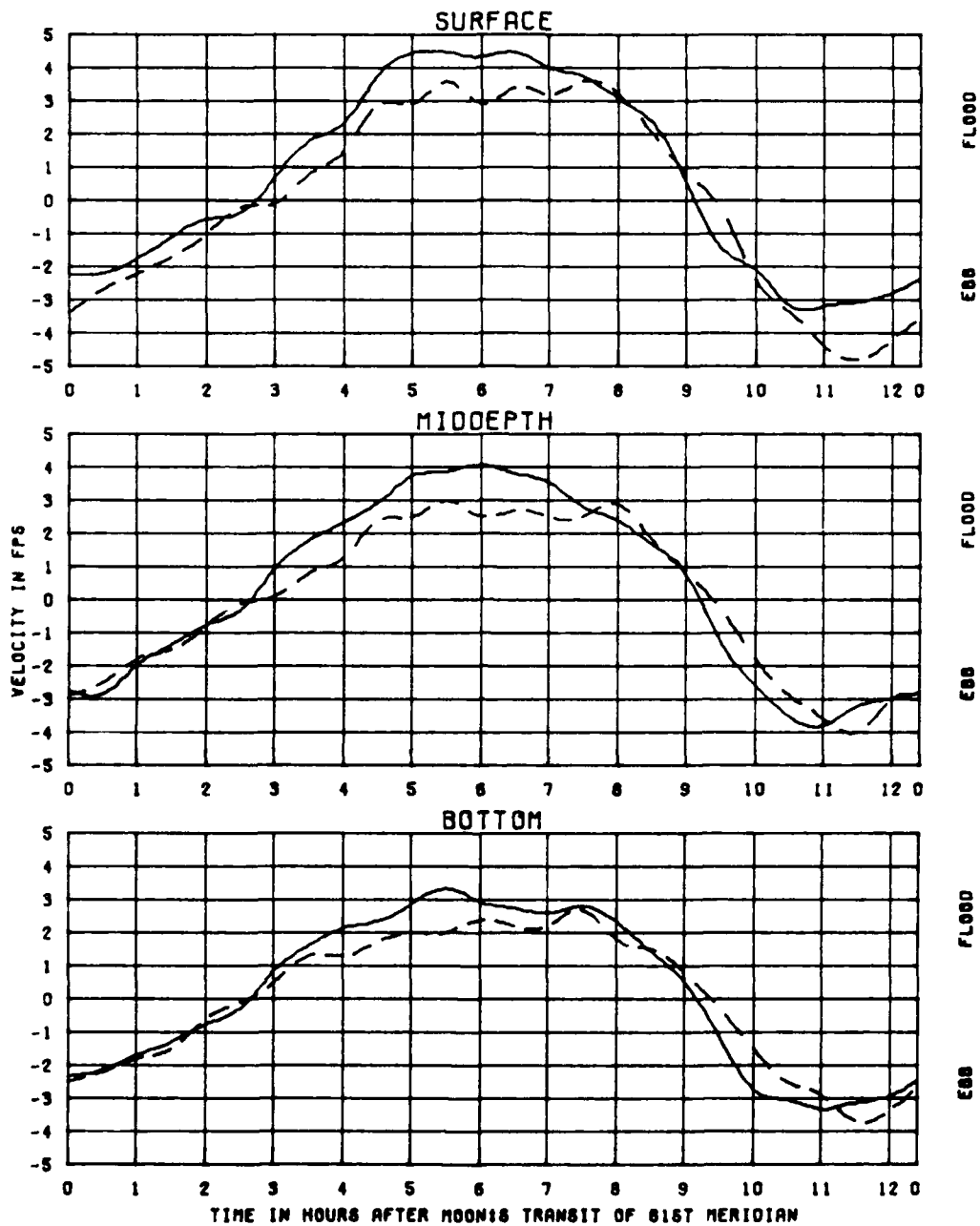
SURFACE

MIDDEPTH

BOTTOM

VELOCITY IN FPS

TIME IN HOURS AFTER MOON'S TRANSIT OF 81ST MERIDIAN
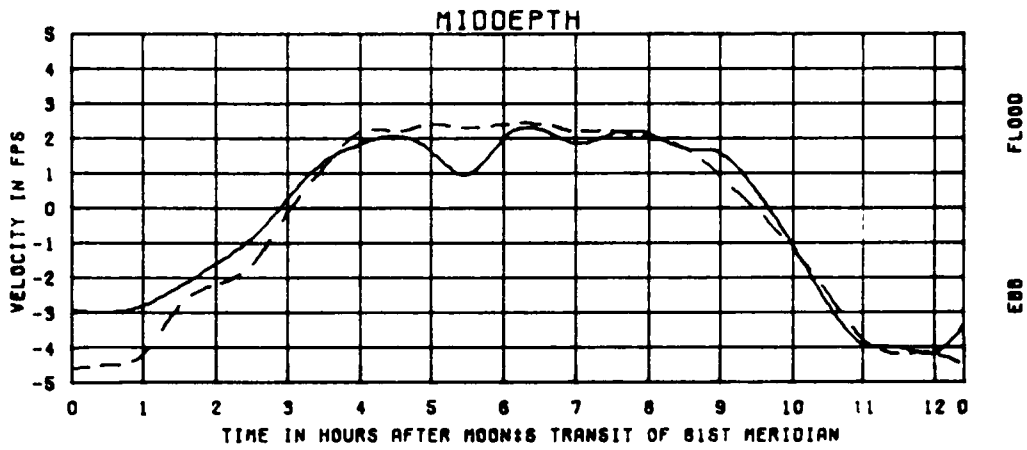
TEST CONDITIONS
TIDE RANGE AT GAGE 1   5.8 FT
OCEAN SALINITY(TOTAL SALT)   32.5 PPT
FRESHWATER INFLOW   1100 CFS

KINGS BAY MODEL

EFFECTS OF
PLAN P4-1
ON VELOCITIES
STATION
2124

LEGEND
BASE ————
PLAN 1 — — —
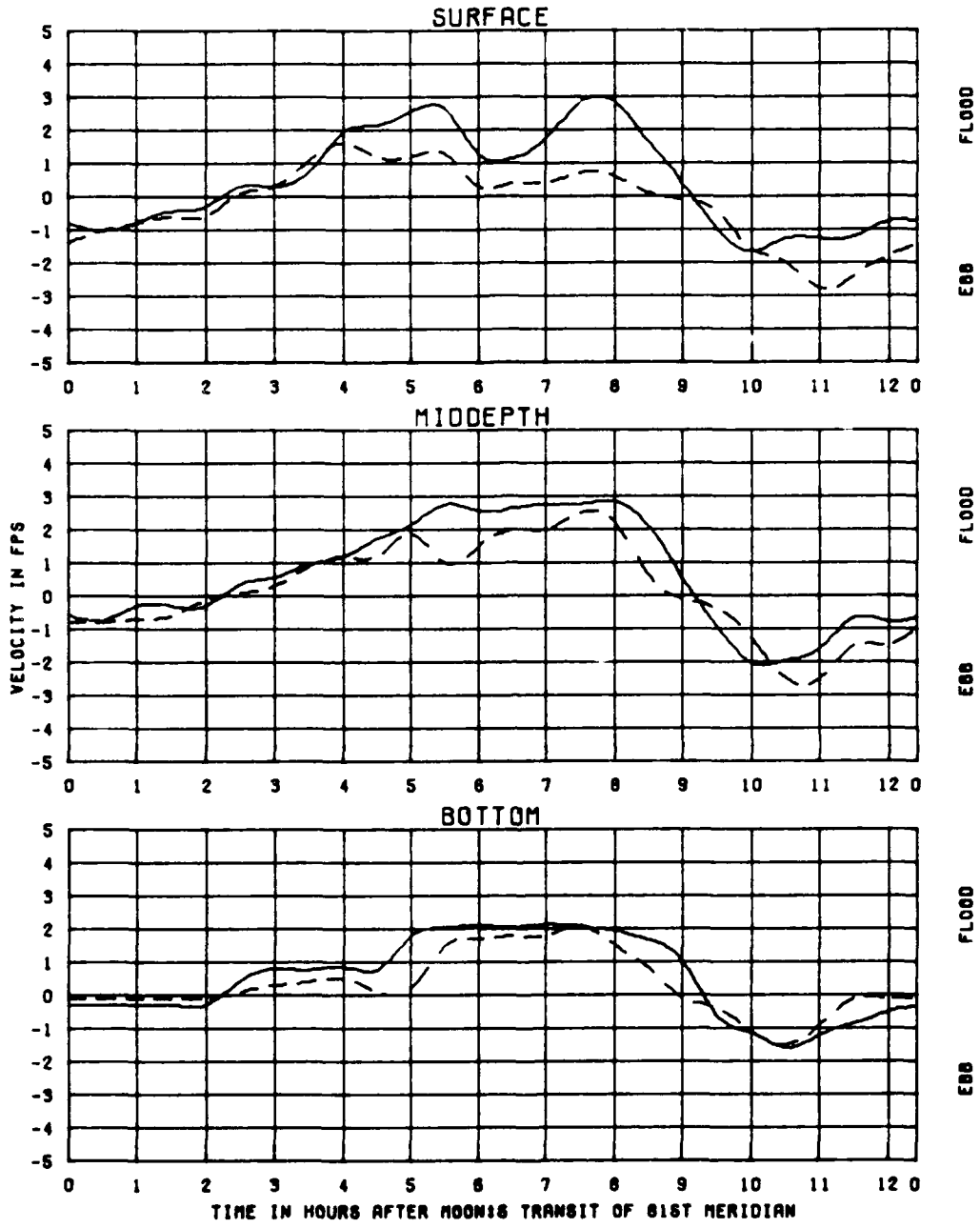
PLATE C6

SURFACE

MIDDEPTH

BOTTOM

TIME IN HOURS AFTER MOON'S TRANSIT OF 81ST MERIDIAN

VELOCITY IN FPS

FLOOD

EBB

TEST CONDITIONS	
TIDE RANGE AT GAGE 1	5.8 FT
OCEAN SALINITY(TOTAL SALT)	32.5 PPT
FRESHWATER INFLOW	1100 CFS

KINGS BAY MODEL

EFFECTS OF
PLAN P4-1
ON VELOCITIES
STATION
50

LEGEND
BASE ————
PLAN 1 — — —
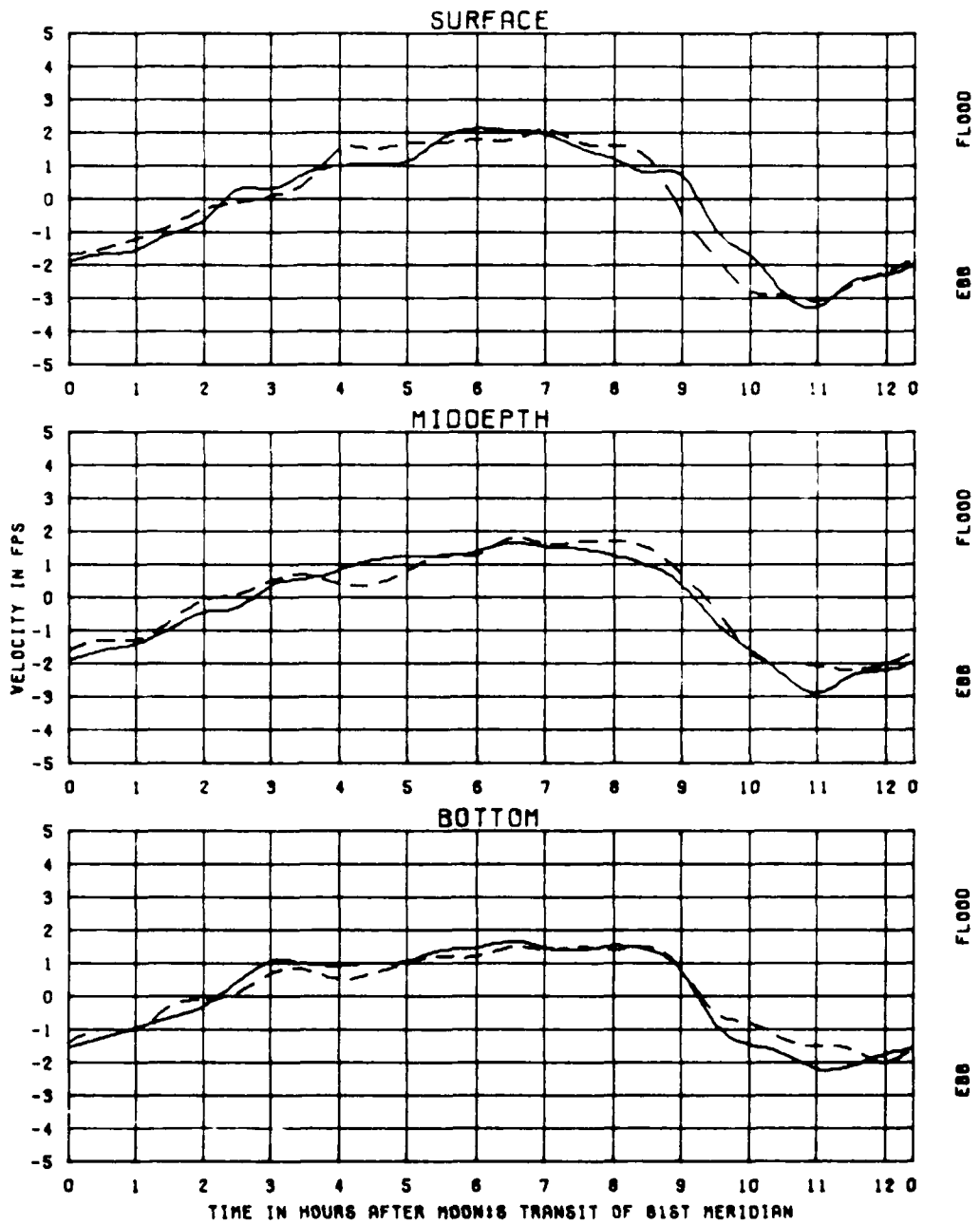
PLATE C7

SURFACE

MIDDEPTH

BOTTOM

VELOCITY IN FPS

TIME IN HOURS AFTER MOON'S TRANSIT OF 81ST MERIDIAN

TEST CONDITIONS		KINGS BAY MODEL
TIDE RANGE AT GAGE 1	5.8 FT	
OCEAN SALINITY(TOTAL SALT)	32.5 PPT	EFFECTS OF
FRESHWATER INFLOW	1100 CFS	PLAN P4-1

ON VELOCITIES
STATION
60

LEGEND
BASE ————
PLAN 1 — — —
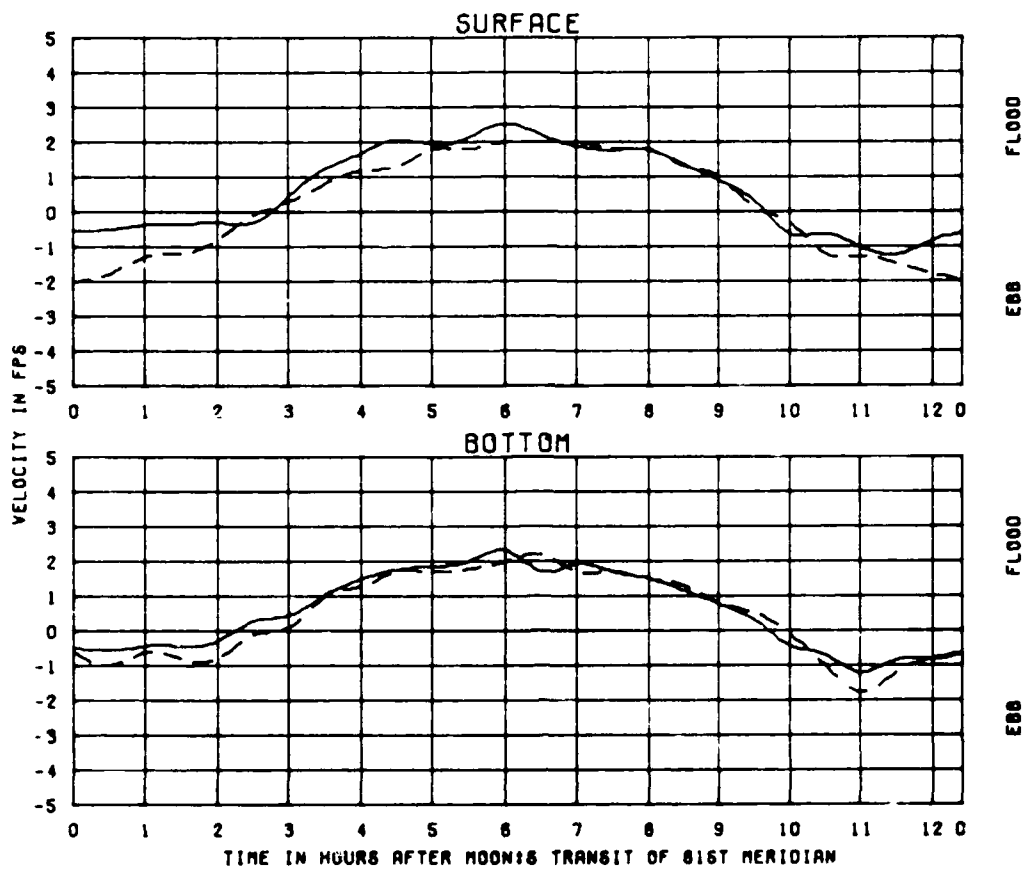
SURFACE

BOTTOM

VELOCITY IN FPS

TIME IN HOURS AFTER MOON'S TRANSIT OF 81ST MERIDIAN

FLOOD

EBB

KINGS BAY MODEL

EFFECTS OF
PLAN P4-1
ON VELOCITIES
STATION
20

LEGEND
BASE   ————
PLAN 1   — — —
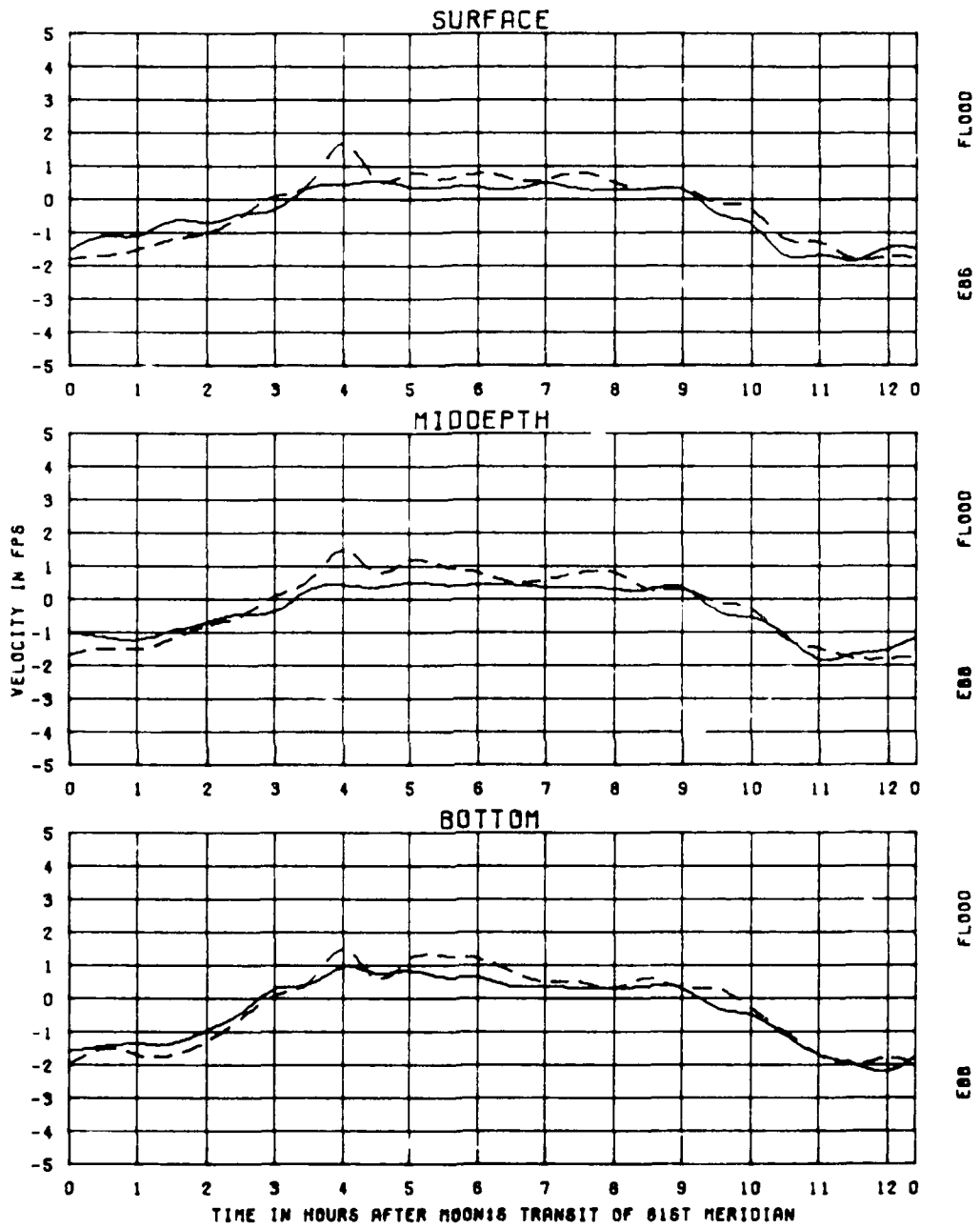
SURFACE

MIDDEPTH

BOTTOM

VELOCITY IN FPS

TIME IN HOURS AFTER MOON'S TRANSIT OF 81ST MERIDIAN
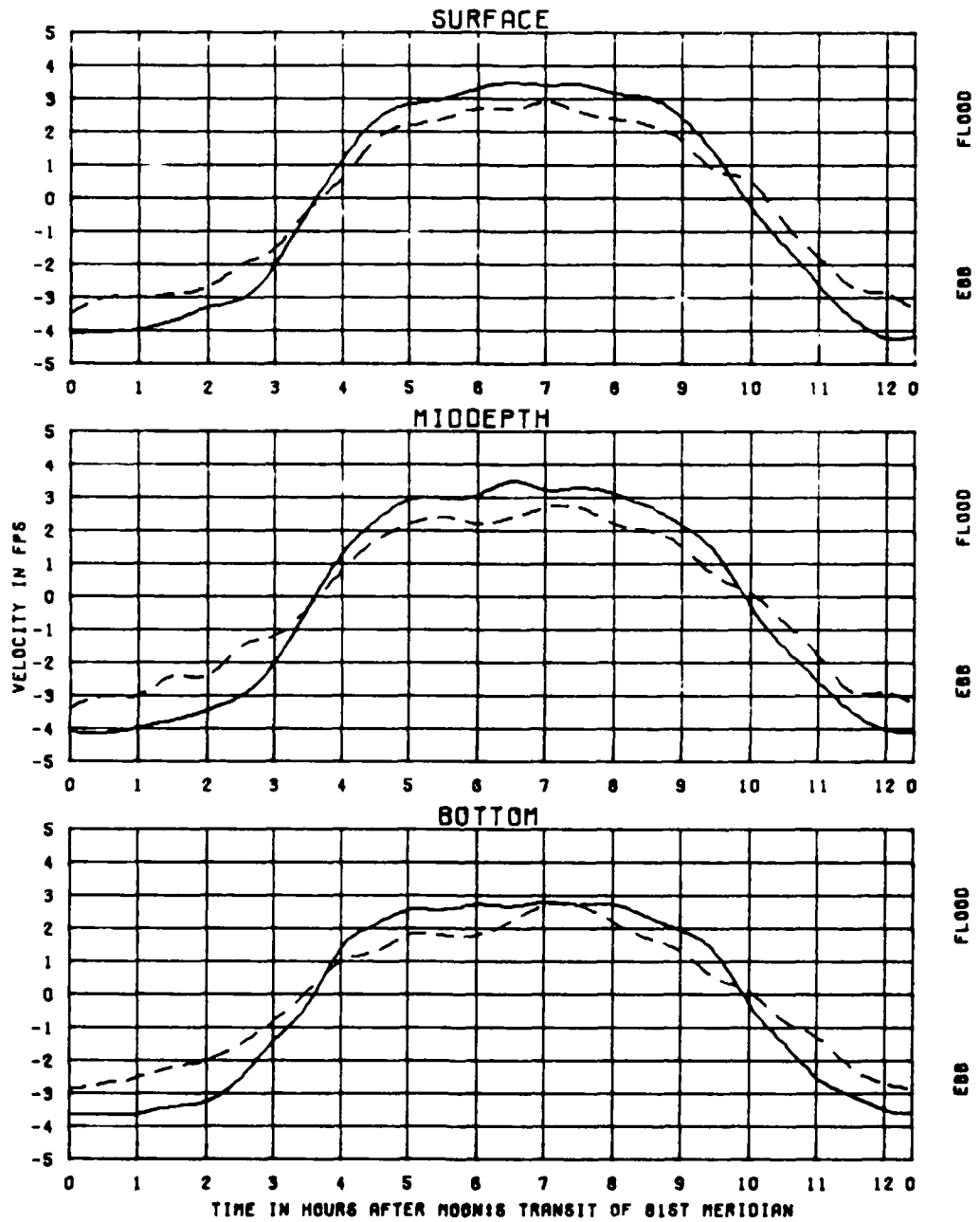
FLOOD

EBB

TEST CONDITIONS
TIDE RANGE AT GAGE 1   5.8 FT
OCEAN SALINITY(TOTAL SALT)   32.5 PPT
FRESHWATER INFLOW   1100 CFS

KINGS BAY MODEL

EFFECTS OF
PLAN P4-1
ON VELOCITIES
STATION
1999

LEGEND
BASE   ————
PLAN 1   — — —
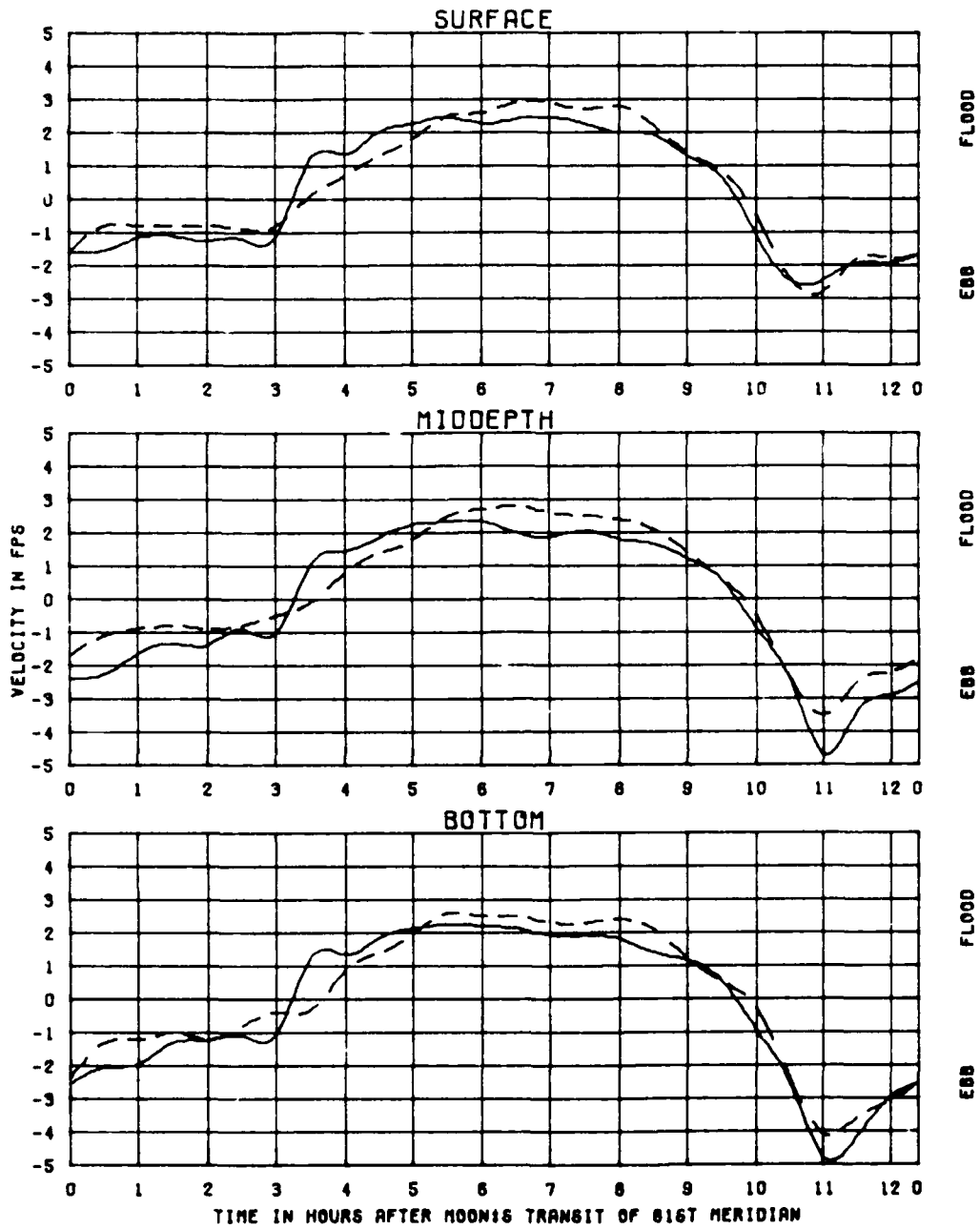
PLATE C10

SURFACE

MIDDEPTH

BOTTOM

VELOCITY IN FPS

TIME IN HOURS AFTER MOON'S TRANSIT OF 61ST MERIDIAN

FLOOD

EBB

TEST CONDITIONS		KINGS BAY MODEL
TIDE RANGE AT GAGE 1	5.8 FT	
OCEAN SALINITY(TOTAL SALT)	32.5 PPT	EFFECTS OF
FRESHWATER INFLOW	1100 CFS	PLAN P4-1

EFFECTS OF
PLAN P4-1
ON VELOCITIES
STATION
1981

LEGEND
BASE ————
PLAN 1 — — —
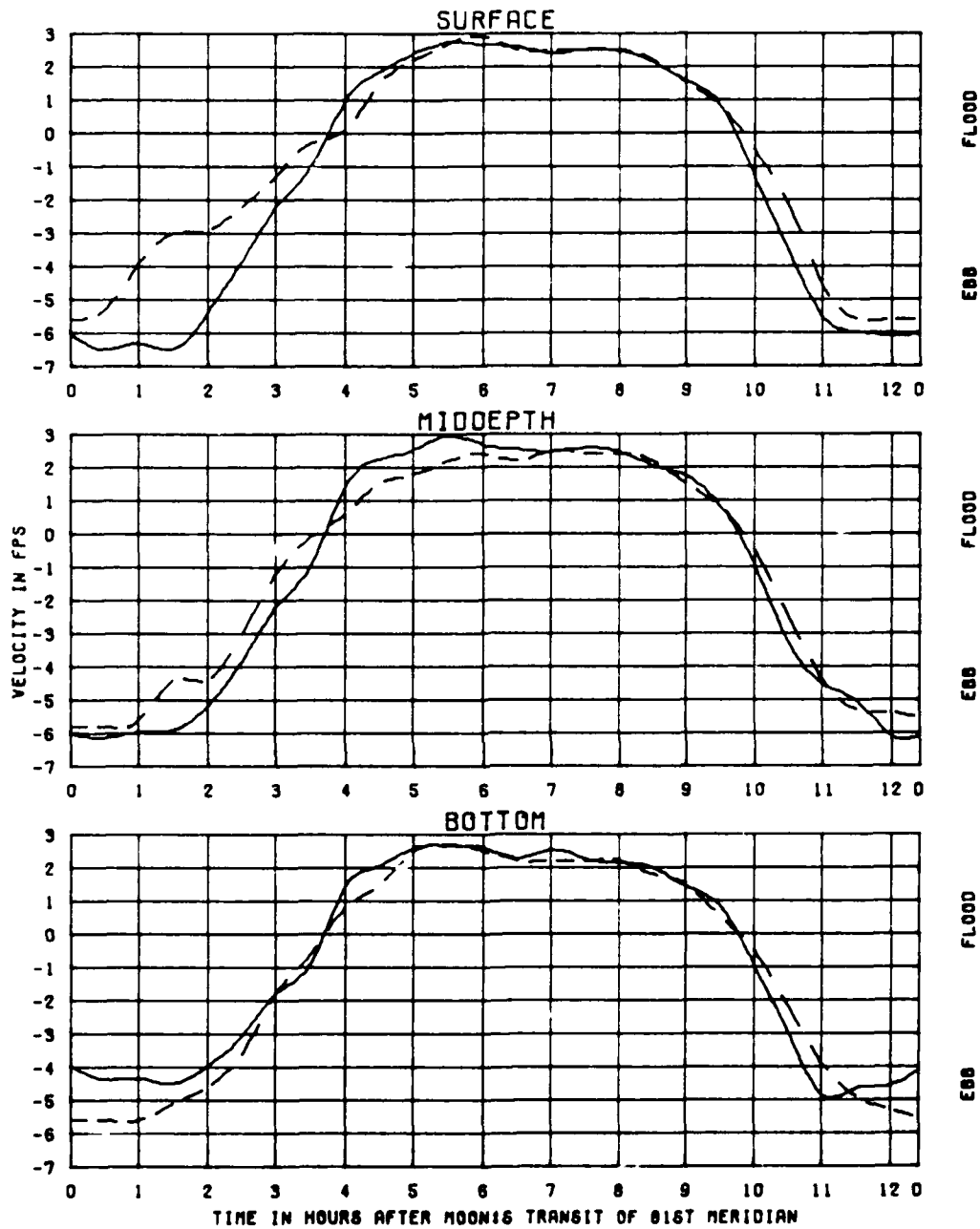
SURFACE

MIDDEPTH

BOTTOM

VELOCITY IN FPS

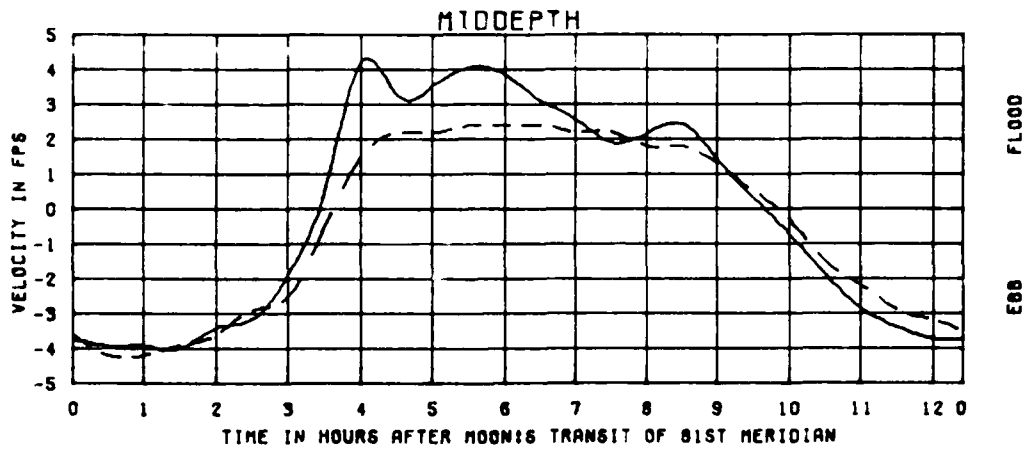TIME IN HOURS AFTER MOON'S TRANSIT OF 81ST MERIDIAN

TEST CONDITIONS
TIDE RANGE AT GAGE 1   5.8 FT
OCEAN SALINITY(TOTAL SALT)   32.5 PPT
FRESHWATER INFLOW   1100 CFS

KINGS BAY MODEL

EFFECTS OF
PLAN P4-1
ON VELOCITIES
STATION
1989

LEGEND
BASE   ————
PLAN 1   — — —
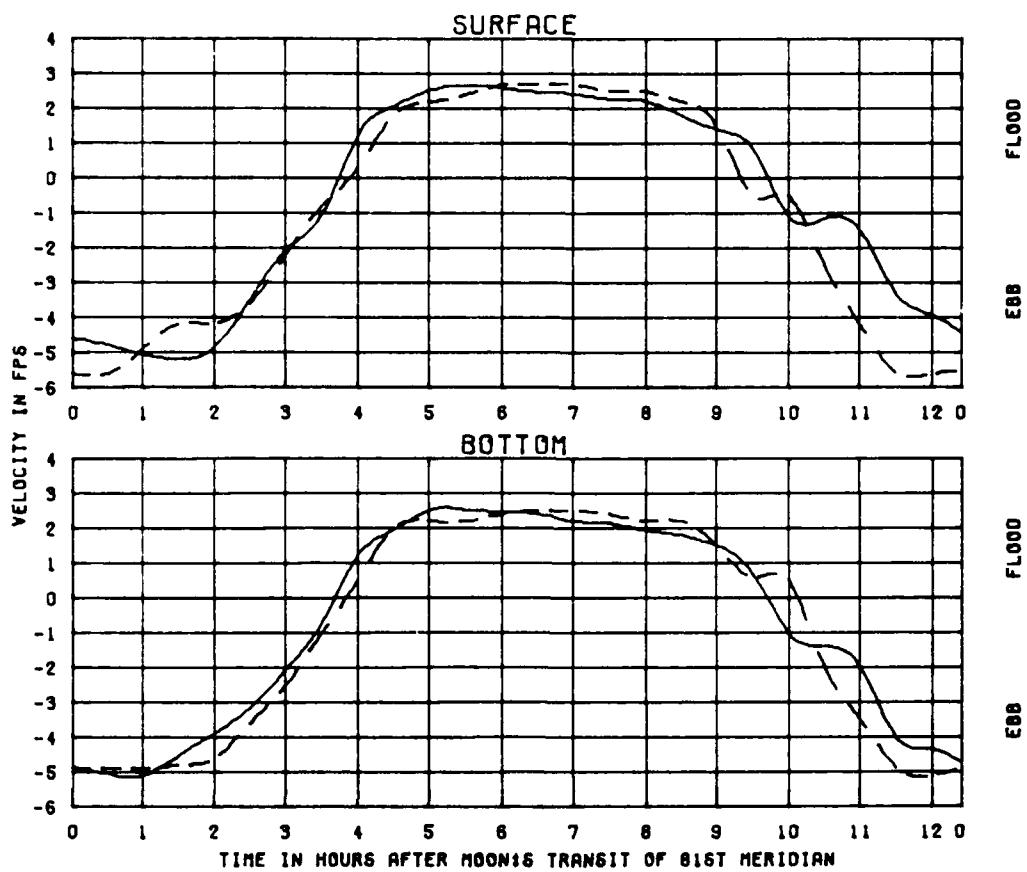
PLATE C12

SURFACE

BOTTOM

VELOCITY IN FPS

TIME IN HOURS AFTER MOON'S TRANSIT OF 81ST MERIDIAN
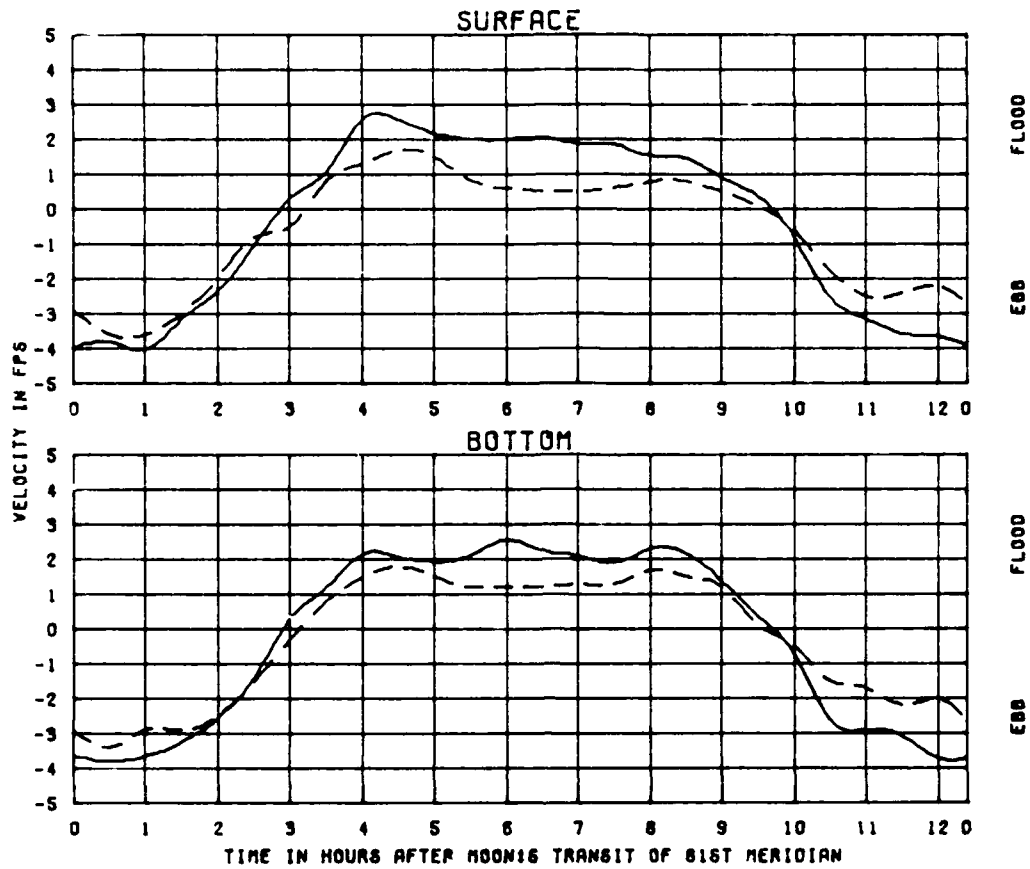
FLOOD

EBB

FLOOD
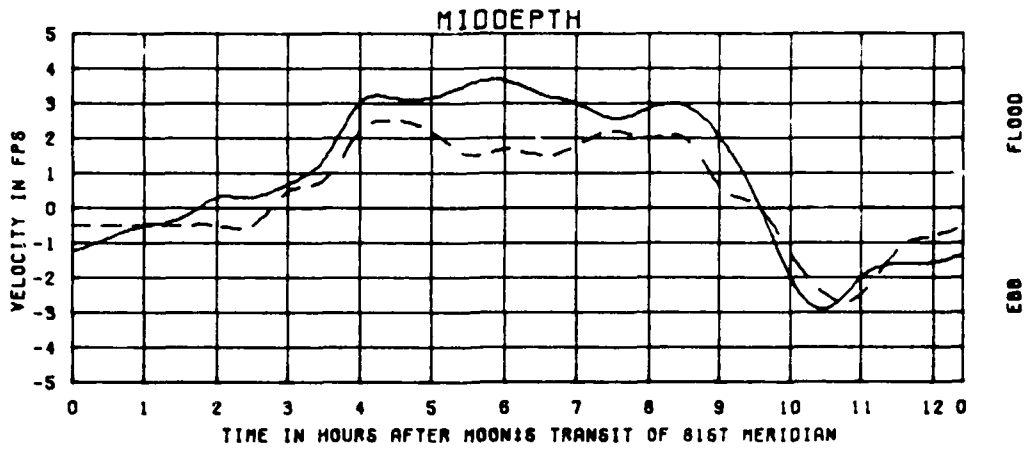
EBB

TEST CONDITIONS
TIDE RANGE AT GAGE 1   5.8 FT
OCEAN SALINITY(TOTAL SALT)   32.5 PPT
FRESHWATER INFLOW   1100 CFS

KINGS BAY MODEL

EFFECTS OF
PLAN P4-1
ON VELOCITIES
STATION
1979

LEGEND
BASE   ———
PLAN 1   — — —
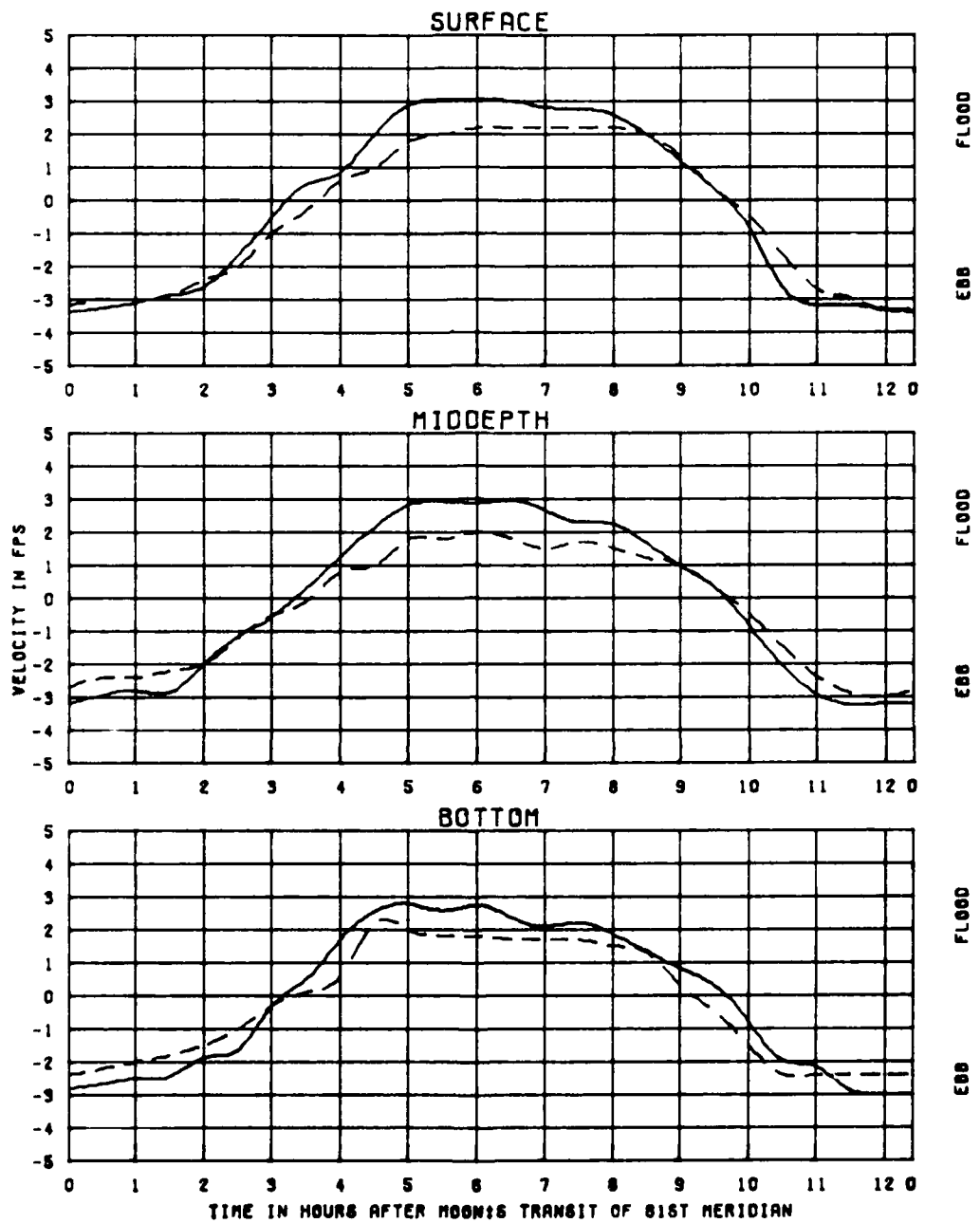
SURFACE

MIDDEPTH

BOTTOM

VELOCITY IN FPS

TIME IN HOURS AFTER MOON'S TRANSIT OF 81ST MERIDIAN

FLOOD

EBB

TEST CONDITIONS		KINGS BAY MODEL
TIDE RANGE AT GAGE 1	5.8 FT	
OCEAN SALINITY(TOTAL SALT)	32.5 PPT	
FRESHWATER INFLOW	1100 CFS	

EFFECTS OF
PLAN P4-1
ON VELOCITIES
STATION
1865

LEGEND
BASE ————
PLAN 1 — — —
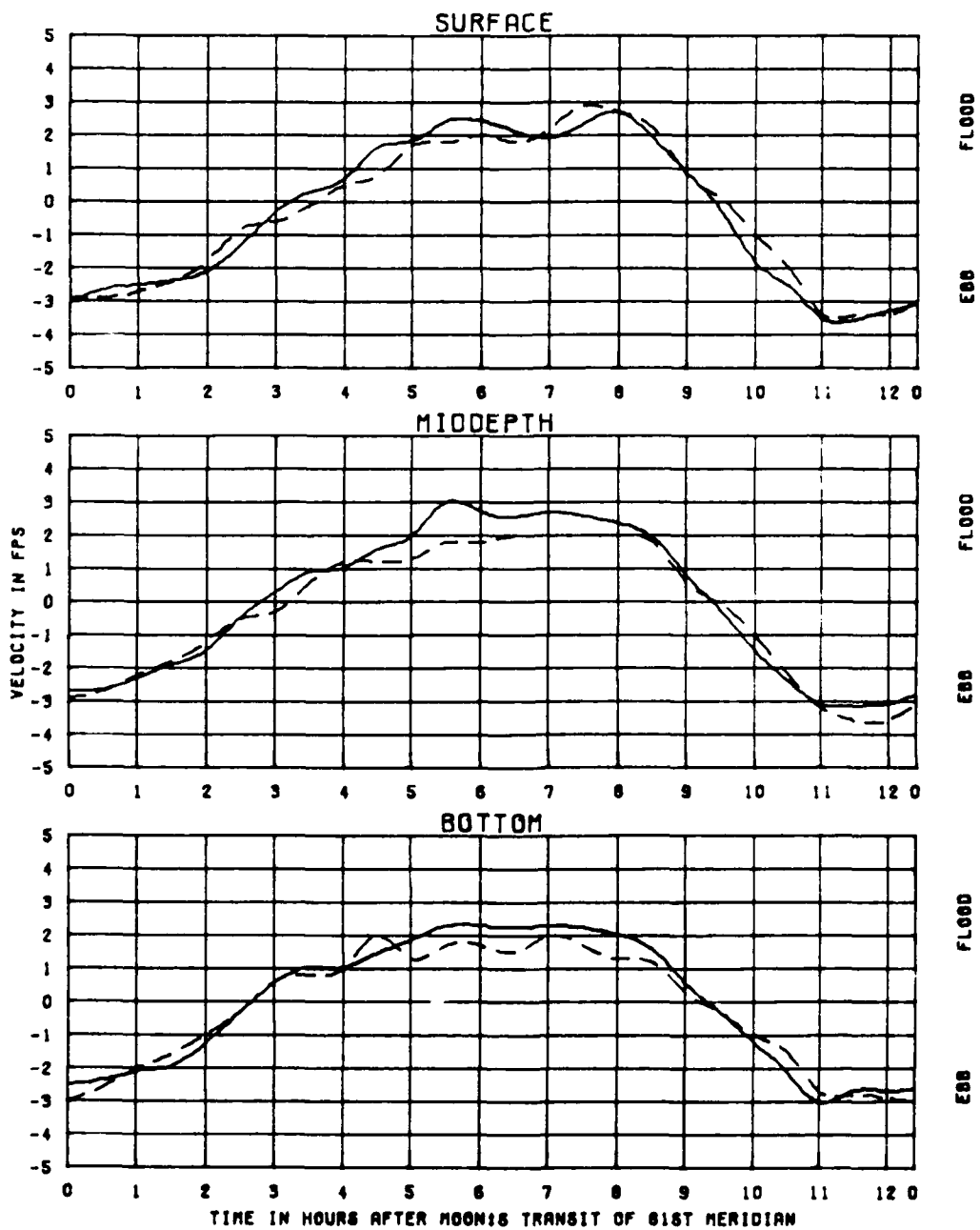
PLATE C14

SURFACE

MIDDEPTH

BOTTOM

TIME IN HOURS AFTER MOON'S TRANSIT OF 81ST MERIDIAN

VELOCITY IN FPS

FLOOD

EBB

TEST CONDITIONS

TIDE RANGE AT GAGE 1	5.8 FT
OCEAN SALINITY(TOTAL SALT)	32.5 PPT
FRESHWATER INFLOW	1100 CFS

KINGS BAY MODEL

EFFECTS OF
PLAN P4-1
ON VELOCITIES
STATION
1869

LEGEND

BASE ——————

PLAN 1 — — —
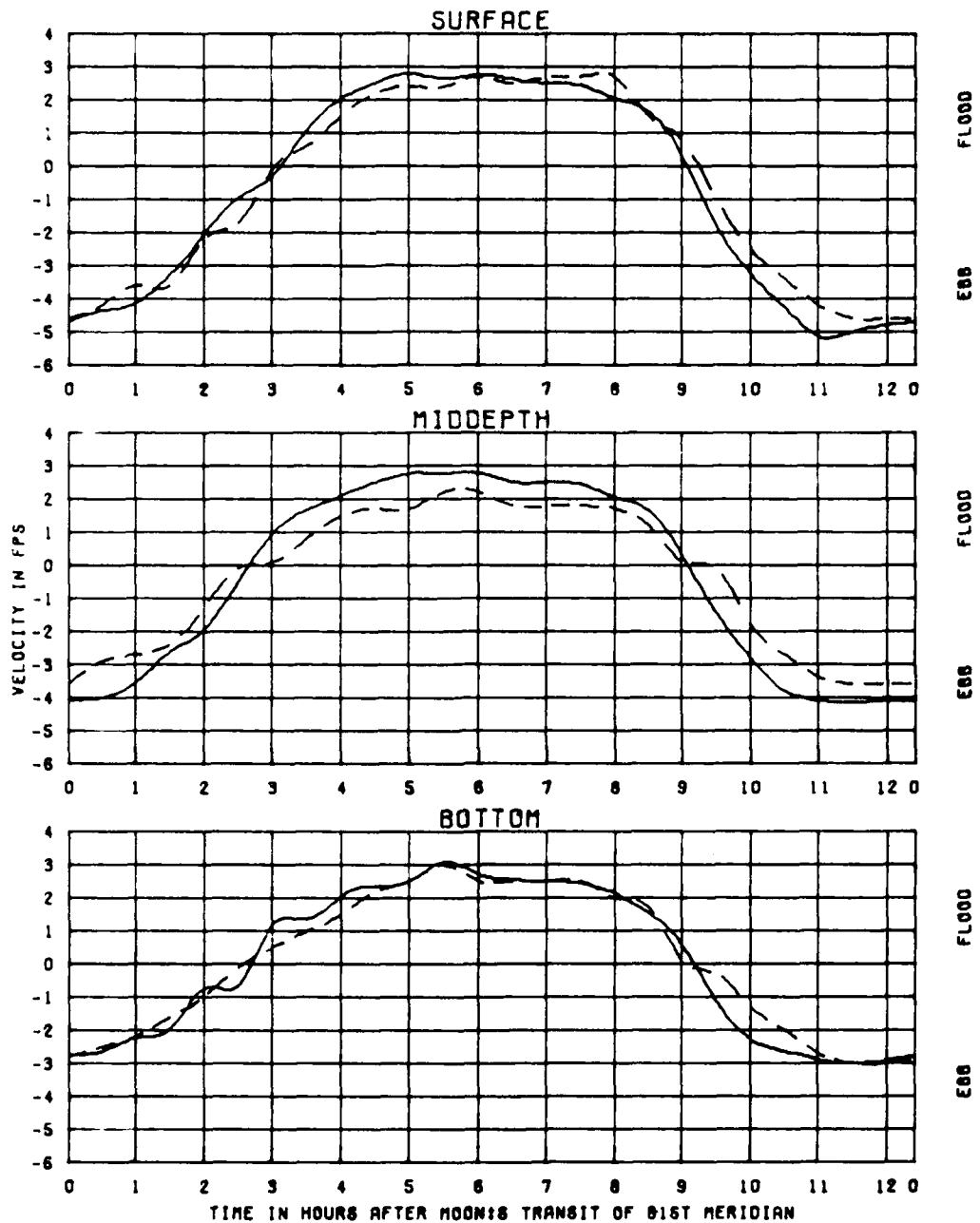
PLATE C15

SURFACE

MIDDEPTH

BOTTOM

TIME IN HOURS AFTER MOON'S TRANSIT OF 81ST MERIDIAN

VELOCITY IN FPS

FLOOD

EBB

TEST CONDITIONS
TIDE RANGE AT GAGE 1   5.8 FT
OCEAN SALINITY(TOTAL SALT)   32.5 PPT
FRESHWATER INFLOW   1100 CFS

KINGS BAY MODEL

EFFECTS OF
PLAN P4-1
ON VELOCITIES
STATION
843

LEGEND
BASE   ————
PLAN 1 — — —

SURFACE

MIDDEPTH

BOTTOM

VELOCITY IN FPS

TIME IN HOURS AFTER MOON'S TRANSIT OF 81ST MERIDIAN

FLOOD

EBB
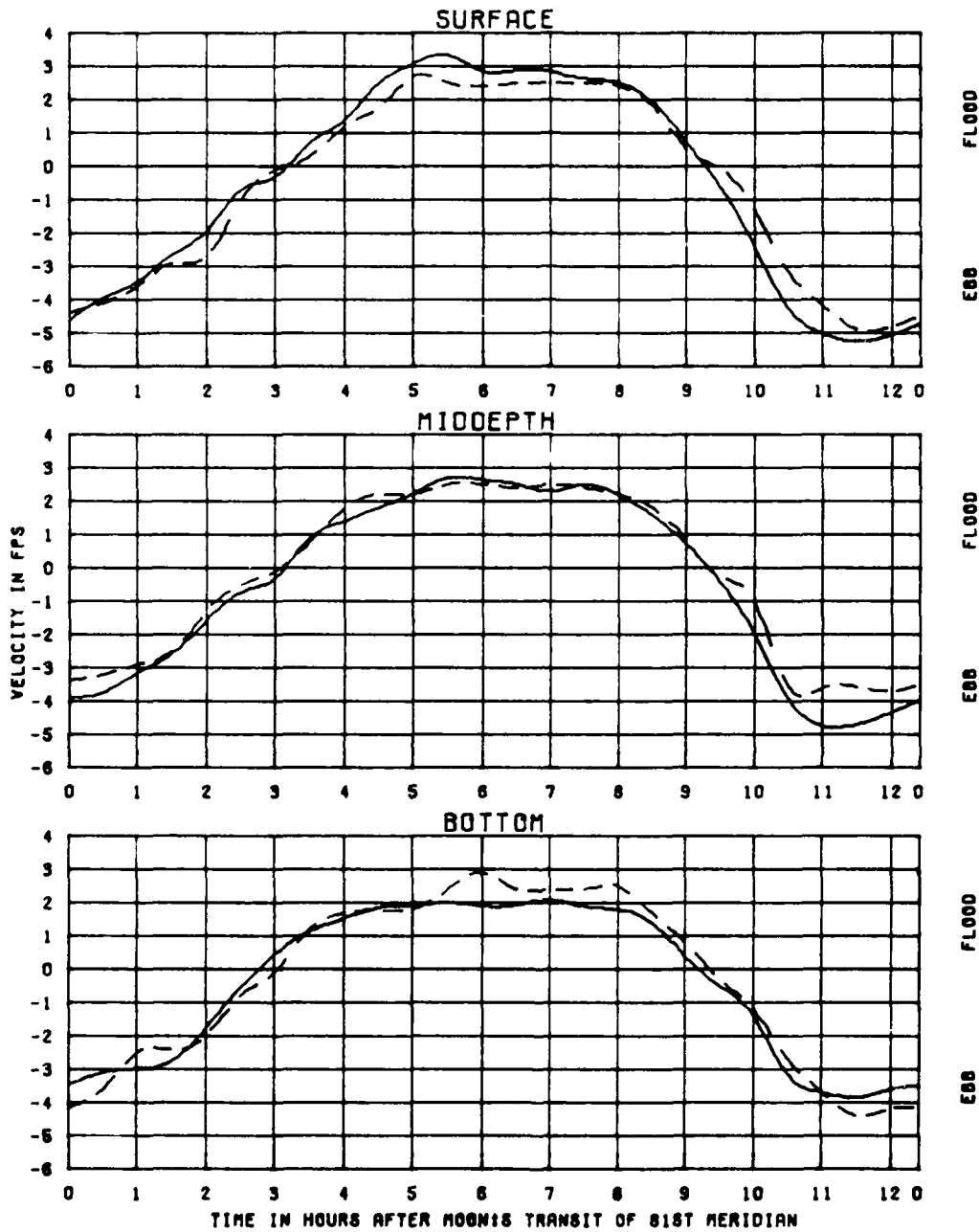
TEST CONDITIONS
TIDE RANGE AT GAGE 1   5.8 FT
OCEAN SALINITY(TOTAL SALT)   32.5 PPT
FRESHWATER INFLOW   1100 CFS

KINGS BAY MODEL

EFFECTS OF
PLAN P4-1
ON VELOCITIES
STATION
1055

LEGEND
BASE   ————
PLAN 1 — — —
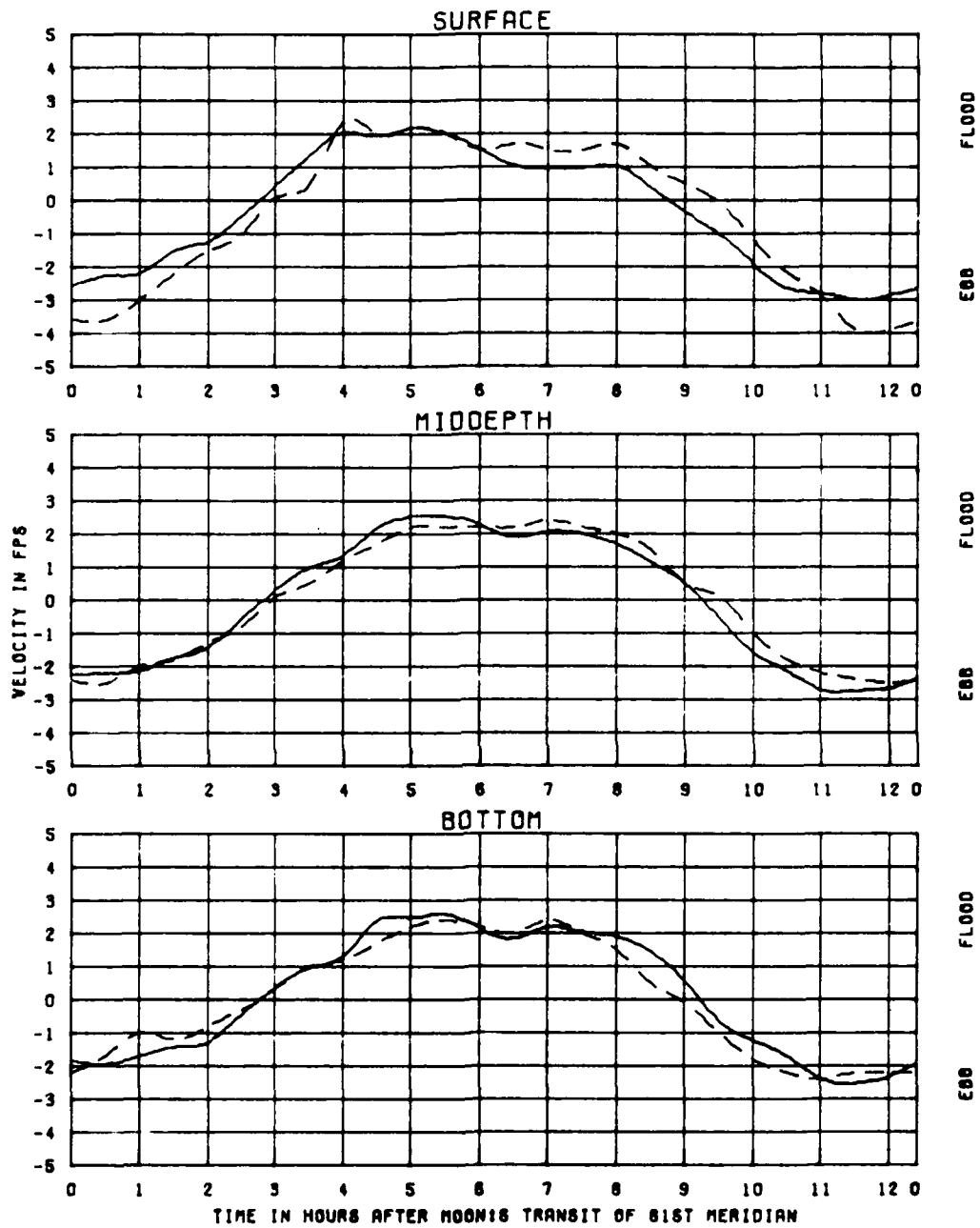
SURFACE

MIDDEPTH

BOTTOM

VELOCITY IN FPS

TIME IN HOURS AFTER MOON'S TRANSIT OF 81ST MERIDIAN

FLOOD

EBB

TEST CONDITIONS
TIDE RANGE AT GAGE 1 .... 5.8 FT
OCEAN SALINITY(TOTAL SALT) .... 32.5 PPT
FRESHWATER INFLOW .... 1100 CFS

KINGS BAY MODEL

EFFECTS OF
PLAN P4-1
ON VELOCITIES
STATION
1153

LEGEND
BASE ———
PLAN 1 — — —
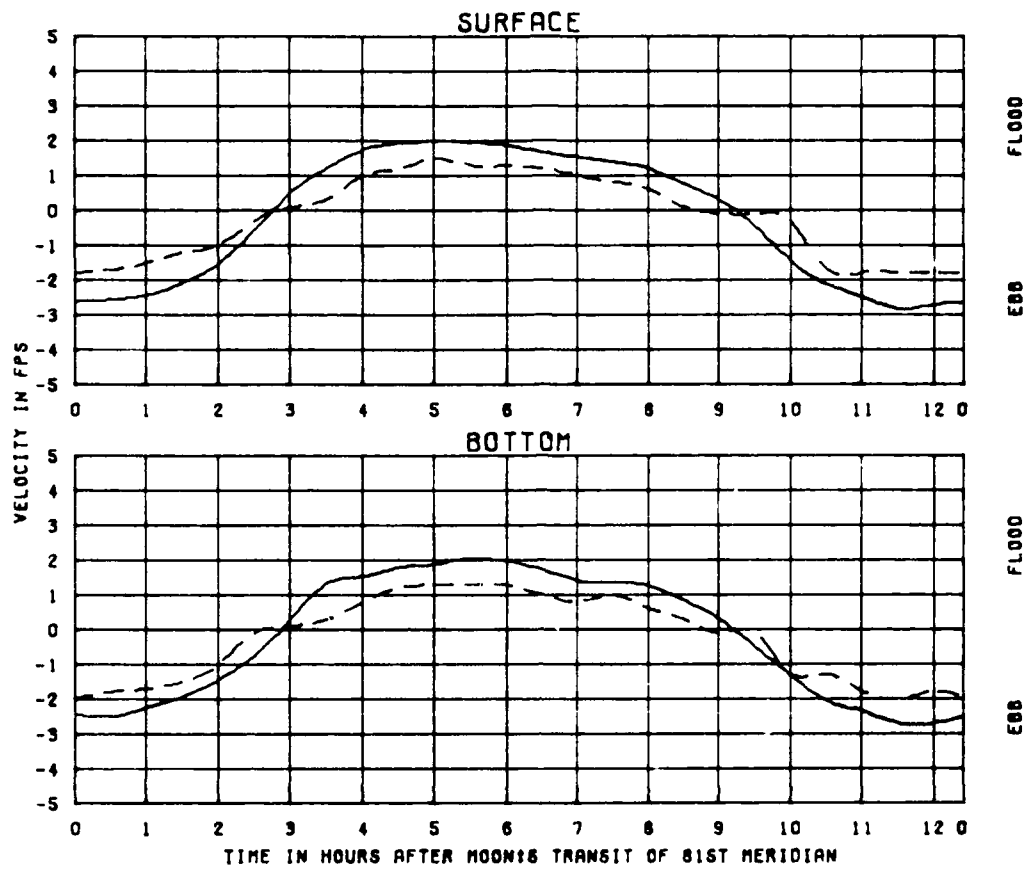
PLATE C18

SURFACE

BOTTOM

VELOCITY IN FPS

FLOOD

EBB

TIME IN HOURS AFTER MOON'S TRANSIT OF 81ST MERIDIAN

TEST CONDITIONS
TIDE RANGE AT GAGE 1   5.8 FT
OCEAN SALINITY(TOTAL SALT)   32.5 PPT
FRESHWATER INFLOW   1100 CFS

KINGS BAY MODEL

EFFECTS OF
PLAN P4-1
ON VELOCITIES
STATION
1883

LEGEND
BASE   ————
PLAN 1 — — —
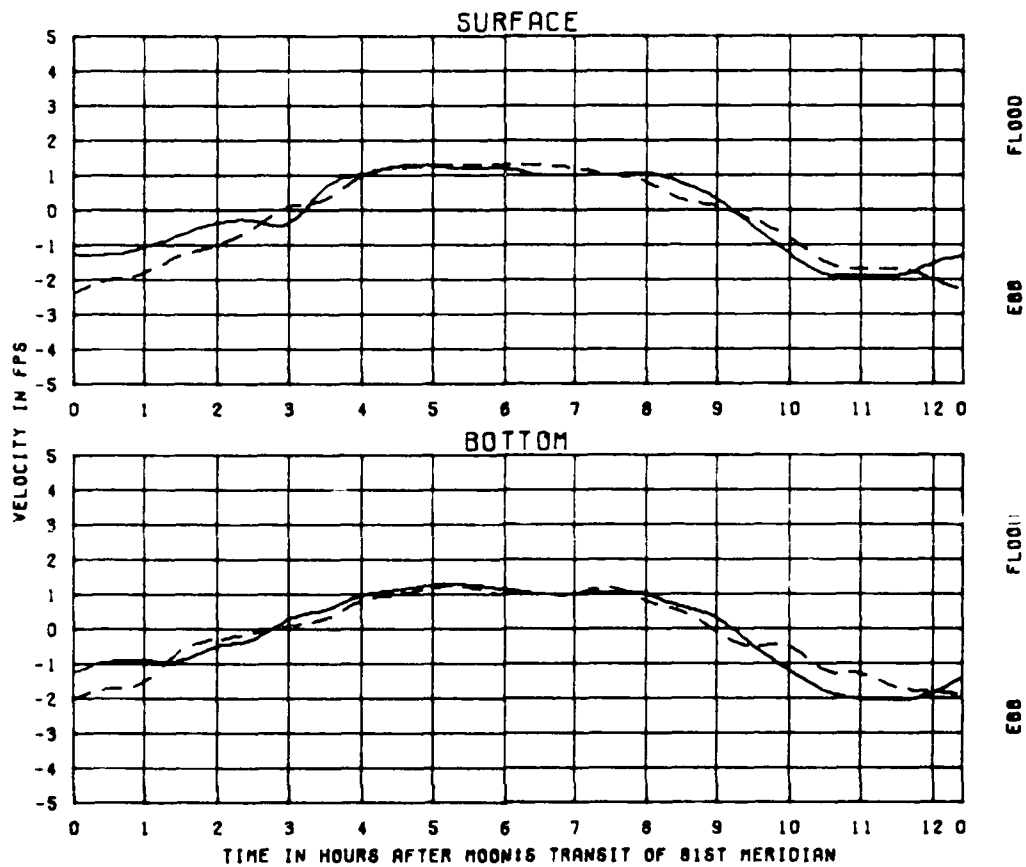
SURFACE

BOTTOM

VELOCITY IN FPS

TIME IN HOURS AFTER MOON'S TRANSIT OF 81ST MERIDIAN

TEST CONDITIONS
TIDE RANGE AT GAGE 1   5.8 FT
OCEAN SALINITY(TOTAL SALT)   32.5 PPT
FRESHWATER INFLOW   1100 CFS

KINGS BAY MODEL

EFFECTS OF
PLAN P4-1
ON VELOCITIES
STATION
396

LEGEND
BASE   ———
PLAN 1   — — —

PLATE C20

SURFACE

MIDDEPTH

BOTTOM

VELOCITY IN FPS

TIME IN HOURS AFTER MOON'S TRANSIT OF 81ST MERIDIAN

FLOOD

EBB

TEST CONDITIONS
TIDE RANGE AT GAGE 1   5.8 FT
OCEAN SALINITY(TOTAL SALT)   32.5 PPT
FRESHWATER INFLOW   1100 CFS

KINGS BAY MODEL

EFFECTS OF
PLAN P4-1
ON VELOCITIES
STATION
1385

LEGEND
BASE   ————
PLAN 1   — — —

SURFACE

MIDDEPTH

BOTTOM

VELOCITY IN FPS

FLOOD / EBB

TIME IN HOURS AFTER MOON'S TRANSIT OF 81ST MERIDIAN

TEST CONDITIONS
TIDE RANGE AT GAGE 1   5.8 FT
OCEAN SALINITY(TOTAL SALT)   32.5 PPT
FRESHWATER INFLOW   1100 CFS

KINGS BAY MODEL

EFFECTS OF
PLAN P4-1
ON VELOCITIES
STATION
650

LEGEND
BASE ————
PLAN 1 — — —

SURFACE

VELOCITY IN FPS

FLOOD

EBB

BOTTOM

FLOOD

EBB

TIME IN HOURS AFTER MOON'S TRANSIT OF 81ST MERIDIAN

TEST CONDITIONS
TIDE RANGE AT GAGE 1   5.8 FT
OCEAN SALINITY(TOTAL SALT)   32.5 PPT
FRESHWATER INFLOW   1100 CFS

KINGS BAY MODEL

**EFFECTS OF
PLAN P4-1
ON VELOCITIES**
STATION
584

LEGEND
BASE ————————
PLAN 1 — — — —

PLATE C23

SURFACE

MIDDEPTH

VELOCITY IN FPS

BOTTOM

TIME IN HOURS AFTER MOON'S TRANSIT OF 81ST MERIDIAN

FLOOD

EBB

TEST CONDITIONS
TIDE RANGE AT GAGE 1   5.8 FT
OCEAN SALINITY(TOTAL SALT)   32.5 PPT
FRESHWATER INFLOW   1100 CFS

KINGS BAY MODEL

EFFECTS OF
PLAN P4-1
ON VELOCITIES
STATION
1915

LEGEND
BASE   ————
PLAN 1 — — —

SURFACE

MIDDEPTH

BOTTOM

VELOCITY IN FPS

TIME IN HOURS AFTER MOON'S TRANSIT OF 81ST MERIDIAN

FLOOD

EBB

TEST CONDITIONS		KINGS BAY MODEL
TIDE RANGE AT GAGE 1	5.8 FT	
OCEAN SALINITY(TOTAL SALT)	32.5 PPT	
FRESHWATER INFLOW	1100 CFS	

EFFECTS OF
PLAN P4-1
ON VELOCITIES
STATION
1851

LEGEND
BASE ————
PLAN 1 — — —

SURFACE / MIDDEPTH / BOTTOM

VELOCITY IN FPS

TIME IN HOURS AFTER MOON'S TRANSIT OF 81ST MERIDIAN

TEST CONDITIONS
TIDE RANGE AT GAGE 1   5.8 FT
OCEAN SALINITY(TOTAL SALT)   32.5 PPT
FRESHWATER INFLOW   1100 CFS

KINGS BAY MODEL

EFFECTS OF
PLAN P4-1
ON VELOCITIES
STATION
1182

LEGEND
BASE   ————
PLAN 1   — — —
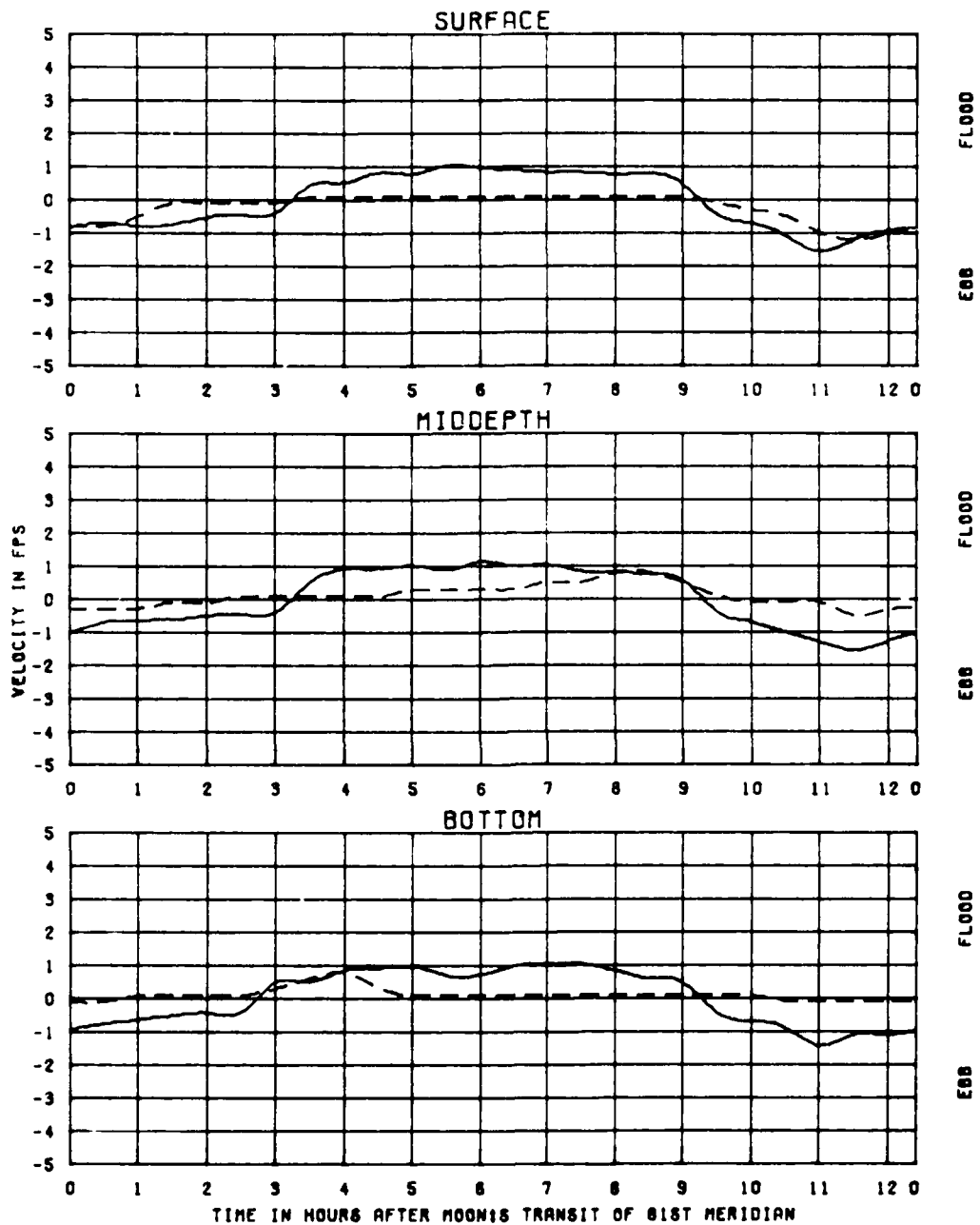
PLATE C26

SURFACE

MIDDEPTH

VELOCITY IN FPS

BOTTOM

TIME IN HOURS AFTER MOON'S TRANSIT OF 81ST MERIDIAN

TEST CONDITIONS
TIDE RANGE AT GAGE 1   5.8 FT
OCEAN SALINITY(TOTAL SALT)   32.5 PPT
FRESHWATER INFLOW   1100 CFS

KINGS BAY MODEL

EFFECTS OF
PLAN P4-1
ON VELOCITIES
STATION
1142

LEGEND
BASE   ————
PLAN 1   — — —
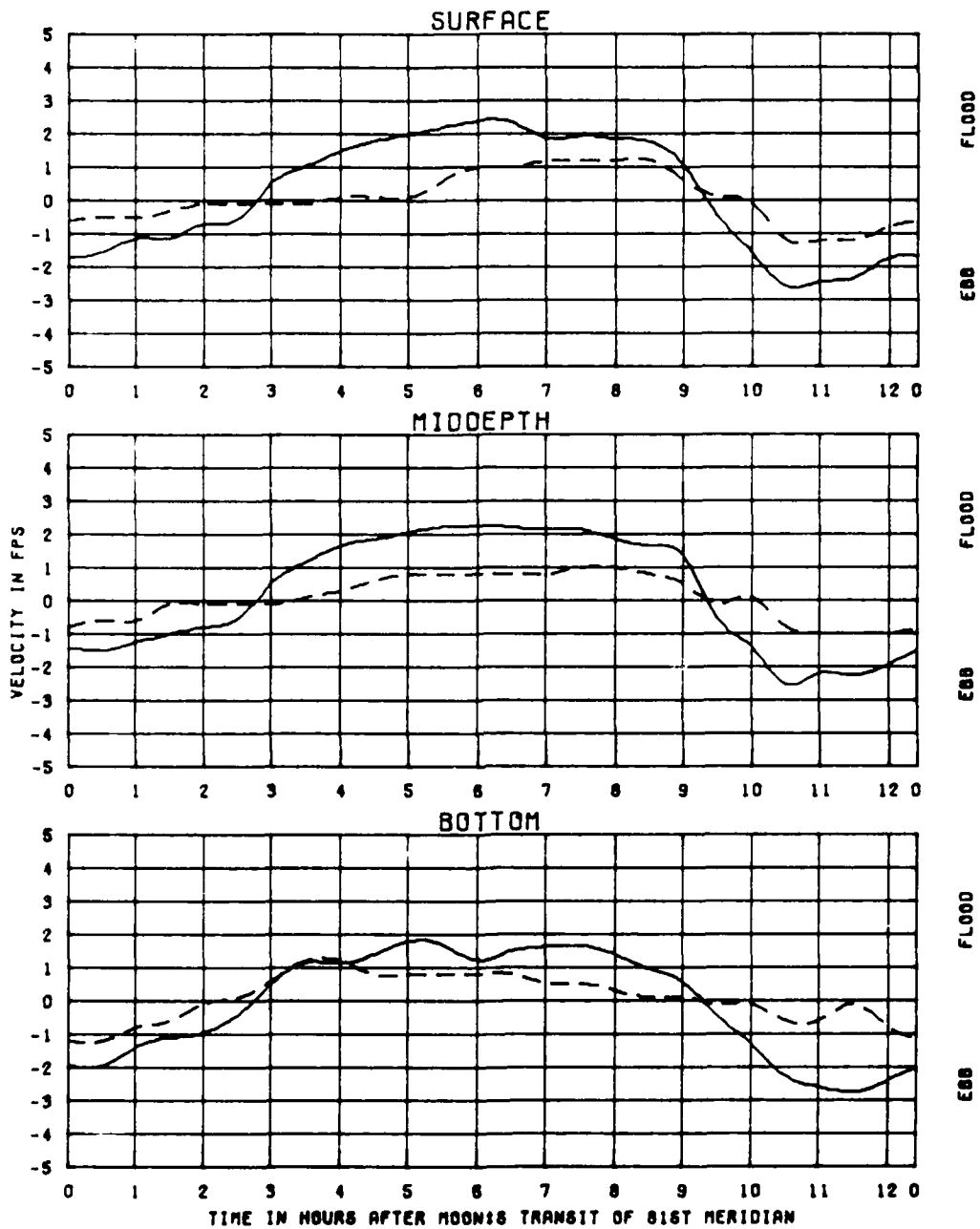
PLATE C27

SURFACE

MIDDEPTH

BOTTOM

VELOCITY IN FPS

FLOOD

EBB

TIME IN HOURS AFTER MOON'S TRANSIT OF 81ST MERIDIAN

TEST CONDITIONS
TIDE RANGE AT GAGE 1   5.8 FT
OCEAN SALINITY(TOTAL SALT)   32.5 PPT
FRESHWATER INFLOW   1100 CFS

KINGS BAY MODEL

EFFECTS OF
PLAN P4-1
ON VELOCITIES
STATION
2074

LEGEND
BASE —————
PLAN 1 — — —
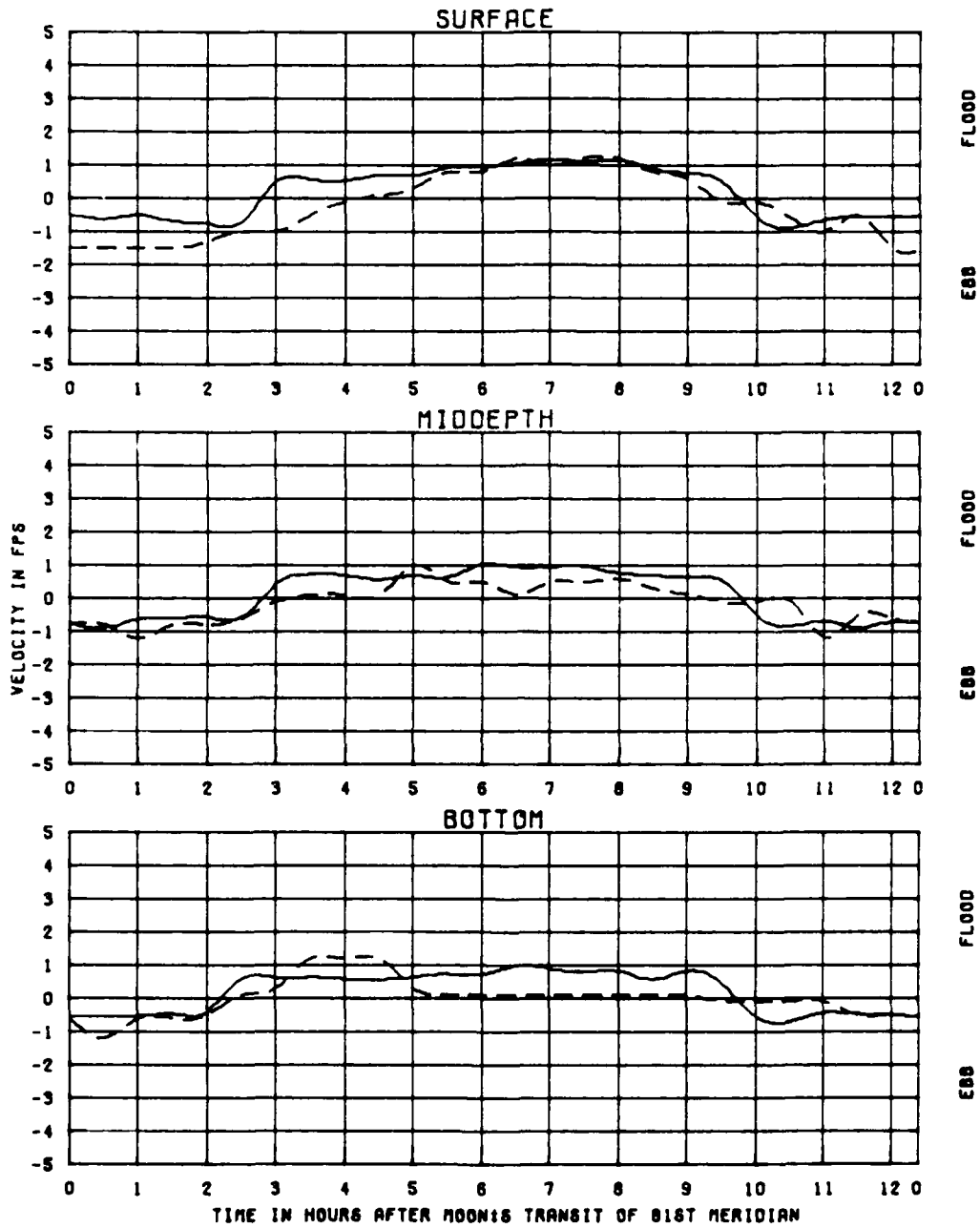
PLATE C28

SURFACE

MIDDEPTH

VELOCITY IN FPS

BOTTOM

TIME IN HOURS AFTER MOON'S TRANSIT OF 81ST MERIDIAN

TEST CONDITIONS
TIDE RANGE AT GAGE 1 — 5.8 FT
OCEAN SALINITY(TOTAL SALT) — 32.5 PPT
FRESHWATER INFLOW — 1100 CFS

KINGS BAY MODEL

EFFECTS OF
PLAN P4-1
ON VELOCITIES
STATION
2089

LEGEND
BASE ———
PLAN 1 — — —

MIDDEPTH

TEST CONDITIONS
TIDE RANGE AT GAGE 1   5.8 FT
OCEAN SALINITY(TOTAL SALT)   32.5 PPT
FRESHWATER INFLOW   1100 CFS

KINGS BAY MODEL

EFFECTS OF
PLAN P4-1
ON VELOCITIES
STATION
1014

LEGEND
BASE   ————
PLAN 1   — — —
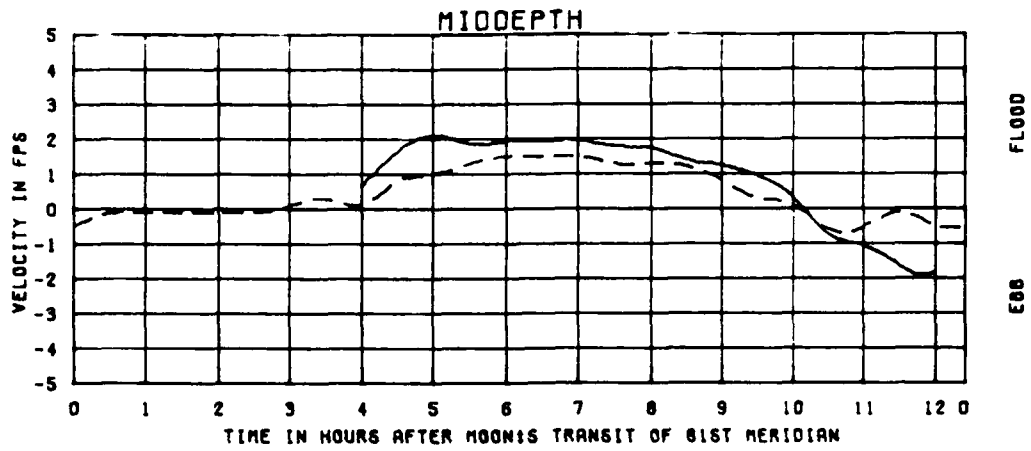
PLATE C30

MIDDEPTH

TEST CONDITIONS
TIDE RANGE AT GAGE 1   5.8 FT
OCEAN SALINITY(TOTAL SALT)   32.5 PPT
FRESHWATER INFLOW   1100 CFS

LEGEND
BASE   —————
PLAN 1   — — —

KINGS BAY MODEL

EFFECTS OF
PLAN P4-1
ON VELOCITIES
STATION
1066

PLATE C31

SURFACE

BOTTOM

VELOCITY IN FPS

TIME IN HOURS AFTER MOON'S TRANSIT OF 81ST MERIDIAN

FLOOD

EBB
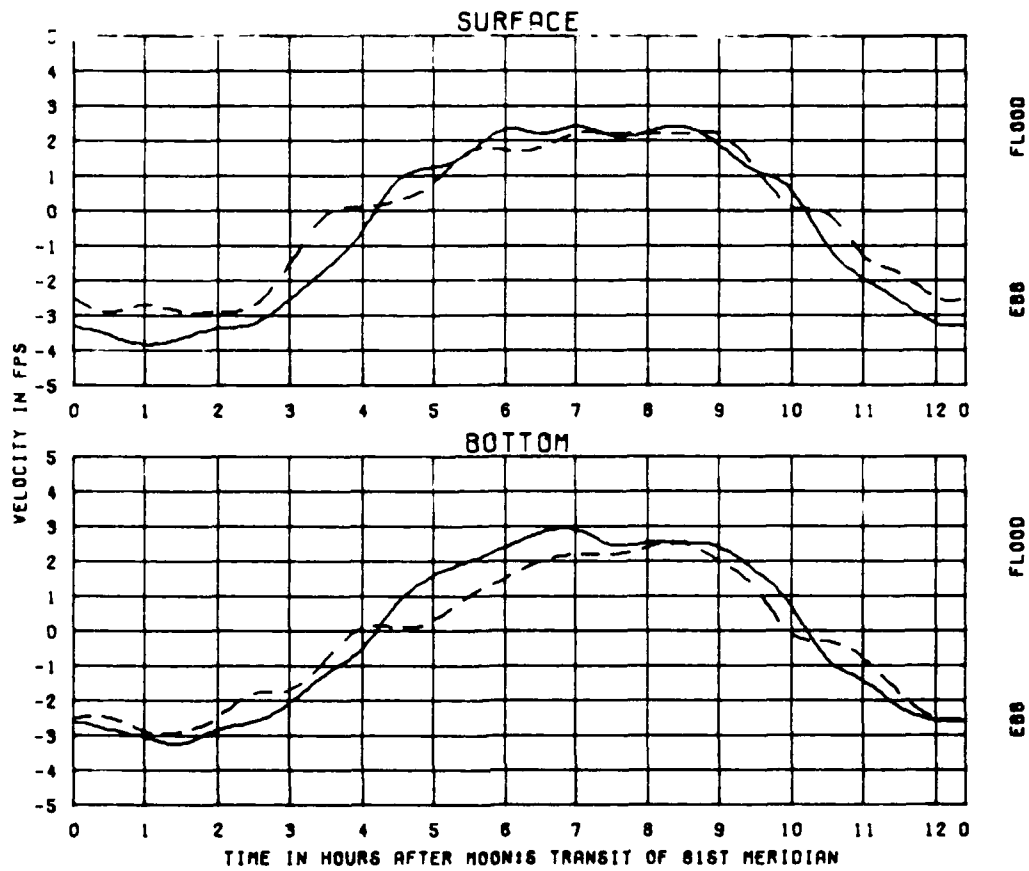
TEST CONDITIONS
TIDE RANGE AT GAGE 1   5.8 FT
OCEAN SALINITY(TOTAL SALT)   32.5 PPT
FRESHWATER INFLOW   1100 CFS

KINGS BAY MODEL

EFFECTS OF
PLAN P4-1
ON VELOCITIES
STATION
230

LEGEND
BASE ————
PLAN 1 — — —
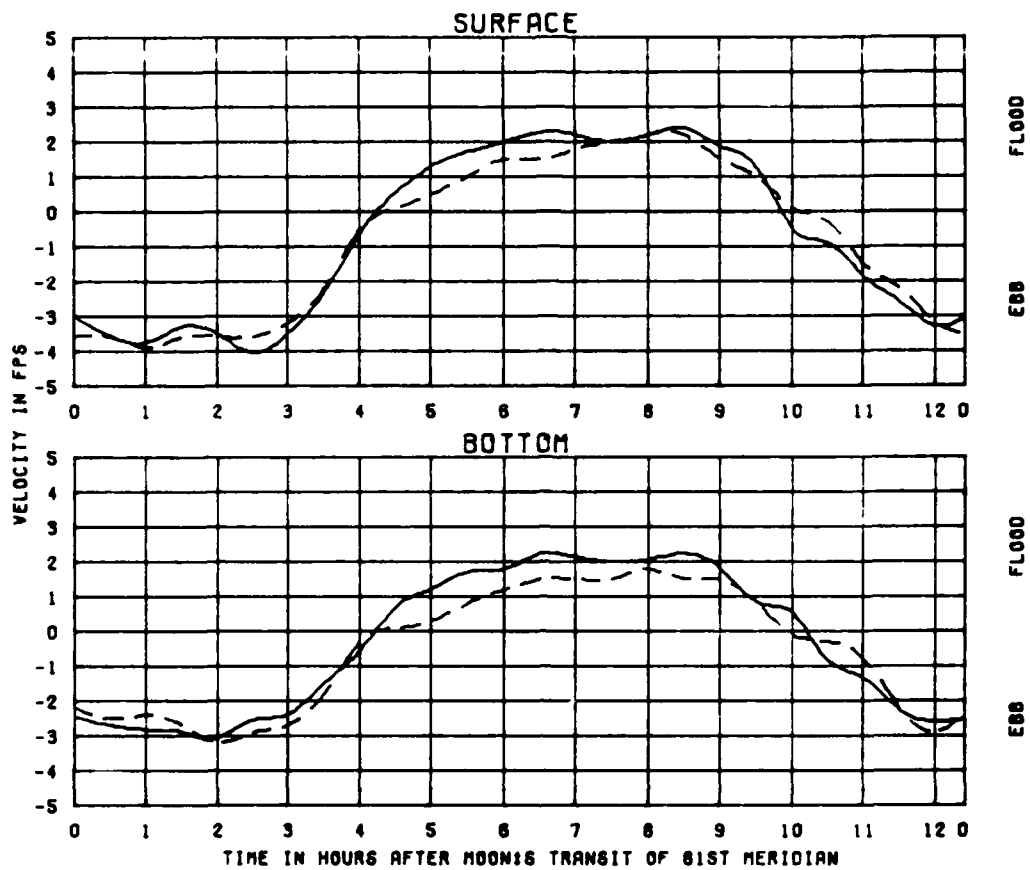
PLATE C32

SURFACE

BOTTOM

TIME IN HOURS AFTER MOON'S TRANSIT OF 81ST MERIDIAN

VELOCITY IN FPS

FLOOD

EBB

FLOOD

EBB

SURFACE

MIDDEPTH

BOTTOM

TIME IN HOURS AFTER MOON'S TRANSIT OF 81ST MERIDIAN

VELOCITY IN FPS

FLOOD

EBB

TEST CONDITIONS

TIDE RANGE AT GAGE 1	5.8 FT
OCEAN SALINITY(TOTAL SALT)	32.5 PPT
FRESHWATER INFLOW	1100 CFS

KINGS BAY MODEL

EFFECTS OF
PLAN P4-1
ON VELOCITIES
STATION
818

LEGEND
BASE ————
PLAN 1 — — —

PLATE C34

MIDDEPTH

TIME IN HOURS AFTER MOON'S TRANSIT OF 81ST MERIDIAN

VELOCITY IN FPS

FLOOD

EBB

TEST CONDITIONS		KINGS BAY MODEL
TIDE RANGE AT GAGE 1	5.8 FT	
OCEAN SALINITY(TOTAL SALT)	32.5 PPT	EFFECTS OF
FRESHWATER INFLOW	1100 CFS	PLAN P4-1
		ON VELOCITIES

LEGEND
BASE ————
PLAN 1 — — —

EFFECTS OF
PLAN P4-1
ON VELOCITIES
STATION

812

SURFACE

BOTTOM

VELOCITY IN FPS

TIME IN HOURS AFTER MOON'S TRANSIT OF 81ST MERIDIAN

FLOOD

EBB

FLOOD

EBB
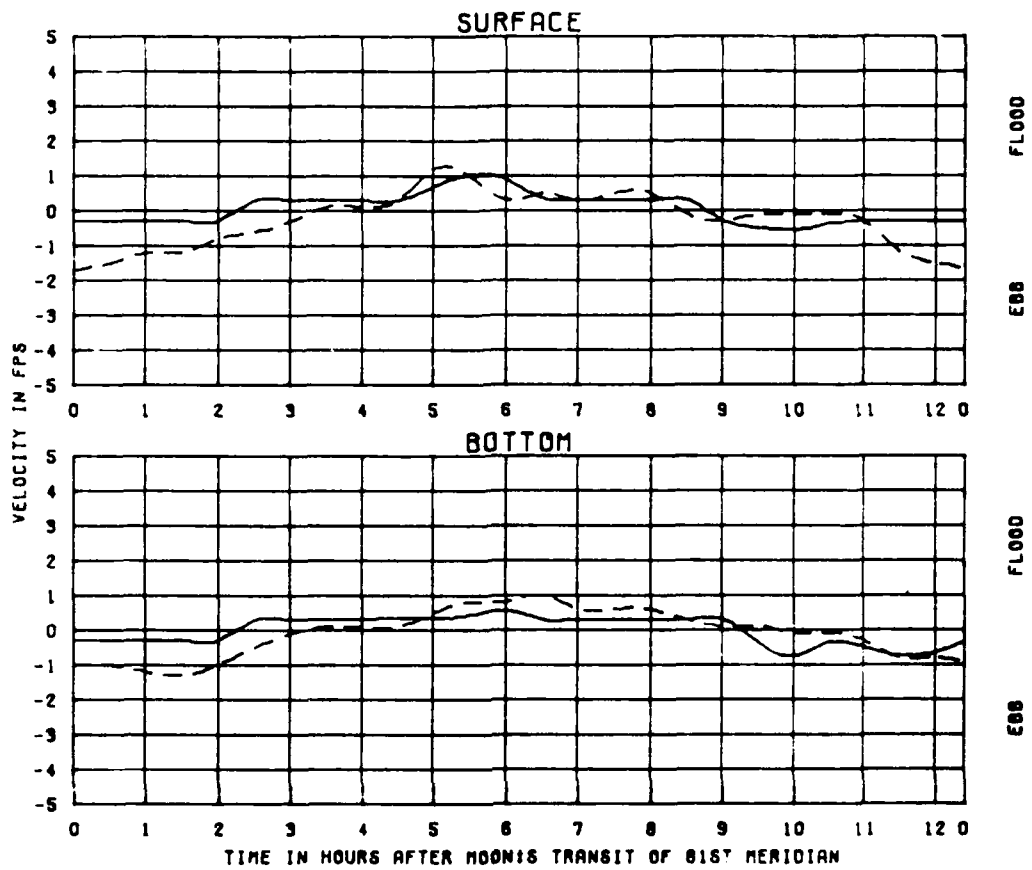
TEST CONDITIONS
TIDE RANGE AT GAGE 1   5.8 FT
OCEAN SALINITY(TOTAL SALT)   32.5 PPT
FRESHWATER INFLOW   1100 CFS

KINGS BAY MODEL

EFFECTS OF
PLAN P4-1
ON VELOCITIES
STATION
1276

LEGEND
BASE
PLAN 1

PLATE C36

SURFACE

BOTTOM

TIME IN HOURS AFTER MOON'S TRANSIT OF 81ST MERIDIAN

MIDDEPTH

TEST CONDITIONS
TIDE RANGE AT GAGE 1   5.8 FT
OCEAN SALINITY(TOTAL SALT)   32.5 PPT
FRESHWATER INFLOW   1100 CFS

KINGS BAY MODEL

EFFECTS OF
PLAN P4-1
ON VELOCITIES
STATION
180

LEGEND
BASE   ————
PLAN 1 — — —

PLATE C38

APPENDIX D: NUMERICAL MODEL MESH 4 PRE-TRIDENT
BASE AND BASIC TRIDENT PLAN COMPARISONS
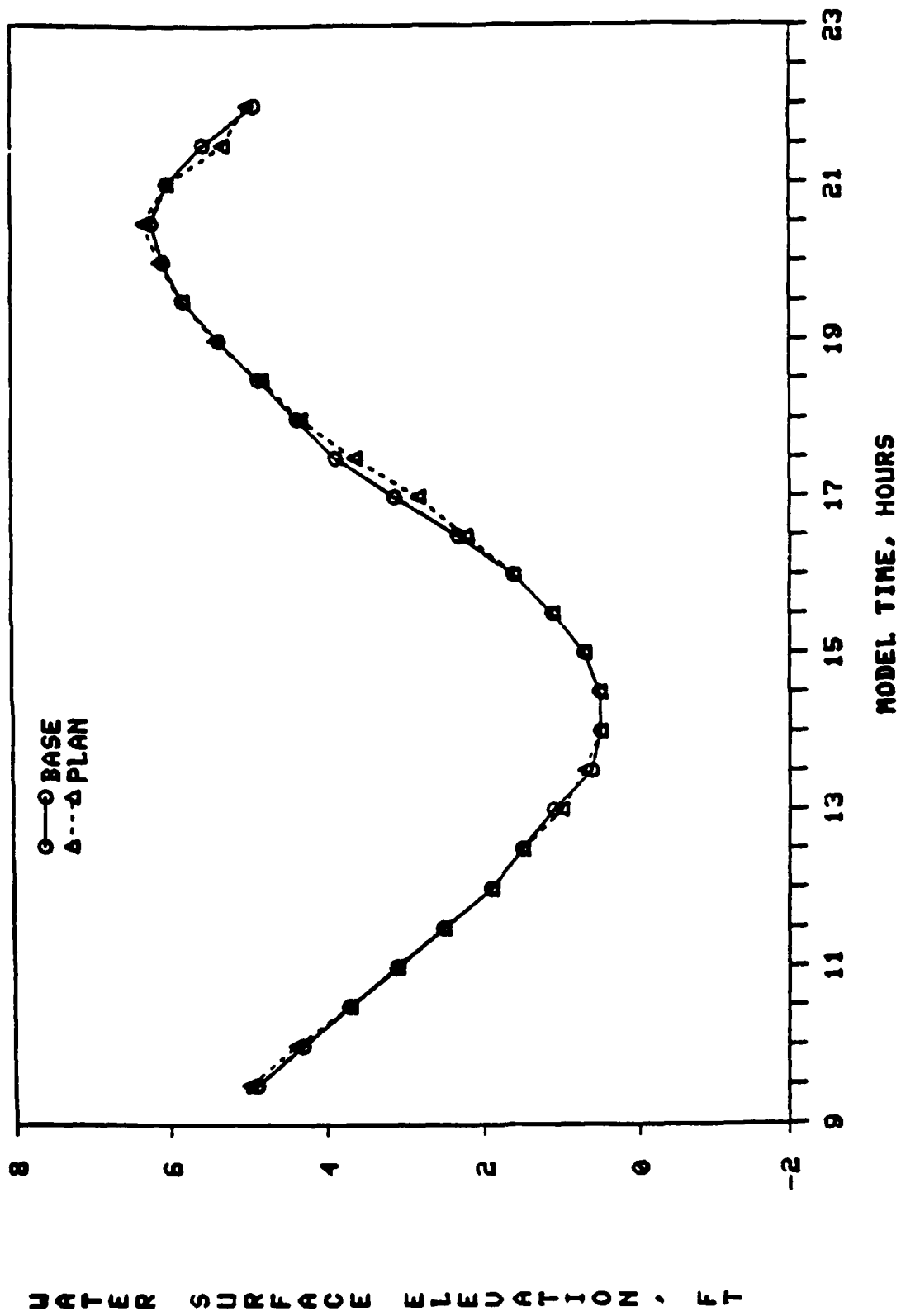
Plate D1. Physical model base and plan water-surface elevations, ocean tide control
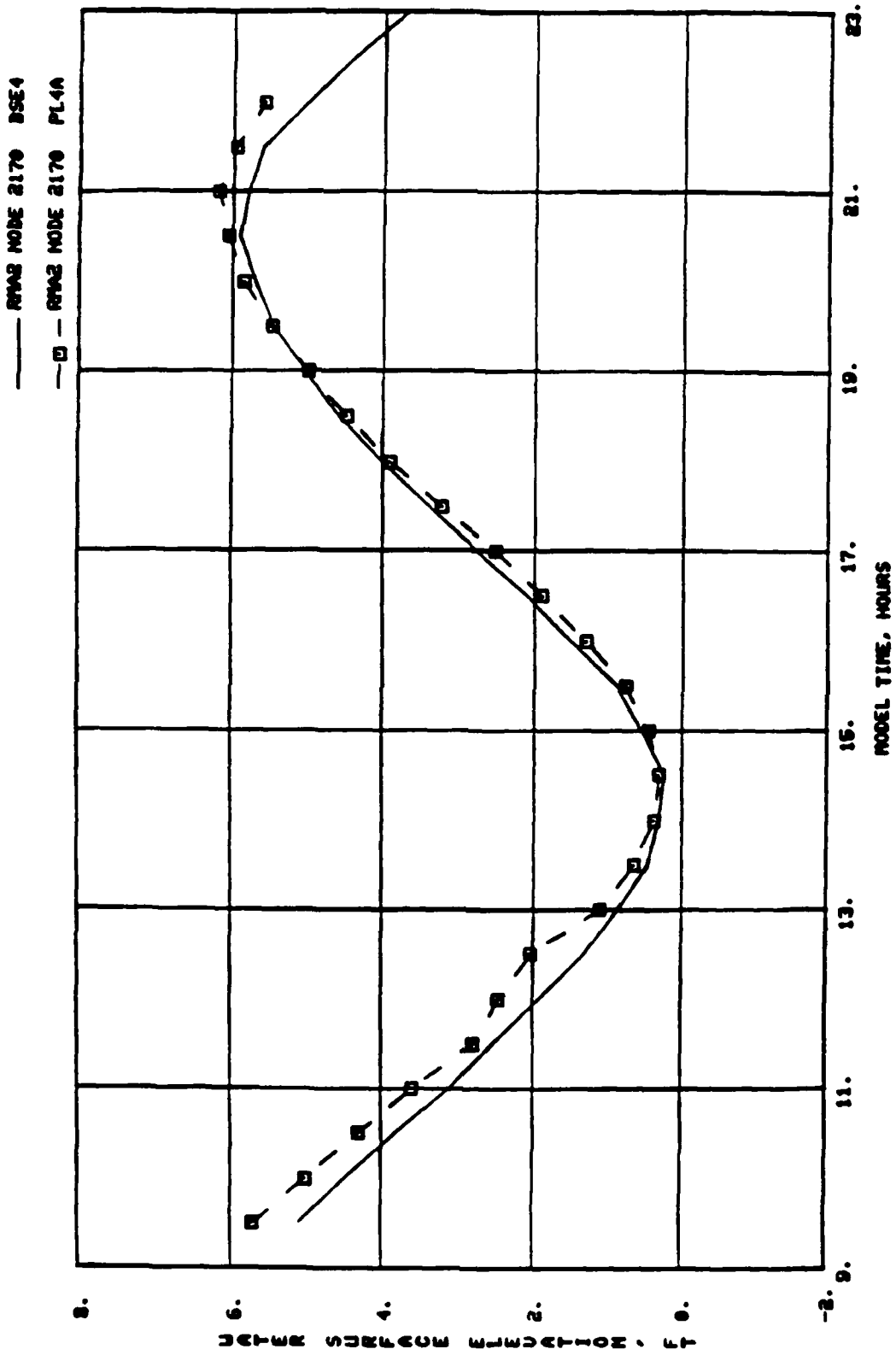
Plate D2. Numerical model base and plan water-surface elevations, node 2170 (ocean boundary)
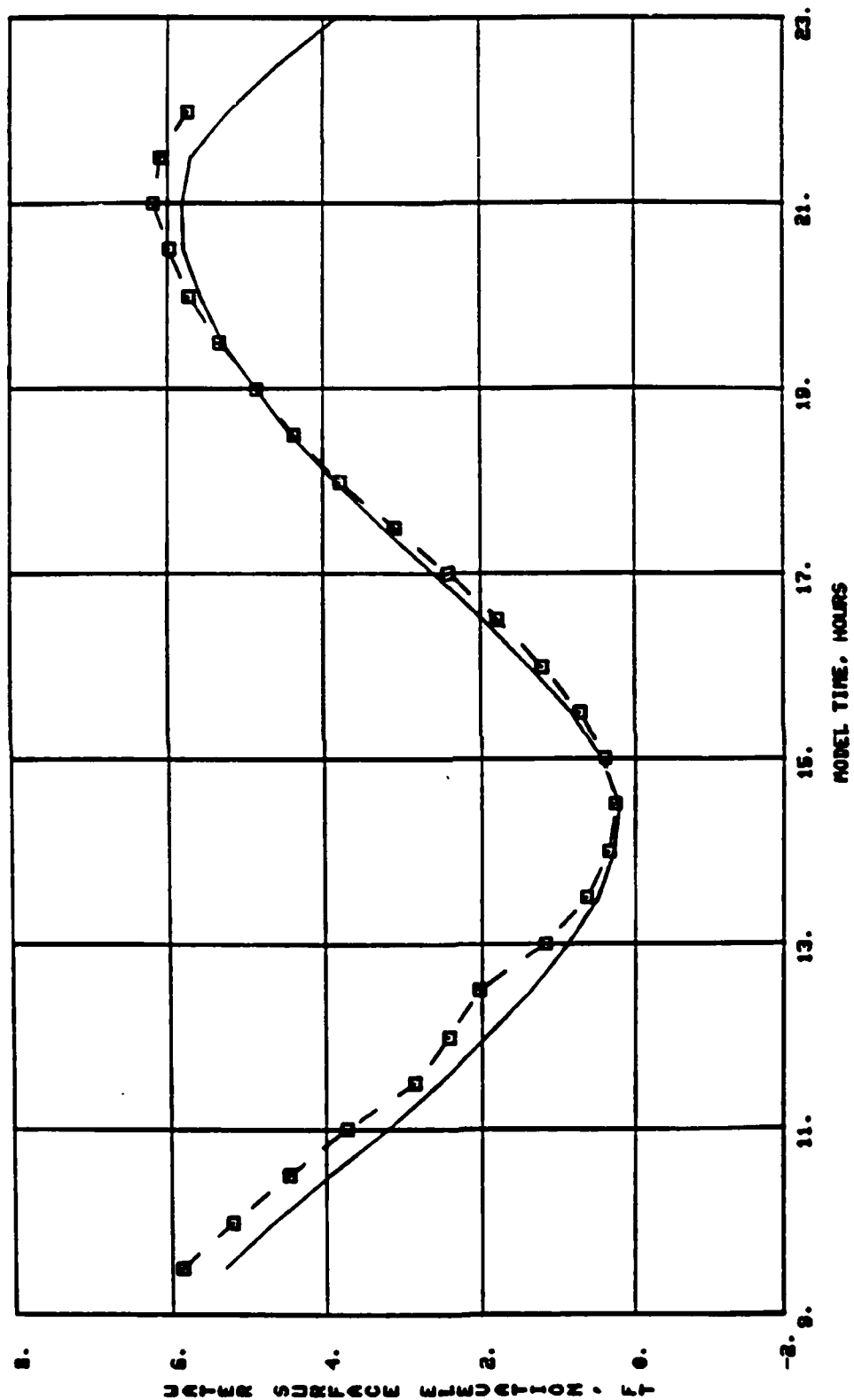
Plate D3. Numerical model base and plan water-surface elevations, node 1939 (same as station 2, physical model, St. Marys Inlet)
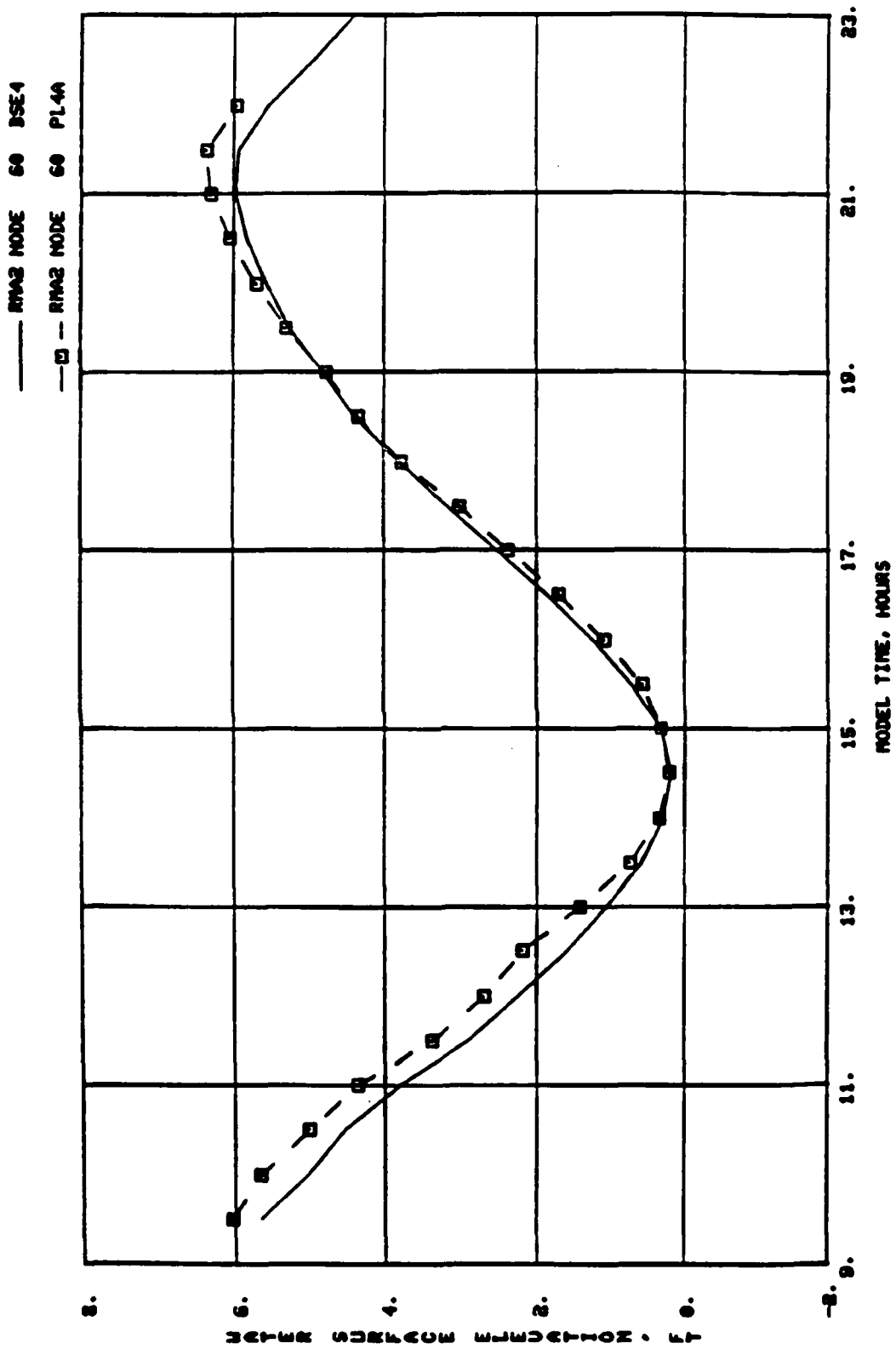
Plate D4. Numerical model base and plan water-surface elevations, node 60 (Amelia River)
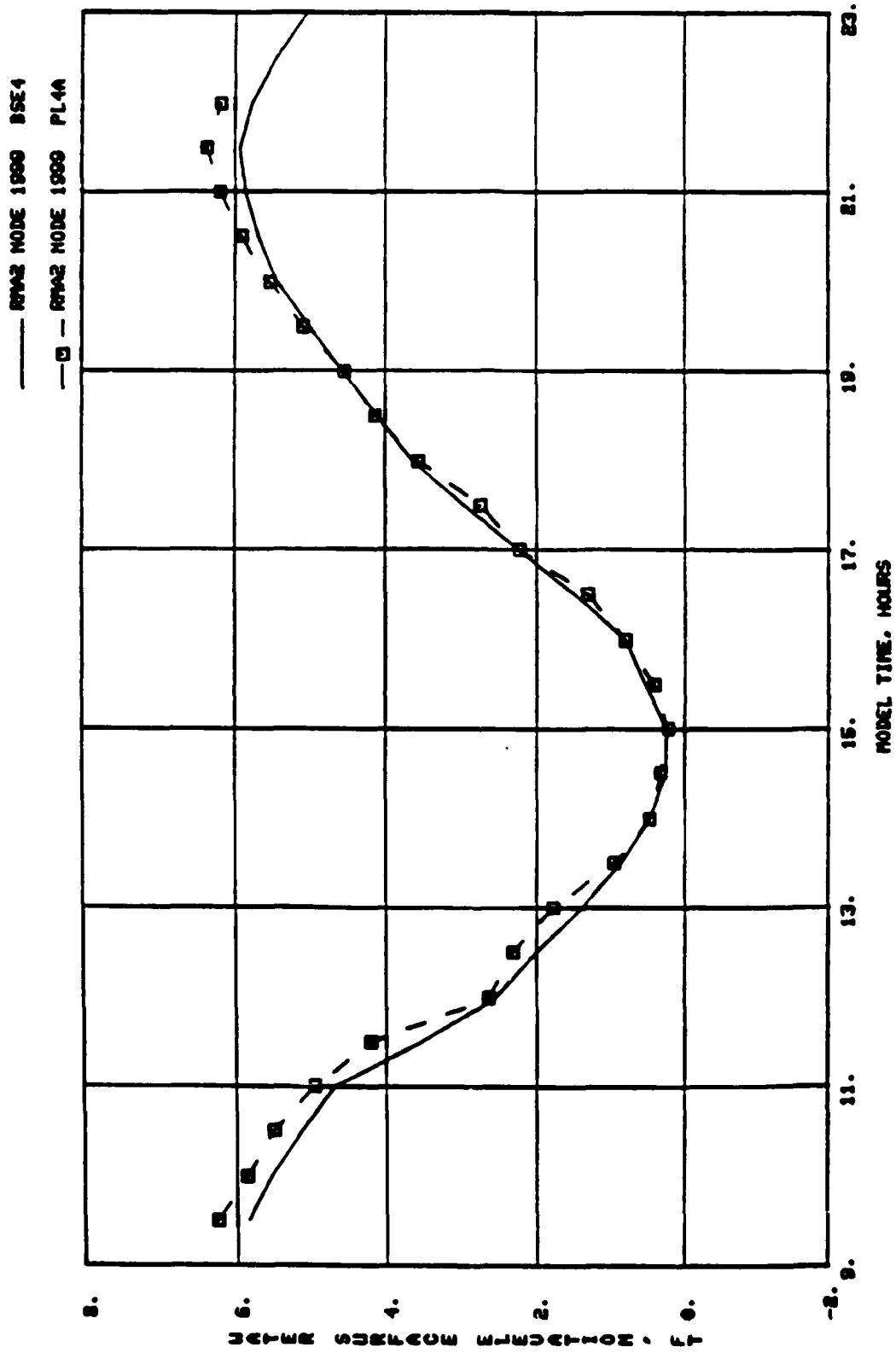
Plate D5. Numerical model base and plan water-surface elevations, node 1999 (Jolly River)
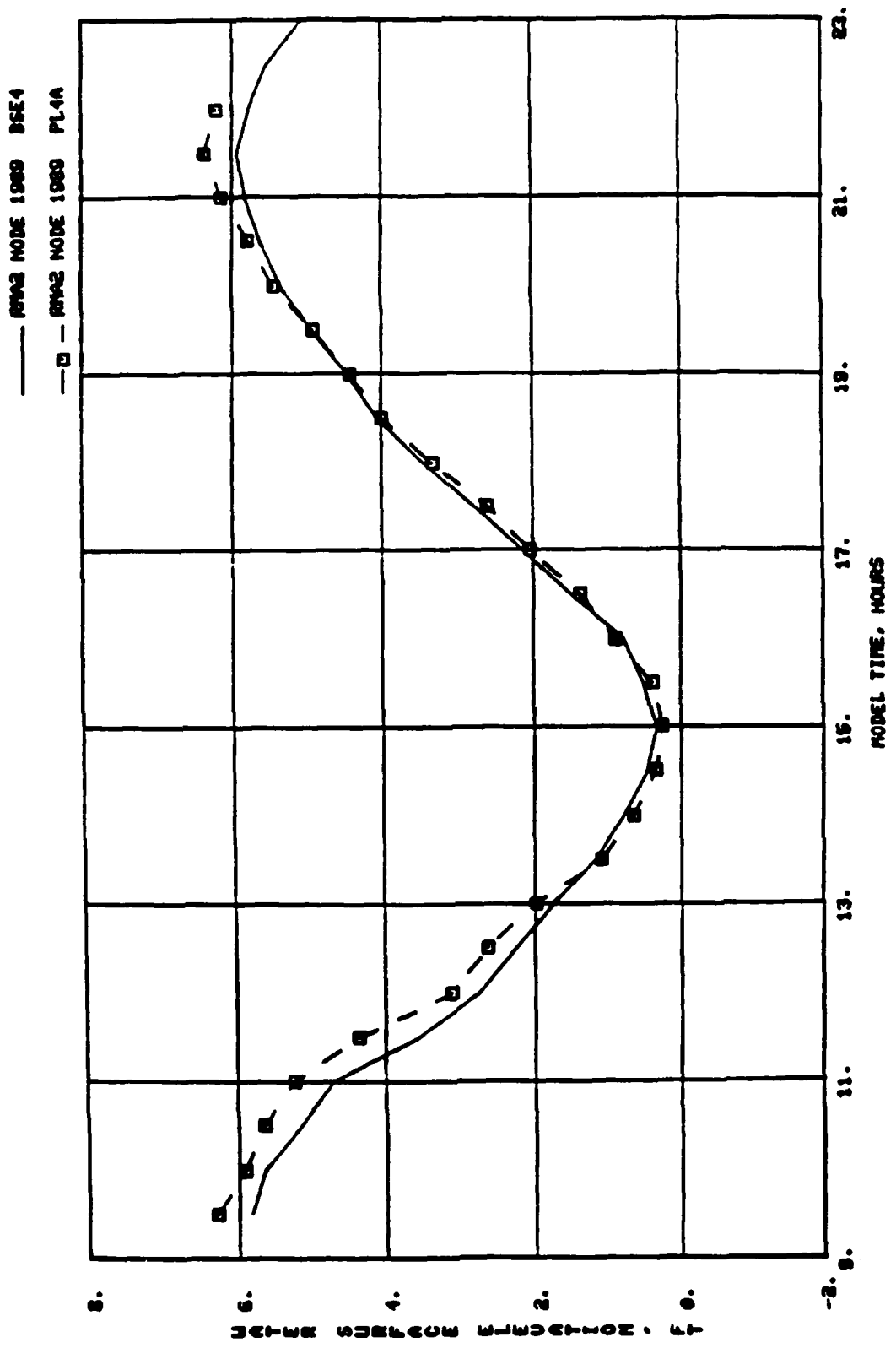
Plate D6. Numerical model base and plan water-surface elevations, node 1989 (St. Marys River)
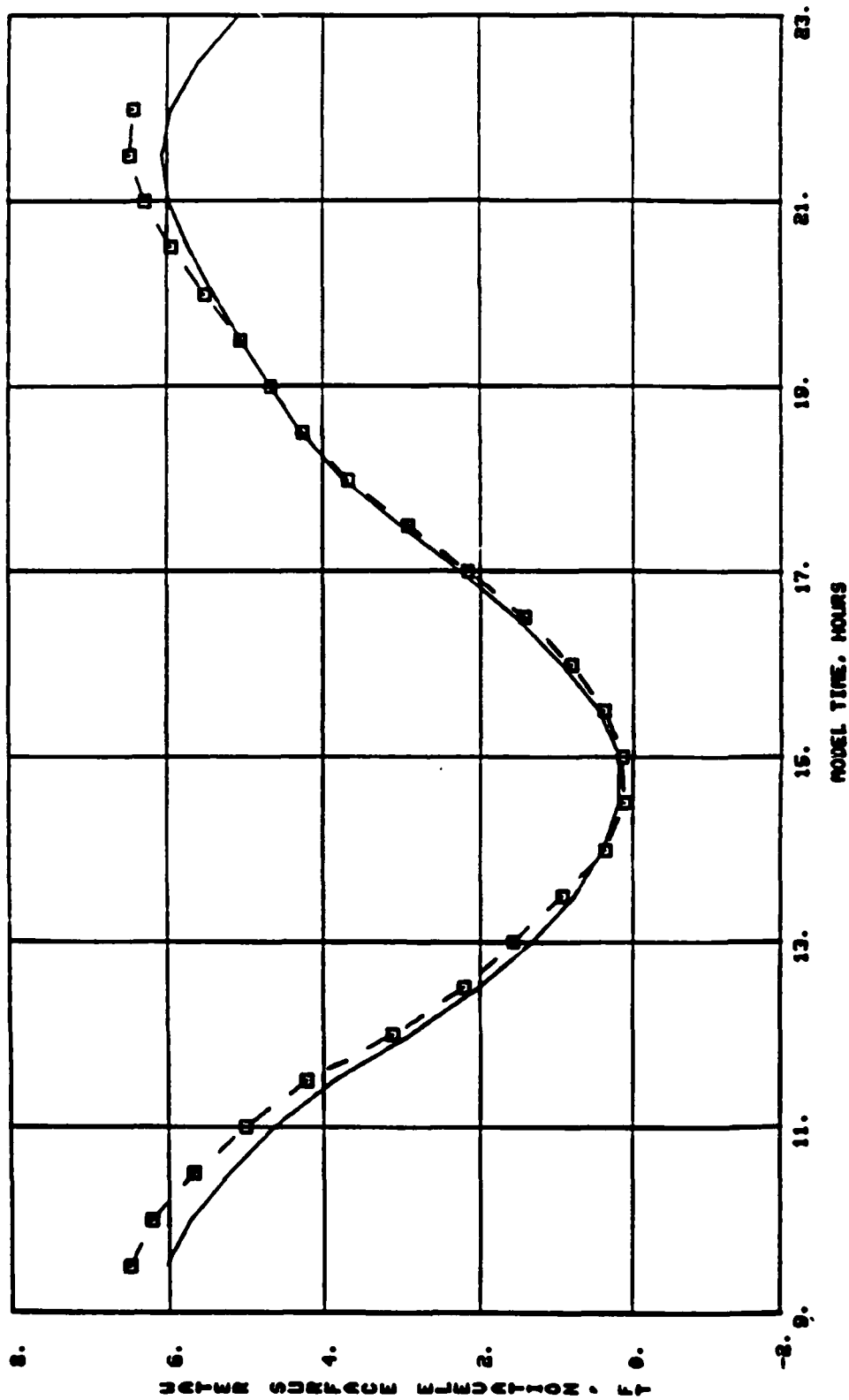
Plate D7. Numerical model base and plan water-surface elevations,
node 1150 (same as station 6, physical model, lower Kings Bay)
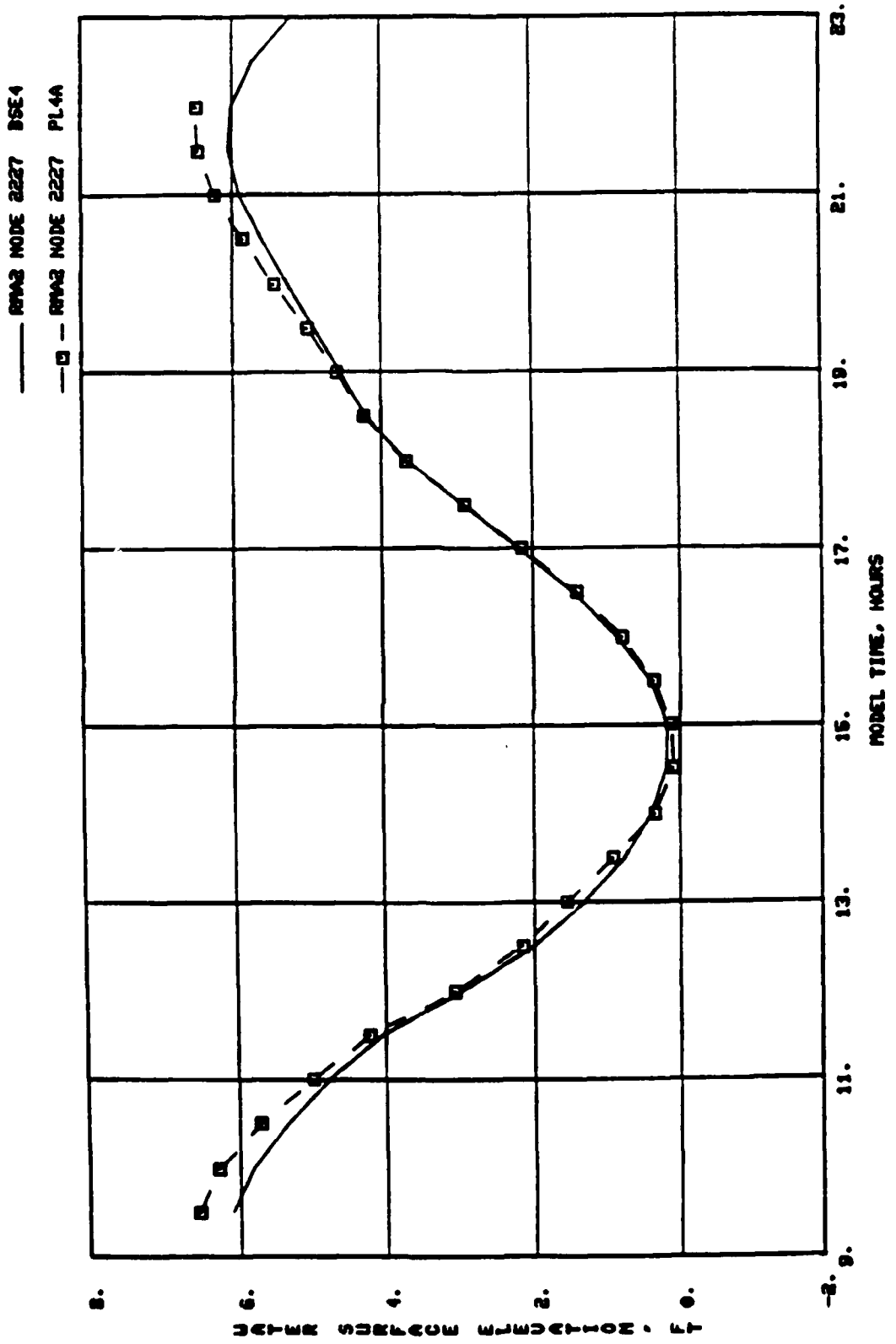
Plate D8. Numerical model base and plan water-surface elevations, node 2227 (same as station 7, physical model, Marianna Creek)
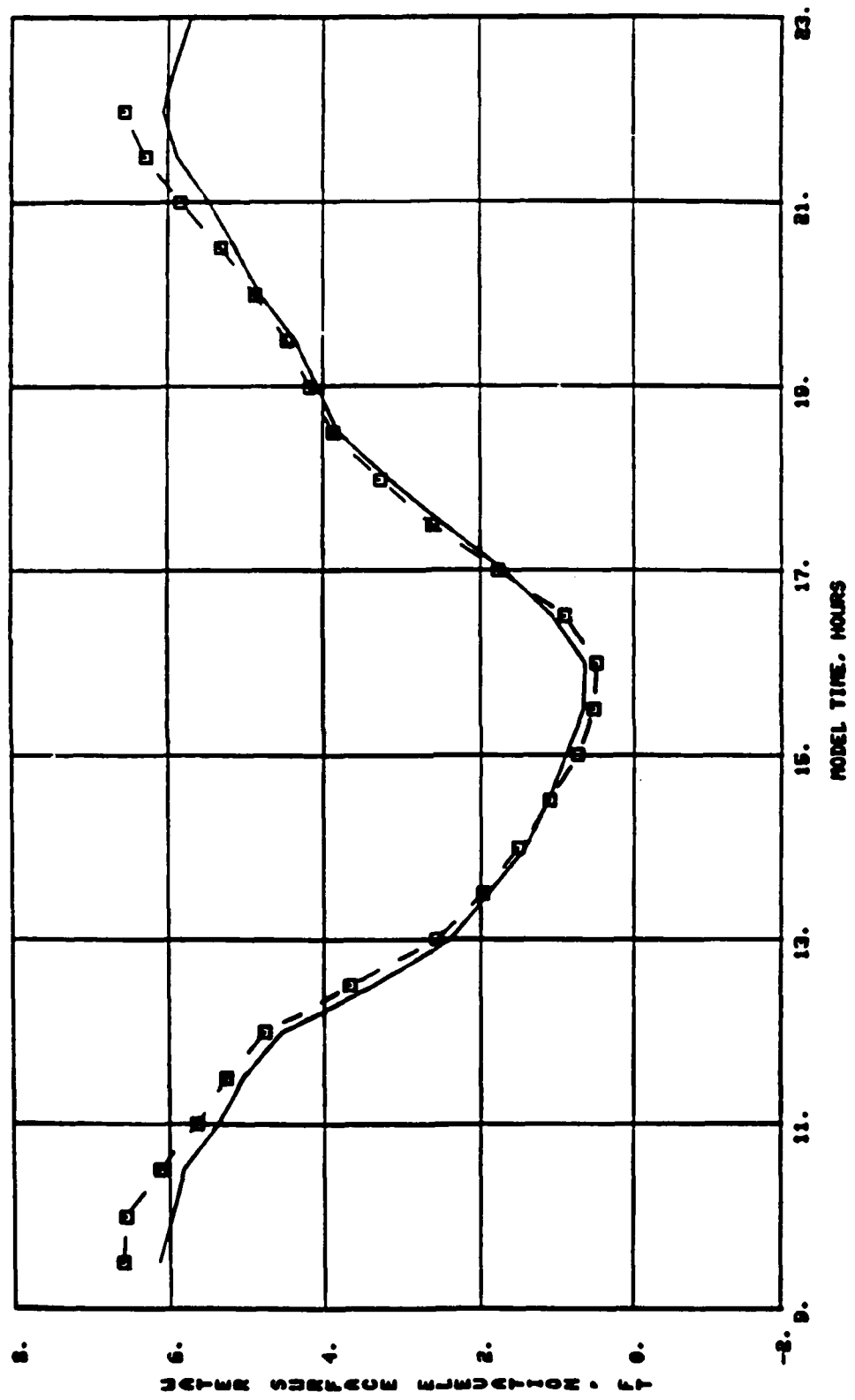
Plate D9. Numerical model base and plan water-surface elevations,
node 240 (Crooked River)
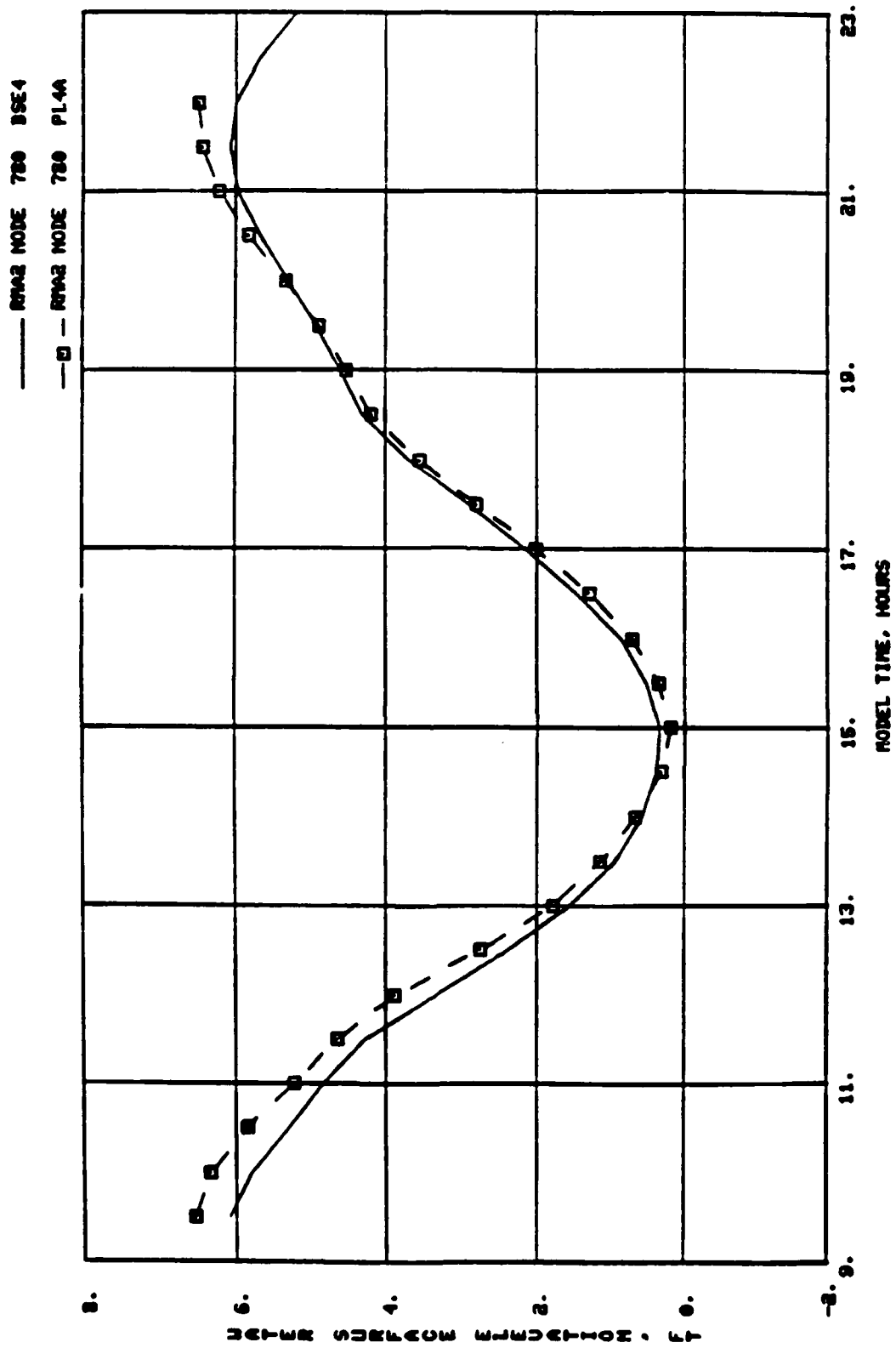
Plate D10. Numerical model base and plan water-surface elevations, node 780 (same as station 9, physical model, upper Cumberland Sound)

D12
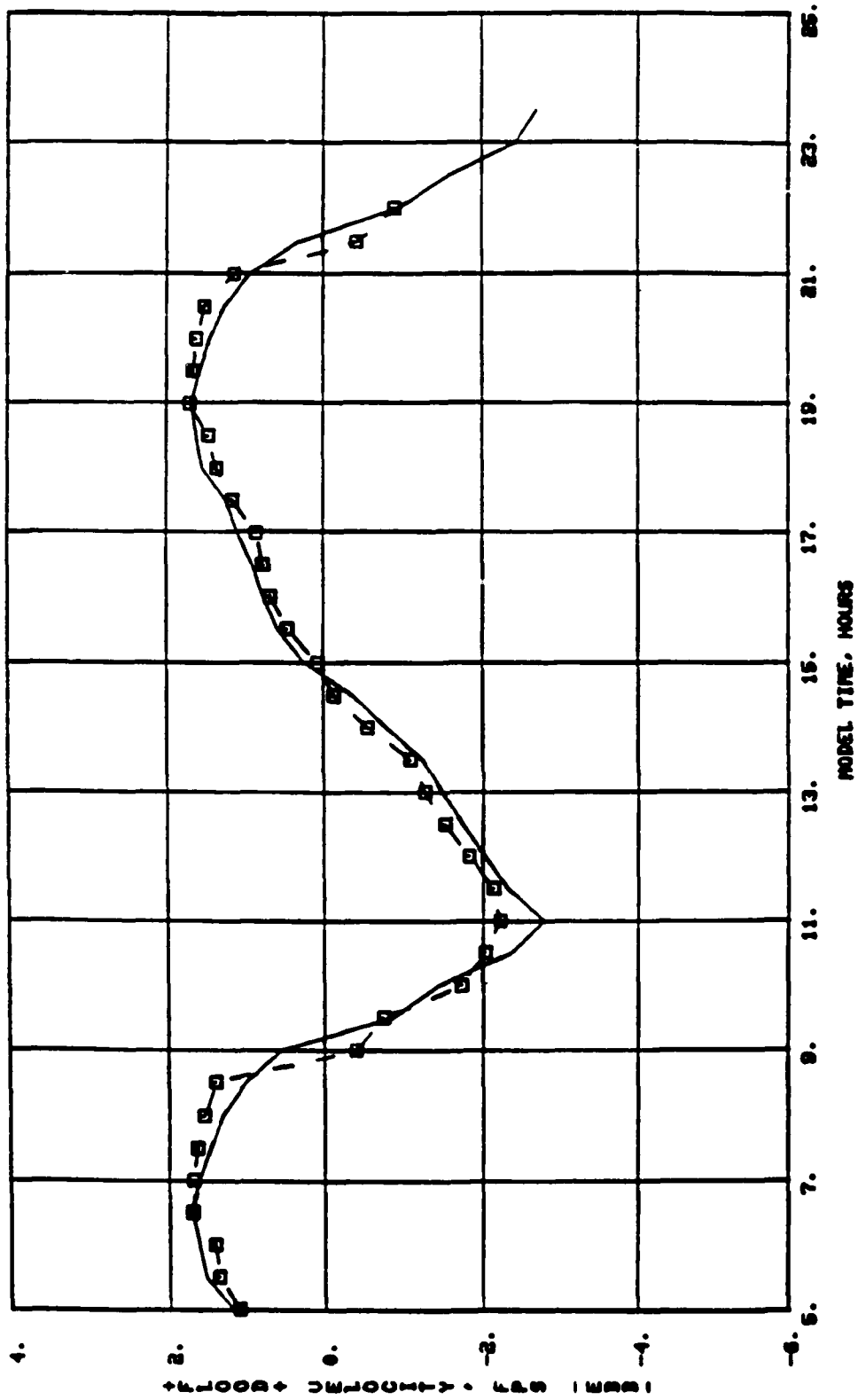
Plate D11. Numerical model base and plan velocities for node 60 (Amelia River boundary)
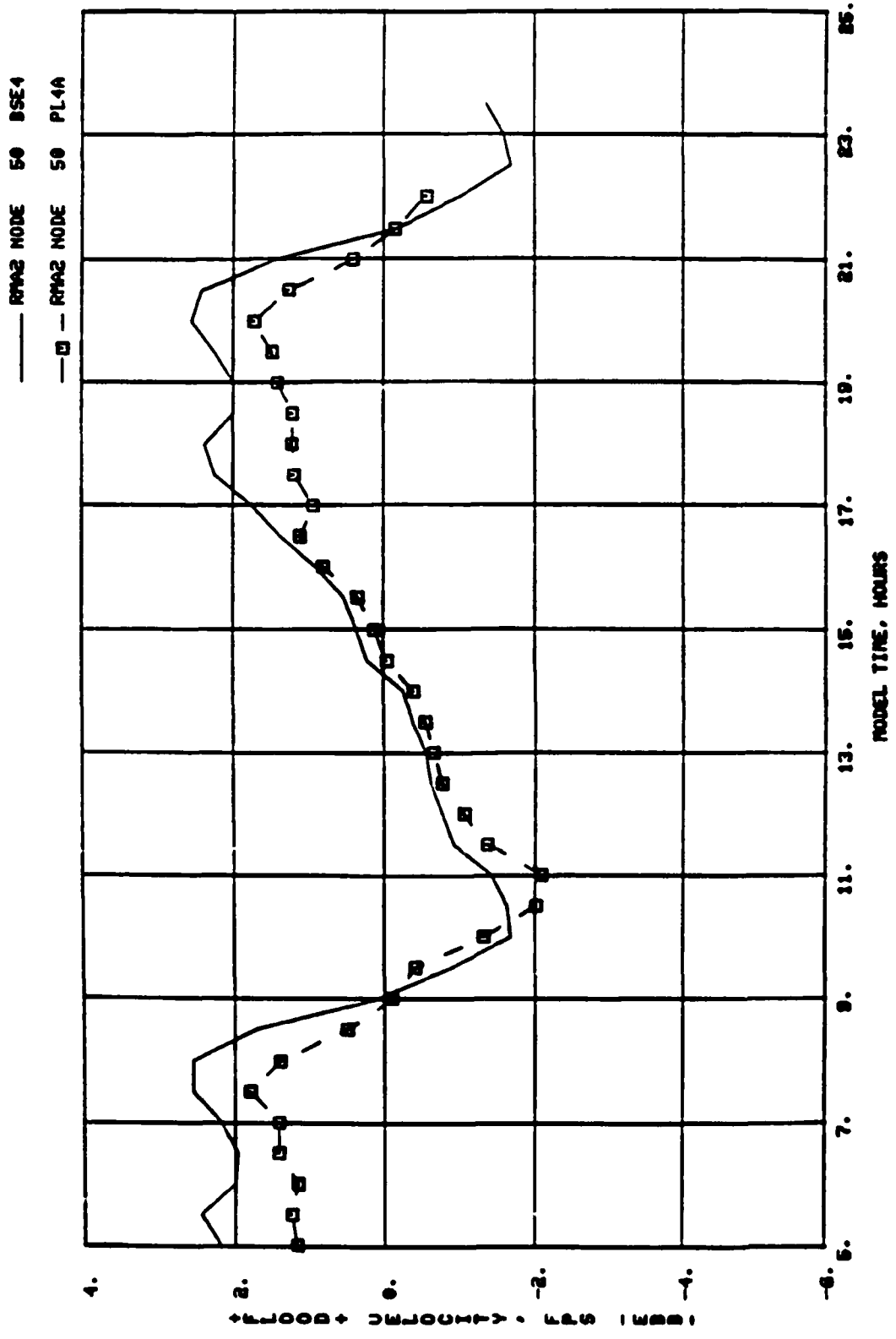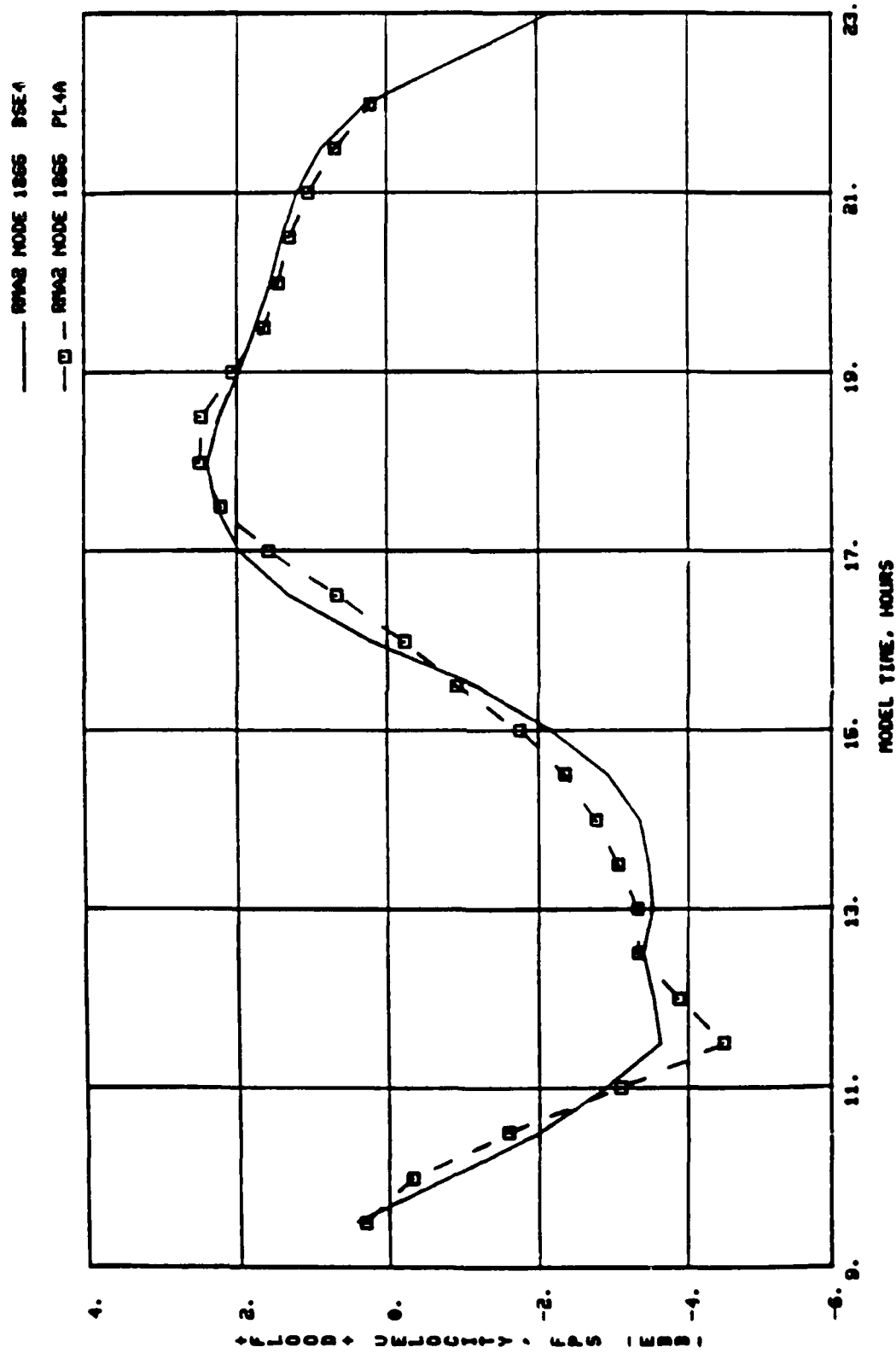
Plate D12. Numerical model base and plan velocities for node 50
(Amelia River boundary)
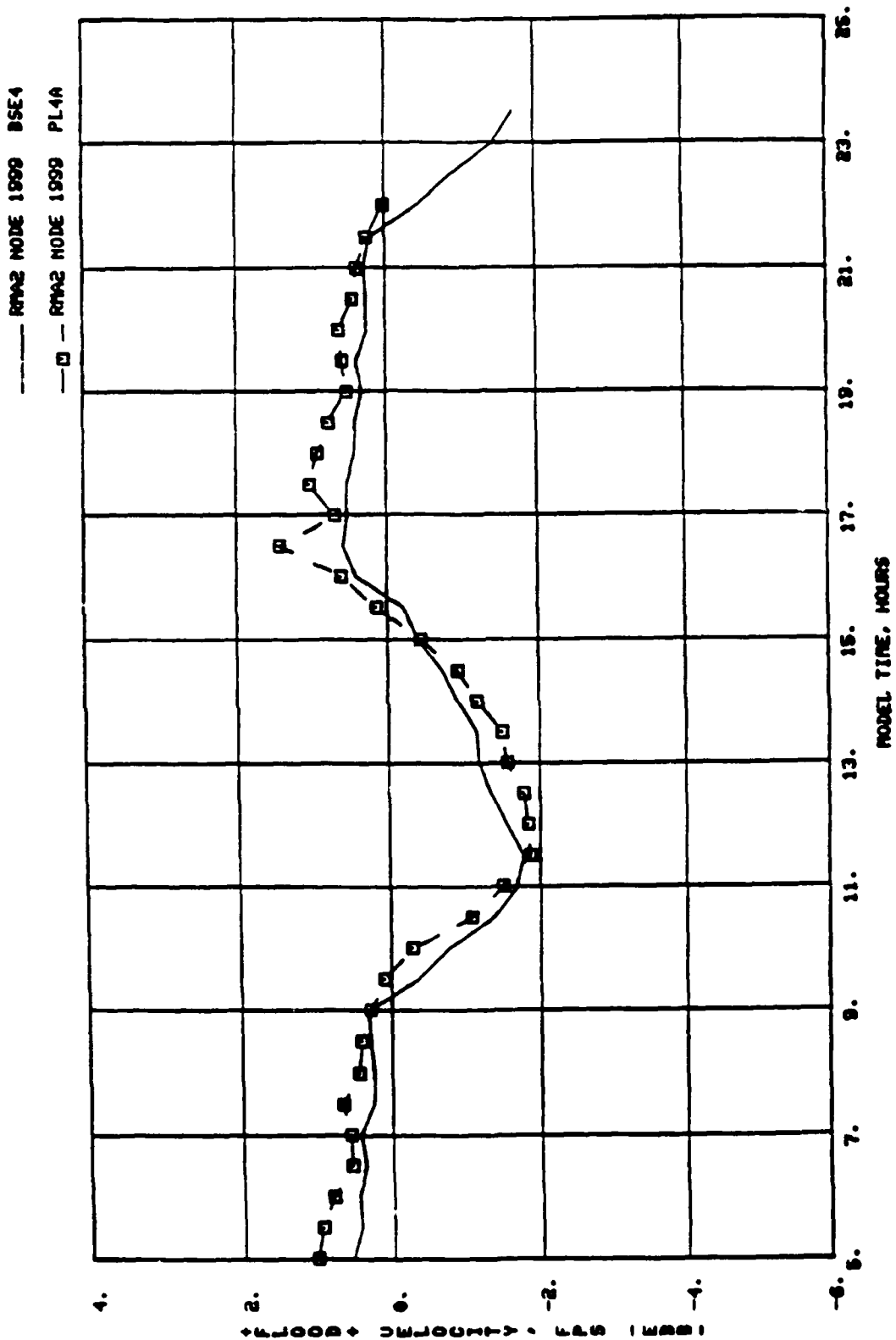
Plate D13. Numerical model base and plan velocities for node 1999 (Jolly River boundary)
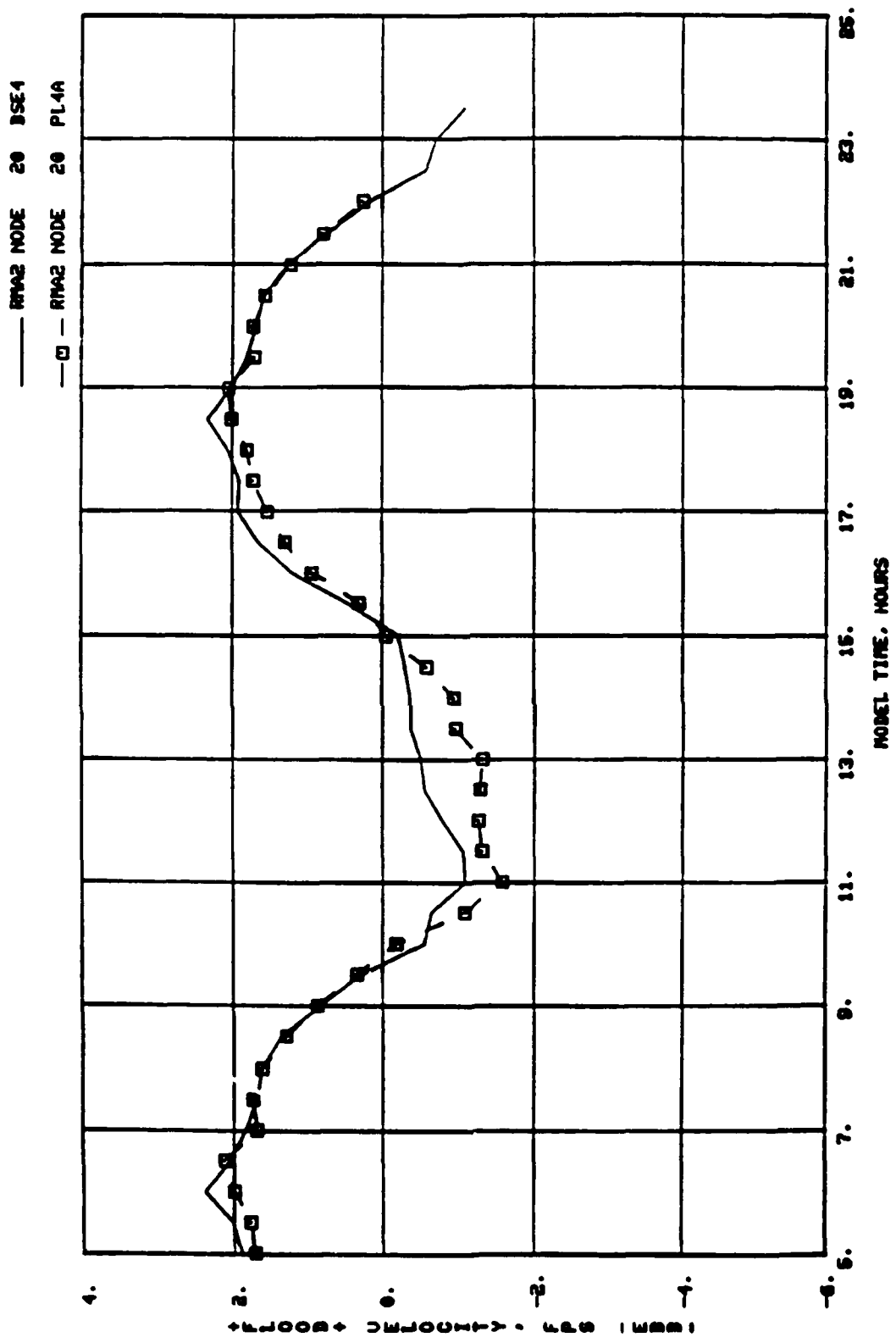
Plate D14. Numerical model base and plan velocities for node 20
(Jolly River boundary)
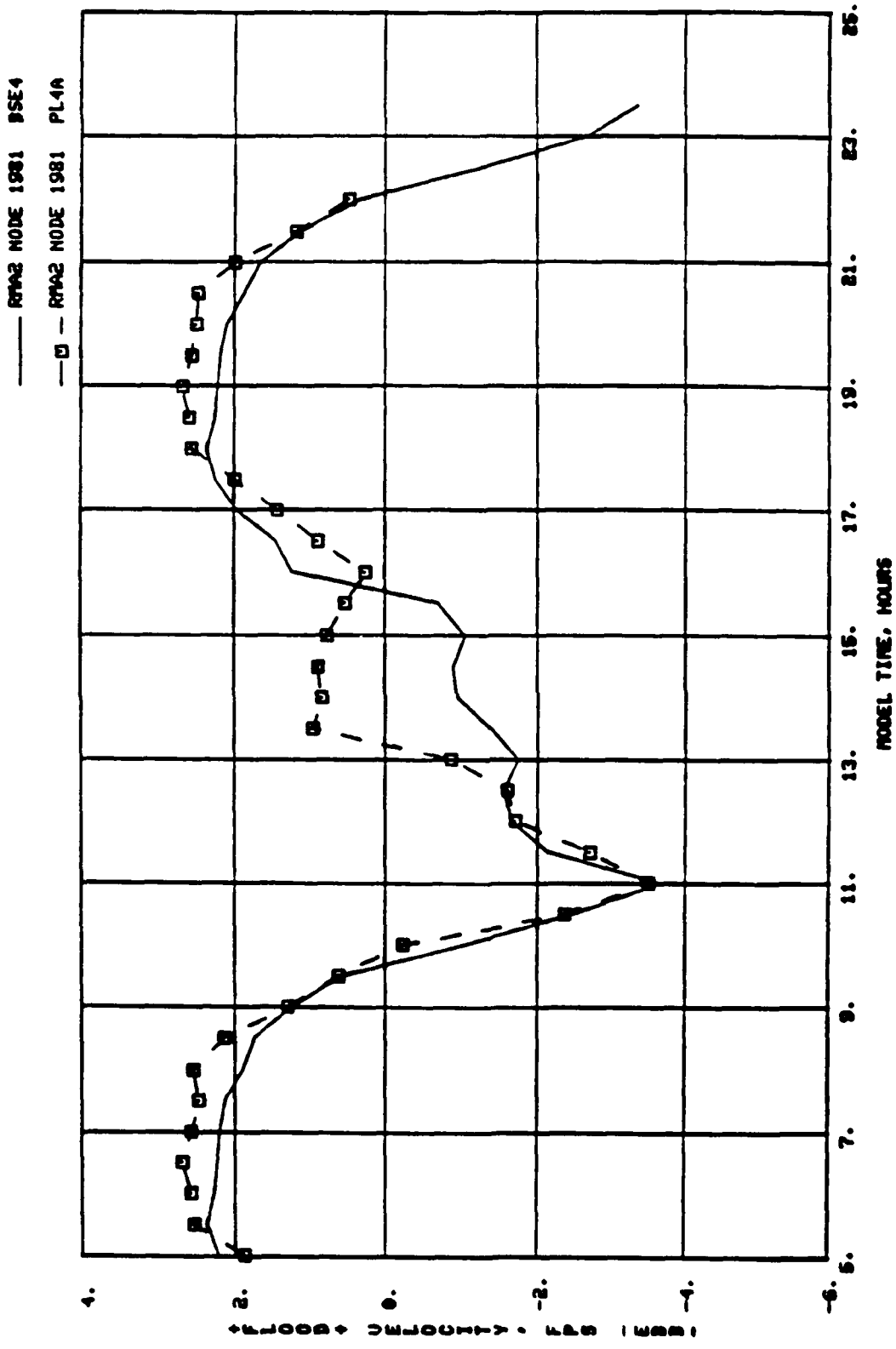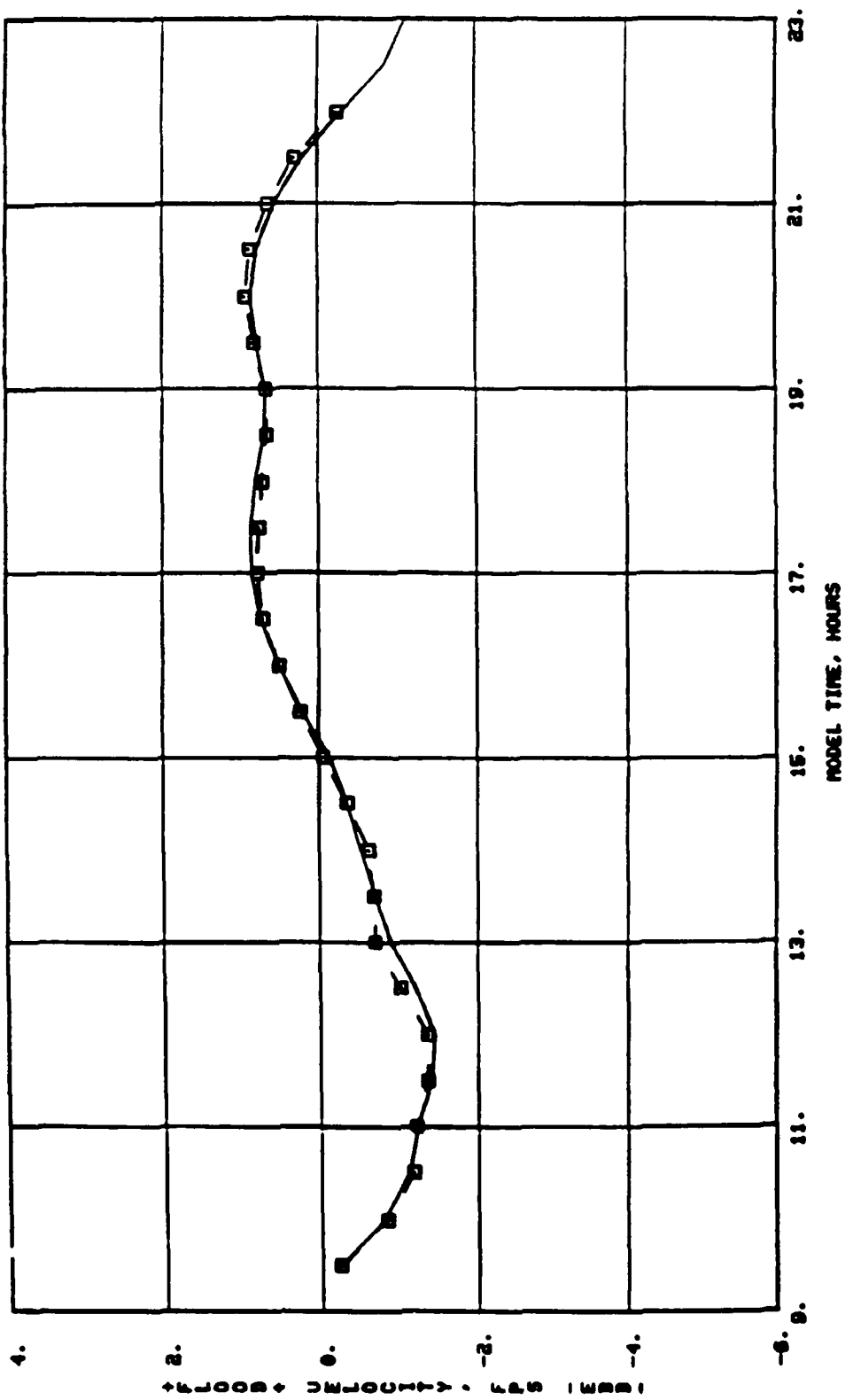
Plate D15. Numerical model base and plan velocities for node 1981
(St. Marys boundary)
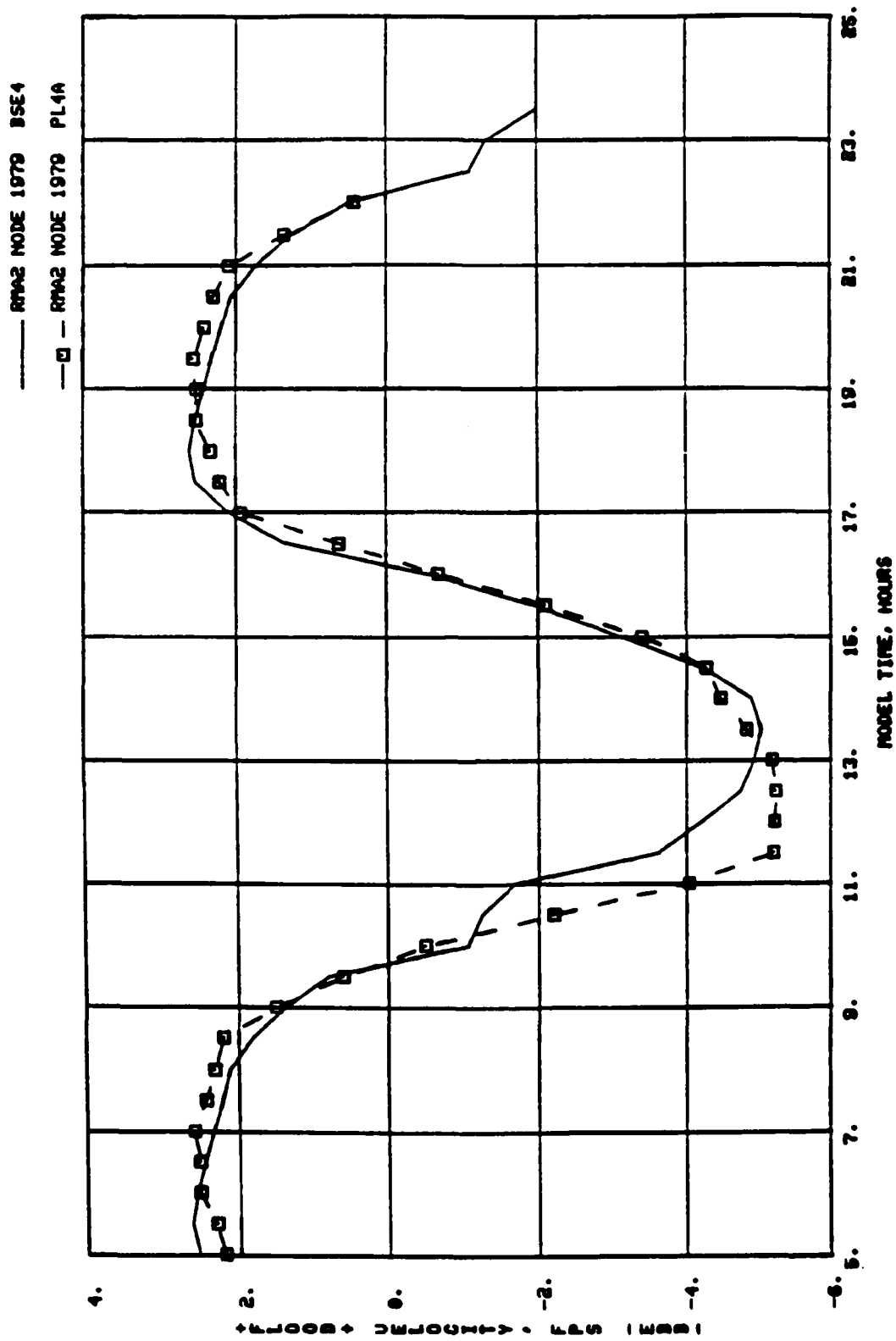
Plate D16. Numerical model base and plan velocities for node 1979 (St. Marys boundary)
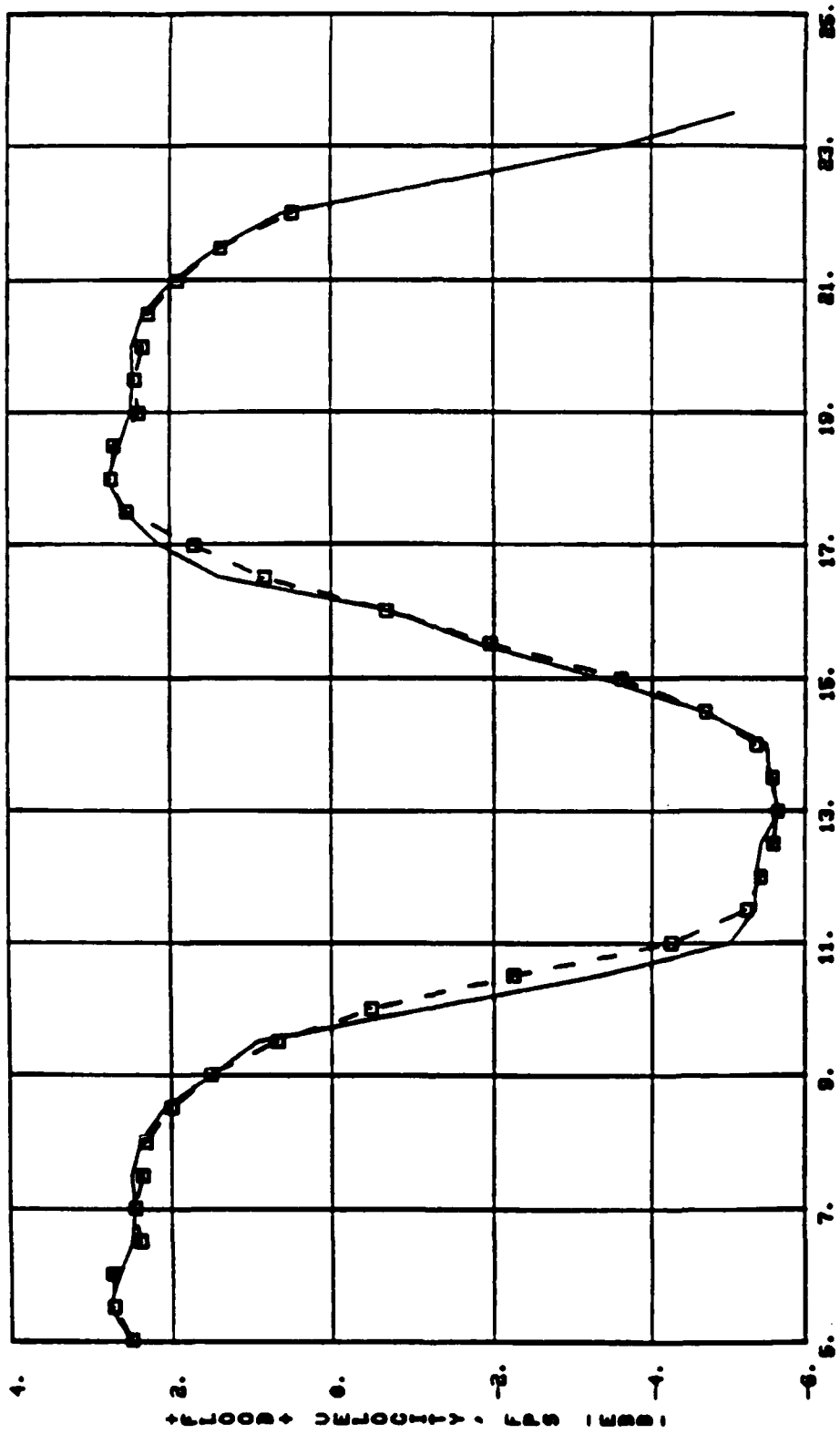
Plate D17. Numerical model base and plan velocities for node 1989
(St. Marys boundary)
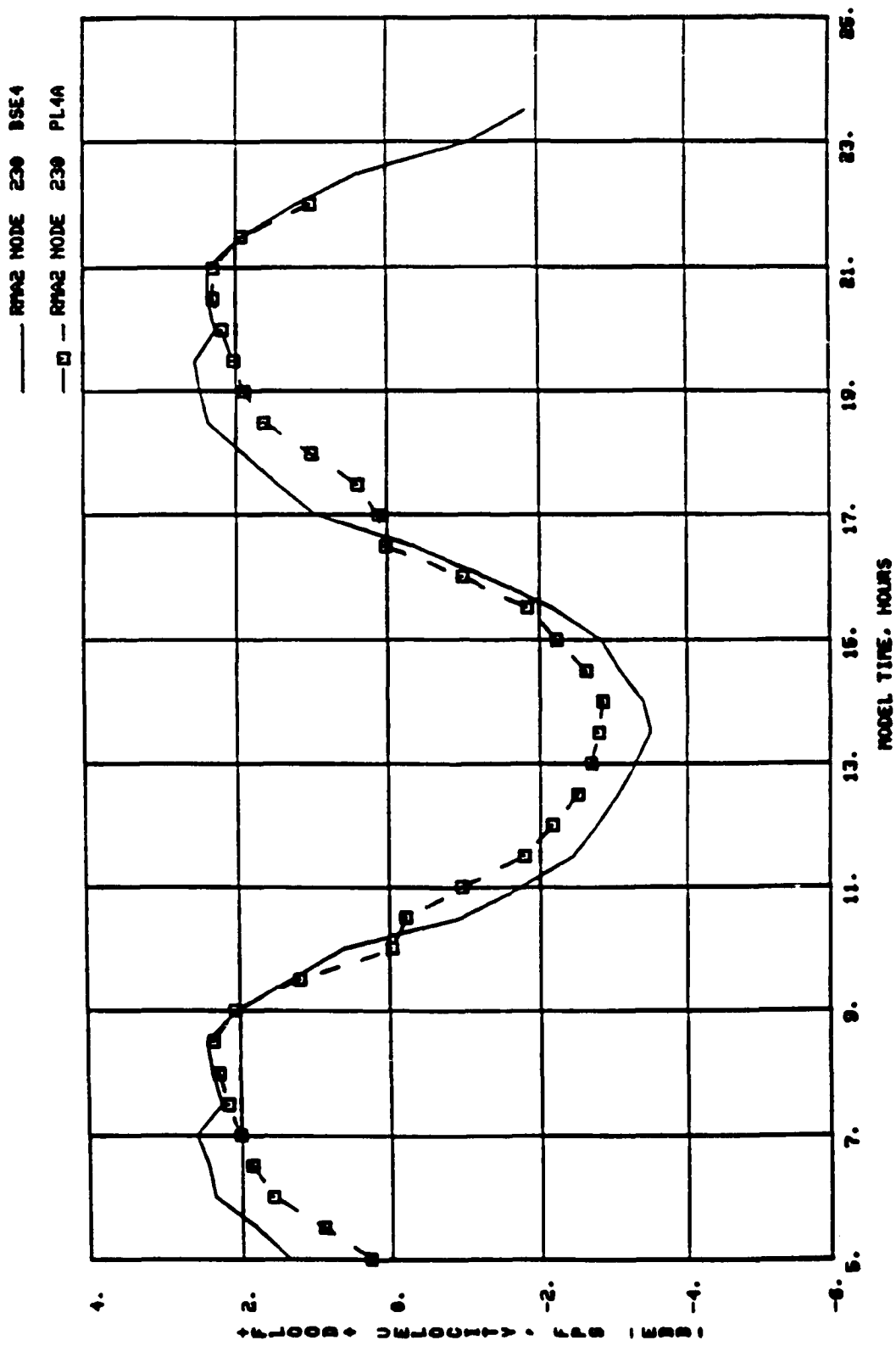
Plate D18. Numerical model base and plan velocities for node 230
(Crooked River boundary)
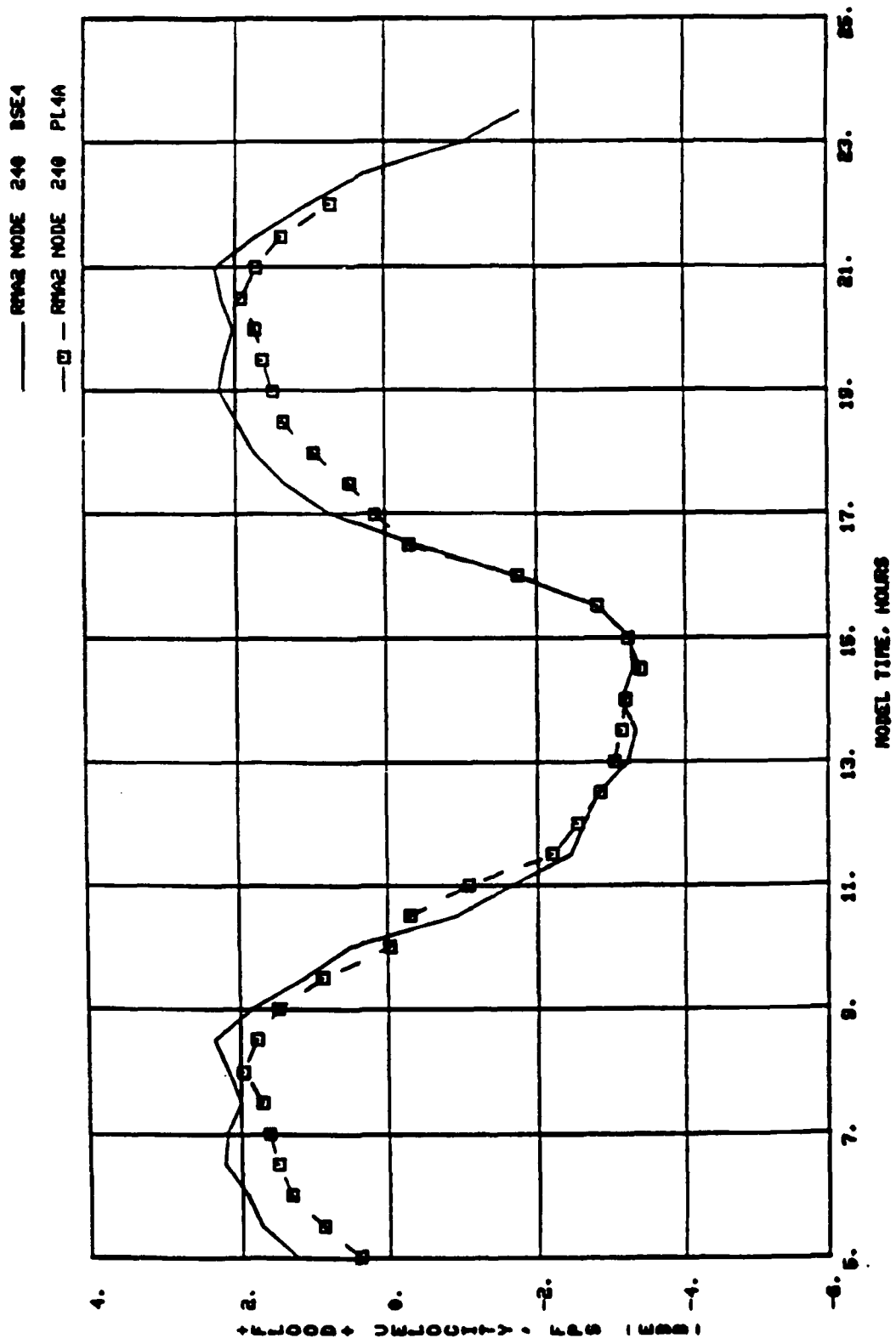
Plate D19. Numerical model base and plan velocities for node 240
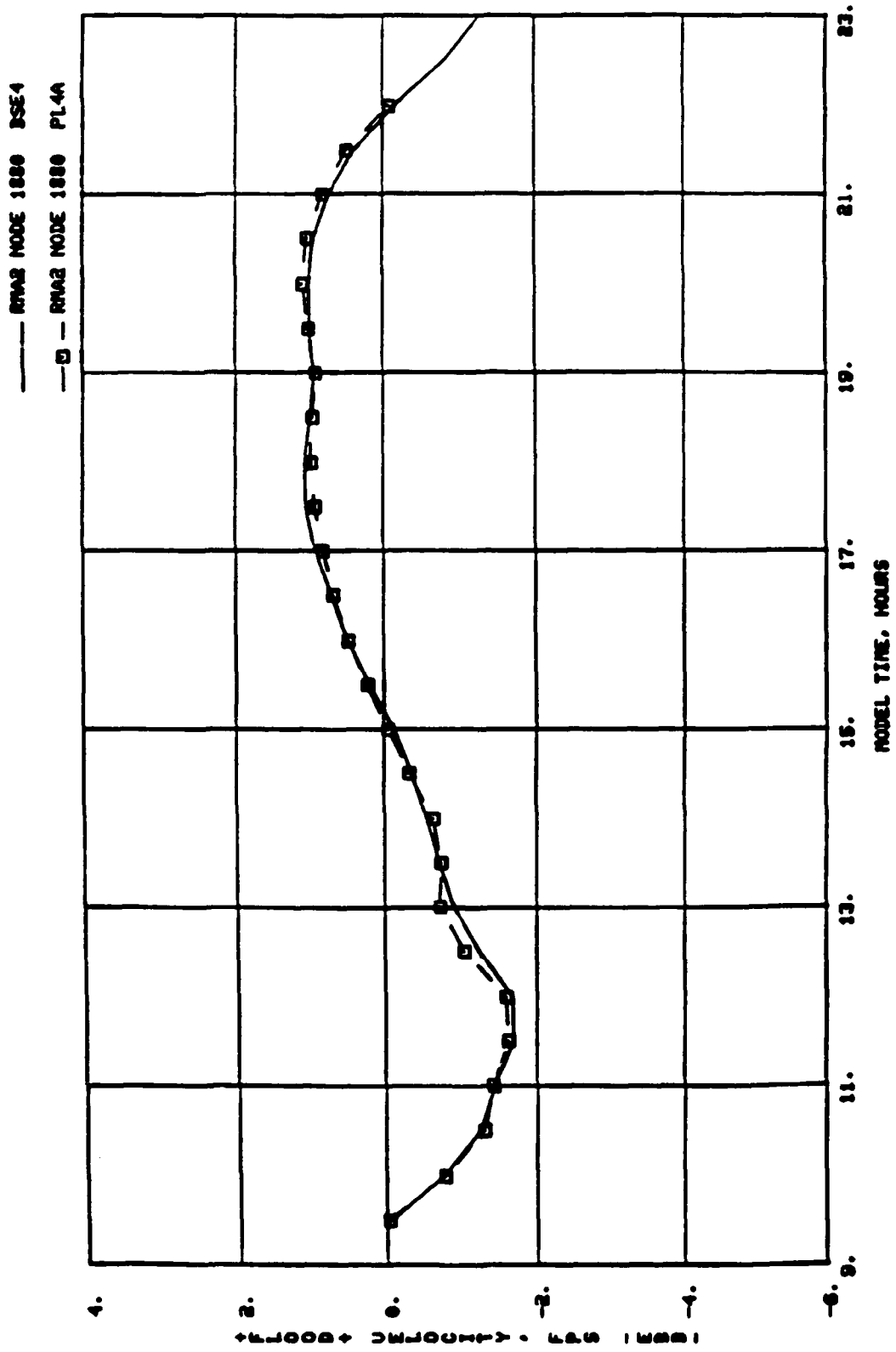(Crooked River boundary)
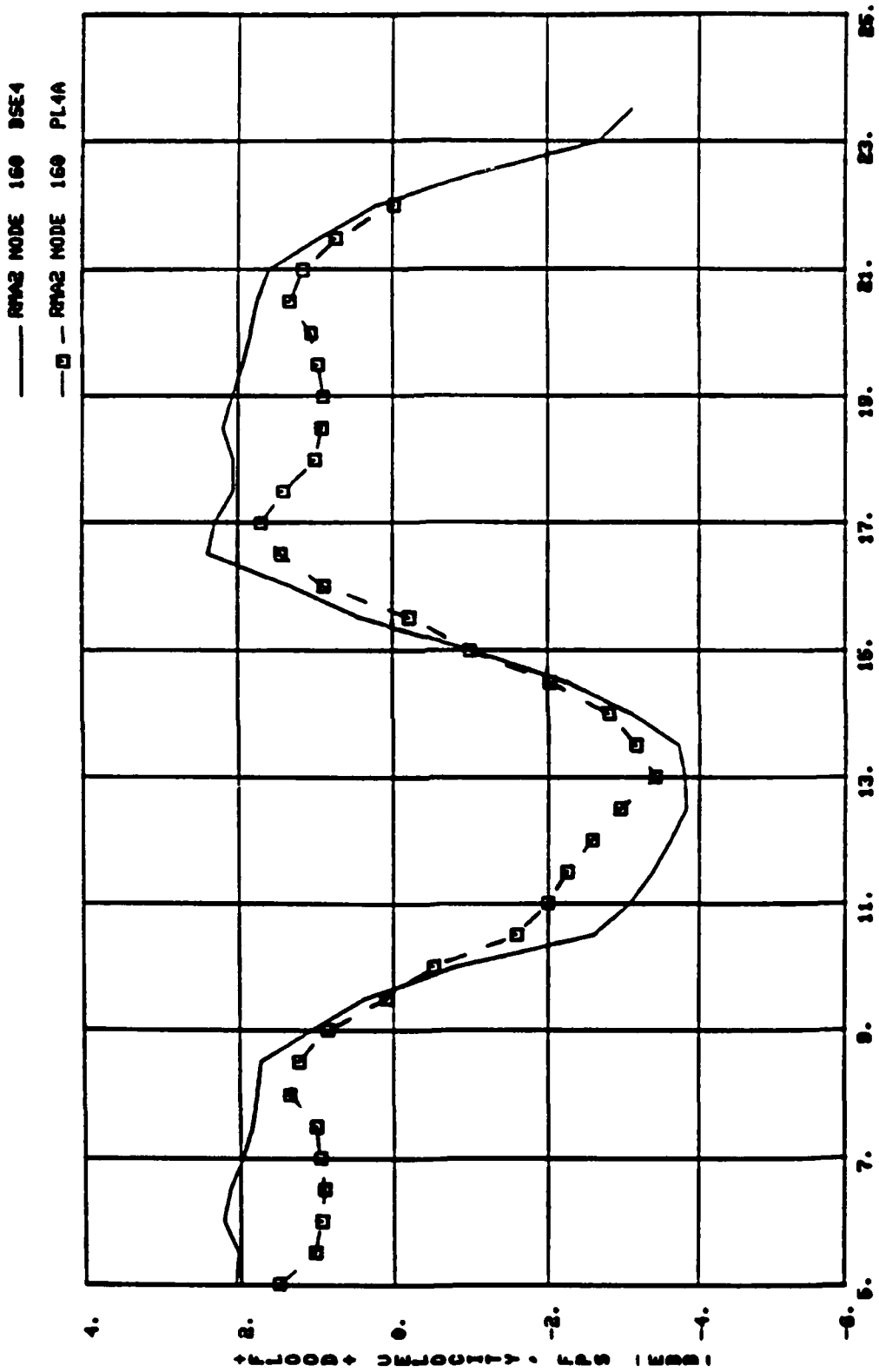
Plate D20. Numerical model base and plan velocities for node 160 (Cumberland River boundary)
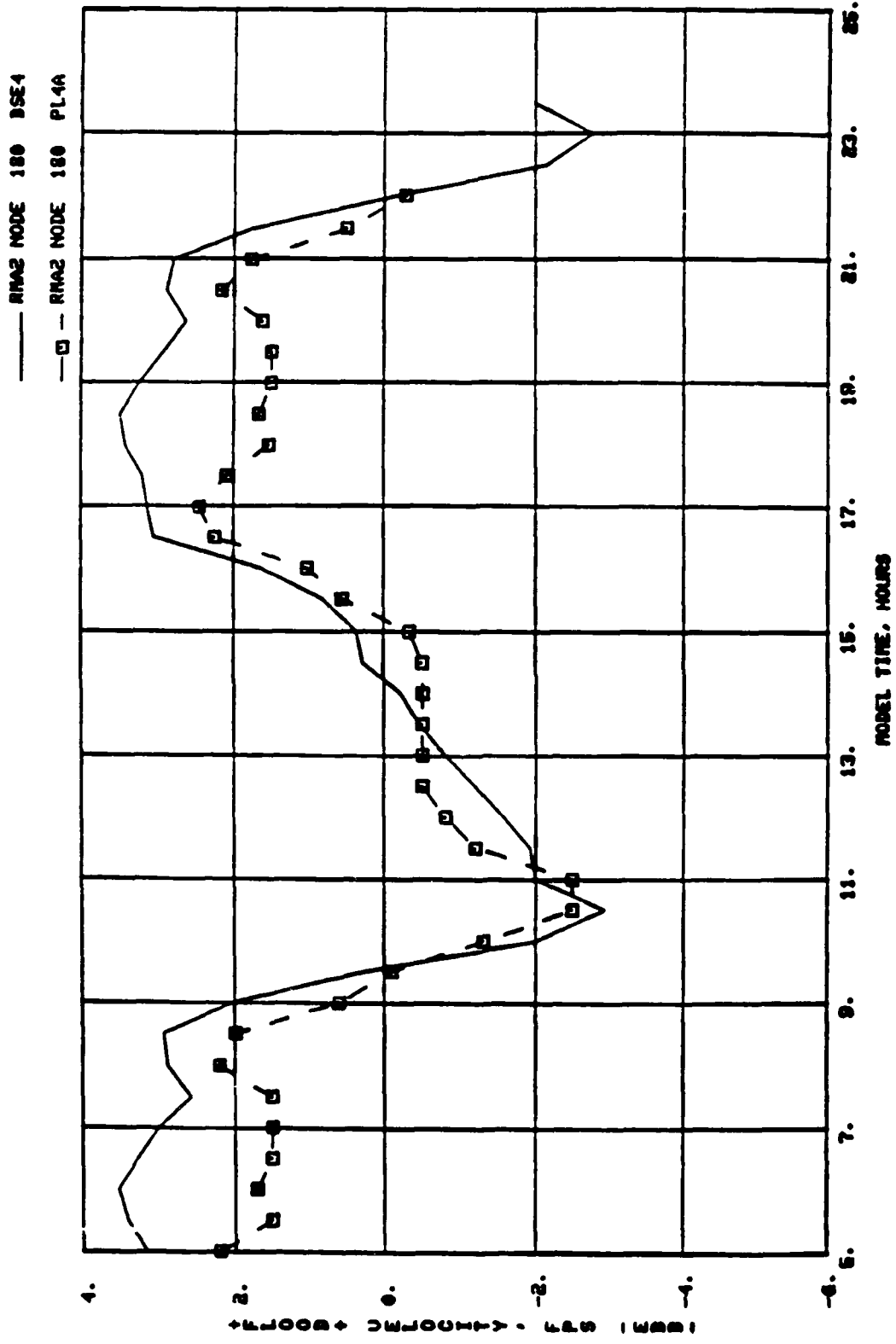
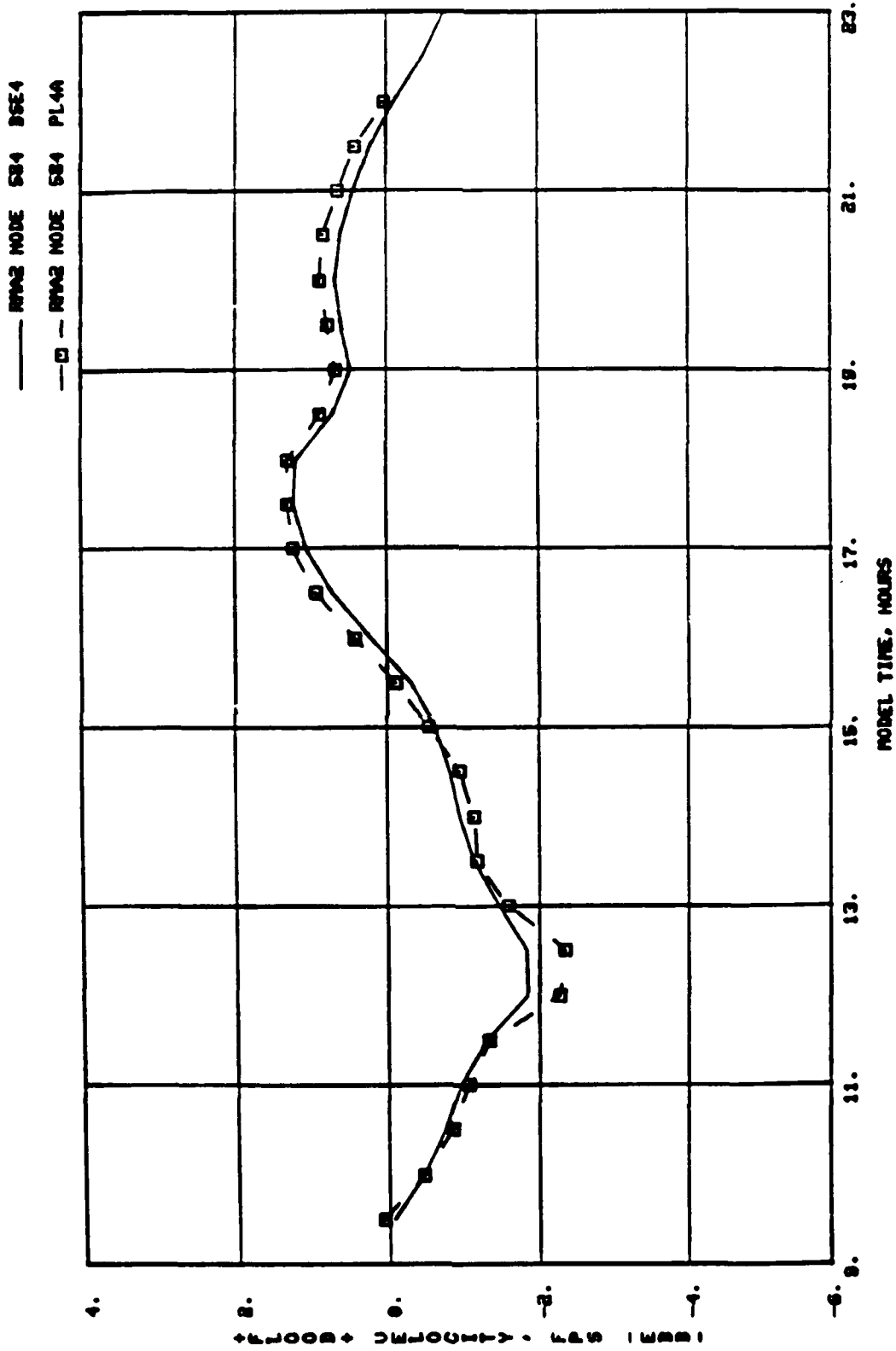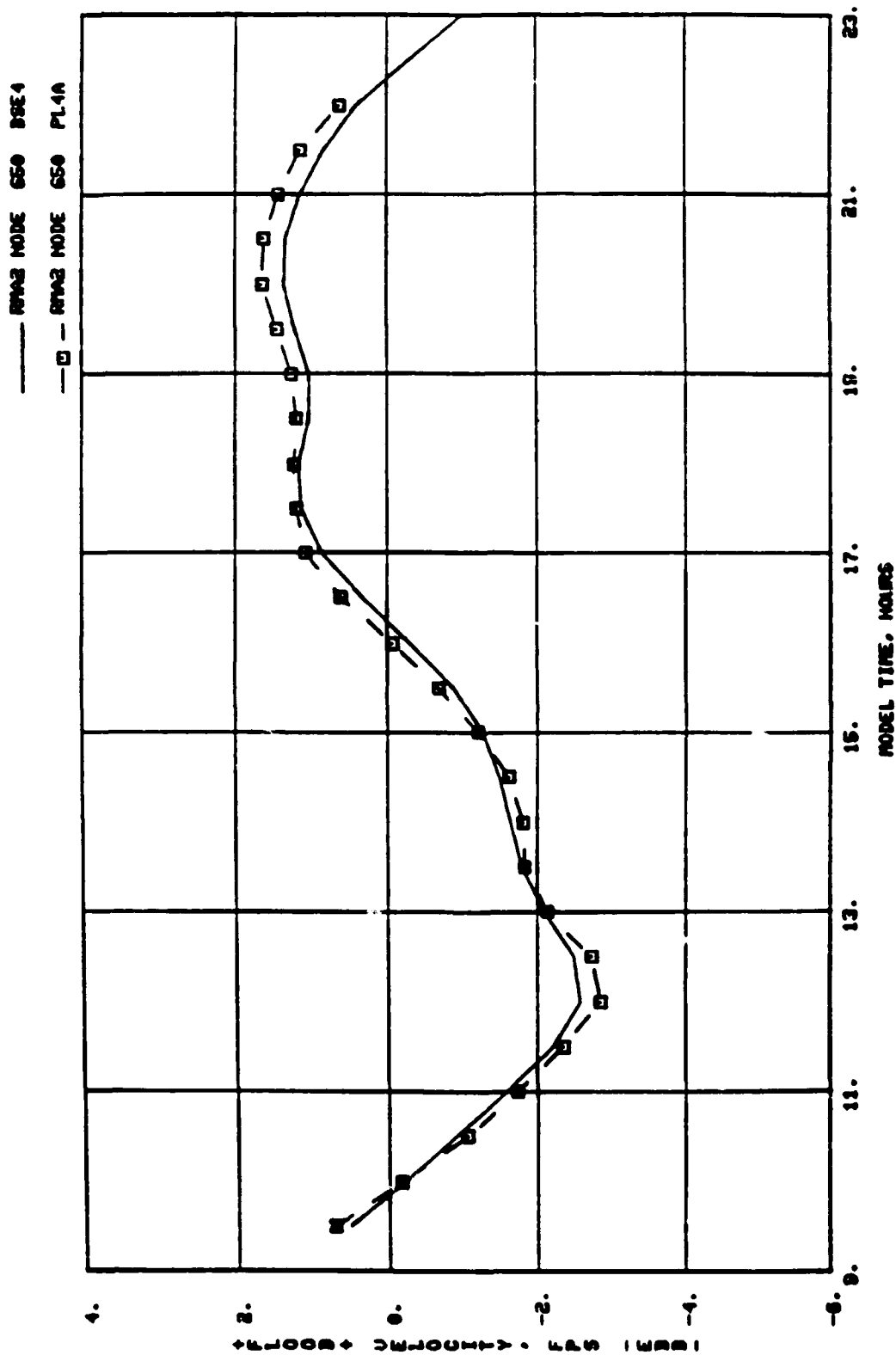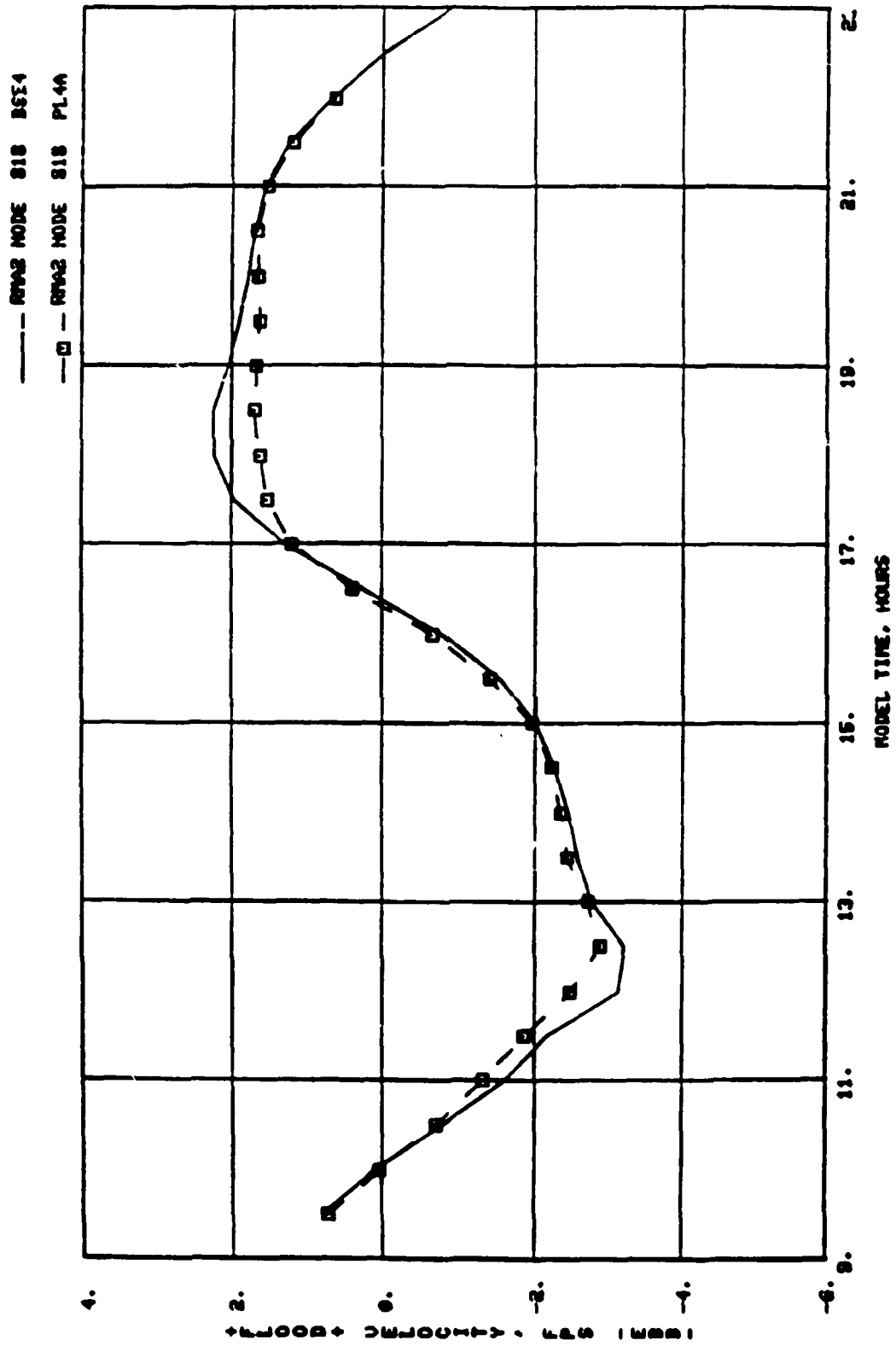Plate D21. Numerical model base and plan velocities for node 180
(Cumberland River boundary)
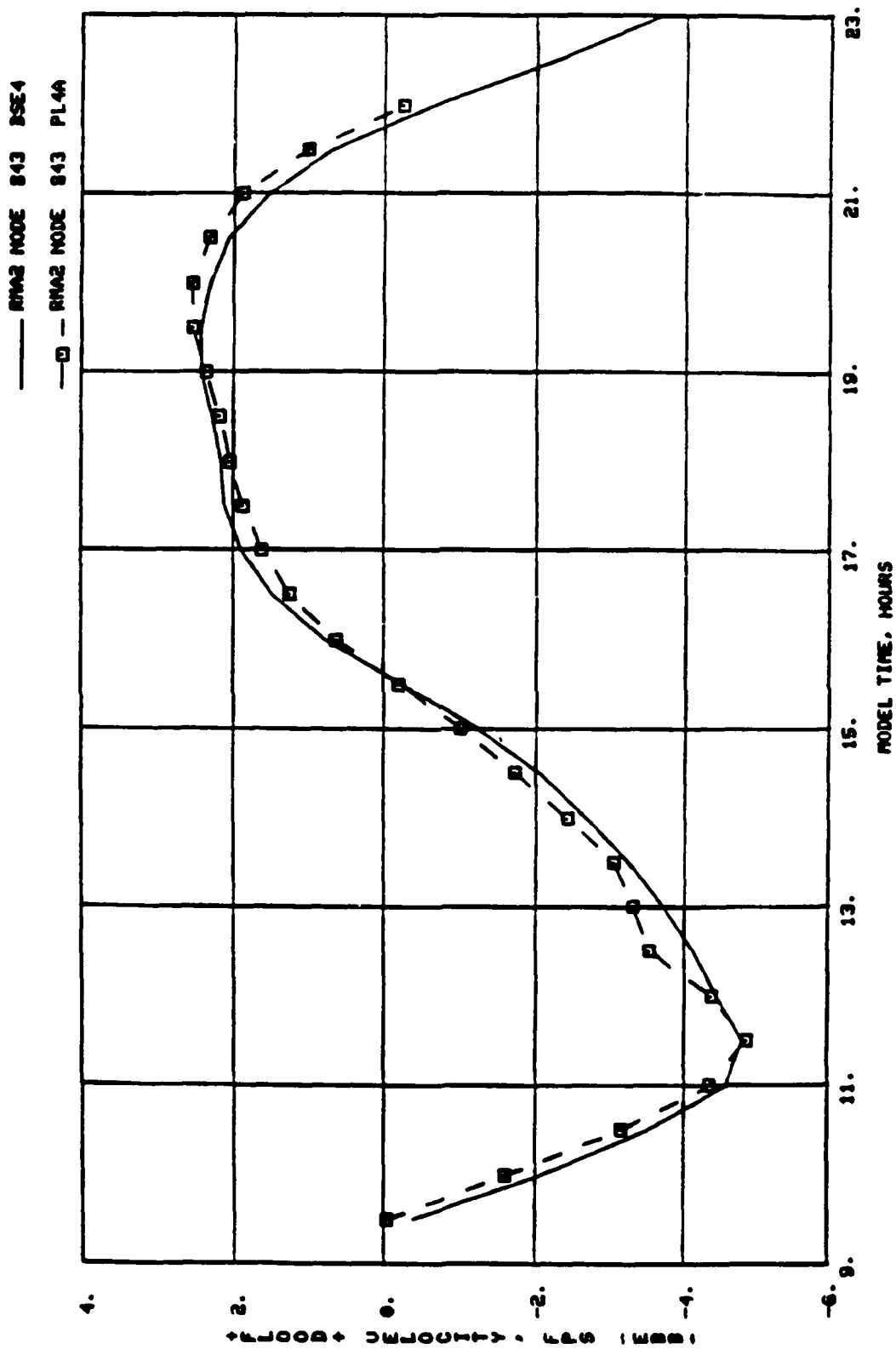
Plate D22. Numerical model base and plan velocities for main submarine channel, node 843
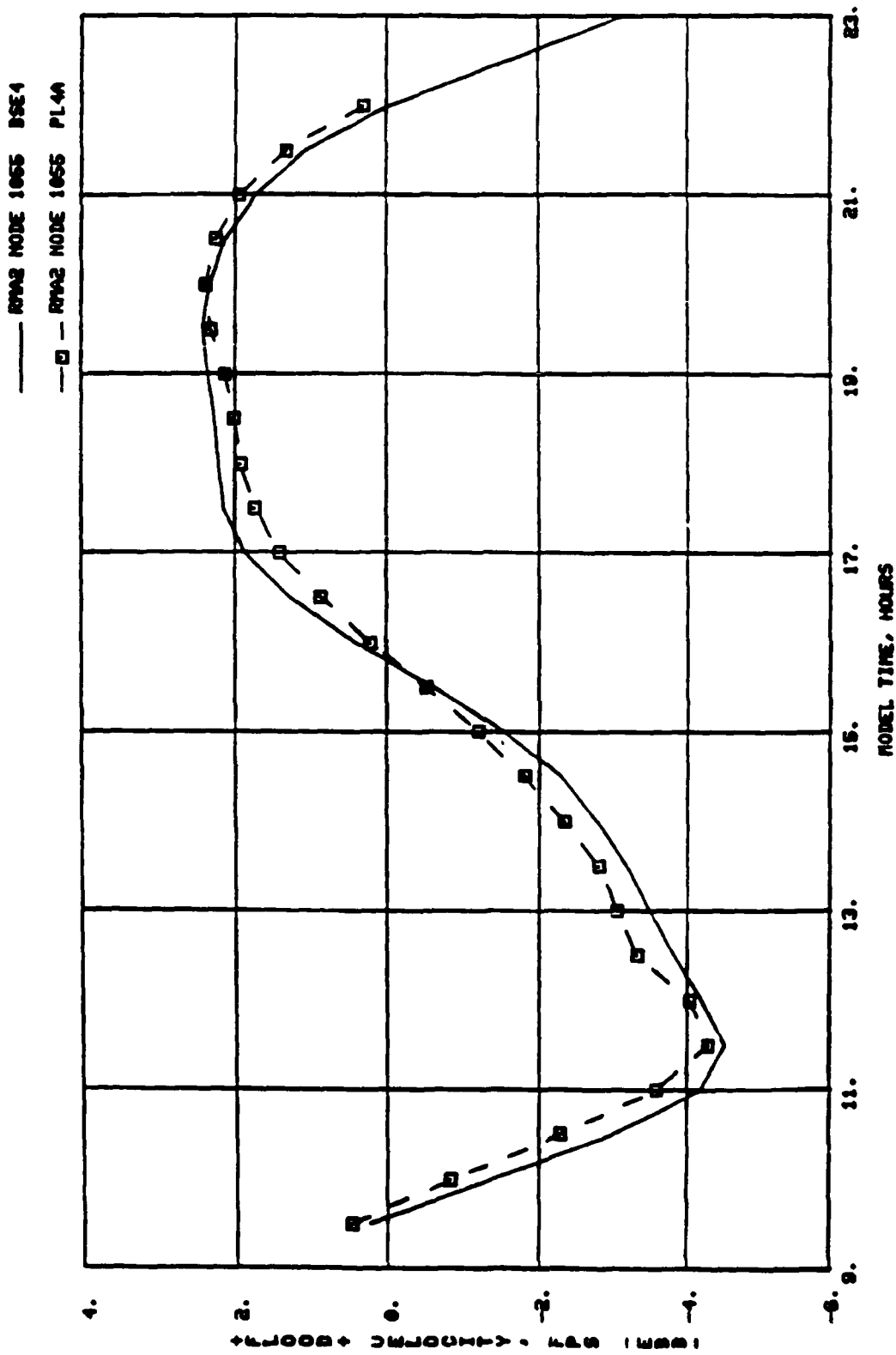
Plate D23. Numerical model base and plan velocities for main submarine channel, node 1055

D25
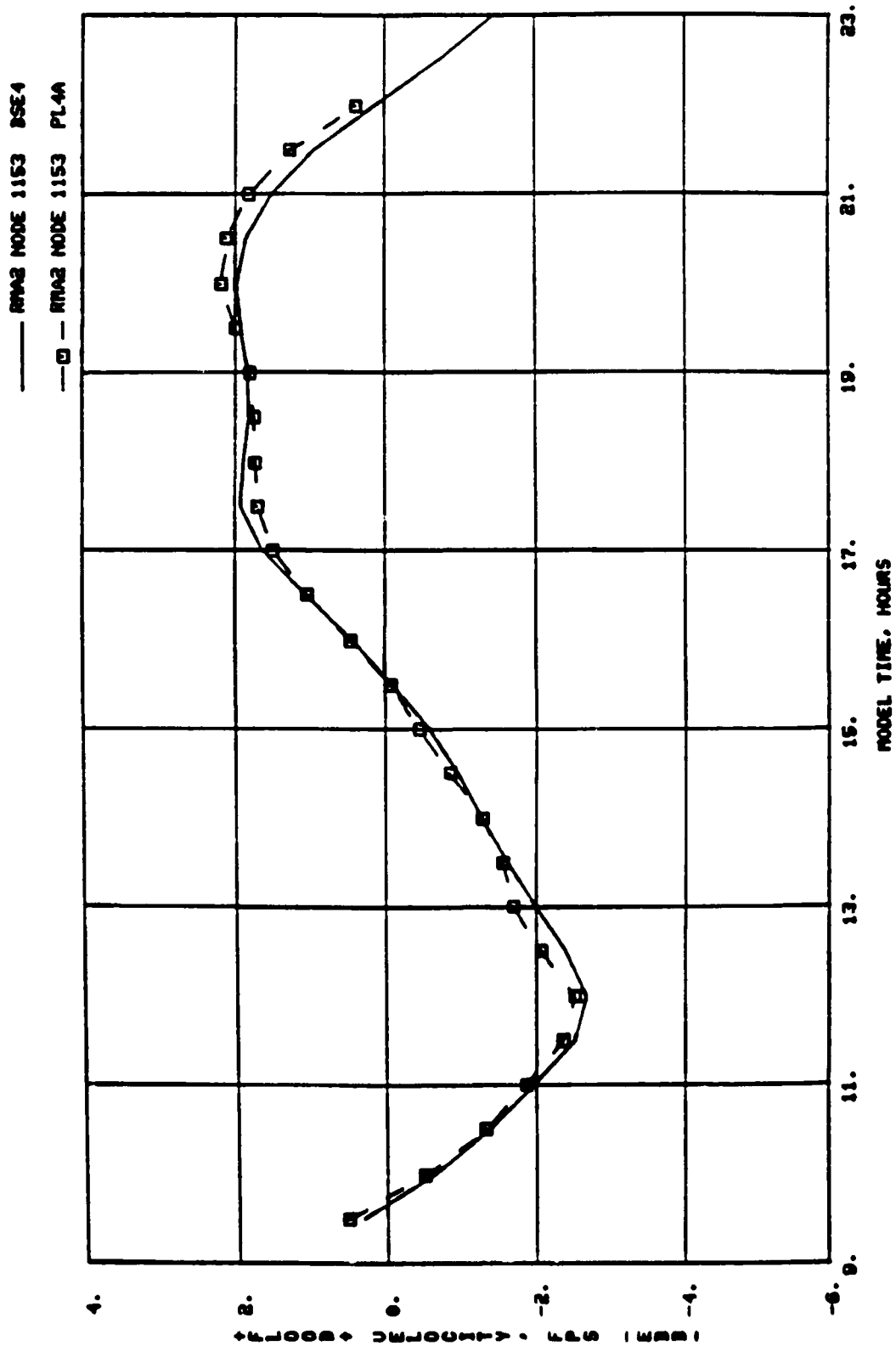
Plate D24. Numerical model base and plan velocities for main submarine
channel, node 1153
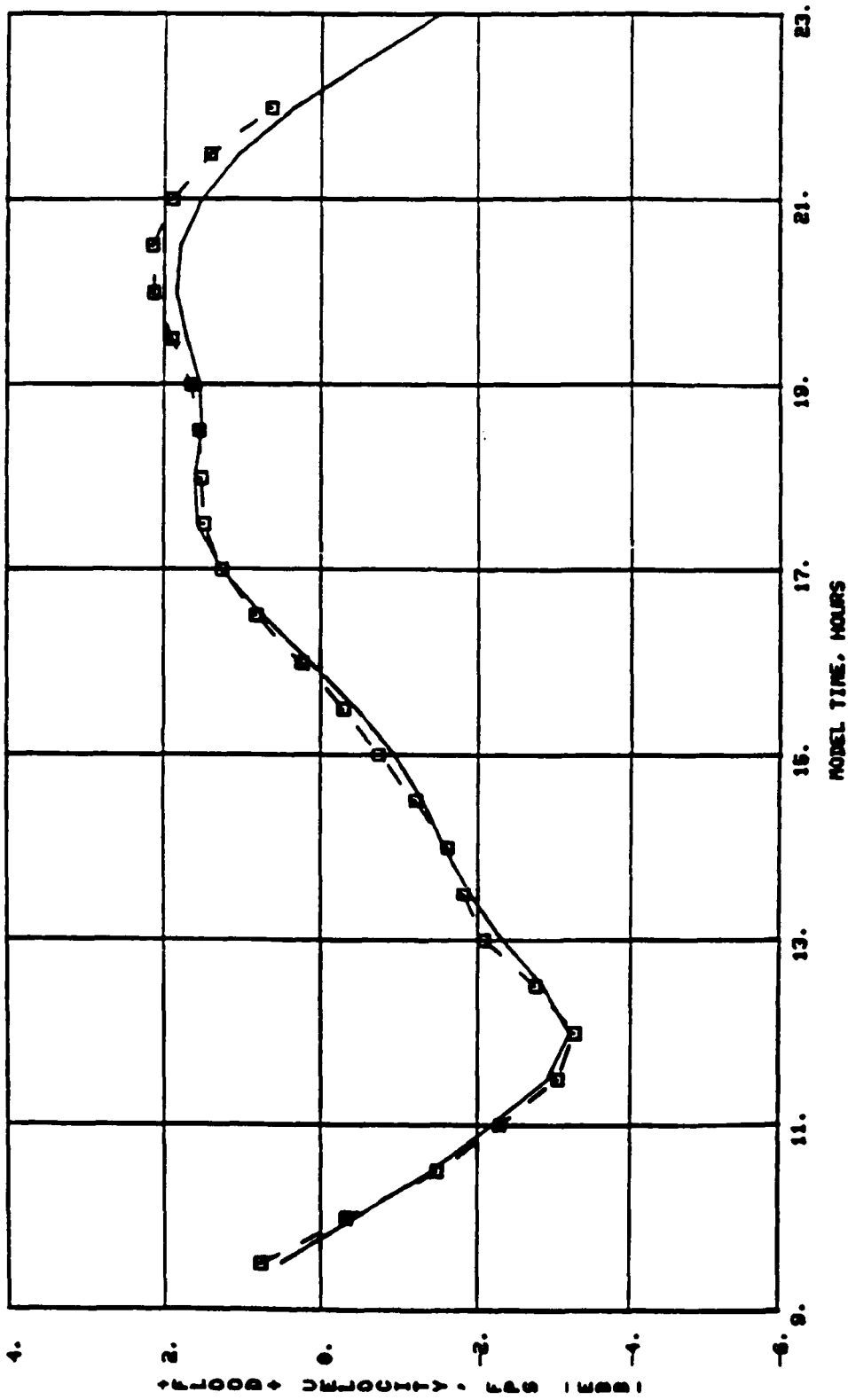
Plate D25. Numerical model base and plan velocities for main submarine
channel, node 1385
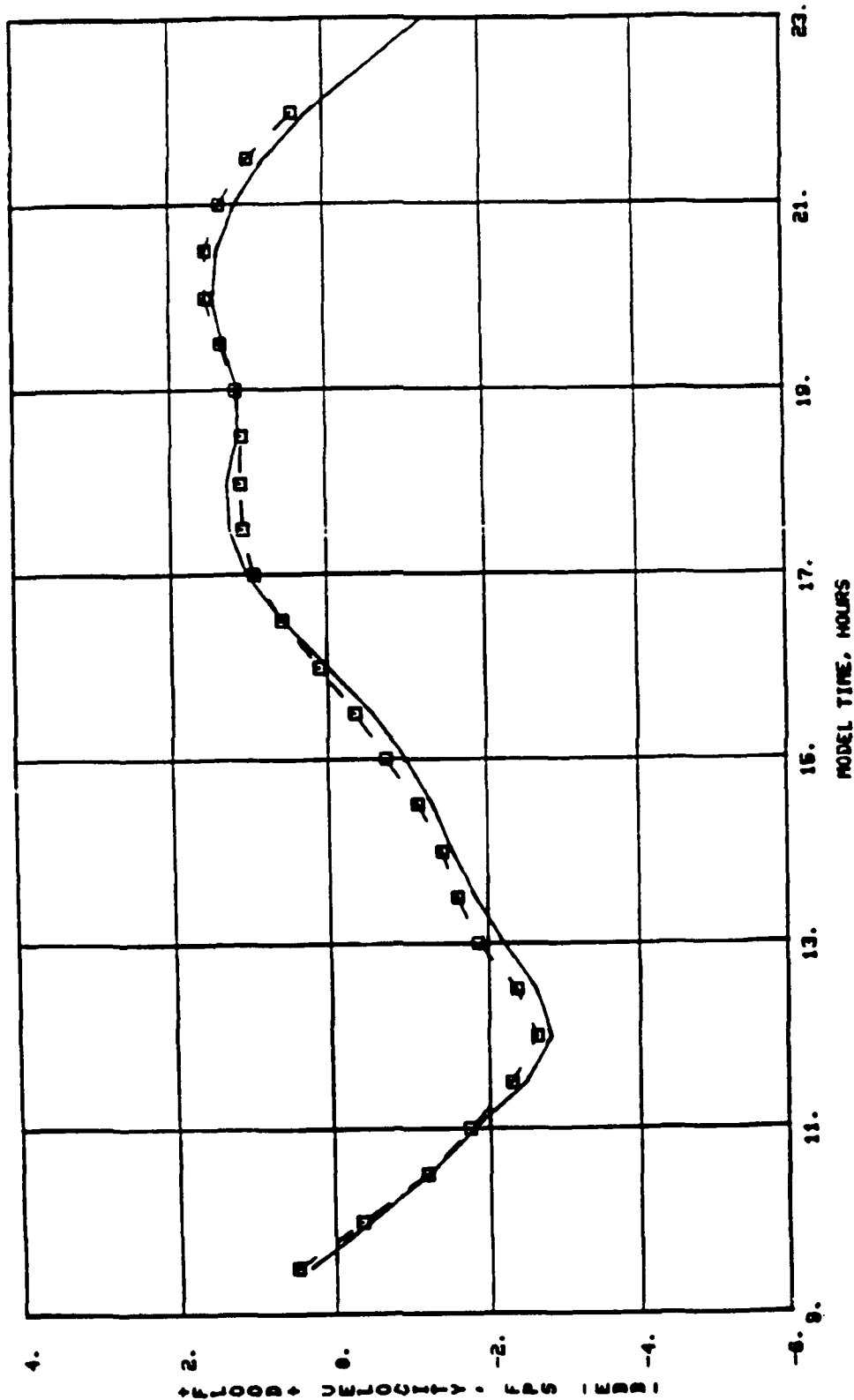
Plate D26. Numerical model base and plan velocities for main submarine
channel, node 1915
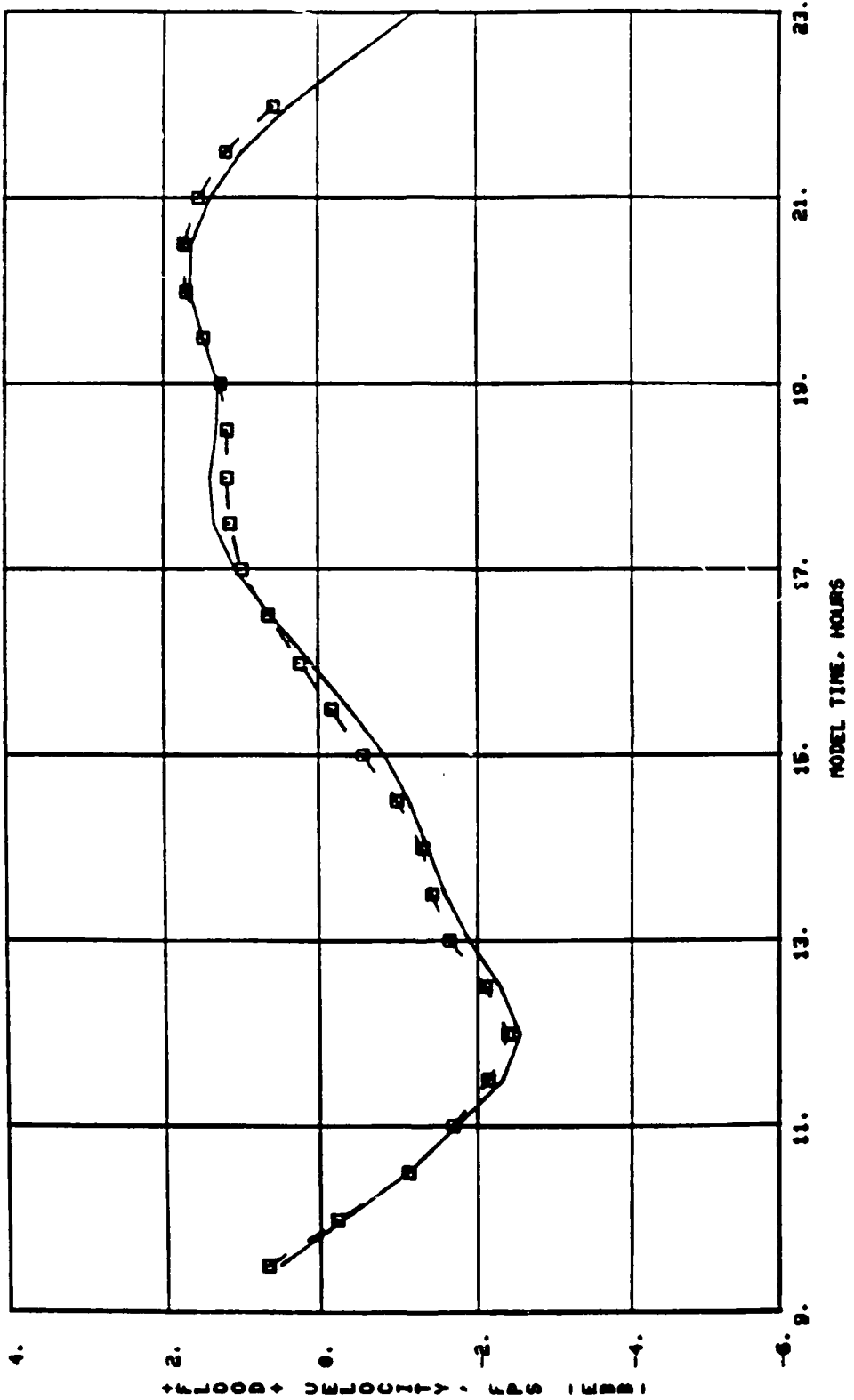
Plate D27. Numerical model base and plan velocities for main submarine channel, node 1851
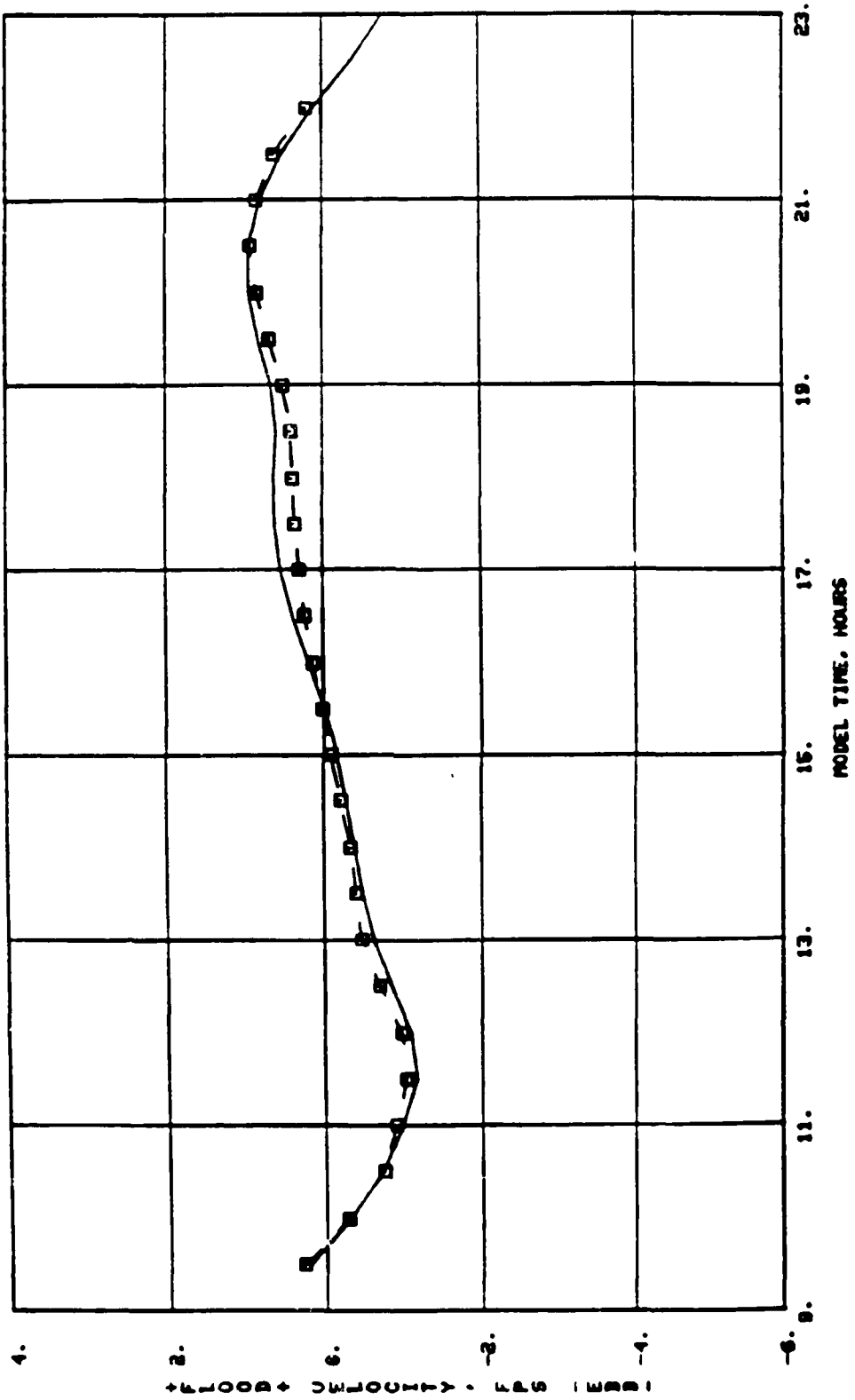
Plate D28. Numerical model base and plan velocities for main submarine channel, node 1182
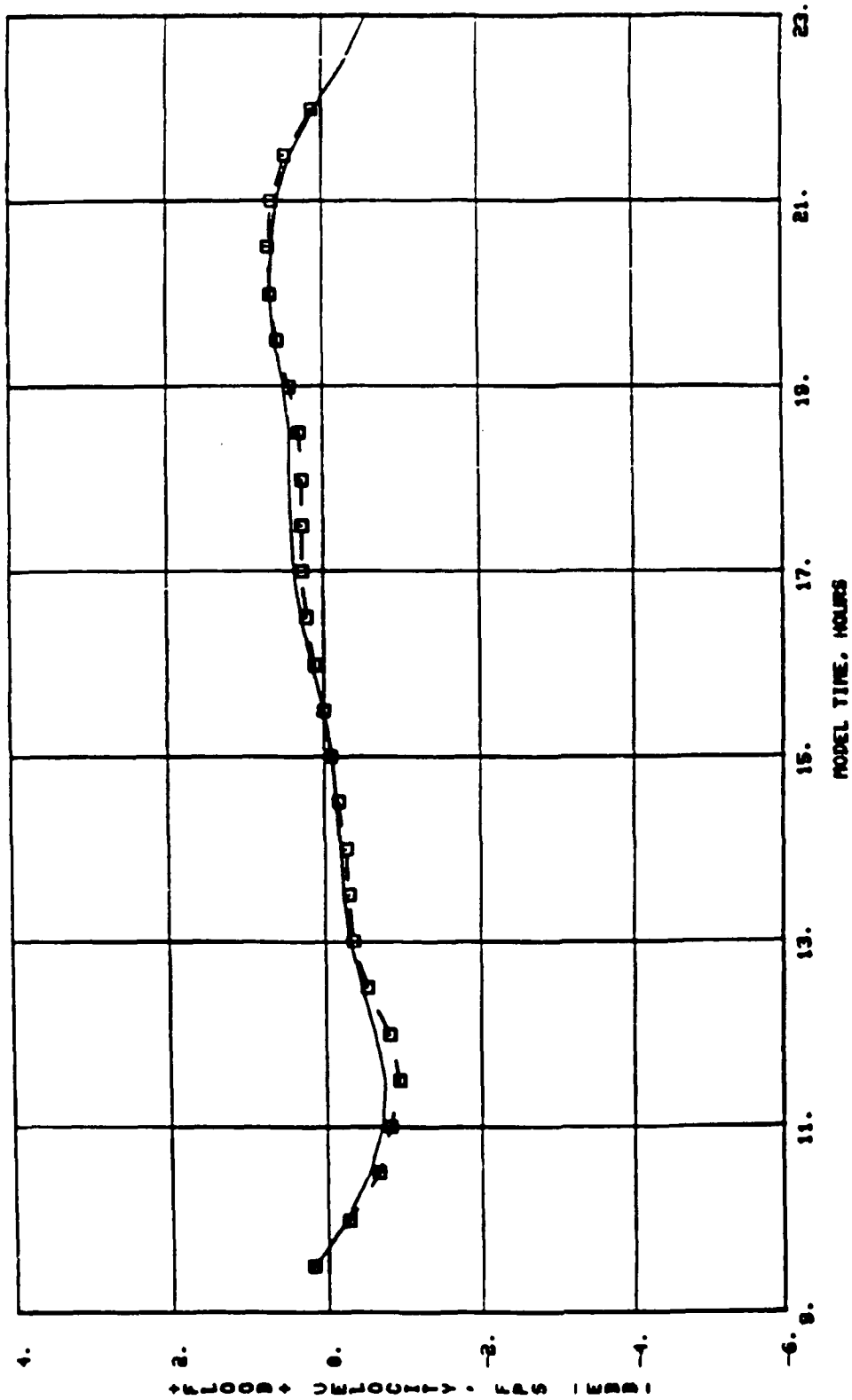
Plate D29. Numerical model base and plan velocities for main submarine channel, node 1142
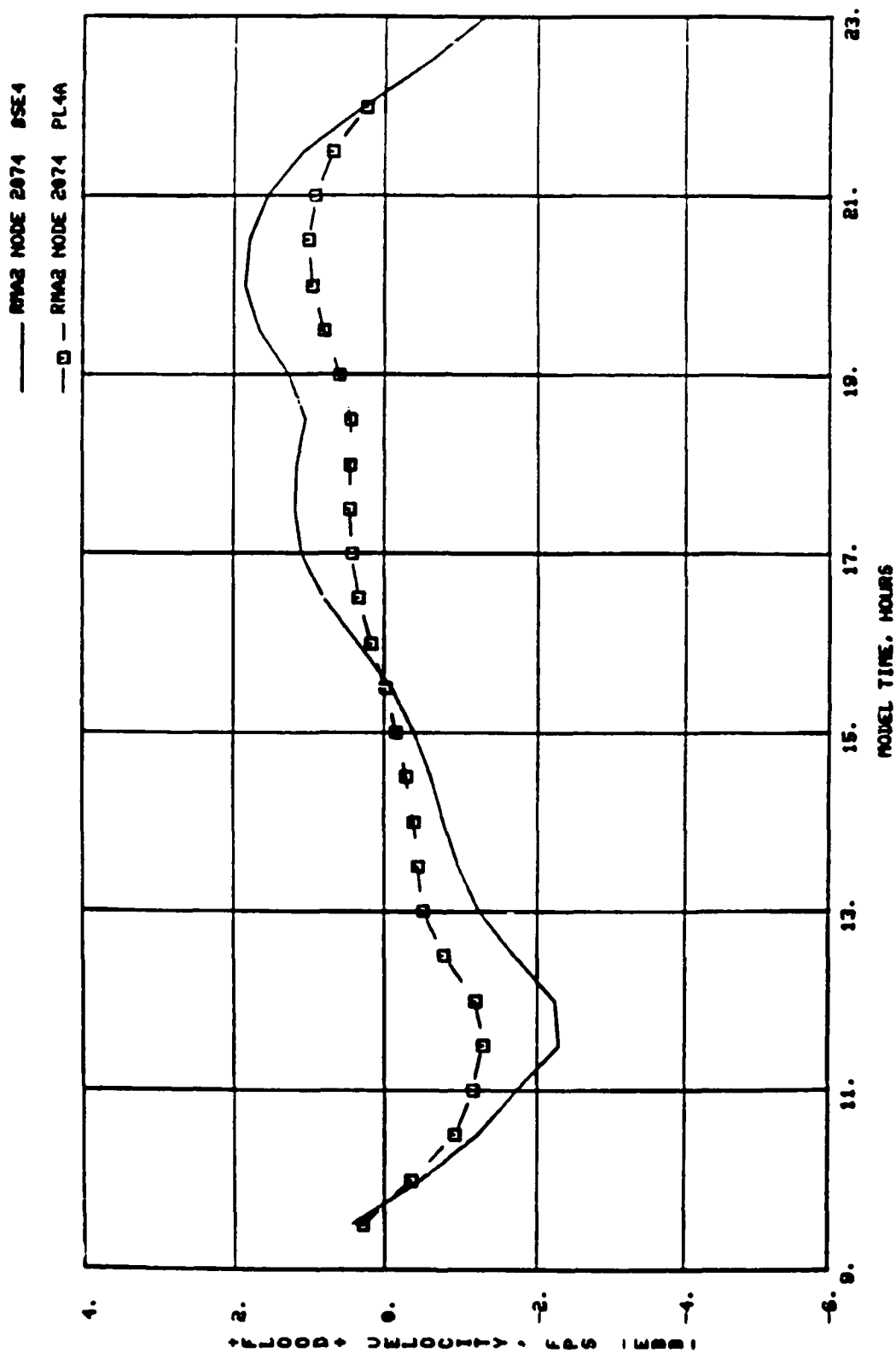
Plate D30. Numerical model base and plan velocities for main submarine channel, node 2074
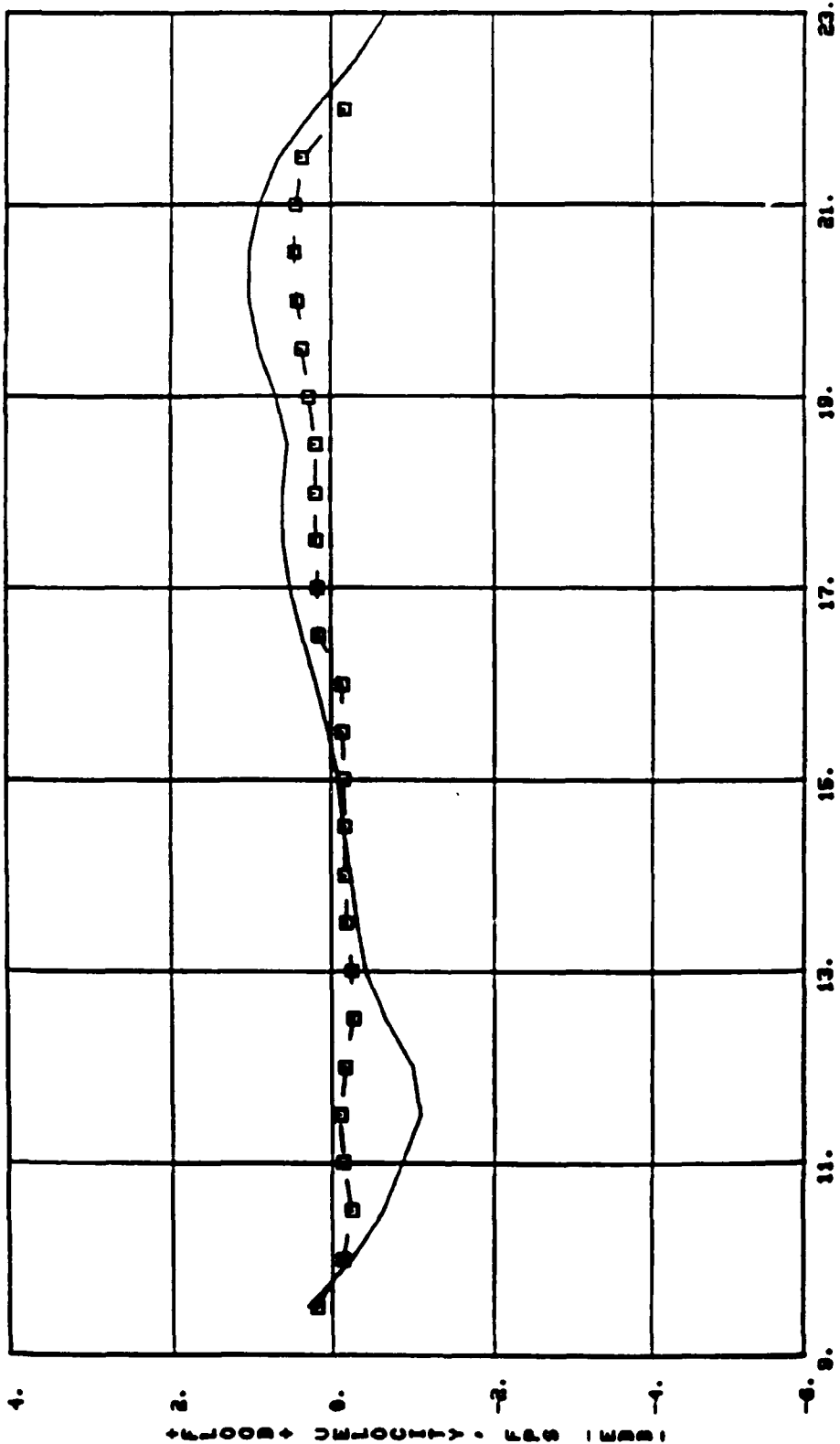
Plate D31. Numerical model base and plan velocities for main submarine channel, node 2089

D33

Plate D32. Numerical model base and plan velocities for node 1865
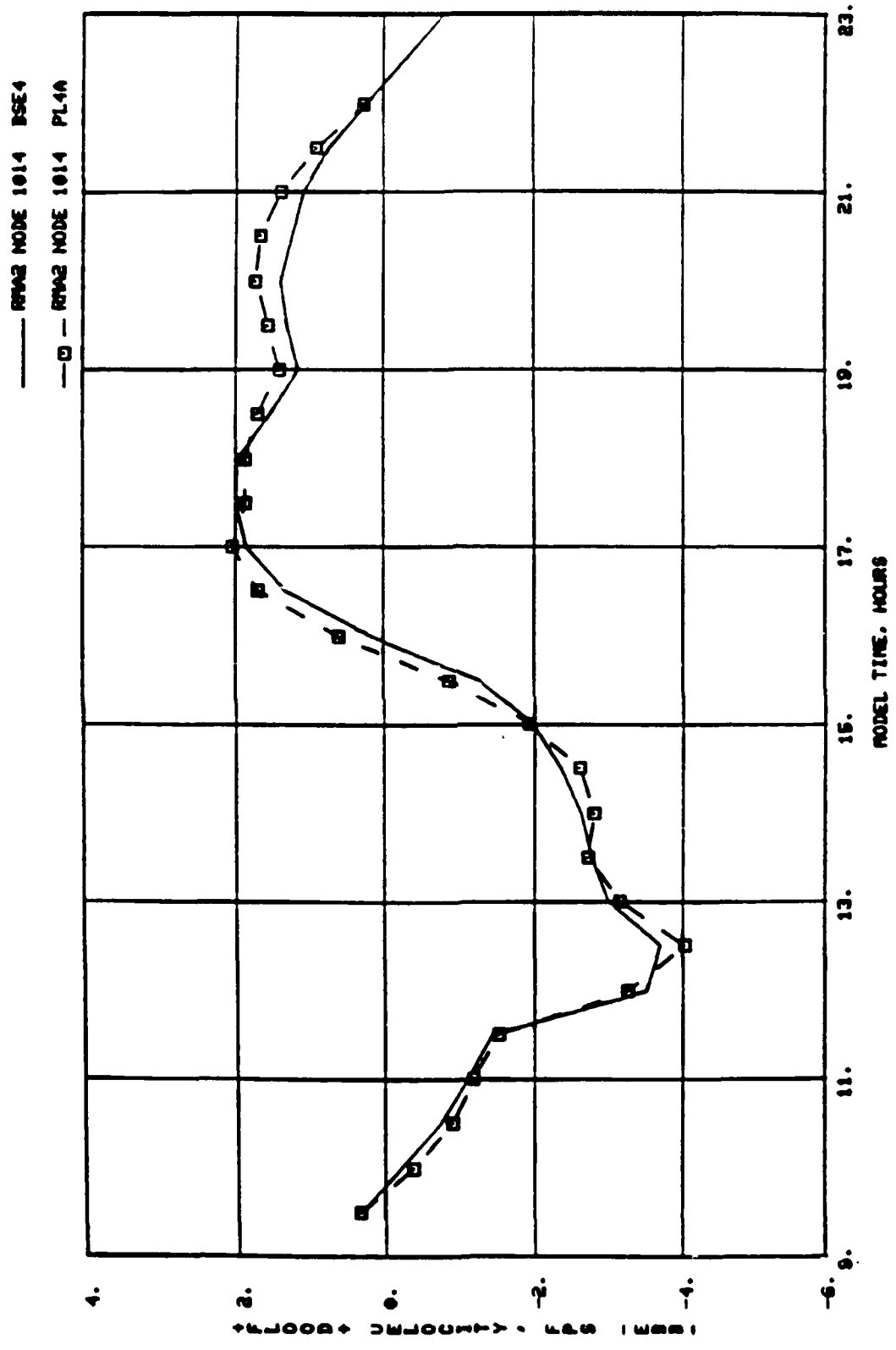(St. Marys River)
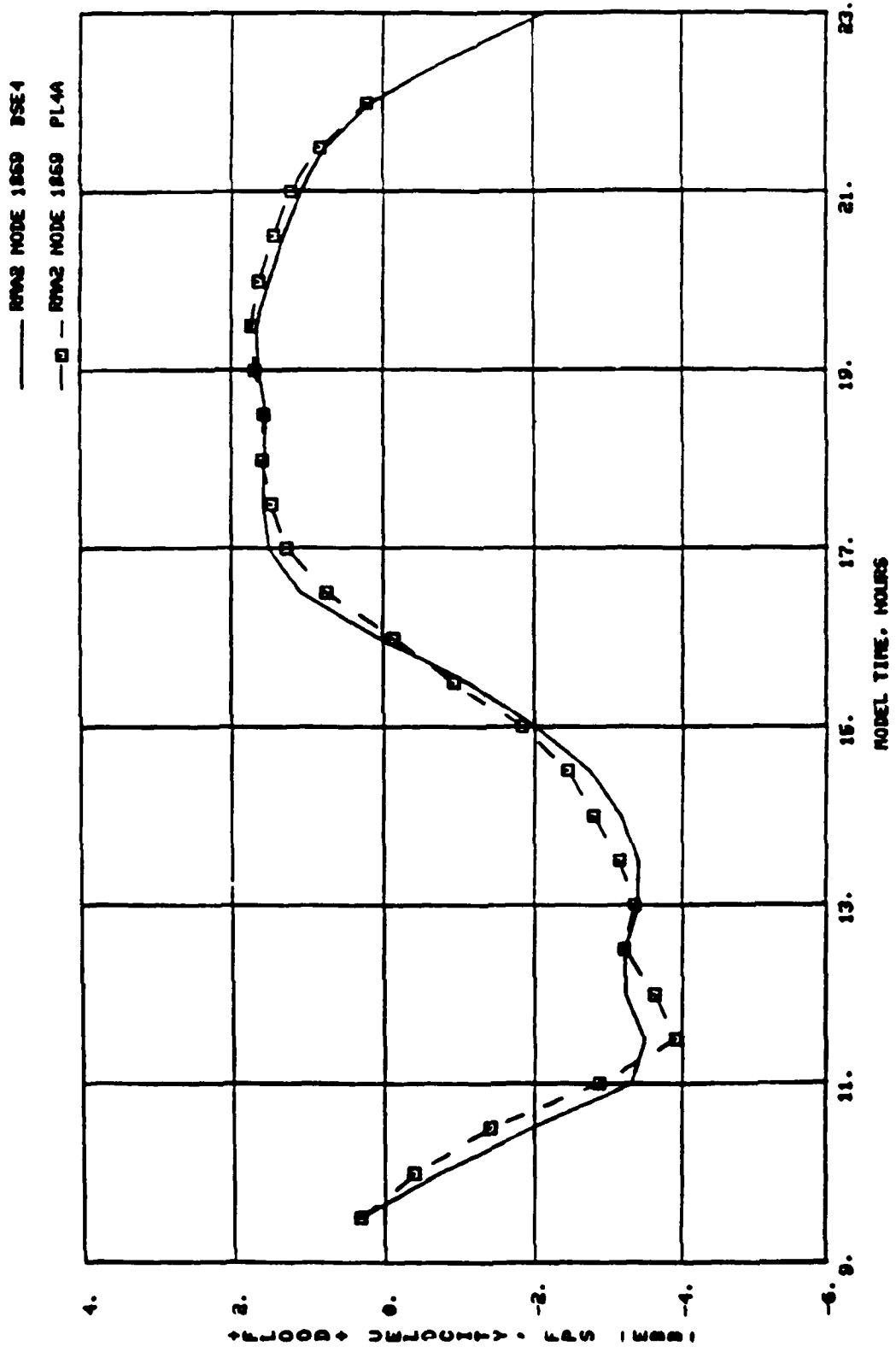
Plate D33.   Numerical model base and plan velocities for node 1869
(St. Marys River)

Plate D34. Numerical model base and plan velocities for node 396 (lower Cumberland Sound)

Plate D35. Numerical model base and plan velocities for node 1880
(lower Cumberland Sound)

Plate D36. Numerical model base and plan velocities for node 584 (Stafford Island channel)

Plate D37. Numerical model base and plan velocities for node 650
(AIWW upper Cumberland Sound)

Plate D38. Numerical model base and plan velocities for node 818
(south branch of Crooked River)
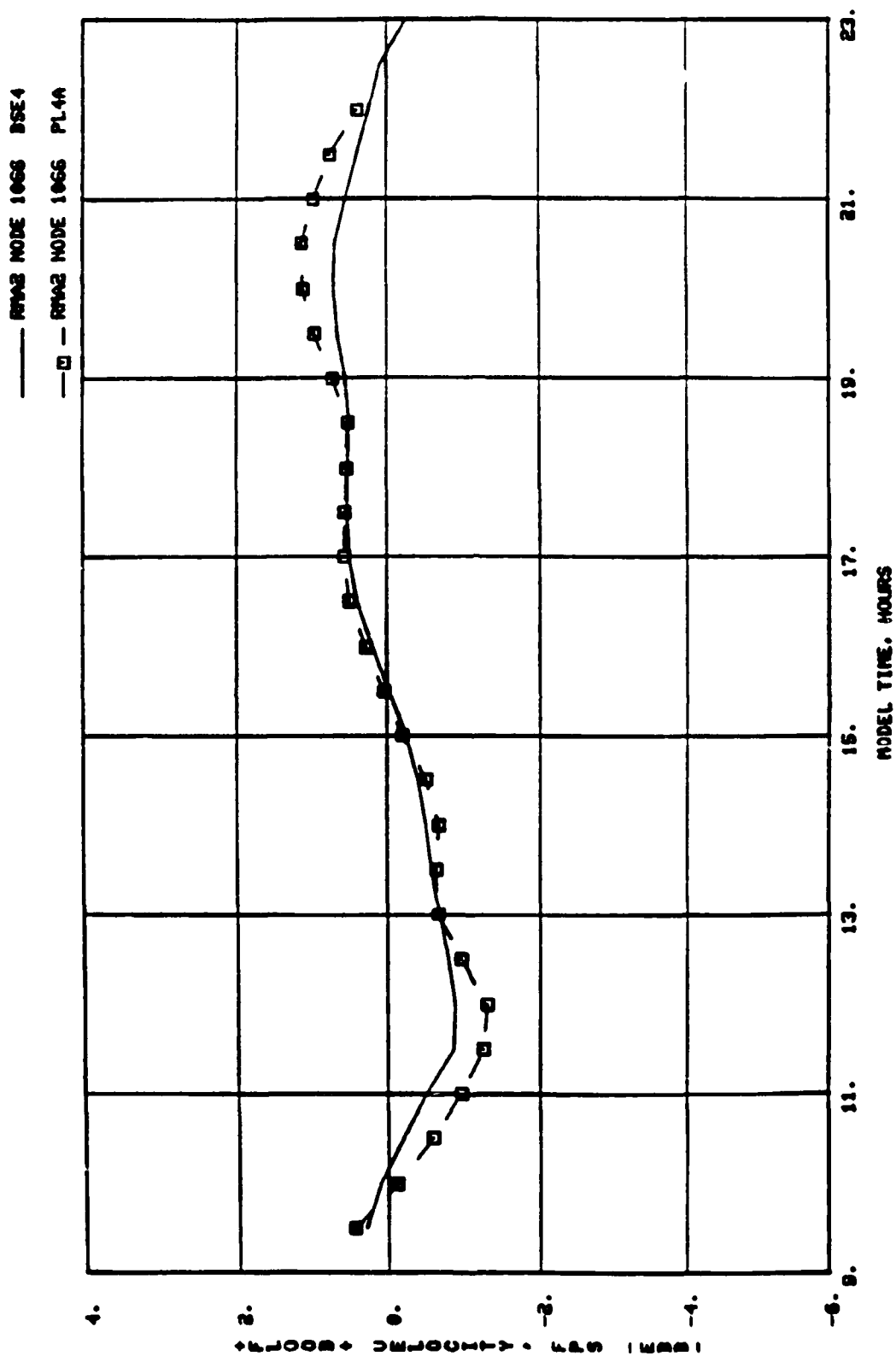
Plate D39. Numerical model base and plan velocities for node 1066 (Back Channel)

Plate D40. Numerical model base and plan velocities for node 1014 (Marianna Creek)
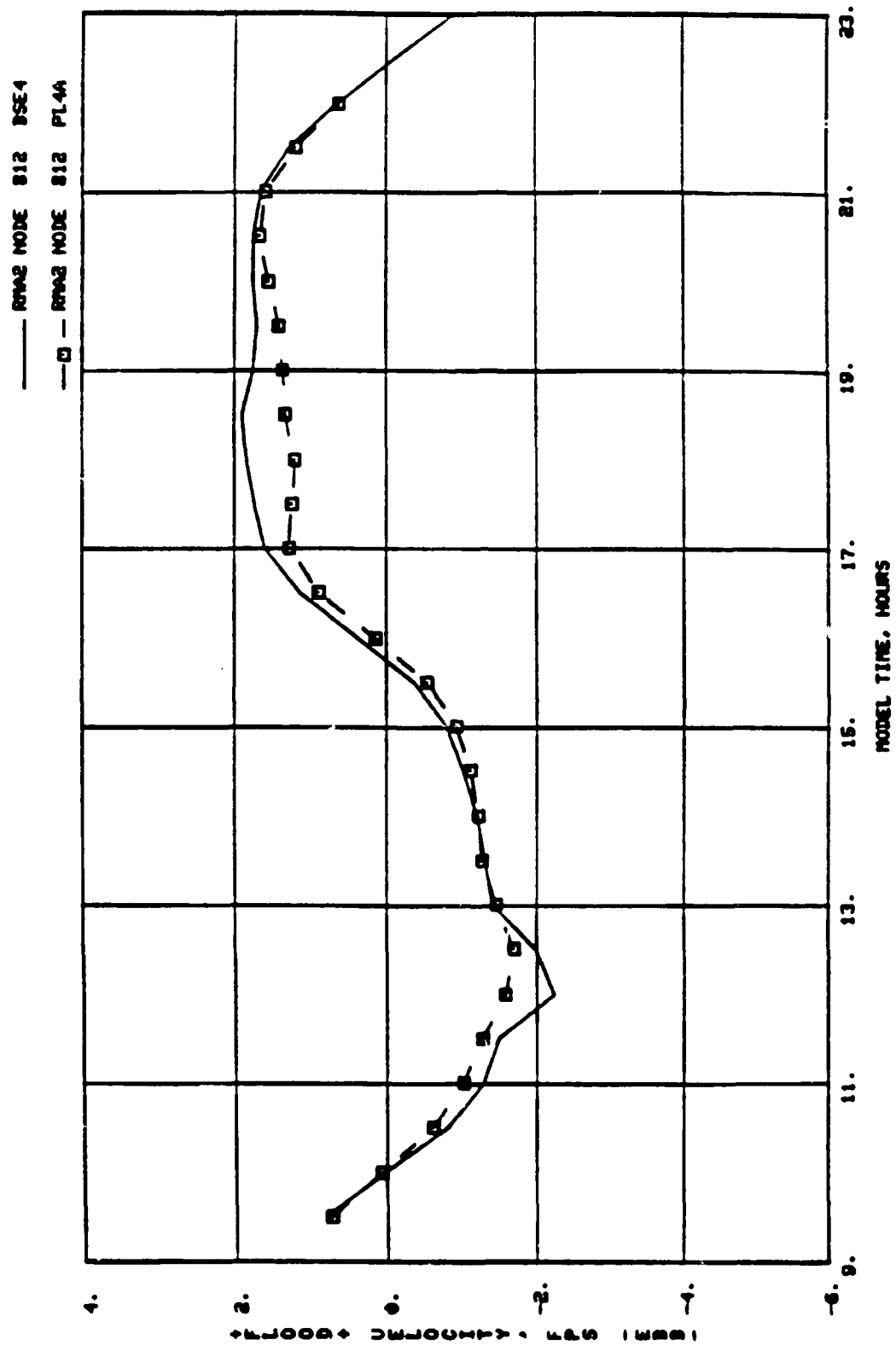
Plate D41. Numerical model base and plan velocities for node 812
(north branch of Crooked River)
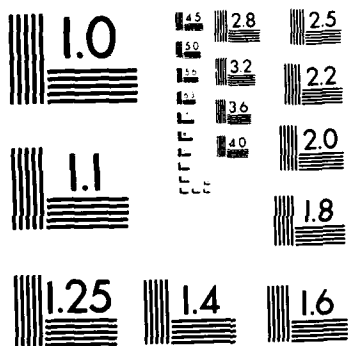
MICROCOPY RESOLUTION TEST CHART
NATIONAL BUREAU OF STANDARDS
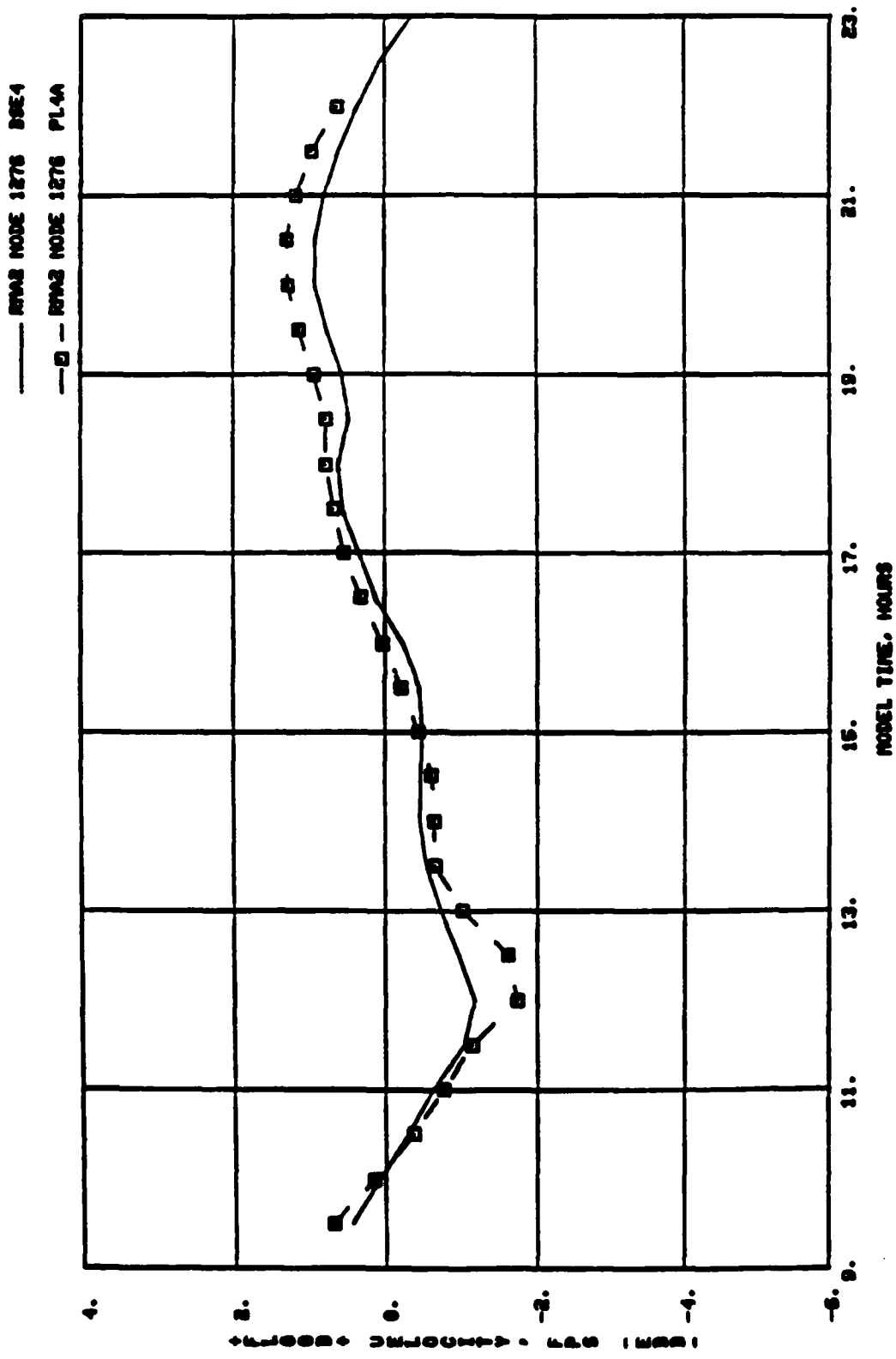STANDARD REFERENCE MATERIAL 1010a
(ANSI and ISO TEST CHART No. 2)

Plate D42. Numerical model base and plan velocities for node 1276 (upper Cumberland Sound)